Introduction to Linear Elasticity

Second Edition

Springer
New York
Berlin
Heidelberg
Barcelona
Hong Kong
London
Milan
Paris
Singapore
Tokyo

Phillip L. Gould

Introduction to Linear Elasticity

Second Edition

With 64 Figures

Springer

Phillip L. Gould
Harold D. Jolley Professor and Chairman
Department of Civil Engineering
Washington University
St. Louis, MO 63130 USA

Library of Congress Cataloging-in-Publication Data
Gould, Phillip L.
Introduction to linear elasticity / Phillip L. Gould.—2nd ed.
p. cm.
Includes bibliographical references and index.
ISBN-13:978-1-4612-8728-5 e-ISBN-13: 978-1-4612-4296-3
DOI: 10.1007/978-1-4612-4296-3
1. Elasticity. I. Title.
QA931.G64 1994
531'.382—dc20 93-5140

Printed on acid-free paper.

Production managed by Ellen Seham; manufacturing supervised by Vincent Scelta.
Typeset by Asco Trade Typesetting Ltd., Hong Kong.

9 8 7 6 5 4 3 (Corrected third printing, 1999)

To my children

Elizabeth Sue
Nathan Charles
Rebecca Blair
Joshua Robert

Preface

"Elasticity is one of the crowning achievements of Western culture!" exclaimed my usually reserved colleague Professor George Zahalak during a meeting to discuss the graduate program in Solid Mechanics. Although my thoughts on the theory of elasticity had not been expressed in such noble terms, it was the same admiration for the creative efforts of the premier physicists, mathematicians and mechanicians of the 19th and 20th centuries that led me to attempt to popularize the basis of solid mechanics in this introductory form.

The book is intended to provide a thorough grounding in tensor-based theory of elasticity, which is rigorous in treatment but limited in scope. It is directed to advanced undergraduate and graduate students in civil, mechanical or aeronautical engineering who may ultimately pursue more applied studies. It is also hoped that a few may be inspired to delve deeper into the vast literature on the subject. A one-term course based on this material may replace traditional Advanced Strength of Materials in the curriculum, since many of the fundamental topics grouped under that title are treated here, while those computational techniques that have become obsolete due to the availability of superior, computer-based numerical methods are omitted.

Little, if any, originality is claimed for this work other than the selection, organization and presentation of the material. The principal historical contributors are noted in the text and several modern references are liberally cited.

My personal interest in the theory of elasticity was kindled at Northwestern University through a course offered by Professor George Herrmann, later of Stanford University. I am also indebted to my colleague Professor S. Sridharan who has class-tested the text, pointed out errors and omissions, and contributed some challenging exercises, as well as to Professor Moujalli Hourani for carefully reading the first edition manuscript. I am grateful to Ms. Kathryn Schallert for typing that manuscript.

For the corrected first edition, the author incorporated the suggestions of many careful readers. He is especially appreciative for the corrections supplied by Mr. A.S. Mosallam and Professor George G. Adams, and for the

clarifications of several points provided by Mr. John C. de C. Henderson. He benefitted from the comments of Dr. Mao Peng who worked most of the exercises. In that printing, a few problems were added to extend the scope of the treatment; Chapter 4 was revised in accordance with the format proposed by Professor Sridharan; and Section 7.10 was replaced by a more meaningful illustration at the urging of Mr. Nathan Gould.

The second edition reflects the scrutiny of G. Tong and Andrea Schokker. The suggestion for the rotating beam problem in Chapter 9 is credited to Mr. Shang-Hyon Shin. The careful proofreading of the new chapters by Xiaofeng Wang and Ying-Xia Cai is especially appreciated.

Phillip L. Gould

Contents

Chapter 5. Formulation, Uniqueness and Solution Strategies

Chapter 6. Extension, Bending and Torsion

Chapter 7. Two-Dimensional Elasticity

Chapter 8. Bending of Thin Plates

Chapter 9. Time-Dependent Effects

Chapter 10. Energy Principles

CHAPTER 1

Introduction and Mathematical Preliminaries

1.1 Scope

The *theory of elasticity* comprises a consistent set of equations which uniquely describe the state of stress, strain and displacement at each point within an elastic deformable body. Solutions of these equations fall into the realm of *applied mathematics*, while applications of such solutions are of *engineering* interest. When elasticity is selected as the basis for an engineering solution, a rigor is accepted that distinguishes this approach from the alternatives, which are mainly based on the strength of materials with its various specialized derivatives such as the theories of rods, beams, plates and shells. The distinguishing feature between the various alternative approaches and the theory of elasticity is the *pointwise* description embodied in elasticity, without resort to expedients such as Navier's hypothesis of plane sections remaining plane.

The theory of elasticity contains *equilibrium* equations relating the stresses; *kinematic* equations relating the strains and displacements; *constitutive* equations relating the stresses and strains; *boundary conditions* relating to the physical domain; and *uniqueness* constraints relating to the applicability of the solution. Origination of the theory of elasticity is attributed to Louis–Marie–Henri Navier, Simon–Denis Poisson and George Green in the first half of the 19th century [1.1].

In subsequent chapters, each component of the theory will be developed in full from the fundamental principles of physics and mathematics. Some limited applications will then be presented to illustrate the potency of the theory as well as its limitations.

1.2 Vector Algebra

A *vector* is a directed line segment in the physical sense. Referred to the unit basis vectors $(\mathbf{e}_x, \mathbf{e}_y, \mathbf{e}_z)$ in the Cartesian coordinate system (x, y, z), an arbitrary vector $\mathbf{A}$ may be written in component form as

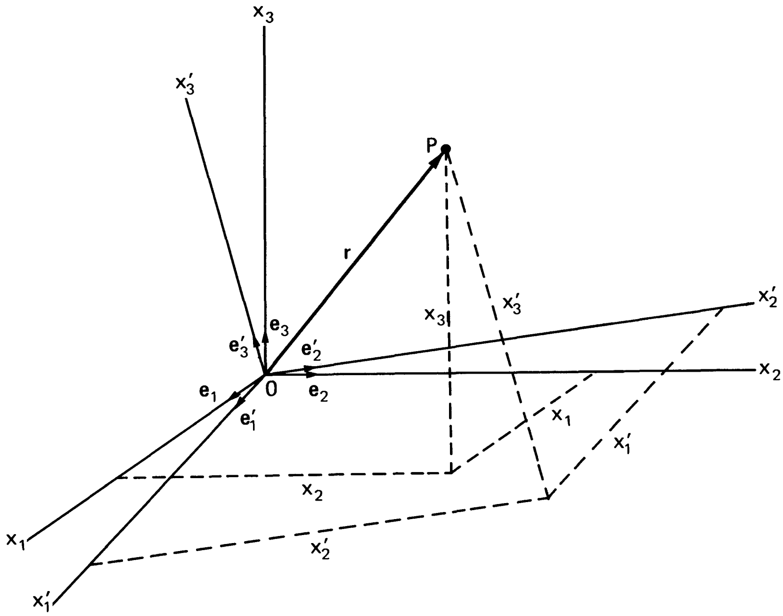

Fig. 1.1. Cartesian coordinate systems (after Tauchert, *Energy Principles in Structural Mechanics*, McGraw–Hill, 1974). Reproduced by permission.

$$\mathbf{A} = A_x\mathbf{e}_x + A_y\mathbf{e}_y + A_z\mathbf{e}_z. \tag{1.1}$$

Alternately, the Cartesian system could be numerically designated as (x_1, x_2, x_3), whereupon

$$\mathbf{A} = A_1\mathbf{e}_1 + A_2\mathbf{e}_2 + A_3\mathbf{e}_3. \tag{1.2}$$

The latter form is common in elasticity. An example is vector $\mathbf{r}$ in Fig. 1.1, where the unit vectors $\mathbf{e}_1$, $\mathbf{e}_2$, and $\mathbf{e}_3$ are identified [1.2].

Beyond the physical representation, it is often sufficient to deal with the components alone as ordered triples,

$$\mathbf{A} = (A_1, A_2, A_3). \tag{1.3}$$

The length or magnitude of $\mathbf{A}$ is given by

$$|\mathbf{A}| = \sqrt{A_1^2 + A_2^2 + A_3^2}. \tag{1.4}$$

Vector equality, addition, and subtraction are trivial. Vector multiplication has two forms. The *inner*, *dot*, or *scalar* product is

$$\begin{aligned} C &= \mathbf{A}\cdot\mathbf{B} \\ &= A_1B_1 + A_2B_2 + A_3B_3 \\ &= |\mathbf{A}||\mathbf{B}|\cos\theta_{AB}. \end{aligned} \tag{1.5}$$

Additionally, there is the *outer*, *cross*, or *vector* product

$$\mathbf{C} = \mathbf{A} \times \mathbf{B}$$
$$= (A_2B_3 - A_3B_2)\mathbf{e}_1 + (A_3B_1 - A_1B_3)\mathbf{e}_2 + (A_1B_2 - A_2B_1)\mathbf{e}_3, \quad (1.6)$$

which is conveniently evaluated as a determinant

$$\mathbf{C} = \mathbf{A} \times \mathbf{B} = \begin{vmatrix} \mathbf{e}_1 & \mathbf{e}_2 & \mathbf{e}_3 \\ A_1 & A_2 & A_3 \\ B_1 & B_2 & B_3 \end{vmatrix};$$

C is perpendicular to the plane containing **A** and **B**.

1.3 Scalar and Vector Fields

1.3.1 Definitions

A *scalar* quantity expressed as a function of the Cartesian coordinates such as

$$f(x_1, x_2, x_3) = \text{constant} \quad (1.7)$$

is known as a *scalar field.* An example is the temperature at a point.

A *vector* quantity similarly expressed, such as $\mathbf{A}(x_1, x_2, x_3)$, is called a *vector field.* An example is the velocity of a particle. We are concerned with changes or derivatives of these fields.

1.3.2 Gradient

The *gradient* of a scalar field f is defined as

$$\begin{aligned} \mathbf{grad}\, f &= \nabla f \\ &= \frac{\partial f}{\partial x_1}\mathbf{e}_1 + \frac{\partial f}{\partial x_2}\mathbf{e}_2 + \frac{\partial f}{\partial x_3}\mathbf{e}_3 \\ &= \left(\frac{\partial f}{\partial x_1}, \frac{\partial f}{\partial x_2}, \frac{\partial f}{\partial x_3}\right), \end{aligned} \quad (1.8)$$

$\mathbf{grad}\, f$ is a *vector* point function which is orthogonal to the surface $f =$ constant, everywhere. Conversely, the components of $\mathbf{grad}\, f$ may be found by the appropriate dot product, for example,

$$\frac{\partial f}{\partial x_1} = \mathbf{e}_1 \cdot \nabla f \quad (1.9)$$

1.3.3 Operators

The del operator ∇ may be treated as a vector

$$\nabla(\ ) = \frac{\partial(\ )}{\partial x_1}\mathbf{e}_1 + \frac{\partial(\ )}{\partial x_2}\mathbf{e}_2 + \frac{\partial(\ )}{\partial x_3}\mathbf{e}_3, \quad (1.10a)$$

while the higher-order scalar operators are written as

$$\nabla^2(\ ) = \nabla \cdot \nabla(\ ) = \frac{\partial^2}{\partial x_1^2}(\ ) + \frac{\partial^2}{\partial x_2^2}(\ ) + \frac{\partial^2}{\partial x_3^2}(\ ) \tag{1.10b}$$

and

$$\begin{aligned}\nabla^4(\ ) &= \nabla^2[\nabla^2(\ )] \\ &= \frac{\partial^4}{\partial x_1^4}(\ ) + \frac{\partial^4}{\partial x_2^4}(\ ) + \frac{\partial^4}{\partial x_3^4}(\ ) + 2\frac{\partial^4}{\partial x_1^2 \partial x_2^2}(\ ) + 2\frac{\partial^4}{\partial x_1^2 \partial x_3^2}(\ ) \\ &\quad + 2\frac{\partial^4}{\partial x_2^2 \partial x_3^2}(\ ) \end{aligned} \tag{1.10c}$$

and are used frequently in the following chapters. The operators are particularly useful because the operation performed is independent of any particular coordinate system, or *invariant*. However, the forms given in Eqs. (1.10) are for Cartesian coordinates; for curvilinear coordinates, such as cylindrical coordinates, the operators must be appropriately transformed. This is developed in Sec. 7.4.

1.3.4 Divergence

The *divergence* of a vector field **A** is defned as

$$\begin{aligned}\operatorname{div} \mathbf{A} &= \nabla \cdot \mathbf{A} \\ &= \frac{\partial A_1}{\partial x_1} + \frac{\partial A_2}{\partial x_2} + \frac{\partial A_3}{\partial x_3},\end{aligned} \tag{1.11}$$

which is a scalar conveniently written as ΔA.

1.3.5 Curl

Since two forms of vector multiplication exist, it is natural to expect another derivative form of **A**. The *curl* of **A** is defined as

$$\begin{aligned}\mathbf{curl}\, \mathbf{A} &= \nabla \times \mathbf{A} \\ &= \begin{vmatrix} \mathbf{e}_1 & \mathbf{e}_2 & \mathbf{e}_3 \\ \dfrac{\partial(\ )}{\partial x_1} & \dfrac{\partial(\ )}{\partial x_2} & \dfrac{\partial(\ )}{\partial x_3} \\ A_1 & A_2 & A_3 \end{vmatrix}\end{aligned} \tag{1.12}$$

in determinant form.

1.3.6 Integral Theorems

Two integral theorems relating vector fields are particularly useful for transforming between contour, area and volume integrals: Green's theorem and the Divergence theorem.

Considering two functions $P(x, y)$ and $Q(x, y)$ which are continuous and have continuous first partial derivatives (C^1 continuous) in a domain D, Green's theorem states that

$$\oint_C (P\,dx + Q\,dy) = \int_A (Q_{,x} - P_{,y})\,dx\,dy \tag{1.13}$$

where A is a closed region of D bounded by C.

Considering a continuously differentiable vector point function **G** in D, the divergence theorem states that

$$\int_V \nabla \cdot \mathbf{G}\,dV = \int_A \mathbf{n} \cdot \mathbf{G}\,dA \tag{1.14}$$

where V is the volume bounded by the oriented surface A and **n** is the positive normal to A.

1.4 Indicial Notation

One of the conveniences of modern treatments of the theory of elasticity is the use of shorthand notation to facilitate the mathematical manipulation of lengthy equations.

Referring to the ordered triple representation for **A** in Eq. (1.3), the three Cartesian components can be symbolized as A_i, where the subscript or *index* i is understood to take the sequential values 1, 2, 3. If we have nine quantities, we may employ a double subscripted notation D_{ij}, where i and j range from 1 to 3 in turn. Later, we will associate these nine components with a higher form of a vector, called a tensor. Further, we may have 27 quantities, C_{ijk}, etc.

While i and j range as stated, an exception is made when two subscripts are identical, such as D_{jj}. The *Einstein summation convention* states that a subscript appearing *twice* is *summed* from 1 to 3. No subscript can appear more than twice. As an example, we have the inner product, Eq. (1.5), rewritten as

$$\begin{aligned} A_i B_i &= \sum_{i=1}^{3} A_i B_i \\ &= A_1 B_1 + A_2 B_2 + A_3 B_3. \end{aligned} \qquad \text{(a)} \quad (1.15)$$

Also,

$$D_{jj} = D_{11} + D_{22} + D_{33}. \qquad \text{(b)} \quad (1.15)$$

It is apparent from the preceding examples that there are two distinct types of indices. The first type appears only once in each term of the equation and ranges from 1 to 3. It is called a *free* index. The second type appears twice in a single term and is summed from 1 to 3. Since it is immaterial which letter is used in this context, a repeated subscript is called a *dummy* index. That is, $D_{ii} = D_{jj} = D_{kk}$.

From the preceding discussion, it may be deduced that the number of individual terms represented by a single product is 3^k, where k is the number of free indices.

There are some situations in which double subscripts occur where the summation convention is not intended. This is indicated by enclosing the subscripts in parentheses [1.3]. For example, the individual components D_{11}, D_{22} and D_{33} could be represented by $D_{(ii)}$.

The *product* of the three components of a vector is expressed by the Pi convention:

$$\prod_{i=1}^{3} A_i = A_1 A_2 A_3. \tag{1.16}$$

Partial differentiation may also be abbreviated using the *comma* convention

$$\frac{\partial A_i}{\partial x_j} = A_{i,j}. \tag{1.17a}$$

Since both i and j are free indices, Eq. (1.17a)represents $3^2 = 9$ quantities. With repeated indices,

$$\begin{aligned}\frac{\partial A_i}{\partial x_i} &= A_{i,i}\\ &= \Delta A\end{aligned} \tag{1.17b}$$

as defined in Eq. (1.11).

Further,

$$\begin{aligned}\frac{\partial D_{ij}}{\partial x_j} &= D_{ij,j}\\ &= D_{i1,1} + D_{i2,2} + D_{i3,3},\end{aligned} \tag{1.17c}$$

which takes on $3^1 = 3$ values for each $i = 1, 2, 3$. This example combines the summation and comma conventions.

1.5 Coordinate Rotation

In Fig. 1.1 (see [1.2]), we show a position vector to point P, $\mathbf{r}$, resolved into components with respect to *two* Cartesian systems, x_i and x_i', having a common origin. The unit vectors in the x_i' system are shown as $\mathbf{e}_i'$ on the figure.

First, we consider the point P with coordinates $P(x_1, x_2, x_3) = P(x_i)$ in the unprimed system and $P(x_1', x_2', x_3') = P(x_i')$ in the primed system. The linear transformation between the coordinates of P is given by

$$\begin{aligned}x_1' &= \alpha_{11}x_1 + \alpha_{12}x_2 + \alpha_{13}x_3\\ x_2' &= \alpha_{21}x_1 + \alpha_{22}x_2 + \alpha_{23}x_3\\ x_3' &= \alpha_{31}x_1 + \alpha_{32}x_2 + \alpha_{33}x_3\end{aligned} \qquad \text{(a)} \quad (1.18)$$

or

$$x'_i = \alpha_{ij} x_j \qquad \text{(b)} \quad (1.18)$$

using the summation convention. Each of the nine quantities α_{ij} is the cosine of the angle between the ith primed and the jth unprimed axis, that is,

$$\alpha_{ij} = \cos(x'_i, x_j) = \frac{\partial x_j}{\partial x'_i} = \mathbf{e}'_i \cdot \mathbf{e}_j = \cos(\mathbf{e}'_i, \mathbf{e}_j) \qquad (1.19)$$

The α_{ij}'s are known as *direction cosines* and are conveniently arranged in tabular form for computation:

	x_1	x_2	x_3
x'_1	α_{11}	α_{12}	α_{13}
x'_2	α_{21}	α_{22}	α_{23}
x'_3	α_{31}	α_{32}	α_{33}.

(1.20)

It is emphasized that, in general, $\alpha_{ij} \neq \alpha_{ji}$. From a computational standpoint, Eq. (1.19) indicates that expressing the unit vectors in the x'_i coordinate system, $\mathbf{e}'_i$, in terms of those in the x_i system, $\mathbf{e}_i$, is tantamount to evaluating the corresponding α_{ij} terms. A numerical example is given in Sections 2.2.6 and 2.4.3.

We next consider the position vector $\mathbf{r}$ and recognize that the *components* are related by Eq. (1.18). Conversely, any quantity which obeys this transformation law is a vector. This somewhat indirect definition of a vector proves to be convenient for defining higher-order quantities, *Cartesian tensors.*

From a computational standpoint, it is often convenient to carry out the transformations indicated in Eq. (1.18) in matrix form as

$$\{\mathbf{x}'\} = [\mathbf{R}]\{\mathbf{x}\}, \qquad (1.21)$$

in which

$$\{\mathbf{x}'\} = \{x'_1 x'_2 x'_3\} \qquad \text{(a)}$$

$$\{\mathbf{x}\} = \{x_1 x_2 x_3\} \qquad \text{(b)} \quad (1.22)$$

$$[\mathbf{R}] = \begin{bmatrix} \alpha_{11} & \alpha_{12} & \alpha_{13} \\ \alpha_{21} & \alpha_{22} & \alpha_{23} \\ \alpha_{31} & \alpha_{32} & \alpha_{33} \end{bmatrix}, \qquad \text{(c)}$$

$[\mathbf{R}]$ is called a *rotation* matrix.

1.6 Cartesian Tensors

A tensor of order n is a set of 3^n quantities which transform from one coordinate system, x_i, to another, x'_i, by a specified law, as follows:

n	order	transformation law
0	zero (scalar)	$A_i' = A_i$
1	one (vector)	$A_i' = \alpha_{ij} A_j$
2	two (dyadic)	$A_{ij}' = \alpha_{ik}\alpha_{jl} A_{kl}$
3	three	$A_{ijk}' = \alpha_{il}\alpha_{jm}\alpha_{kn} A_{lmn}$
4	four	$A_{ijkl}' = \alpha_{im}\alpha_{jn}\alpha_{kp}\alpha_{lq} A_{mnpq}$

Order zero and order one tensors are familiar physical quantities, whereas the higher-order tensors are useful to describe physical quantities with a corresponding number of associated directions.

Second-order tensors (dyadics) are particularly prevalent in elasticity and the transformation may be carried out in a matrix format, analogous to Eq. (1.21), as

$$[\mathbf{A}'] = [\mathbf{R}][\mathbf{A}][\mathbf{R}]^T, \tag{1.23}$$

in which

$$[\mathbf{A}'] = \begin{bmatrix} A_{11}' & A_{12}' & A_{13}' \\ A_{21}' & A_{22}' & A_{23}' \\ A_{31}' & A_{32}' & A_{33}' \end{bmatrix} \tag{1.24}$$

and [A] is similar. The superscript T indicates the transpose operation.

It may be helpful to visualize a tensor of order n as having n unit vectors or directions associated with each component. Thus, a scalar has no directional association (isotropic) and a vector is directed in one direction. A second-order tensor has two associated directions, perhaps one direction *in* which it acts and another defining the surface *on* which it is acting.

1.7 Algebra of Cartesian Tensors

Tensor arithmetic and algebra are similiar to matrix operations in regard to addition, subtraction, equality and scalar multiplication. Multiplication of two tensors of order n and m produces a new tensor of order $n + m$. For example,

$$A_i B_{jk} = C_{ijk} \tag{1.25}$$

For two repeated indices the summation convention holds, as shown in Eq. (1.15b).

1.8 Operational Tensors

Additional tensor operations are facilitated by the use of the *Kronecker delta* δ_{ij} defined such that

$$\delta_{ij} = 1 \quad \text{if } i = j$$
$$\delta_{ij} = 0 \quad \text{if } i \neq j \tag{1.26}$$

and the *permutation symbol* ε_{ijk} defined such that

$$\varepsilon_{ijk} = \tfrac{1}{2}(i - j)(j - k)(k - i) \tag{1.27}$$

Thus

$\varepsilon_{ijk} = 0$ if any two of i, j, k are equal

$\varepsilon_{ijk} = 1$ for an even permutation (forward on the number line 1, 2, 3, 1, 2, 3, ...)

$\varepsilon_{ijk} = -1$ for an odd permutation (backward on the number line)

Hence, $\varepsilon_{112} = 0$, $\varepsilon_{231} = +1$, $\varepsilon_{321} = -1$.

The Kronecker delta δ_{ij} is used to change the subscripts in a tensor by multiplication, as illustrated in the following:

$$\begin{aligned} \delta_{ij}A_i &= \delta_{1j}A_1 + \delta_{2j}A_2 + \delta_{3j}A_3 = A_j \\ \delta_{ij}D_{jk} &= \delta_{i1}D_{1k} + \delta_{i2}D_{2k} + \delta_{i3}D_{3k} = D_{ik} \\ \delta_{ij}C_{ijk} &= \delta_{11}C_{11k} + \delta_{22}C_{22k} + \delta_{33}C_{33k} = C_{iik} = A_k. \end{aligned} \tag{1.28}$$

The last illustration, in which two subscripts in C_{ijk} were made identical by δ_{ij}, results in C_{ijk} being changed from a third- to a first-order tensor. This is known as *contraction*, and generally reduces the order of the original tensor by two.

The Kronecker delta δ_{ij} is also useful in vector algebra and for coordinate transformations. Starting with the dot product of two unit vectors

$$\mathbf{e}_i \cdot \mathbf{e}_j = \delta_{ij} \tag{1.29}$$

and seeking the component of a vector $\mathbf{A} = A_i\mathbf{e}_i$ in the j direction, A_j, we do the following:

$$\begin{aligned} \mathbf{e}_j \cdot \mathbf{A} &= (\mathbf{e}_j \cdot \mathbf{e}_i)A_i \\ &= \delta_{ji}A_i \\ &= A_j. \end{aligned} \tag{1.30}$$

Next, we consider Eq. (1.29) for transformed coordinates:

$$\begin{aligned} \delta_{ij} &= \mathbf{e}'_i \cdot \mathbf{e}'_j \\ &= (\alpha_{ik}\mathbf{e}_k) \cdot (\alpha_{jl}\mathbf{e}_l) \\ &= \alpha_{ik}\alpha_{jl}\mathbf{e}_k \cdot \mathbf{e}_l \\ &= \alpha_{ik}\alpha_{jl}\delta_{kl} \\ &= \alpha_{ik}\alpha_{jk}. \end{aligned} \tag{1.31}$$

Equation (1.31) is useful for demonstrating some important properties of direction cosines.

First, taking $i = j$ and summing only on k, we get

$$\begin{aligned} 1 &= \alpha_{(i)k}\alpha_{(i)k} \\ &= \alpha_{i1}^2 + \alpha_{i2}^2 + \alpha_{i3}^2 \end{aligned} \tag{1.32}$$

Expanding Eq. (1.32), we have

$$\begin{aligned} i = 1:&\quad \alpha_{11}^2 + \alpha_{12}^2 + \alpha_{13}^2 = 1 \\ i = 2:&\quad \alpha_{21}^2 + \alpha_{22}^2 + \alpha_{23}^2 = 1 \\ i = 3:&\quad \alpha_{31}^2 + \alpha_{32}^2 + \alpha_{33}^2 = 1, \end{aligned}$$

which is the *normality* property of direction cosines.

Then, taking $i \neq j$, we get

$$\begin{aligned} 0 &= \alpha_{ik}\alpha_{jk} \\ &= \alpha_{i1}\alpha_{j1} + \alpha_{i2}\alpha_{j2} + \alpha_{i3}\alpha_{j3}. \end{aligned} \tag{1.34}$$

Expanding Eq. (1.34), we have

$$\begin{aligned} i = 1, j = 2:&\ \alpha_{11}\alpha_{21} + \alpha_{12}\alpha_{22} + \alpha_{13}\alpha_{23} = 0 \\ i = 1, j = 3:&\ \alpha_{11}\alpha_{31} + \alpha_{12}\alpha_{32} + \alpha_{13}\alpha_{33} = 0 \\ i = 2, j = 1:&\ \alpha_{21}\alpha_{11} + \alpha_{22}\alpha_{12} + \alpha_{23}\alpha_{13} = 0 \\ i = 2, j = 3:&\ \alpha_{21}\alpha_{31} + \alpha_{22}\alpha_{32} + \alpha_{23}\alpha_{33} = 0 \\ i = 3, j = 1:&\ \alpha_{31}\alpha_{11} + \alpha_{32}\alpha_{12} + \alpha_{33}\alpha_{13} = 0 \\ i = 3, j = 2:&\ \alpha_{31}\alpha_{21} + \alpha_{32}\alpha_{22} + \alpha_{33}\alpha_{23} = 0, \end{aligned}$$

which is the *orthogonality* property of direction cosines.

The permutation symbol ε_{ijk} is useful for vector cross-product operations. If we take

$$\begin{aligned} \varepsilon_{ijk}A_jB_k\mathbf{e}_i &= (\varepsilon_{123}A_2B_3 + \varepsilon_{132}A_3B_2)\mathbf{e}_1 + (\varepsilon_{213}A_1B_3 + \varepsilon_{231}A_3B_1)\mathbf{e}_2 \\ &\quad + (\varepsilon_{312}A_1B_2 + \varepsilon_{321}A_2B_1)\mathbf{e}_3 \\ \varepsilon_{ijk}A_jB_k\mathbf{e}_i &= (A_2B_3 - A_3B_2)\mathbf{e}_1 + (A_3B_1 - A_1B_3)\mathbf{e}_2 \\ &\quad + (A_1B_2 - A_2B_1)\mathbf{e}_3 \end{aligned} \tag{1.36}$$

we obtain an expression which is identical to Eq. (1.6). Thus, $\varepsilon_{ijk}A_jB_k$ gives the components of $\mathbf{A} \times \mathbf{B}$.

1.9 Computational Examples

To illustrate computations and manipulations using Cartesian tensors, we present the following illustrations:

(1) Show that $\delta_{ij}\delta_{jk} = \delta_{ik}$:
Expanding $\delta_{ij}\delta_{jk}$, we get

$$\delta_{ij}\delta_{jk} = \delta_{i1}\delta_{1k} + \delta_{i2}\delta_{2k} + \delta_{i3}\delta_{3k} = 1 \times \delta_{ik} \quad \text{for a selected } i = 1, 2 \text{ or } 3$$

(2) Show that $\varepsilon_{ijk}A_jA_k = 0$:
Expanding $\varepsilon_{ijk}A_jA_k$, we find

$$\begin{aligned}\varepsilon_{ijk}A_jA_k &= \varepsilon_{123}A_2A_3 + \varepsilon_{132}A_3A_2 + \varepsilon_{231}A_3A_1 + \varepsilon_{213}A_1A_3 \\ &\quad + \varepsilon_{312}A_1A_2 + \varepsilon_{321}A_2A_1 \\ &= +1 - 1 + 1 - 1 + 1 - 1 \\ &= 0.\end{aligned}$$

(3) Prove that the product of two first-order tensors is a second-order tensor: Let A_i and B_j be two first-order tensors and C_{ij} be their product, then

$$A_i = \alpha_{ik}A_k$$

$$B_j = \alpha_{jl}B_l$$

$$A_iB_j = \alpha_{ik}\alpha_{jl}A_kB_l = \alpha_{ik}\alpha_{jl}C_{kl} = C_{ij}$$

so that C_{ij} transforms as a second-order tensor.

Exercises

1.1 Show that (after [1.2]):
(a) $\delta_{ij}\delta_{ij} = 3$
(b) $\varepsilon_{ijk}\varepsilon_{kji} = -6$

1.2 Prove that if $\delta_{ij} = \delta'_{ij}$, then δ_{ij} is a second-order tensor (after [1.2]).

1.3 Prove that the product of a first- and a second-order tensor is a third-order tensor.

1.4 Two first-order tensors are related by

$$A_i = C_{ij}B_j.$$

Prove that C_{ij} is a second-order tensor.

1.5 Show that if B_i is a first-order tensor, $B_{i,j}$ is a second-order tensor [1.2].

1.6 If a square matrix [C] has the property

$$[\mathbf{C}]^{-1} = [\mathbf{C}]^T$$

it is said to be orthogonal. This property is used in the derivation of Eq. (1.23). Show that the matrix of direction cosines $[A]$ is orthogonal.

1.7 Write the operator $\nabla^2(\ )$ defined in Eq. 1.10(b) in indicial notation.

References

[1.1] Westergaard, H. M., *Theory of Elasticity and Plasticity* (Dover Publications, Inc., New York, 1964).

[1.2] Tauchert, T. R., *Energy Principles in Structural Mechanics* (McGraw–Hill Book Company, Inc., New York, 1974).

[1.3] Ma, Y. and Desai, C. S., "Alternative Definition of Finite Strains," *Journal of Engineering Mechanics*, ASCE, v. 116, No. 4, April, 1990, pp. 901–919.

CHAPTER 2

Traction, Stress and Equilibrium

2.1 Introduction

An approach to the solution of problems in solid mechanics is to establish relationships first between applied loads and internal stresses and, subsequently, to consider deformations. Another approach is to examine deformations initially, and then proceed to the stresses and applied loads. Regardless of the eventual solution path selected, it is necessary to derive the component relationships individually. In this chapter, the first set of equations, which describe equilibrium between external and internal forces and stresses, are derived.

2.2 State of Stress

2.2.1 Traction and Couple-Stress Vectors

A deformable body subject to external loading is shown in Fig. 2.1. There may be loads applied over the exterior, properly called *surface forces*, and loads distributed within the interior, known as *body forces*. An example of the latter is the effect of gravity which produces the *self-weight* of the body.

Focusing on an element with an area ΔA_n on or within the body and oriented as specified by the unit normal $\mathbf{n}$, we accumulate the resultant force $\Delta \mathbf{F}_n$ and moment $\Delta \mathbf{M}_n$. Both are vector quantities and are *not*, in general, parallel to $\mathbf{n}$. Next, we seek the intensity of the resultants on the area ΔA_n in the form [2.1]

$$\lim_{\Delta A_n \to 0} \frac{\Delta \mathbf{F}_n}{\Delta A_n} = \frac{d\mathbf{F}_n}{dA_n} = \mathbf{T}_n \qquad \text{(a)}$$

$$\lim_{\Delta A_n \to 0} \frac{\Delta \mathbf{M}_n}{\Delta A_n} = \frac{d\mathbf{M}_n}{dA_n} = \mathbf{C}_n, \qquad \text{(b)} \qquad (2.1)$$

where $\mathbf{T}_n$ is known as the stress vector or *traction*, and $\mathbf{C}_n$ is called the *couple-stress vector.*

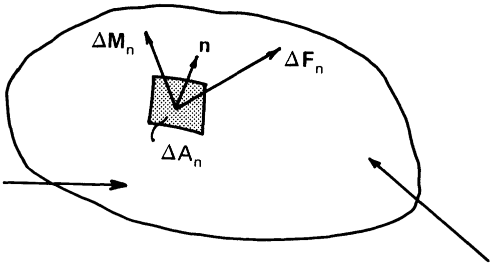

Fig. 2.1. Deformable body under external loading (after Tauchert, *Energy Principles in Structural Mechanics*, McGraw–Hill, 1974). Reproduced with permission.

The elementary theory of elasticity proceeds on the assumption that $\mathbf{C}_n = 0$ [2.2], while the traction $\mathbf{T}_n$ represents the stress intensity at the point for the particular orientation of area element specified by $\mathbf{n}$. A complete description at the point requires that the state of stress be known for all directions, so that $\mathbf{T}_n$ itself is necessary, but not sufficient, for this purpose.

2.2.2 Components of Stress

We now study an infinitesimal rectangular parallelepiped at the point in question and erect a set of Cartesian coordinates x_i parallel to the sides, as shown in Fig. 2.2[2.1]. Corresponding to each coordinate axis is a unit vector $\mathbf{e}_i$. Shown in the figure are the tractions $\mathbf{T}_i$ acting on each face i, with the subscript chosen corresponding to the face normal $\mathbf{e}_i$. It is again emphasized that, in general, $\mathbf{T}_i$ is *not* parallel to $\mathbf{e}_i$, which is perpendicular to the face of the parallelepiped.

Each traction may be written in terms of its Cartesian components in the form

$$\mathbf{T}_i = \sigma_{ij}\mathbf{e}_j, \tag{2.2}$$

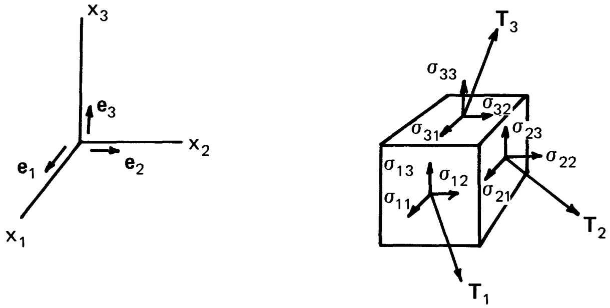

Fig. 2.2. Components of stress (after Tauchert, *Energy Principles in Structural Mechanics*, McGraw–Hill, 1974). Reproduced with permission.

which is expanded explicitly into the three equations

$$\mathbf{T}_1 = \sigma_{11}\mathbf{e}_1 + \sigma_{12}\mathbf{e}_2 + \sigma_{13}\mathbf{e}_3 \qquad \text{(a)}$$

$$\mathbf{T}_2 = \sigma_{21}\mathbf{e}_1 + \sigma_{22}\mathbf{e}_2 + \sigma_{23}\mathbf{e}_3 \qquad \text{(b)} \quad (2.3)$$

$$\mathbf{T}_3 = \sigma_{31}\mathbf{e}_1 + \sigma_{32}\mathbf{e}_2 + \sigma_{33}\mathbf{e}_3. \qquad \text{(c)}$$

The coeffcients $\sigma_{11}, \sigma_{12}, \ldots, \sigma_{33}$ are known as components of stress or, simply, as stresses, while the entire array forms the stress tensor when the appropriate transformation rule is verified. The subscript and sign conventions for components of stress σ_{ij} are as follows:

(1) The *first* subscript i refers to the *normal* $\mathbf{e}_i$ which denotes the face *on* which $\mathbf{T}_i$ acts.
(2) The *second* subscript j corresponds to the *direction* $\mathbf{e}_j$ *in* which the stress acts.
(3) The so-called *normal* or *extensional* components $\sigma_{(ii)}$ are positive if they produce tension, and negative if they produce compression. The *shearing* components $\sigma_{ij}(i \neq j)$ are positive if directed in the positive x_j direction while acting on the face with the unit normal $+\mathbf{e}_i$, or if directed in the negative x_j direction while acting on the face with unit normal $-\mathbf{e}_i$.

While it is sometimes vital to distinguish between tension and compression, the difference between the positive and negative shear directions is quite arbitrary for most materials. See Sections 11.4.3 and 11.4.4.

2.2.3 Stress at a Point

We are now in a position to pursue the main thrust of this section, and thus establish sufficient conditions to completely describe the state of stress at a point. We will show that this may be accomplished by specifying the tractions $\mathbf{T}_i$ on each of the three planes $\mathbf{e}_i$ which, by Eq. (2.3), is equivalent to specifying the nine components of stress σ_{ij}. Then, if the traction $\mathbf{T}_n$ acting on any *arbitrary* element of surface, defined by an appropriate $\mathbf{n}$, may be evaluated, then the proposition is proved and the stress tensor σ_{ij}, referred to any convenient Cartesian system, completely specifies the state of stress at the point.

The differential tetrahedron in Fig. 2.3[2.2] shows the traction $\mathbf{T}_n$ acting on the plane identified by $\mathbf{n}$, along with tractions on the faces indicated by $\mathbf{e}_i$ and the body force per unit volume $\mathbf{f}$[2.1]. The force on the sloping face is $\mathbf{T}_n dA_n$, while the force on each of the other faces is $-\mathbf{T}_i dA_i$, $i = 1, 2, 3$, since they have unit normals in the negative $\mathbf{e}_i$ directions.

The areas of the planes are related by [2.3]

$$dA_i = dA_n \cos(\mathbf{n}, \mathbf{e}_i) = dA_n \mathbf{n} \cdot \mathbf{e}_i \qquad (2.4)$$

so that

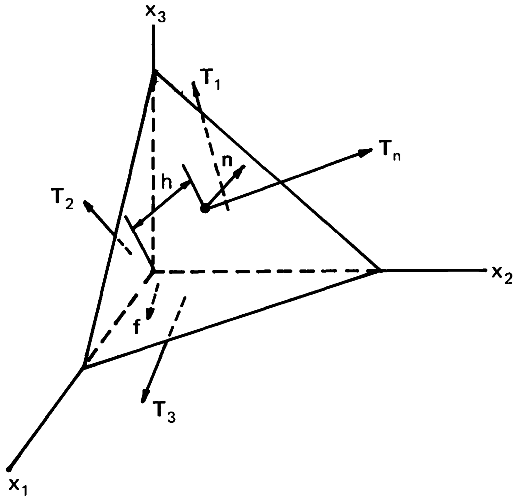

Fig. 2.3. Tractions (after Tauchert, *Energy Principles in Structural Mechanics*, McGraw–Hill, 1974). Reproduced with permission.

$$dA_n = \frac{dA_i}{\mathbf{n}\cdot\mathbf{e}_i} = \frac{dA_i}{n_i}, \tag{2.5}$$

where

$$n_i = \mathbf{n}\cdot\mathbf{e}_i = \cos(\mathbf{n}, \mathbf{e}_i) \tag{2.6}$$

is the component of $\mathbf{n}$ in the $\mathbf{e}_i$ direction and also a direction cosine.

Force equilibrium for the tetrahedron gives

$$\mathbf{T}_n dA_n - \mathbf{T}_1 dA_1 - \mathbf{T}_2 dA_2 - \mathbf{T}_3 dA_3 + \mathbf{f}(\tfrac{1}{3}h dA_n) = 0, \tag{2.7}$$

where h is the height of the tetrahedron. Using Eq. (2.5), Eq. (2.7) becomes

$$\left(\mathbf{T}_n - \mathbf{T}_i n_i + \mathbf{f}\frac{h}{3}\right) dA_n = 0. \tag{2.8}$$

Next, resolving $\mathbf{T}_n$ into Cartesian components $T_i\mathbf{e}_i$ and taking the limit as $h \to 0$, equilibrium is satisfied if

$$T_i\mathbf{e}_i = \mathbf{T}_i n_i. \tag{2.9}$$

The next step is to write $\mathbf{T}_i$ in terms of the stress components using Eq. (2.2). However, it is convenient first to change the dummy index on the r.h.s. of Eq. (2.9) from i to j, thus

$$\mathbf{T}_i n_i = \mathbf{T}_j n_j = \sigma_{ji} n_j \mathbf{e}_i, \tag{2.10}$$

which permits coefficients of $\mathbf{e}_i$ in Eqs. (2.9) and (2.10) to be equated, yielding

$$T_i = \sigma_{ji} n_j. \tag{2.11}$$

Conversely, if the components T_i are known, the magnitude of $\mathbf{T}_n$ may be evaluated as

$$T_n = |\mathbf{T}_n| = (T_i T_i)^{1/2}. \tag{2.12}$$

Since T_n represents a component of traction acting on any arbitrary plane as defined by $\mathbf{n}$, knowledge of the stress components referred to the Cartesian coordinates is indeed sufficient to specify completely the state of stress at the point. In Eq. (2.11), T_i and n_j are both components of vectors (order 1 tensors) so that the σ_{ji} are components of an order 2 tensor $\boldsymbol{\sigma}$. Therefore, if the stress components are known in one coordinate system, say the x_i system, they may be evaluated for another coordinate system, say the x_i' system, by the transformation law for second-order tensors

$$\sigma_{ij}' = \alpha_{ik}\alpha_{jl}\sigma_{kl}, \tag{2.13}$$

where each direction cosine

$$\alpha_{ij} = \cos(x_i', x_j) \tag{2.14}$$

as introduced in Sec. 1.5, represents the cosine of the angle between the x_i' and x_j axes.

Since transformation rules play an important role in the theory of elasticity, it is worth restating that $\alpha_{ij} \neq \alpha_{ji}$, that is, the direction cosines are *not* symmetric.

2.2.4 Stress on a Normal Plane

It is sometimes useful to resolve $\mathbf{T}_n$ into components that are normal and tangential to the differential surface element dA_n, as shown in Fig. 2.4. The normal component is calculated by

$$\begin{aligned}\sigma_{nn} = |\mathbf{N}| &= \mathbf{T}_n \cdot \mathbf{n} \\ &= T_i \mathbf{e}_i \cdot \mathbf{n} \\ &= T_i n_i \end{aligned} \tag{2.15}$$

or, from Eq. (2.11),

$$\sigma_{nn} = \sigma_{ji} n_j n_i. \tag{2.16}$$

The tangential component is

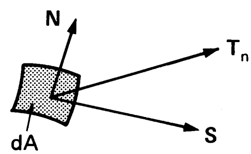

Fig. 2.4. Differential surface element.

$$\begin{aligned}\sigma_{ns} = |\mathbf{S}| &= \mathbf{T}_n \cdot \mathbf{s} \\ &= T_i \mathbf{e}_i \cdot \mathbf{s} \\ &= T_i s_i \\ &= \sigma_{ji} n_j s_i,\end{aligned} \tag{2.17}$$

where

$$s_i = \mathbf{e}_i \cdot \mathbf{s}. \tag{2.18}$$

It is often expedient to calculate σ_{ns} using the Pythagorian theorem as

$$\sigma_{ns} = (T_i T_i - \sigma_{nn}^2)^{1/2}. \tag{2.19}$$

Carrying the resolution one step further, the Cartesian components of **N** and **S** may be evaluated using (k) to designate the axes:

$$\begin{aligned}\sigma_{nn(k)} = \mathbf{N} \cdot \mathbf{e}_k &= \sigma_{nn} \mathbf{n} \cdot \mathbf{e}_k \\ &= \sigma_{nn} n_k \\ &= \sigma_{ji} n_j n_i n_k \quad \text{where } k = 1, 2, 3\end{aligned} \tag{2.20}$$

from Eq. (2.16). For σ_{ns}, simple subtraction gives

$$\sigma_{ns(k)} = T_k - \sigma_{nn(k)} \qquad k = 1, 2, 3, \tag{2.21a}$$

where T_k are the Cartesian components of **T**, as given by Eq. (2.11). The expression may be written explicity as

$$\begin{aligned}\sigma_{ns(k)} &= \sigma_{jk} n_j - \sigma_{ji} n_j n_i n_k \\ &= (\delta_{ki} - n_i n_k) \sigma_{ij} n_j\end{aligned} \tag{2.21b}$$

An application of this resolution is presented in Section 11.2.3.

2.2.5 Dyadic Representation of Stress

Conceptually, it may be helpful to view the stress tensor as a vector-like quantity having a magnitude and associated direction(s), specified by unit vectors. The *dyadic*, attributed to the mathematician J. Willard Gibbs [2.4], is such a representation. We write the stress tensor or stress dyadic as

$$\begin{aligned}\boldsymbol{\sigma} &= \sigma_{ij} \mathbf{e}_i \mathbf{e}_j \\ &= \sigma_{11} \mathbf{e}_1 \mathbf{e}_1 + \sigma_{12} \mathbf{e}_1 \mathbf{e}_2 + \sigma_{13} \mathbf{e}_1 \mathbf{e}_3 + \sigma_{21} \mathbf{e}_2 \mathbf{e}_1 + \sigma_{22} \mathbf{e}_2 \mathbf{e}_2 + \sigma_{23} \mathbf{e}_2 \mathbf{e}_3 \\ &\quad + \sigma_{31} \mathbf{e}_3 \mathbf{e}_1 + \sigma_{32} \mathbf{e}_3 \mathbf{e}_2 + \sigma_{33} \mathbf{e}_3 \mathbf{e}_3,\end{aligned} \tag{2.22}$$

where the juxtaposed double vectors are termed *dyads*. The corresponding tractions are evaluated by an operation analogous to the scalar or dot product operation in vector arithmetic:

$$\mathbf{T}_i = \boldsymbol{\sigma} \cdot \mathbf{e}_i = \sigma_{ij}\mathbf{e}_j. \tag{2.23}$$

The dot $(\cdot)$ operation of $\mathbf{e}_i$ on $\boldsymbol{\sigma}$ selects the components with the second vector of the dyad equal to $\mathbf{e}_i$ since $\mathbf{e}_i \cdot \mathbf{e}_j = \delta_{ij}$. Equation (2.23) is identical to Eq. (2.2).

Similarly, the normal and tangential components of the traction $\mathbf{T}_n$ on a plane defined by normal $\mathbf{n}$ are

$$\begin{aligned}\sigma_{nn} &= \boldsymbol{\sigma} \cdot \mathbf{n} \cdot \mathbf{n} \\ &= \mathbf{T}_n \cdot \mathbf{n} \\ &= \sigma_{ij} n_i n_j\end{aligned} \tag{2.24}$$

and

$$\begin{aligned}\sigma_{ns} &= \boldsymbol{\sigma} \cdot \mathbf{n} \cdot \mathbf{s} \\ &= \mathbf{T}_n \cdot \mathbf{s} \\ &= \sigma_{ij} n_i s_j\end{aligned} \tag{2.25}$$

as previously found in Eqs. (2.16) and (2.17), respectively.

2.2.6 Computational Example

The problem statement follows.

(1) The components of stress at a point in Cartesian coordinates are given by $\sigma_{xx} = 500$; $\sigma_{xy} = \sigma_{yx} = 500$; $\sigma_{yy} = 1000$; $\sigma_{yz} = \sigma_{zy} = -750$, $\sigma_{zx} = 800$; $\sigma_{zz} = -300$.

(2) A plane is defined by the unit vector

$$\mathbf{n} = \frac{1}{2}\mathbf{e}_x + \frac{1}{2}\mathbf{e}_y + \frac{1}{\sqrt{2}}\mathbf{e}_z.$$

(3) It is desired to compute the traction and the normal and tangential components on the plane.

(4) Note: At this point in the development, the given state of stress cannot be verified as correct or admissible. The values are chosen in order to illustrate a computational format for the equations developed thus far.

(5) Let $x, y, z = x_1, x_2, x_3$.

The solution in component form is as follows.

(1) Evaluate n_i by using Eq. (2.6),

$$n_i = \mathbf{n} \cdot \mathbf{e}_i,$$

$$n_1 = 1/2; \quad n_2 = 1/2; \quad n_3 = 1/\sqrt{2}.$$

(2) Evaluate T_i by using Eq. (2.11),

$$
\begin{aligned}
T_i &= \sigma_{ji} n_j; \\
T_1 &= \sigma_{11} n_1 + \sigma_{21} n_2 + \sigma_{31} n_3 \\
&= (500)(1/2) + (500)(1/2) + (800)(1/\sqrt{2}) \\
&= 1066; \\
T_2 &= \sigma_{12} n_1 + \sigma_{22} n_2 + \sigma_{32} n_3 \\
&= (500)(1/2) + (1000)(1/2) + (-750)(1/\sqrt{2}) \\
&= 220; \\
T_3 &= \sigma_{13} n_1 + \sigma_{23} n_2 + \sigma_{33} n_3 \\
&= (800)(1/2) + (-750)(1/2) + (-300)(1/\sqrt{2}) \\
&= -187.
\end{aligned}
$$

(3) Evaluate $|\mathbf{T}_n|$ by using Eq. (2.12),

$$
\begin{aligned}
|\mathbf{T}_n| &= (T_i T_i)^{1/2} \\
&= [(1066)^2 + (220)^2 + (-187)^2]^{1/2} \\
&= 1104.
\end{aligned}
$$

(4) Evaluate σ_{nn} and σ_{ns} by using Eq. (2.15),

$$
\begin{aligned}
\sigma_{nn} &= T_i n_i \\
&= (1066)(1/2) + (220)(1/2) + (-187)(1/\sqrt{2}) = 511,
\end{aligned}
$$

or using Eq. (2.16),

$$\sigma_{nn} = \sigma_{ji} n_j n_i,$$

where

j	i	$(+)$	$(-)$
1	1	$(500)(1/2)(1/2)$	
1	2	$(500)(1/2)(1/2)$	
1	3	$(800)(1/2)(1/\sqrt{2})$	
2	1	$(500)(1/2)(1/2)$	
2	2	$(1000)(1/2)(1/2)$	
2	3		$(750)(1/2)(1/\sqrt{2})$
3	1	$(800)(1/2)(1/\sqrt{2})$	
3	2		$(750)(1/\sqrt{2})(1/2)$
3	3		$(300)(1/\sqrt{2})(1/\sqrt{2})$
		1191	680

$$\sigma_{nn} = 1191 - 680 = 511.$$

Using Eq. (2.19),

$$\sigma_{ns} = (T_i T_i - \sigma_{nn}^2)^{1/2};$$

$$\sigma_{ns} = [(1104)^2 - (511)^2]^{1/2} = 979.$$

Finally the Cartesian components are computed from Eq. (2.20) as

$$\sigma_{nn(1)} = \sigma_{nn} n_1 = 511(1/2) = 256$$

$$\sigma_{nn(2)} = \sigma_{nn} n_2 = 511(1/2) = 256$$

$$\sigma_{nn(3)} = \sigma_{nn} n_3 = 511(1/\sqrt{2}) = 361$$

and Eq. (2.21a) as

$$\sigma_{ns(1)} = T_1 - \sigma_{nn(1)} = 1066 - 256 = 810$$

$$\sigma_{ns(2)} = T_2 - \sigma_{nn(2)} = 220 - 256 = -36$$

$$\sigma_{ns(3)} = T_3 - \sigma_{nn(3)} = -187 - 361 = -548.$$

To check,

$$\sigma_{ns} = [(810)^2 + (-36)^2 + (-548)^2]^{1/2} = 979.$$

The solution in dyadic form is as follows.

(1) The stress dyadic $\boldsymbol{\sigma}$ from Eq. (2.22);

$$\begin{aligned}\boldsymbol{\sigma} &= \sigma_{ij}\mathbf{e}_i\mathbf{e}_j \\ &= 500\mathbf{e}_1\mathbf{e}_1 + 500\mathbf{e}_1\mathbf{e}_2 + 800\mathbf{e}_1\mathbf{e}_3 + 500\mathbf{e}_2\mathbf{e}_1 + 1000\mathbf{e}_2\mathbf{e}_2 \\ &\quad - 750\mathbf{e}_2\mathbf{e}_3 + 800\mathbf{e}_3\mathbf{e}_1 - 750\mathbf{e}_3\mathbf{e}_2 - 300\mathbf{e}_3\mathbf{e}_3.\end{aligned}$$

(2) Evaluate $\mathbf{T}_n$ from Eq. (2.23);

$$\begin{aligned}\mathbf{T}_n &= \boldsymbol{\sigma}\cdot\mathbf{n} \\ &= [500(1/2) + 500(1/2) + 800(1/\sqrt{2})]\mathbf{e}_1 \\ &\quad + [500(1/2) + 1000(1/2) - 750(1/\sqrt{2})]\mathbf{e}_2 \\ &\quad + [800(1/2) - 750(1/2) - 300(1/\sqrt{2})]\mathbf{e}_3 \\ &= 1066\mathbf{e}_1 + 220\mathbf{e}_2 - 187\mathbf{e}_3;\end{aligned}$$

$$|\mathbf{T}_n| = [(1066)^2 + (220)^2 + (-187)^2]^{1/2} = 1104.$$

(3) Evaluate σ_{nn} and σ_{ns} from Eq. (2.24);

$$\begin{aligned}\sigma_{nn} &= \mathbf{T}_n\cdot\mathbf{n} \\ &= (1066)(1/2) + 220(1/2) - 187(1/\sqrt{2}) = 511.\end{aligned}$$

From Eq. (2.19),

$$\begin{aligned}\sigma_{ns} &= (T_i T_i - \sigma_{nn}^2)^{1/2} \\ &= [(1104)^2 - (511)^2] = 979.\end{aligned}$$

2.3 Equilibrium

2.3.1 Physical and Mathematical Principles

The state of stress at a point in any direction has been shown to be completely determined by the components of the Cartesian stress tensor σ_{ij}. Naturally, the stresses vary within the body. The equations governing the distribution of stresses are known as the equations of equilibrium and are derived from the application of the fundamental physical principles of linear and angular momentum to the region shown in Fig. 2.5, with surface area A and volume V.

The principle of linear momentum is

$$\int_V \mathbf{f}\,dv + \int_A \mathbf{T}\,dA = \int_V \rho\ddot{\mathbf{u}}\,dV \tag{2.26}$$

in which ρ is the mass density; $\mathbf{u}$ the displacement vector; and the symbol $(\ddot{\ })$ signifies differentiation twice with respect to time.

The principle of angular momentum is

$$\int_V (\mathbf{r}\times\mathbf{f})\,dV + \int_A (\mathbf{r}\times\mathbf{T})\,dA = \int_V (\mathbf{r}\times\rho\ddot{\mathbf{u}})\,dV; \tag{2.27}$$

in which $\mathbf{r}$ is the position vector as shown in Fig. 2.5.

Also useful in the derivation is the divergence theorem stated as Eq. (1.14)

$$\int_V \nabla\cdot\mathbf{G}\,dV = \int_A \mathbf{n}\cdot\mathbf{G}\,dA; \tag{2.28}$$

The preceding equations may be written in component form. The body forces are

$$\mathbf{f} = f_i\mathbf{e}_i \qquad \text{(a)} \quad (2.29)$$

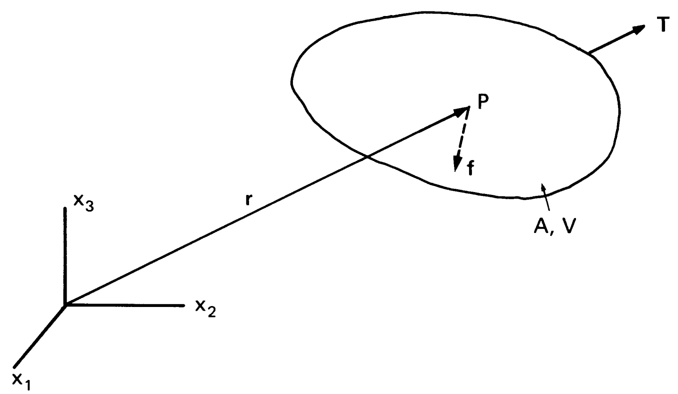

Fig. 2.5. Body in equilibrium in Cartesian space.

and the tractions are

$$\mathbf{T} = T_i \mathbf{e}_i$$
$$= \sigma_{ji} n_j \mathbf{e}_i; \qquad \text{(b)} \quad (2.29)$$

from Eq. (2.11). Considering the position vector $\mathbf{r}$ to point $P(x_i)$

$$\mathbf{r} = x_j \mathbf{e}_j; \qquad \text{(c)}$$
$$\mathbf{r} \times \mathbf{f} = \varepsilon_{ijk} x_j f_k \mathbf{e}_i; \qquad \text{(d)}$$
$$\mathbf{r} \times \mathbf{T} = \varepsilon_{ijk} x_j T_k \mathbf{e}_i \qquad (2.29)$$
$$= \varepsilon_{ijk} x_j \sigma_{lk} n_l \mathbf{e}_i. \qquad \text{(e)}$$

For static problems, the r.h.s. of Eqs. (2.26) and (2.27) are zero. Substituting Eqs. (2.29) into Eqs. (2.26), (2.27) and (2.28), we have the static equations of linear and angular momentum and the divergence theorem in component form as, respectively,

$$\int_V f_i \, dV + \int_A \sigma_{ji} n_j \, dA = 0; \qquad (2.30)$$

$$\int_V \varepsilon_{ijk} x_j f_k \, dV + \int_A \varepsilon_{ijk} x_j \sigma_{lk} n_l \, dA = 0; \qquad (2.31)$$

$$\int_V G_{i,i} \, dV = \int_A n_i G_i \, dA. \qquad (2.32)$$

2.3.2 Linear Momentum

We assume that the stresses σ_{ij} are C^1 continuous and apply Eq. (2.32) to Eq. (2.30), giving

$$\int_V (f_i + \sigma_{ji,j}) \, dV = 0. \qquad (2.33)$$

With every element of V in equilibrium, the region of integration is arbitrary and Eq. (2.33) is satisfied if the integrand vanishes. Therefore,

$$\sigma_{ji,j} + f_i = 0 \qquad (2.34)$$

represents three equations of equilibrium in terms of the nine unknown components of stress σ_{ij}.

2.3.3 Angular Momentum

Taking $\varepsilon_{ijk} x_j \sigma_{lk}$ for G_i and n_l for n_i, Eq. (2.32) is applied to Eq. (2.31) and gives

$$\int_V [\varepsilon_{ijk} x_j f_k + (\varepsilon_{ijk} x_j \sigma_{lk})_{,l}] \, dV = 0. \qquad (2.35)$$

The second term of the integrand is expanded by product differentiation as

$$(\varepsilon_{ijk}x_j\sigma_{lk})_{,l} = \varepsilon_{ijk}\sigma_{lk}x_{j,l} + \varepsilon_{ijk}x_j\sigma_{lk,l}. \tag{2.36}$$

Further, it is recognized that x_j, the component of $\mathbf{r}$ in the x_j direction, changes only in that direction; that is,

$$x_{j,l} = \delta_{jl}. \tag{2.37}$$

Thus Eq. (2.35) becomes

$$\int_V \varepsilon_{ijk}(x_j f_k + \delta_{jl}\sigma_{lk} + x_j\sigma_{lk,l})\,dV = 0. \tag{2.38}$$

The first and third terms of the integrand combine into

$$\varepsilon_{ijk}x_j(f_k + \sigma_{lk,l}) = 0 \tag{2.39}$$

from Eq. (2.34), and the remaining term becomes

$$\varepsilon_{ijk}\delta_{jl}\sigma_{lk} = \varepsilon_{ijk}\sigma_{jk} \tag{2.40}$$

so that the equation reduces to

$$\int_V \varepsilon_{ijk}\sigma_{jk}\,dV = 0, \tag{2.41}$$

which is satisfied if

$$\varepsilon_{ijk}\sigma_{jk} = 0. \tag{2.42}$$

Equation (2.42) may be evaluated for $i = 1, 2, 3$. For $i = 1$, $\sigma_{23} - \sigma_{32} = 0$; for $i = 2$, $\sigma_{31} - \sigma_{13} = 0$; for $i = 3$, $\sigma_{12} - \sigma_{21} = 0$ or, in general,

$$\sigma_{ij} = \sigma_{ji} \tag{2.43}$$

which is a statement of the *symmetry* of the stress tensor and which furthermore implies that σ_{ij} has but six independent components, instead of nine components. Equation (2.43) is very important in the entire field of solid mechanics.

We may now rewrite Eq. (2.11) as

$$T_i = \sigma_{ij}n_j \tag{2.44}$$

and Eq. (2.34) as

$$\sigma_{ij,j} + f_i = 0, \tag{2.45}$$

which is now a set of three equations in six unknowns. Since they are used repeatedly, it is useful to write the latter equations in explicit form:

$$\begin{aligned}
&\sigma_{11,1} + \sigma_{12,2} + \sigma_{13,3} + f_1 = 0 && \text{(a)}\\
&\sigma_{21,1} + \sigma_{22,2} + \sigma_{23,3} + f_2 = 0 && \text{(b)} \quad (2.46)\\
&\sigma_{31,1} + \sigma_{32,2} + \sigma_{33,3} + f_3 = 0, && \text{(c)}
\end{aligned}$$

which represents a system which is still statically indeterminate.

2.3.4 Computational Example

Although it is not possible to solve the equilibrium equations alone since there are more unknowns than equations, it is possible to test a given set of stresses against the equilibrium equations, Eqs. (2.46).

We take the components of stress for an elastic body to be given by

$$\sigma_{11} = x^2 + y + 3z^2; \quad \sigma_{22} = 2x + y^2 + 2z; \quad \sigma_{33} = -2x + y + z^2$$

$$\sigma_{12} = \sigma_{21} = -xy + z^3; \quad \sigma_{13} = \sigma_{31} = y^2 - xz; \quad \sigma_{23} = \sigma_{32} = x^2 - yz$$

$$f_1 = f_2 = f_3 = 0$$

and show that this state of stress satisfies equilibrium when the values are substituted into Eqs. (2.46a, b, c), respectively:

$$2x - x - x = 0$$

$$-y + 2y - y = 0$$

$$-z - z + 2z = 0.$$

2.4 Principal Stress

2.4.1 Definition and Derivation

We consider Fig. 2.6(a), a normal section through the body. The traction $\mathbf{T}_n$ acts on the plane defined by $\mathbf{n}$ that appears edgewise in the figure. $\mathbf{T}_n$ is not

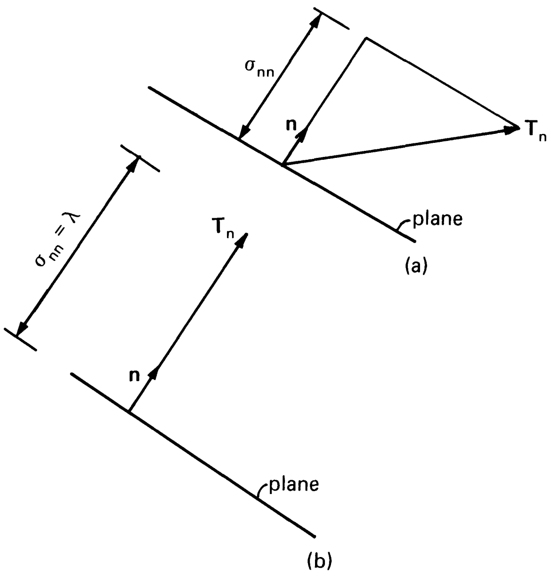

Fig. 2.6. (a) Normal section; (b) principal plane.

necessarily shown true in this view but the normal component σ_{nn} is in the plane of the figure.

Using the dyadic form,

$$\sigma_{nn} = \mathbf{T}_n \cdot \mathbf{n} = \boldsymbol{\sigma} \cdot \mathbf{n} \cdot \mathbf{n}. \tag{2.47}$$

We seek the orientation of a plane (given by the direction of $\mathbf{n}$) such that σ_{nn} is an extremum (maximum or minimum). Such a plane (or planes) are called *principal.*

From differential calculus, the extremum is achieved when $d\sigma_{nn}/dn = 0$. From Eq. (2.47), treating the sought-after direction n as a variable,

$$\frac{d\sigma_{nn}}{dn} = \mathbf{n} \cdot \frac{d(\boldsymbol{\sigma} \cdot \mathbf{n})}{dn} + (\boldsymbol{\sigma} \cdot \mathbf{n}) \cdot \frac{d\mathbf{n}}{dn}. \tag{2.48}$$

Since $\boldsymbol{\sigma}$ is not a function of $\mathbf{n}$, Eq. (2.48) becomes

$$\begin{aligned} \frac{d\sigma_{nn}}{dn} &= 2(\boldsymbol{\sigma} \cdot \mathbf{n}) \cdot \frac{d\mathbf{n}}{dn} \\ &= 2\mathbf{T}_n \cdot \frac{d\mathbf{n}}{dn} \\ &= 0. \end{aligned} \tag{2.49}$$

If $\mathbf{T}_n \cdot (d\mathbf{n}/dn) = 0$, $\mathbf{T}_n$ is normal to $d\mathbf{n}/dn$. Furthermore, $d\mathbf{n}/dn$ is itself normal to $\mathbf{n}$. Therefore, $\mathbf{T}_n$ must be *parallel* to n for Eq. (2.49) to hold. The condition corresponding to the extremum is shown in Fig. 2.6(b). Obviously, the tangential component $\sigma_{ns} = 0$, and the normal component for this case is designated as

$$\sigma_{nn} = |\mathbf{T}_n| = \lambda. \tag{2.50}$$

We may express the preceding by

$$\mathbf{T}_n = \lambda \mathbf{n} \tag{2.51}$$

or, in component form, by dotting each side with $\mathbf{e}_i$, as

$$T_i = \lambda n_i. \tag{2.52}$$

Also, from Eq. (2.11), we have

$$T_i = \sigma_{ji} n_j. \tag{2.53}$$

Equating Eqs. (2.52) and (2.53) and employing the index changing property of the Kronecker-delta,

$$\lambda n_i = \lambda n_j \delta_{ij} = \sigma_{ji} n_j \tag{2.54}$$

or

$$(\sigma_{ji} - \lambda \delta_{ij}) n_j = 0. \tag{2.55}$$

Equation (2.55) is a set of three homogeneous algebraic equations in four unknowns, n_j with $j = 1, 2, 3$, and λ. The components n_j determine the orientation of the *principal plane* and λ is called the *principal stress.* This is known as a linear eigenvalue problem and, using Cramer's rule, it may be shown that a nontrivial solution may be found if the determinant of the coefficients of n_j vanish, that is,

$$|\sigma_{ji} - \lambda\delta_{ij}| = 0 \qquad \text{(a)} \quad (2.56)$$

or, in expanded form,

$$\begin{vmatrix} \sigma_{11} - \lambda & \sigma_{12} & \sigma_{13} \\ \sigma_{21} & \sigma_{22} - \lambda & \sigma_{23} \\ \sigma_{31} & \sigma_{32} & \sigma_{33} - \lambda \end{vmatrix} = 0. \qquad \text{(b)} \quad (2.56)$$

Equation (2.56b) provides a cubic equation for λ, indicating that three principal stresses, $\lambda_1 = \sigma^{(1)}$, $\lambda_2 = \sigma^{(2)}$, $\lambda_3 = \sigma^{(3)}$, exist. Corresponding to each principal stress is a distinct orientation, evaluated by substituting, in turn, a known value of $\sigma^{(k)}$, that is, $\sigma^{(1)}$, $\sigma^{(2)}$, $\sigma^{(3)}$, into Eq. (2.55) and solving for the corresponding components of $n_j^{(k)}$, that is, $n_j^{(1)}$, $n_j^{(2)}$ and $n_j^{(3)}$. Since Eq. (2.55) originally represented three equations in four unknowns, it is a linearly dependent set that must be supplemented by an additional relationship

$$n_j^{(k)} n_j^{(k)} = 1 \qquad (2.57)$$

expressing the "length" of the unit normal with $k = 1, 2, 3$ in turn.

Since the principal stresses at a point represent the greatest magnitudes of tension and compression that can exist under a particular loading case, they are of great importance in engineering design.

2.4.2 Computational Format, Stress Invariants and Principal Coordinates

It is often expedient to substitute the numerical values of the stresses, which have been calculated with respect to a selected Cartesian coordinate system, into Eq. (2.56) and to expand, simplify and solve the determinant as an algebraic equation.

It may be shown [2.2] that a general expansion of Eq. (2.56) is

$$\lambda^3 - Q_1\lambda^2 + Q_2\lambda - Q_3 = 0, \qquad (2.58)$$

in which

$$\begin{aligned} Q_1 &= \sigma_{11} + \sigma_{22} + \sigma_{33} \\ &= \sigma_{ii} \quad \text{is the sum of the main diagonal of } [\sigma_{ij}], \qquad \text{(a)} \end{aligned}$$

$$\begin{aligned} Q_2 &= \begin{vmatrix} \sigma_{11} & \sigma_{21} \\ \sigma_{12} & \sigma_{22} \end{vmatrix} + \begin{vmatrix} \sigma_{11} & \sigma_{31} \\ \sigma_{13} & \sigma_{33} \end{vmatrix} + \begin{vmatrix} \sigma_{22} & \sigma_{32} \\ \sigma_{23} & \sigma_{33} \end{vmatrix} \\ &= \tfrac{1}{2}\varepsilon_{mik}\varepsilon_{mjl}\sigma_{ij}\sigma_{kl} \quad \text{is the sum of the minors of the main diagonal of } [\sigma_{ij}], \qquad \text{(b)} \quad (2.59) \end{aligned}$$

$$Q_3 = \begin{vmatrix} \sigma_{11} & \sigma_{12} & \sigma_{13} \\ \sigma_{21} & \sigma_{22} & \sigma_{23} \\ \sigma_{31} & \sigma_{32} & \sigma_{33} \end{vmatrix}$$

$$= \tfrac{1}{6}\varepsilon_{mik}\varepsilon_{nil}\sigma_{ij}\sigma_{kl}\sigma_{mn} \quad \text{is the determinant of } [\sigma_{ij}]. \qquad \text{(c)}$$

It is instructive to examine the coefficients of Eq. (2.59) in terms of scalar quantities that can be constructed out of the tensor σ_{ij}, that is,

$$\begin{aligned} P_1 &= \sigma_{ii}; \\ P_2 &= \sigma_{ij}\sigma_{ij}; \\ P_3 &= \sigma_{ij}\sigma_{jk}\sigma_{ki}. \end{aligned} \tag{2.60}$$

Such scalar quantities (no free indices) constructed from a tensor are obviously independent of any particular coordinate system and are therefore known as *invariants*. For a principal coordinate system that coincides with the directions of the principal stresses and is, subsequently, shown to be orthogonal, all the σ_{ij}, with $i \neq j$, terms vanish so that P_1, P_2 and P_3 may be written in terms of the principal stresses as

$$\begin{aligned} P_1 &= \sigma^{(1)} + \sigma^{(2)} + \sigma^{(3)}; \\ P_2 &= \sigma^{(1)^2} + \sigma^{(2)^2} + \sigma^{(3)^2}; \\ P_3 &= \sigma^{(1)^3} + \sigma^{(2)^3} + \sigma^{(3)^3}. \end{aligned} \tag{2.61}$$

Finally, it may be shown that [2.2]

$$\begin{aligned} Q_1 &= P_1; \\ Q_2 &= \tfrac{1}{2}(P_1^2 - P_2); \\ Q_3 &= (P_1^3 - 3P_1P_2 + 2P_3); \end{aligned} \tag{2.62}$$

so that Q_1, Q_2 and Q_3 are likewise *invariant*. Invariants are quite important in many applications of the theory of elasticity. For example, see Herrmann et al. [2.5]. In the literature, they are commonly denoted as

$$\begin{aligned} J_1 &= P_1 = \sigma_{ii} \\ J_2 &= \tfrac{1}{2}P_2 = \tfrac{1}{2}\sigma_{ij}\sigma_{ij} \\ J_3 &= \tfrac{1}{3}P_3 = \tfrac{1}{3}\sigma_{ij}\sigma_{jk}\sigma_{ki} \end{aligned} \tag{2.63}$$

We next take up the problem of evaluating the components of the normals to the principal planes $n_j^{(k)}$. This is carried out by back-substitutions of each computed $\sigma^{(k)}$ into two permutations of Eqs. (2.55), along with the use of Eq. (2.57). Care should be taken to insure that the two equations extracted from Eqs. (2.55) are linearly independent. As an illustration, we take $i = 1, 2$ in Eq. (2.55) giving

$$i = 1: \quad [\sigma_{11} - \sigma^{(k)}]n_1^{(k)} + \sigma_{21}n_2^{(k)} = -\sigma_{31}n_3^{(k)}; \qquad \text{(a)}$$
$$i = 2: \quad \sigma_{12}n_1^{(k)} + [\sigma_{22} - \sigma^{(k)}]n_2^{(k)} = -\sigma_{32}n_3^{(k)} \qquad \text{(b)} \quad (2.64)$$
$$n_1^{(k)2} + n_2^{(k)2} + n_3^{(k)2} = 1. \qquad \text{(c)}$$

Considering (a) and (b), we solve for $n_1^{(k)}$ and $n_2^{(k)}$ in terms of $n_3^{(k)}$ using Cramer's rule

$$n_1^{(k)} = n_3^{(k)}\frac{D_1}{D}; \qquad \text{(a)}$$
$$n_2^{(k)} = n_3^{(k)}\frac{D_2}{D}, \qquad \text{(b)} \quad (2.65)$$

where

$$D_1 = \begin{vmatrix} -\sigma_{31} & \sigma_{21} \\ -\sigma_{32} & \sigma_{22} - \sigma^{(k)} \end{vmatrix}, \qquad \text{(a)}$$
$$D_2 = \begin{vmatrix} \sigma_{11} - \sigma^{(k)} & -\sigma_{31} \\ \sigma_{12} & -\sigma_{32} \end{vmatrix}, \qquad \text{(b)} \quad (2.66)$$
$$D = \begin{vmatrix} \sigma_{11} - \sigma^{(k)} & \sigma_{21} \\ \sigma_{12} & \sigma_{22} - \sigma^{(k)} \end{vmatrix}. \qquad \text{(c)}$$

Then, substituting into Eq. (2.64c) gives

$$n_3^{(k)2}\left[\left(\frac{D_1}{D}\right)^2 + \left(\frac{D_2}{D}\right)^2 + 1\right] = 1. \qquad (2.67)$$

With $\sigma^{(k)}$ real, $n_3^{(k)}$ will be real, and $n_1^{(k)}$ and $n_2^{(k)}$ are found from Eq. (2.65). Finally,

$$\mathbf{n}^{(k)} = n_1^{(k)}\mathbf{e}_1 + n_2^{(k)}\mathbf{e}_2 + n_3^{(k)}\mathbf{e}_3. \qquad (2.68)$$

The procedure is carried out for each $\sigma^{(k)}$, $k = 1, 2, 3$, in turn.

It now remains to show that the calculated $\mathbf{n}^{(k)}$ corresponding to the principal directions are orthogonal. We consider $k = 1$ and $k = 2$ and form

$$\sigma_{ij}n_j^{(1)} = \sigma^{(1)}n_i^{(1)}, \qquad \text{(a)}$$
$$\sigma_{ij}n_j^{(2)} = \sigma^{(2)}n_i^{(2)}. \qquad \text{(b)} \quad (2.69)$$

We multiply Eq. (2.69a) by $n_i^{(2)}$ and Eq. (2.69b) by $n_i^{(1)}$ giving

$$\sigma_{ij}n_j^{(1)}n_i^{(2)} = \sigma^{(1)}n_i^{(1)}n_i^{(2)}, \qquad \text{(a)}$$
$$\sigma_{ij}n_j^{(2)}n_i^{(1)} = \sigma^{(2)}n_i^{(2)}n_i^{(1)}. \qquad \text{(b)} \quad (2.70)$$

Since i and j are repeated indices, the l.h.s. of Eqs. (2.70) are equal; hence, equating the r.h.s.,

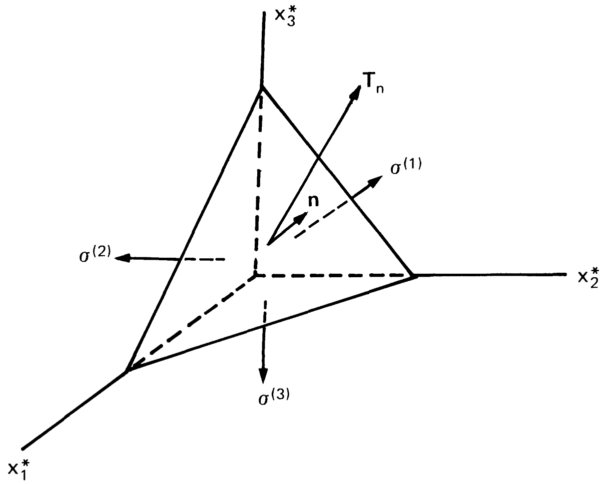

Fig. 2.7. Principal coordinates and stresses (after Tauchert, *Energy Principles in Structural Mechanics*, McGraw–Hill, 1974). Reproduced with permission.

$$(\sigma^{(1)} - \sigma^{(2)})n_i^{(1)}n_i^{(2)} = 0 \tag{2.71}$$

and, if $\sigma^{(1)}$ and $\sigma^{(2)}$ are different, $n_i^{(1)}$ and $n_i^{(2)}$ must be orthogonal.

Once the principal stresses are evaluated and the principal planes are located, it is generally convenient to refer further computations to the *principal coordinates* that have now been shown to be orthogonal. Referring to Fig. 2.7 and designating the principal coordinates by x_i^*, it is obvious that the state of stress is relatively simple with only direct stresses and no shearing stresses acting. The components of the traction $\mathbf{T}_n$ on any other plane are found from Eq. (2.11) as

$$\begin{aligned} T_1^* &= \sigma^{(1)}n_1^* && \text{(a)} \\ T_2^* &= \sigma^{(2)}n_2^* && \text{(b)} \quad (2.72) \\ T_3^* &= \sigma^{(3)}n_3^*, && \text{(c)} \end{aligned}$$

where

$$n_i^* = \mathbf{n}\cdot\mathbf{e}_i^*. \qquad \text{(d)}$$

Other illustrations using principal coordinate solutions are given in Section 2.5.

2.4.3 Computational Example

As a continuation of the analysis in Section 2.2.6, we now seek the principal stresses and directions for the state of stress previously enumerated. Eq.

(2.56b) becomes

$$\begin{vmatrix} 500-\lambda & 500 & 800 \\ 500 & 1000-\lambda & -750 \\ 800 & -750 & -300-\lambda \end{vmatrix} = 0. \tag{2.73}$$

It is convenient to work with the stress × 10^{-3}. Expanding the determinant directly gives

$$\bar{\lambda}^3 - 1.2\bar{\lambda}^2 - 1.4025\bar{\lambda} + 1.59625 = 0, \tag{2.74}$$

where $\bar{\lambda} = \lambda \times 10^{-3}$.

We may also compute the coefficients by using the invariants as described in Eqs. (2.60) and (2.62) and compare the values to those in Eq. (2.74).

$$P_1 = \sigma_{ii} = 0.500 + 1.000 - 0.300 = 1.2$$

$$-Q_1 = -P_1 = 1.2 \quad \surd$$

$$\begin{aligned} P_2 &= \sigma_{ij}\sigma_{ij} \\ &= (0.500)^2 + 2(0.500)^2 + 2(0.800)^2 + (1.00)^2 + 2(-0.750)^2 + (0.300)^2 \\ &= 4.245 \end{aligned}$$

$$Q_2 = \tfrac{1}{2}[(1.2)^2 - 4.245] = -1.4025 \quad \surd$$

or, using the sum of the minors of the main diagonal of σ_{ij},

$$\begin{aligned} Q_2 &= [(1.00)(-0.300) - (-0.750)(-0.750)] \\ &\quad + [(0.500)(-0.300) - (0.800)(0.800)] \\ &\quad + [(0.500)(1.000) - (0.500)(0.500)] \\ &= -1.4025 \quad \surd \end{aligned}$$

$$\begin{aligned} Q_3 &= \det[\sigma_{ij}] \\ &= (0.500)(1.00)(-0.300) + 2(0.800)(0.500)(-0.750) \\ &\quad - (0.800)(0.800)(1.000) - (-0.750)(-0.750)(0.500) \\ &\quad - (0.500)(0.500)(-0.300) \\ &= -1.59625 \\ -Q_3 &= +1.59625 \quad \surd. \end{aligned}$$

Solving a cubic equation may be tedious, but straightforward procedures are found in standard mathematics texts. The solution to Eq. (2.74) may be verified as

$$\bar{\lambda}_1 = -1.168; \quad \bar{\lambda}_2 = 1.380; \quad \bar{\lambda}_3 = 0.988$$

so that the principal stresses are

$$\begin{aligned} \sigma^{(1)} &= -1168 \\ \sigma^{(2)} &= 1380 \\ \sigma^{(3)} &= 988 \end{aligned} \tag{2.75}$$

From Eqs. (2.64)–(2.67), the corresponding unit vectors are

$$\begin{aligned} \mathbf{n}^{(1)} &= -0.4903\mathbf{e}_1 + 0.3838\mathbf{e}_2 + 0.7825\mathbf{e}_3 && \text{(a)} \\ \mathbf{n}^{(2)} &= -0.2514\mathbf{e}_1 - 0.9207\mathbf{e}_2 + 0.2988\mathbf{e}_3 && \text{(b)} \\ \mathbf{n}^{(3)} &= 0.8298\mathbf{e}_1 - 0.0749\mathbf{e}_2 + 0.5530\mathbf{e}_3 && \text{(c)} \end{aligned} \tag{2.76}$$

or, in general, $\mathbf{n}^{(j)} = n_{ji}\mathbf{e}_i$. (d)

The unit normals $\mathbf{n}^{(j)}$ now become the basis vectors $\mathbf{e}_j^*$ for the principal coordinate system x_j^*; and the components n_{ji} are the direction cosines for the transformation between the x_j^* and x_i axes.

2.5 Stresses in Principal Coordinates

2.5.1 Stresses on an Oblique Plane

It was noted in Section 2.4.2 that the principal coordinates, once established, provide a convenient basis for further analysis. We first consider a plane oblique to the x_i^* axis as shown in Fig. 2.7, with direction cosines n_i^*. From Eq. (2.16), with $\sigma_{(ii)} = \sigma^{(i)}$ and $\sigma_{ij}(i \neq j) = 0$, we may write the normal component of the traction as

$$\begin{aligned} \sigma_{nn} &= \sigma^{(i)} n_i^* n_i^* \\ &= \sigma^{(1)}(n_1^*)^2 + \sigma^{(2)}(n_2^*)^2 + \sigma^{(3)}(n_3^*)^2. \end{aligned} \tag{2.77}$$

The shearing component is found from Eq. (2.19) by taking

$$\begin{aligned} T_i T_i &= \sigma^{(i)} n_i^* \sigma^{(i)} n_i^* \\ &= (\sigma^{(1)})^2(n_1^*)^2 + (\sigma^{(2)})^2(n_2^*)^2 + (\sigma^{(3)})^2(n_3^*)^2 \end{aligned} \tag{2.78}$$

along with σ_{nn} from Eq. (2.77).

Expanding, we have

$$\begin{aligned} \sigma_{ns} &= \{\sigma^{(i)} n_i^* \sigma^{(i)} n_i^* - [\sigma^{(i)} n_i^* n_i^*]^2\}^{1/2} \\ &= \{(\sigma^{(1)})^2(n_1^*)^2 + (\sigma^{(2)})^2(n_2^*)^2 + (\sigma^{(3)})^2(n_3^*)^2 - (\sigma^{(1)})^2(n_1^*)^4 \\ &\quad - (\sigma^{(2)})^2(n_2^*)^4 - (\sigma^{(3)})^2(n_3^*)^4 \\ &\quad - 2\sigma^{(1)}\sigma^{(2)}(n_1^*)^2(n_2^*)^2 - 2\sigma^{(1)}\sigma^{(3)}(n_1^*)^2(n_3^*)^2 \\ &\quad - 2\sigma^{(2)}\sigma^{(3)}(n_2^*)^2(n_3^*)^2\}^{1/2}, \end{aligned} \tag{2.79}$$

which may be simplified if Eq. (1.32), the normality of the direction cosines

$$(n_i^* n_i^*)^2 = 1, \tag{2.80}$$

is introduced into Eq. (2.79). Replacing $(n_1^*)^4$ with $(n_1^*)^2[1 - (n_2^*)^2 - (n_3^*)^2]$, etc., this allows the relatively compact form [2.7]

$$\sigma_{ns} = \{[\sigma^{(1)} - \sigma^{(2)}]^2 (n_1^*)^2 (n_2^*)^2 + [\sigma^{(2)} - \sigma^{(3)}]^2 (n_2^*)^2 (n_3^*)^2 + [\sigma^{(3)} - \sigma^{(1)}]^2 (n_3^*)^2 (n_1^*)^2\}^{1/2} \tag{2.81}$$

to be derived. Equation (2.81) reveals that if all of the principal stresses are equal, the shearing stress is zero on any plane.

2.5.2 Stresses on Octahedral Planes

Of particular interest in the theory of material failure is the state of stress on the octahedral planes, which are defined as planes having equal direction cosines with each of the principal planes. There are obviously eight such planes, one in each octant of the coordinate system. The octahedral plane in the $+x_1^*$, $+x_2^*$, $+x_3^*$ octant may be represented by the triangular surface in Fig. 2.7 where the normal to the surface

$$\mathbf{n}^* = 1/\sqrt{3}(\mathbf{n}^{(1)} + \mathbf{n}^{(2)} + \mathbf{n}^{(3)}) \tag{2.82}$$

and the respective direction cosines are

$$n_1^* = n_2^* = n_3^* = 1/\sqrt{3}. \tag{2.83}$$

Substituting Eq. (2.83) into Eqs. (2.77) and (2.81) gives the octahedral normal stress

$$\begin{aligned} \sigma_{nn}^{\text{oct}} &= \tfrac{1}{3}[\sigma^{(1)} + \sigma^{(2)} + \sigma^{(3)}] \\ &= \tfrac{1}{3}\sigma_{ii}, \end{aligned} \tag{2.84a}$$

which is simply the *average* of the principal stresses, and the octahedral shearing stress

$$\sigma_{ns}^{\text{oct}} = \tfrac{1}{3}\{[\sigma^{(1)} - \sigma^{(2)}]^2 + [\sigma^{(2)} - \sigma^{(3)}]^2 + [\sigma^{(3)} - \sigma^{(1)}]^2\}^{1/2}. \tag{2.84b}$$

2.5.3 Absolute Maximum Shearing Stress

The absolute maximum shearing stress at a point may also be of interest in regard to the capacity of the material.

We first observe that both terms of Eq. (2.79) are positive. Therefore, for σ_{ns} to be a maximum, the second term should be a minimum. This is true if the orientation of σ_{ns} is such that

$$\frac{\partial}{\partial n_i^*}[\sigma^{(i)} n_i^* n_i^*]^2 = 0$$

or (2.85)

$$4[\sigma^{(i)^2} n_i^* n_i^*] n_k^* = 0,$$

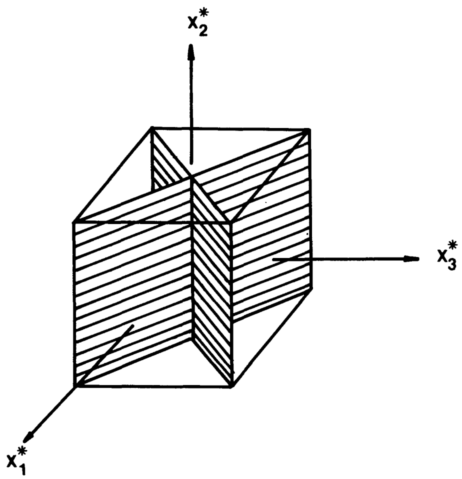

Fig. 2.8. Planes with maximum shearing stresses (after Ugural and Fenster, *Advanced Strength and Applied Elasticity*, Elsevier, 1975). Reproduced with permission.

where the last subscript is changed to k to avoid a triple repeated index. Equation (2.85) is satisfied only if $n_k^* = 0$, indicating that the planes for which σ_{ns} is maximum will be *parallel* to one of the principal axes.

Now, examining Eq. (2.81), two of the three terms will vanish due to $n_k^* = 0$. The nonzero term which makes σ_{ns} the largest is the one which contains the bracketed term with the largest principal stress *difference*. Since this is the only term not containing n_k^*, the maximum shearing stress acts on plane(s) parallel to n_k^*. For example, if $\sigma^{(1)}$ and $\sigma^{(3)}$ are the maximum and minimum principal stresses, then $n_2^* = 0$. In general, with i and j indicating the directions of the maximum and minimum principal stresses,

$$(\sigma_{ns}^{\max})^2 = [\sigma^{(i)} - \sigma^{(j)}]^2 (n_i^*)^2 (n_j^*)^2. \tag{2.86}$$

Since $(n_j^*)^2 = 1 - (n_i^*)^2$, the maximum value of the r.h.s. of Eq. (2.86) occurs when $(n_i^*)^2 = \frac{1}{2} = (n_j^*)^2$ and the absolute maximum shearing stress is

$$\sigma_{ns}^{\max} = \tfrac{1}{2}[\sigma^{(i)} - \sigma^{(j)}] \tag{2.87}$$

acting on the planes *bisecting* the planes of maximum and minimum principal stress. For example, if $i = 1$ and $j = 3$,

$$\sigma_{ns}^{\max} = \tfrac{1}{2}[\sigma^{(1)} - \sigma^{(3)}], \tag{2.88}$$

and the corresponding planes are shown in Fig. 2.8.

2.5.4 Computational Example

Using the principal stresses found in Section 2.4.3, we may evaluate the stresses on the octahedral planes from Eq. (2.84) as

$$\sigma_{nn}^{oct} = \tfrac{1}{3}(-1168 + 1380 + 988) = 400$$

$$\sigma_{ns}^{oct} = \tfrac{1}{3}\{[-1168 - 1380]^2 + [1380 - 988]^2 + [988 - (-1168)]^2\}^{1/2}$$
$$= 1120.$$

The maximum shearing stress is found from Eq. (2.87), with $i = 2$ and $j = 1$,

$$\sigma_{ns}^{max} = \tfrac{1}{2}[1380 - (-1168)] = 1274,$$

and acts on planes bisecting the x_1^* and x_2^* axis and parallel to x_3^*.

2.6 Properties and Special States of Stress

2.6.1 Projection Theorem

We focus on any point, say P, of the continuum shown in Fig. 2.5. It has been established that any number of tractions may be calculated at P, each associated with a single plane passing through P and identified by the corresponding unit normal. The projection theorem is a relationship between any two tractions at P, say $\mathbf{T}^{(a)}$ and $\mathbf{T}^{(b)}$, and their associated normals, say $\mathbf{n}^{(a)}$ and $\mathbf{n}^{(b)}$, and is stated to be

$$\mathbf{T}^{(a)} \cdot \mathbf{n}^{(b)} = \mathbf{T}^{(b)} \cdot \mathbf{n}^{(a)}, \tag{2.89}$$

or, in component form, as

$$T_i^{(a)} n_i^{(b)} = T_i^{(b)} n_i^{(a)} \tag{2.90}$$

meaning that the projection of the traction acting on the first plane onto the second plane is equal to the projection of the traction acting on the second plane onto the first plane.

The proof is easily demonstrated by substituting Eq. (2.11) into both sides of Eq. (2.90) to obtain

$$\begin{aligned} \sigma_{ji} n_j^{(a)} n_i^{(b)} &= \sigma_{ji} n_j^{(b)} n_i^{(a)} \\ &= \sigma_{ij} n_j^{(a)} n_i^{(b)} \end{aligned} \tag{2.91}$$

since the i and j became dummy indices. As $\sigma_{ij} = \sigma_{ji}$, the expressions are identical. The projection theorem may be used to define several of special states of stress.

2.6.2 Plane Stress

Suppose that on one plane passing through P, there are no stresses, that is, $\mathbf{T} = 0$. The projection theorem states that the traction on any other plane passing through P must be perpendicular to the normal to the stress-free plane; hence, it is parallel to that plane. Conversely, if it is established that the traction on any plane is parallel to another plane, then the latter plane will also be stress-free. This is known as a state of *plane stress* and is of practical use since it allows the elasticity problem to be reduced from three to two dimensions, which greatly facilitates the mathematical solution. It is obvious that if one of the principal stresses is zero, the state of stress is plane.

2.6.3 Linear Stress

If there are two nonparallel planes on which $\mathbf{T} = 0$, the traction on any other plane must be parallel to both of these planes and also to their line of intersection. This is a state of *linear stress* and is essentially a one-dimensional problem. For this state, two principal stresses vanish.

2.6.4 Pure Shear

If, for any coordinate system

$$\sigma_{11}^* = \sigma_{22}^* = \sigma_{33}^* = 0,$$

then the state of stress is called *pure shear* since only shear stresses σ_{ij}, with $i \neq j$, exist. Also, for pure shear, $\sigma_{ii} = 0$ for any coordinate system.

2.6.5 Hydrostatic Stress

If the principal stresses $\sigma^{(i)}$ are all equal, then the stress state is hydrostatic and the shearing stresses are zero; examine Eq. (2.81).

Exercises

2.1 Find the components of the traction on a plane defined by $n_1 = 1/\sqrt{2}$, $n_2 = 1/\sqrt{2}$, $n_3 = 0$ for the following states of stress:

(a) $\sigma_{11} = \sigma, \quad \sigma_{12} = 0, \quad \sigma_{13} = 0,$

$\sigma_{22} = \sigma, \quad \sigma_{23} = 0, \quad \sigma_{33} = \sigma,$

(b) $\sigma_{11} = \sigma, \quad \sigma_{12} = \sigma, \quad \sigma_{13} = 0,$

$\sigma_{22} = \sigma, \quad \sigma_{23} = 0, \quad \sigma_{33} = 0.$

2.2 The state of stress at a point P in a structure is given by

$$\sigma_{11} = 20{,}000, \quad \sigma_{22} = -15{,}000, \quad \sigma_{33} = 3000$$
$$\sigma_{12} = 2000, \quad \sigma_{23} = 2000, \quad \sigma_{31} = 1000.$$

(a) Compute the scalar components T_1, T_2, and T_3 of the traction $\mathbf{T}$ on the plane passing through P whose outward normal vector $\mathbf{n}$ makes equal angles with the coordinate axes x_1, x_2, and x_3 (from [2.1]).
(b) Compute the normal and tangential components of stress on this plane.
(c) Write the stress dyadic for the state of stress and repeat parts (a) and (b).

2.3 The state of stress at a point is given by the components of stress tensor σ_{ij}. A plane is defined by the direction cosines of the normal $(1/2, 1/2, 1/\sqrt{2})$. State the general conditions for which the traction on the plane has the same direction as the x_2 axis and a magnitude of 1.0.

2.4 Determine the body forces for which the following stress field describes a state of equilibrium (from [2.6]):

$$\sigma_{xx} = -2x^2 - 3y^2 - 5z, \quad \sigma_{xy} = z + 4xy - 6,$$
$$\sigma_{yy} = -2y^2 + 7, \quad \sigma_{xz} = -3x + 2y + 1,$$
$$\sigma_{zz} = 4x + y + 3z - 5 \quad \sigma_{yz} = 0.$$

2.5 Determine whether the following stress field is admissible in an elastic body when body forces are negligible.

$$\boldsymbol{\sigma} = \begin{bmatrix} yz + 4 & z^2 + 2x & 5y + z \\ \cdot & xz + 3y & 8x^3 \\ \cdot & \cdot & 2xyz \end{bmatrix}.$$

2.6 At a given point in a body

$$\sigma_{11} = \sigma_{22} = \sigma_{33} = -p,$$
$$\sigma_{12} = \sigma_{23} = \sigma_{31} = 0.$$

Show that the normal stresses there are equal to $-p$ and that the shearing stresses vanish for any other Cartesian coordinate system (from [2.1]).

2.7 Expand the stress transformation law from the tensor form Eq. (2.13) for a two-dimensional state of stress by assuming that the stress components in the x_3 direction are zero and by considering a rotation about the x_3 axis. Compare the resulting expressions with the Mohr's circle representation [2.1].

2.8 The stress tensor at a point $P(x, y, z)$ in a solid is

$$\boldsymbol{\sigma} = \begin{bmatrix} 3 & 1 & 1 \\ 1 & 0 & 2 \\ 1 & 2 & 0 \end{bmatrix}.$$

(a) Show that the principal stresses are 4, 1, -2.
(b) Find the orientation of the principal planes.
(c) Compute the octahedral stresses at P.
(d) Determine the magnitude and orientation of the absolute maximum shearing stress at P.

2.9 The stress tensor at a point $P(x, y, z)$ in a solid is

$$\boldsymbol{\sigma} = \begin{bmatrix} 120 & 40 & 30 \\ 40 & 150 & 20 \\ 30 & 20 & 100 \end{bmatrix};$$

(a) Determine the stresses with respect to a set of axes x', y', z' for which the matrix of direction cosines is

$$[\alpha_{ij}] = \begin{bmatrix} \frac{1}{2} & -\frac{\sqrt{3}}{2} & 0 \\ \frac{\sqrt{3}}{2} & \frac{1}{2} & 0 \\ 0 & 0 & 1 \end{bmatrix};$$

(b) Compute the principal stresses using both the x, y, z and x', y', z' axes as the basis (from [2.6]).

(c) Find the orientation of the principal planes with respect to the x, y, z axes.
(d) Compute the stress invariants for both coordinate systems, and verify that they are equal.

2.10 For an octahedral plane with a normal defined by Eq. (2.82), show that the traction on the plane is

$$\mathbf{T}_n^* = \sigma_{nn}^{\text{oct}}\mathbf{n}^* + \mathbf{T}_{ns}^*$$

where σ_{nn}^{oct} is defined by Eq. (2.84a) and where the magnitude of the shearing component $\mathbf{T}_{ns}^*$ is σ_{ns}^{oct}, Eq. (2.84b).

References

[2.1] Tauchert, T. R., *Energy Principles in Structural Mechanics* (McGraw–Hill Book Company, Inc., New York, 1974).
[2.2] Pearson, C. E., *Theoretical Elasticity* (Harvard Monographs in *Applied Science*, No 6. Harvard Univ. Press, Cambridge. MA, 1959).
[2.3] Westergaard, H. M., *Theory of Elasticity and Plasticity* (Dover Publications, Inc., New York. 1964).
[2.4] Davis. H. F., *Introduction to Vector Analysis* (Allyn and Bacon. Inc., Boston, 1961).
[2.5] Herrmann, L. R., Hamidi. R., Shafigh–Nobari, F., and Lim, C. K., "Nonlinear Behavior of Elastomeric Bearings. 1: Theory," *Journal of Engineering Mechanics*, ASCE, Vol. 114, No. 11, Nov. 1988, pp. 1811–1830.
[2.6] Ugural, A. C., and Fenster, S. K., *Advanced Strength and Applied Elasticity* (Elsevier-North Holland, New York, 1975).

CHAPTER 3

Deformations

3.1 Introduction

Displacements with respect to a reference coordinate system may be physically observed, calculated, or measured (at least on the surface) for a deformed elastic body. Each displacement may be considered to have two components, one of which is due to *relative* movements or *distortions* within the body and the other which is uniform throughout the body, so-called *rigid body* motion. The relationships between the displacements and the corresponding internal distortions are known as the *kinematic* or the *strain-displacement* equations of the theory of elasticity and may take several forms depending on the expected magnitude of the distortions and displacements.

3.2 Strain

We consider the undeformed and the deformed positions of an elastic body shown in Fig. 3.1. It is convenient to designate two sets of Cartesian coordinates x_i and X_i with $i = 1, 2, 3$, called *initial* coordinates and *final* coordinates, respectively, that denote the undeformed and deformed positions of the body [3.1]. Then, we select a reference point $P(\bar{x}_i)$ on the undeformed body and $p(\bar{X}_i)$ on the deformed body, where $\bar{x}_i$ and $\bar{X}_i$ indicate specific values of the coordinates x_i and X_i. Also, we locate neighboring points $Q(\bar{x}_i + d\bar{x}_i)$ and $q(\bar{X}_i + d\bar{X}_i)$ that are separated from P and p by differential distances ds and dS, respectively. The latter are given in component form by

$$(ds)^2 = d\bar{x}_1^2 + d\bar{x}_2^2 + d\bar{x}_3^2 = d\bar{x}_i d\bar{x}_i; \qquad \text{(a)}$$

$$(dS)^2 = d\bar{X}_1^2 + d\bar{X}_2^2 + d\bar{X}_3^2 = d\bar{X}_i d\bar{X}_i. \qquad \text{(b)} \qquad (3.1)$$

In Fig. 3.1, $\mathbf{u}$ represents the displacement of P to p, and $\mathbf{u} + d\mathbf{u}$ the displacement of Q to q. From the force diagram in Fig. 3.1, we note

$$d\mathbf{s} + (\mathbf{u} + d\mathbf{u}) = \mathbf{u} + d\mathbf{S}, \qquad (3.2)$$

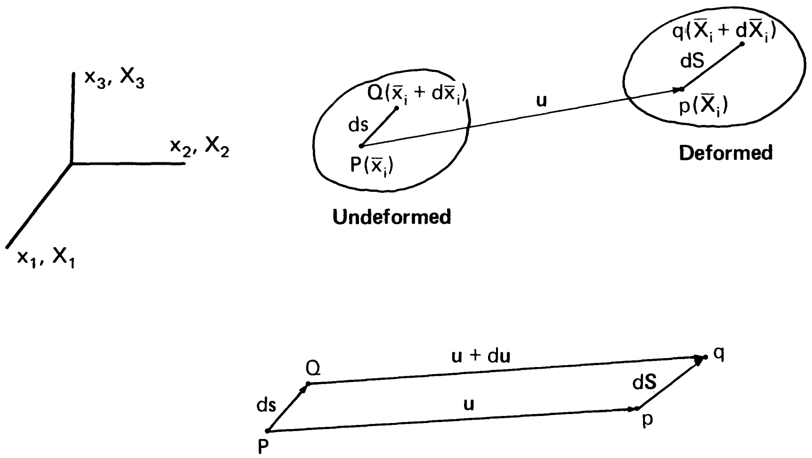

Fig. 3.1. Displacement vector in Cartesian space.

or

$$d\mathbf{u} = d\mathbf{S} - d\mathbf{s}. \tag{3.3}$$

We may consider this relationship in component form using Eq. (3.1) as

$$(dS)^2 - (ds)^2 = d\bar{X}_i d\bar{X}_i - d\bar{x}_i d\bar{x}_i. \tag{3.4}$$

We may now select either the initial or the final coordinates as the basis for further computations. First, we choose the initial coordinates x_i so that

$$\begin{aligned}
\bar{X}_i &= \bar{X}_i(x_1, x_2, x_3) && \text{(a)}\\
d\bar{X}_i &= \frac{\partial X_i}{\partial x_1} d\bar{x}_1 + \frac{\partial X_i}{\partial x_2} d\bar{x}_2 + \frac{\partial X_i}{\partial x_3} d\bar{x}_3 &&\\
&= X_{i,j} d\bar{x}_j && \text{(b)}\\
\mathbf{u} &= u_1 \mathbf{e}_{x_1} + u_2 \mathbf{e}_{x_2} + u_3 \mathbf{e}_{x_3} = u_i \mathbf{e}_{x_i}, && \text{(c)}\\
u_i &= X_i - x_i, && \text{(d)}
\end{aligned} \tag{3.5}$$

in component form. Substituting Eqs. (3.5b and d) into Eq. (3.4), introducing another dummy subscript k and applying Eq. (2.37),

$$\begin{aligned}
(dS)^2 - (ds)^2 &= X_{i,j} d\bar{x}_j X_{i,k} d\bar{x}_k - d\bar{x}_i d\bar{x}_i\\
&= (X_{i,j} X_{i,k} - \delta_{ij}\delta_{ik}) d\bar{x}_j d\bar{x}_k\\
&= [(x_i + u_i)_{,j}(x_i + u_i)_{,k} - \delta_{jk}] d\bar{x}_j d\bar{x}_k\\
&= [(\delta_{ij} + u_{i,j})(\delta_{ik} + u_{i,k}) - \delta_{jk}] d\bar{x}_j d\bar{x}_k\\
&= [\delta_{jk} + u_{j,k} + u_{k,j} + u_{i,j} u_{i,k} - \delta_{jk}] d\bar{x}_j d\bar{x}_k\\
&= (u_{j,k} + u_{k,j} + u_{i,j} u_{i,k}) d\bar{x}_j d\bar{x}_k.
\end{aligned} \tag{3.6}$$

It is convenient to interchange the dummy indices i and k, so that

$$(dS)^2 - (ds)^2 = (u_{i,j} + u_{j,i} + u_{k,i}u_{k,j})\,d\bar{x}_i\,d\bar{x}_j$$
$$= 2\varepsilon_{ij}^L\,d\bar{x}_i\,d\bar{x}_j, \tag{3.7}$$

in which

$$\varepsilon_{ij}^L = \tfrac{1}{2}(u_{i,j} + u_{j,i} + u_{k,i}u_{k,j}) \tag{3.8}$$

are components of the *Lagrangian*, or *Material*, strain tensor $\boldsymbol{\varepsilon}^L$.

We may repeat the procedure with the final coordinates X_i as the basis, so that

$$\bar{x}_i = \bar{x}_i(X_1, X_2, X_3) \tag{3.9a}$$

$$d\bar{x}_i = \frac{\partial x_i}{\partial X_1}d\bar{X}_1 + \frac{\partial x_i}{\partial X_2}d\bar{X}_2 + \frac{\partial x_i}{\partial X_3}d\bar{X}_3$$
$$= x_{i,j}\,d\bar{X}_j \tag{3.9b}$$

and

$$\mathbf{u} = u_1\mathbf{e}_{X_1} + u_2\mathbf{e}_{X_2} + u_3\mathbf{e}_{X_3} = u_i\mathbf{e}_{X_i}. \tag{3.9c}$$

Substituting Eq. (3.9b) and Eq. 3.5(d) into Eq. (3.4) gives

$$(dS)^2 - (ds)^2 = d\bar{X}_i\,d\bar{X}_i - x_{i,j}\,d\bar{X}_j x_{i,k}\,d\bar{X}_k$$
$$= (\delta_{ij}\delta_{ik} - x_{i,j}x_{i,k})\,d\bar{X}_j\,d\bar{X}_k$$
$$= [\delta_{jk} - (X_i - u_i)_{,j}(X_i - u_i)_{,k}]\,d\bar{X}_j\,d\bar{X}_k$$
$$= [\delta_{jk} - (\delta_{ij} - u_{i,j})(\delta_{ik} - u_{i,k})]\,d\bar{X}_j\,d\bar{X}_k$$
$$= [\delta_{jk} - \delta_{jk} + u_{k,j} + u_{j,k} - u_{i,j}u_{i,k}]\,d\bar{X}_j\,d\bar{X}_k$$
$$= (u_{j,k} + u_{k,j} - u_{i,j}u_{i,k})\,d\bar{X}_j\,d\bar{X}_k \tag{3.10}$$

or, interchanging i and k,

$$(dS)^2 - (ds)^2 = (u_{i,j} + u_{j,i} - u_{k,i}u_{k,j})\,d\bar{X}_i\,d\bar{X}_j$$
$$= 2\varepsilon_{ij}^E\,d\bar{X}_i\,d\bar{X}_j, \tag{3.11}$$

in which

$$\varepsilon_{ij}^E = \tfrac{1}{2}(u_{i,j} + u_{j,i} - u_{k,i}u_{k,j}) \tag{3.12}$$

are components of the *Eulerian*, or *Spatial*, strain tensor $\boldsymbol{\varepsilon}^E$.

If the displacement *gradients* $u_{k,i}$ are *small* in comparison to *unity*, then products of such terms are negligible in Eqs. (3.8) and (3.12), and they may be dropped. For such cases, we also consider the initial and final coordinate systems to be coincident, so that

$$\frac{\partial(\ )}{\partial x_i} = \frac{\partial(\ )}{\partial X_i}, \tag{3.13}$$

then

$$\varepsilon_{ij}^L = \varepsilon_{ij}^E = \varepsilon_{ij} = \tfrac{1}{2}(u_{i,j} + u_{j,i}). \tag{3.14}$$

The components ε_{ij} refer to the small or *infinitestimal* strain tensor $\boldsymbol{\varepsilon}$. Note that no restriction is placed on the magnitude of the u_i terms but only the gradients. It is thus at least theoretically possible at this point to describe relatively large displacements by infinitestimal strains.

The equations represented by Eq. (3.14) are a cornerstone of the development of the linear theory of elasticity and are called the *strain-displacement*, or *kinematic*, equations written in explicit form as

$$\begin{aligned}
\varepsilon_{11} &= u_{1,1} = \partial u_1/\partial x_1 && \text{(a)}\\
\varepsilon_{22} &= u_{2,2} = \partial u_2/\partial x_2 && \text{(b)}\\
\varepsilon_{33} &= u_{3,3} = \partial u_3/\partial x_3 && \text{(c)}\\
\varepsilon_{12} &= \varepsilon_{21} = \tfrac{1}{2}(u_{1,2} + u_{2,1}) = \tfrac{1}{2}(\partial u_1/\partial x_2 + \partial u_2/\partial x_1) && \text{(d)}\\
\varepsilon_{13} &= \varepsilon_{31} = \tfrac{1}{2}(u_{1,3} + u_{3,1}) = \tfrac{1}{2}(\partial u_1/\partial x_3 + \partial u_3/\partial x_1) && \text{(e)}\\
\varepsilon_{23} &= \varepsilon_{32} = \tfrac{1}{2}(u_{2,3} + u_{3,2}) = \tfrac{1}{2}(\partial u_2/\partial x_3 + \partial u_3/\partial x_2). && \text{(f)}
\end{aligned} \tag{3.15}$$

Noting that the u_i terms constitute a vector or first-order tensor, the $u_{i,j}$ terms represent a tensor of order 2, and, therefore, $\boldsymbol{\varepsilon}$ is a second-order tensor that transforms just as the stress tensor $\boldsymbol{\sigma}$:

$$\varepsilon'_{ij} = \alpha_{ik}\alpha_{jl}\varepsilon_{kl}. \tag{3.16}$$

3.3 Physical Interpretation of Strain Tensor

The physical definition of strain is familiar from elementary strength of materials. Here, it has been introduced from a mathematical standpoint and it remains to reconcile the notions.

First, we consider the components $\varepsilon_{(ii)}$, which are called *extensional* strains [3.1]. For example, consider a fiber parallel to the x_2 coordinate axis of initial length ds and final length dS, for which $dx_1 = 0$, $dx_3 = 0$, $dx_2 = ds$. Equation (3.7) becomes

$$(dS)^2 - (ds)^2 = 2\varepsilon_{22}\, ds^2 \tag{3.17}$$

for the case of infinitesimal strain.

Considering the l.h.s. of Eq. (3.17),

$$(dS)^2 - (ds)^2 = (dS - ds)(dS + ds) \tag{3.18}$$

and

$$\frac{dS - ds}{ds} = \frac{(dS)^2 - (ds)^2}{ds(dS + ds)}. \tag{3.19}$$

Substituting Eq. (3.17) into the r.h.s. of Eq. (3.19), we have

$$\frac{dS - ds}{ds} = \frac{2\varepsilon_{22}\, ds^2}{ds(dS + ds)}$$

$$\simeq \frac{2\varepsilon_{22}\, ds^2}{2ds^2}$$

$$= \varepsilon_{22}, \tag{3.20}$$

since the difference between $ds\, dS$ and ds^2 is of higher order for distortions $d\mathbf{u}/\mathbf{u}$, which are small compared to unity. Therefore,

$$\varepsilon_{22} = \frac{dS - ds}{ds} \tag{3.21}$$

which is the *relative elongation* of a fiber parallel to the x_2 coordinate axis. Similar interpretations are true for ε_{11} and ε_{33}.

The components ε_{ij} are called *shearing* strains and may be interpreted by considering intersecting fibers initially parallel to two of the coordinate axes [3.1]. For example, we select fibers parallel to the x_1 and x_3 axes, as shown in Fig. 3.2, with initial lengths $ds^{(1)}$ and $ds^{(3)}$. These fibers have final lengths of $dS^{(1)}$ and $dS^{(3)}$ and have rotated through angles $\beta^{(1)}$ and $\beta^{(3)}$, respectively. The total change in the initially right angle is

$$\beta^{(1)} + \beta^{(3)} = \beta. \tag{3.22}$$

We consider vectors coincident with the fibers given in component form by

$$d\mathbf{S}^{(1)} = dS_i^{(1)}\mathbf{e}_{x_i} \qquad \text{(a)}$$

and (3.23)

$$d\mathbf{S}^{(3)} = dS_i^{(3)}\mathbf{e}_{x_i}, \qquad \text{(b)}$$

in which the components may be written in terms of the initial coordinates as

$$dS_i^{(1)} = \frac{\partial S_i^{(1)}}{\partial x_j} dx_j^{(1)} = S_{i,j}^{(1)}\, dx_j^{(1)}; \qquad \text{(a)}$$

$$dS_i^{(3)} = \frac{\partial S_i^{(3)}}{\partial x_k} dx_k^{(3)} = S_{i,k}^{(3)}\, dx_k^{(3)}. \qquad \text{(b)} \tag{3.24}$$

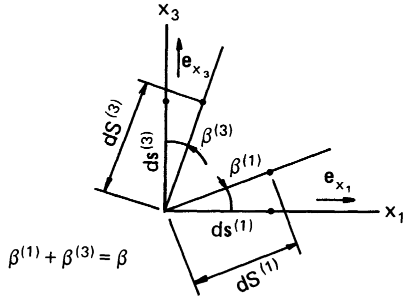

Fig. 3.2. Shearing strains.

The scalar product of the vectors is

$$d\mathbf{S}^{(1)} \cdot d\mathbf{S}^{(3)} = dS^{(1)}\,dS^{(3)} \cos\left(\frac{\pi}{2} - \beta\right). \tag{3.25}$$

Considering first the l.h.s. of Eq. (3.25), in view of Eqs. (3.23), (3.24), (3.3) and also Eq. (2.37),

$$\begin{aligned} d\mathbf{S}^{(1)} \cdot d\mathbf{S}^{(3)} &= S^{(1)}_{i,j}\,dx^{(1)}_j\,S^{(3)}_{i,k}\,dx^{(3)}_k \\ &= (s^{(1)}_i + u_i)_{,j}(s^{(3)}_i + u_i)_{,k}\,dx^{(1)}_j\,dx^{(3)}_k \\ &= (\delta_{ij} + u_{i,j})(\delta_{ik} + u_{i,k})\,dx^{(1)}_j\,dx^{(3)}_k \\ &= (\delta_{jk} + u_{k,j} + u_{j,k} + u_{i,j}u_{i,k})\,dx^{(1)}_j\,dx^{(3)}_k. \end{aligned} \tag{3.26}$$

The product term is zero for infinitesimal theory and, considering the initial orientation of the fibers, we obtain

$$\begin{aligned} &dx^{(1)}_1 = ds^{(1)}; \quad dx^{(1)}_2 = dx^{(1)}_3 = 0; \\ &dx^{(3)}_3 = ds^{(3)}; \quad dx^{(3)}_1 = dx^{(3)}_2 = 0. \end{aligned} \tag{3.27}$$

Therefore, Eq. (3.26) has a nonzero value only for $j = 1$ and $k = 3$, for which $\delta_{jk} = 0$. Thus,

$$d\mathbf{S}^{(1)} \cdot d\mathbf{S}^{(3)} \simeq (u_{3,1} + u_{1,3})\,ds^{(1)}\,ds^{(3)}. \tag{3.28}$$

Now equating the r.h.s. of Eqs. (3.25) and (3.28),

$$dS^{(1)}\,dS^{(3)} \cos\left(\frac{\pi}{2} - \beta\right) = (u_{3,1} + u_{1,3})\,ds^{(1)}\,ds^{(3)} \tag{3.29}$$

Neglecting the differences between the squares of the initial and final lengths of the fibers and assuming small angles of rotation β such that $\cos\left(\frac{\pi}{2} - \beta\right) = \sin\beta \cong \beta$.

$$\beta = (u_{1,3} + u_{3,1}) = 2\varepsilon_{13}. \tag{3.30}$$

That is, the strain component ε_{13} is equal to *one-half* of the increase in the angle between two fibers initially parallel to the x_1 and x_3 axes. Similar interpretations are obvious for ε_{12} and ε_{23}.

It should be noted that the shearing strains are frequently taken as the *total* angle increase β rather than *one-half* this value [3.2]. Such a definition is termed an "engineering" strain but is awkward because it violates the tensor character of ε_{ij}. Nevertheless, we should be aware of this form, since engineering strains are helpful for physical interpretation and useful in deriving material laws as demonstrated in Sec. 4.3.

Since the strain tensor is formed from the displacement gradients, it is interesting to separate $u_{i,j}$ into two parts

$$u_{i,j} = \varepsilon_{ij} + \omega_{ij}, \tag{3.31}$$

where

$$\omega_{ij} = \tfrac{1}{2}(u_{i,j} - u_{j,i}), \tag{3.32}$$

from Eq. (3.14). For $i = j$, $\omega_{ij} = 0$, while for $i \neq j$, $\omega_{ij} = -\omega_{ji}$, thus the ω_{ij} are elements of a skew-symmetric tensor $\boldsymbol{\omega}$. For the previous example,

$$\omega_{13} = \tfrac{1}{2}(u_{1,3} - u_{3,1}). \tag{3.33}$$

From Eqs. (3.22) and (3.30), we find

$$\beta = \beta^{(1)} + \beta^{(3)} = (u_{1,3} + u_{3,1}) = 2\varepsilon_{13}. \tag{3.34}$$

By comparison,

$$\omega_{13} = \frac{\beta^{(1)} - \beta^{(3)}}{2}, \tag{3.35}$$

which may be interpreted as the *average* rotation of all fibers around the x_2 axis. For a rigid body rotation, $\varepsilon_{13} = 0$, $\beta^{(1)} = -\beta^{(3)}$ and $\omega_{13} = \beta^{(1)}$. For this reason, $\boldsymbol{\omega}$ is called the rotation tensor [3.3].

The physical notions of strain discussed in this section are closely intertwined with the mathematical definitions in the preceding section. This connection extends into the nonlinear Lagrangian and Eulerian strain tensors as well, but is understandably more complex than the linear case. A recent unified definition of finite strains by Ma and Desai [3.4] contains both of the classical nonlinear tensors as special cases and isolates a special case which is essentially a mean of the two. The resulting strain tensor possesses some linear charactertics that assist in physical interpretation and exhibits good computational performances for some classical one- and two-dimensional problems.

3.4 Principal Strains

Since we have shown that the strains have the same second-order tensor character as the stresses, we expect to be able to identify a system of principal strains that are the eigenvalues determined from the characteristic equation

$$|\varepsilon_{ji} - \lambda\delta_{ji}| = 0, \tag{3.36}$$

which is analogous to Eq. (2.56a). The three roots $\lambda_1, \lambda_2, \lambda_3$ are the principal strains $\varepsilon^{(k)}$, with $k = 1, 2, 3$.

The corresponding eigenvectors designate the directions associated with each of the principal strains and are computed from

$$(\varepsilon_{ji} - \lambda\delta_{ji})n_j = 0 \tag{3.37}$$

along with Eq. (2.57). The direction of principal strain are denoted by $n_j^{(k)}$, with $k = 1$, 2 and 3. These directions are mutually perpendicular and, for isotropic elastic materials (to be discussed in Chapter 4), coincide with the directions of the principal stresses. Obviously, the largest extension experienced by any fiber at a point is equal to the largest principal strain.

Strains on oblique planes, octahedral strains and the absolute maximum shearing strain are obtained relative to the principal coordinates in a manner analogous to obtaining corresponding stress quantities, described in Section 2.5. Also for completeness, we define the strain invariants R_1, R_2 and R_3 analogous to Q_1, Q_2 and Q_3 in Eqs. (2.58) and (2.59), with the σ_{ij} replaced by ε_{ij} in each case. Of particular physical significance is

$$R_1 = \varepsilon_{ii} = u_{i,i}, \tag{3.38}$$

which is called the cubical strain, and is related to the volume change as shown in Sec. 3.5.

3.5 Volume and Shape Changes

It is sometimes convenient to separate the components of strain into those that cause changes in the *volume* and those that cause changes in the *shape* of a differential element.

Consider a volume element oriented with the *principal* directions, similar to that shown in Fig. 2.2, but with the shearing stresses equal to zero. The original length of each side is taken as $dx^{(k)}$ and the final length as $dX^{(k)}$, where

$$dX^{(k)} = dx^{(k)}(1 + \varepsilon^{(k)}). \tag{3.39}$$

The original volume is found as

$$dv = \prod_{k=1}^{3} dx^{(k)} \tag{3.40a}$$

and the final volume by

$$\begin{aligned} dV &= \prod_{k=1}^{3} dX^{(k)} \\ &= \prod_{k=1}^{3} (1 + \varepsilon^{(k)})\, dx^{(k)}. \end{aligned} \tag{3.40b}$$

Now, the *dilatation* is defined as the relative change in volume

$$\begin{aligned} \Delta &= \frac{dV - dv}{dv} \\ &= \frac{dv\left\{\left[\prod_{k=1}^{3} (1 + \varepsilon^{(k)})\right] - 1\right\}}{dv} \\ &= [(1 + \varepsilon^{(1)})(1 + \varepsilon^{(2)})(1 + \varepsilon^{(3)})] - 1 \end{aligned}$$

$$= \varepsilon^{(1)} + \varepsilon^{(2)} + \varepsilon^{(3)} + \text{higher-order terms}$$

$$\cong \prod_{k=1}^{3} \varepsilon^{(k)}. \tag{3.41}$$

which is simply the sum of the diagonal terms of the tensor.

The dilatation Δ is also equal to the sum of the principal strains ε_{ii}, which is the first strain invariant R_1 and the *divergence* of the displacement vector $\nabla \cdot \mathbf{u} = u_{i,i}$, defined by Eq. (3.5c).

Changes in shape of the volume element are denoted by the shearing strains ε_{ij}, with $i \neq j$, sometimes called the *detrusions* [3.2].

The preceding separation of the strains into dilatational and detrusional components may be formalized by the resolution of the strain tensor into two terms [3.3],

$$\boldsymbol{\varepsilon} = \boldsymbol{\varepsilon}_M + \boldsymbol{\varepsilon}_D, \tag{3.42}$$

in which

$$\boldsymbol{\varepsilon}_M = \begin{bmatrix} \varepsilon_M & 0 & 0 \\ 0 & \varepsilon_M & 0 \\ 0 & 0 & \varepsilon_M \end{bmatrix} = \textit{mean normal strain} \tag{3.43}$$

$$\boldsymbol{\varepsilon}_D = \begin{bmatrix} \varepsilon_{11} - \varepsilon_M & \varepsilon_{12} & \varepsilon_{13} \\ \varepsilon_{12} & \varepsilon_{22} - \varepsilon_M & \varepsilon_{23} \\ \varepsilon_{13} & \varepsilon_{23} & \varepsilon_{33} - \varepsilon_M \end{bmatrix} = \textit{strain deviator}, \tag{3.44}$$

and where

$$\begin{aligned} \varepsilon_M &= \tfrac{1}{3}(\varepsilon_{11} + \varepsilon_{22} + \varepsilon_{33}) \\ &= \tfrac{1}{3}(\varepsilon^{(1)} + \varepsilon^{(2)} + \varepsilon^{(3)}) \\ &= \tfrac{1}{3}R_1 \end{aligned} \tag{3.45}$$

The mean normal strain $\boldsymbol{\varepsilon}_M$ corresponds to a state of equal elongation in all directions for an element at a given point. The element would remain similar to the original shape but change in volume with a dilatation of ε_{ii}. For this reason, $\boldsymbol{\varepsilon}_M$ may be termed the *volumetric* component of strain.

The strain deviator, or *deviatoric* component, $\boldsymbol{\varepsilon}_D$ has a dilatation, calculated from Eq. (3.41), of

$$\begin{aligned} \Delta &= \sum_{i=1}^{3} \varepsilon_D^{(i)} \\ &= \varepsilon_{D_{ii}} \\ &= (\varepsilon_{11} - \varepsilon_M) + (\varepsilon_{22} - \varepsilon_M) + (\varepsilon_{33} - \varepsilon_M) \\ &= \varepsilon_{11} + \varepsilon_{22} + \varepsilon_{33} - 3[\tfrac{1}{3}(\varepsilon_{11} + \varepsilon_{22} + \varepsilon_{33})] \\ &= 0. \end{aligned} \tag{3.46}$$

This characterizes a change in *shape* of an element with no change in *volume*.

The invariants of the strain deviator tensor play an important role in the theory of plasticity since shape changes are of importance.

Corresponding to the deformations associated with the mean normal strain and strain deviator, we define the principal stresses associated with changes in the volume and the shape as

$$\boldsymbol{\sigma} = \boldsymbol{\sigma}_M + \boldsymbol{\sigma}_D \tag{3.47}$$

in which

$$\boldsymbol{\sigma}_M = \begin{bmatrix} \sigma_M & 0 & 0 \\ 0 & \sigma_M & 0 \\ 0 & 0 & \sigma_M \end{bmatrix} = \textit{mean normal stress} \tag{3.48}$$

$$\boldsymbol{\sigma}_D = \begin{bmatrix} \sigma_{11} - \sigma_M & \sigma_{12} & \sigma_{13} \\ \sigma_{12} & \sigma_{22} - \sigma_M & \sigma_{23} \\ \sigma_{13} & \sigma_{23} & \sigma_{33} - \sigma_M \end{bmatrix} = \textit{stress deviator}, \tag{3.49}$$

and where

$$\begin{aligned} \sigma_M &= \tfrac{1}{3}(\sigma_{11} + \sigma_{22} + \sigma_{33}) \\ &= \tfrac{1}{3}(\sigma^{(1)} + \sigma^{(2)} + \sigma^{(3)}) \end{aligned} \tag{3.50}$$

In indicial form, the volumetric and deviatoric components of stress are, respectively,

$$\sigma_{M_{ij}} = \tfrac{1}{3}\sigma_{kk}\delta_{ij} \tag{3.51}$$

and

$$\begin{aligned} \sigma_{D_{ij}} &= \sigma_{ij} - \sigma_{M_{ij}} \\ &= \sigma_{ij} - \tfrac{1}{3}\sigma_{kk}\delta_{ij}. \end{aligned} \tag{3.52}$$

For principal axes

$$\begin{aligned} \boldsymbol{\sigma}_D &= \begin{bmatrix} \sigma^{(1)} - \sigma_M & 0 & 0 \\ 0 & \sigma^{(2)} - \sigma_M & 0 \\ 0 & 0 & \sigma^{(3)} - \sigma_M \end{bmatrix} \\ &= \begin{bmatrix} \sigma_D^{(1)} & 0 & 0 \\ 0 & \sigma_D^{(2)} & 0 \\ 0 & 0 & \sigma_D^{(3)} \end{bmatrix}. \end{aligned} \tag{3.53}$$

Note that the sum of the diagonals of $\boldsymbol{\sigma}_D$ is

$$\sigma_{D_{ii}} = \sigma^{(1)} + \sigma^{(2)} + \sigma^{(3)} - 3\cdot\tfrac{1}{3}[\sigma^{(1)} + \sigma^{(2)} + \sigma^{(3)}] = 0. \tag{3.54}$$

The stress deviator tensor referred to the principal axes, Eq. (3.53), is the basis of the reknown von Mises yield condition, discussed in Sec. 11.3.3.

3.6 Compatibility

If we examine Eq. (3.14), $\varepsilon_{ij} = \frac{1}{2}(u_{i,j} + u_{j,i})$, we see that the components of strain may be computed once the displacements are known, provided that they are once differentiable. However, the inverse problem of calculating the displacements from the strains is not so direct since there are six independent equations and only three unknowns. Conditions of *compatibility*, imposed on the components of strain $\varepsilon_{(jj)}$, may be shown to be necessary and sufficient [3.5] to insure a continuous single-valued displacement field $\mathbf{u}$.

The usual procedure is to eliminate the displacements between the equations repeatedly to produce equations with only strains as unknowns. First, we take two normal components $\varepsilon_{(ll)}$ and $\varepsilon_{(mm)}$ and the shearing component ε_{lm} with the summation convention suspended. Taking second partials, we have

$$\begin{aligned} \varepsilon_{(ll,mm)} &= u_{(l,lmm)} && \text{(a)} \\ \varepsilon_{(mm,ll)} &= u_{(m,mll)} && \text{(b)} \\ \varepsilon_{(lm,lm)} &= \tfrac{1}{2}(u_{(l,mlm)} + u_{(m,llm)}) \\ &= \tfrac{1}{2}(u_{(l,lmm)} + u_{(m,mll)}), && \text{(c)} \end{aligned} \qquad (3.55)$$

with interchangeability of the order of differentiation assumed. Next, we equate Eq. (3.55a) plus Eq. (3.55b) to twice Eq. (3.55c) to get

$$\varepsilon_{(ll,mm)} + \varepsilon_{(mm,ll)} = 2\varepsilon_{(lm,lm)}. \qquad (3.56)$$

Then, we take one normal component $\varepsilon_{(ll)}$ and three shearing components ε_{lm}, ε_{ln}, ε_{mn} and write the second partials

$$\begin{aligned} \varepsilon_{(ll,mn)} &= u_{(l,lmn)} && \text{(a)} \\ \varepsilon_{(lm,ln)} &= \tfrac{1}{2}(u_{(l,mln)} + u_{(m,lln)}) && \text{(b)} \\ \varepsilon_{(ln,lm)} &= \tfrac{1}{2}(u_{(l,nlm)} + u_{(n,llm)}) && \text{(c)} \\ \varepsilon_{(mn,ll)} &= \tfrac{1}{2}(u_{(m,nll)} + u_{(n,mll)}). && \text{(d)} \end{aligned} \qquad (3.57)$$

We find that Eq. (3.57a) can be equated to Eq. (3.57b) plus Eq. (3.57c) minus Eq. (3.57d) to give

$$\varepsilon_{(lm,ln)} + \varepsilon_{(ln,lm)} - \varepsilon_{(mn,ll)} = \varepsilon_{(ll,mn)}. \qquad (3.58)$$

Equations (3.56) and (3.58) are six equations relating the components of strain that insure that these components will integrate into a unique displacement field. They are of importance and may be written explicitly as

$$\begin{aligned} \varepsilon_{11,22} + \varepsilon_{22,11} &= 2\varepsilon_{12,12} && \text{(a)} \\ \varepsilon_{22,33} + \varepsilon_{33,22} &= 2\varepsilon_{23,23} && \text{(b)} \\ \varepsilon_{33,11} + \varepsilon_{11,33} &= 2\varepsilon_{31,31} && \text{(c)} \end{aligned}$$

$$\varepsilon_{12,13} + \varepsilon_{13,12} - \varepsilon_{23,11} = \varepsilon_{11,23} \qquad \text{(d)}$$

$$\varepsilon_{23,21} + \varepsilon_{21,23} - \varepsilon_{31,22} = \varepsilon_{22,31} \qquad \text{(e)}$$

$$\varepsilon_{31,32} + \varepsilon_{32,31} - \varepsilon_{12,33} = \varepsilon_{33,12}. \qquad \text{(f)} \quad (3.59)$$

These are known as the *St. Venant* compatibility equations which may also be extracted from the tensor equation

$$\varepsilon_{ij,kl} + \varepsilon_{kl,ij} = \varepsilon_{ik,jl} + \varepsilon_{jl,ik}, \tag{3.60}$$

which represents $3^4 = 81$ equations, only six of which are distinct; for example, for $i = 1$, $j = 1$, $k = 2$, $l = 2$, we get

$$\varepsilon_{11,22} + \varepsilon_{22,11} = \varepsilon_{12,12} + \varepsilon_{12,12} = 2\varepsilon_{12,12}, \tag{3.61}$$

which is also Eq. (3.59a). It has been shown that these equations are not strictly "independent. A further differential combination of the six equations produces three identities connecting the equations, which are known as the Bianchi formulas. One may not, however, choose any three of the six, so that the usual approach is to include all six in the formulation [3.7].

Even though we have the compatibility equations, the formulation is still incomplete in that there is no connection between the equilibrium equations Eqs. (2.34), three equations in six unknowns σ_{ij}, and the kinematic equations Eqs. (3.14), Six equations in nine unknowns ε_{ij} and u_i. We will seek the connection between the equilibrium and the kinematic equations in the laws of physics governing material behavior, considered in the next chapter.

3.7 Computational Example

A displacement field is given by

$$\mathbf{u} = [(3x^2y + 6) \times 10^{-2}]\mathbf{e}_x + [(y^2 + 6xz) \times 10^{-2}]\mathbf{e}_y + [(6z^2 + 2yz + 10) \times 10^{-2}]\mathbf{e}_z. \tag{3.62}$$

We seek to compute the components of the strain and rotation tensors ε_{ij} and ω_{ij}, and to verify the compatibility equations.

(1) The partial derivatives $\times\ 10^{-2}$ with $x = 1$, $y = 2$, $z = 3$ are

$$u_{1,1} = 6xy; \quad u_{1,2} = 3x^2; \quad u_{1,3} = 0;$$

$$u_{1,11} = 6y; \quad u_{1,12} = 6x; \quad u_{1,112} = 6.$$

$$u_{2,1} = 6z; \quad u_{2,2} = 2y; \quad u_{2,3} = 6x;$$

$$u_{2,13} = 6; \quad u_{2,22} = 2.$$

$$u_{3,1} = 0; \quad u_{3,2} = 2z; \quad u_{3,3} = 12z + 2y;$$

$$u_{3,23} = 2; \quad u_{3,33} = 12.$$

(2) The strain tensor is

$$\varepsilon = \begin{bmatrix} 6xy & \frac{1}{2}(3x^2 + 6y) & 0 \\ \frac{1}{2}(3x^2 + 6z) & 2y & \frac{1}{2}(6x + 2z) \\ 0 & \frac{1}{2}(6x + 2z) & 12z + 2y \end{bmatrix} \times 10^{-2}.$$

(3) The rotation tensor is

$$\omega = \begin{bmatrix} 0 & \frac{1}{2}(3x^2 - 6z) & 0 \\ -\frac{1}{2}(3x^2 - 6z) & 0 & \frac{1}{2}(6x - 2z) \\ 0 & -\frac{1}{2}(6x - 2z) & 0 \end{bmatrix} \times 10^{-2}.$$

For any given points (x, y, z), the strains and average rotations may be computed as the elements of ε_{ij} and ω_{ij}, respectively, and the principal strains and directions determined.

(4) Compatibility: Since only nonzero second partial derivatives enter into Eqs. (3.59), we consider $\varepsilon_{12,11} = 3$ and $\varepsilon_{21,11} = 3$. Neither of these appears in Eqs. (3.59), thus the latter equations are identically satisfied. Beyond this trivial example we may observe that all strain fields which are *linear* will identically satisfy the compatibility relations. This is of some importance in generating numerical or approximate solutions to the equations of the theory of elasticity since linear approximations are otherwise convenient.

Exercises

3.1 The components of a displacement field are (from [3.6])

$$u_x = (x^2 + 20) \times 10^{-4},$$
$$u_u = 2yz \times 10^{-3},$$
$$u_z = (z^2 - xy) \times 10^{-3}.$$

(a) Consider two points in the undeformed system (2, 5, 7) and (3, 8, 9). Find the change in distance between these points.
(b) Compute the components of the strain tensor.
(c) Compute the components of the rotation tensor.
(d) Compute the strain at (2, −1, 3).
(e) Does the displacement field satisfy compatibility?

3.2 The strain field at a point $P(x, y, z)$ in an elastic body is given by

$$\varepsilon = \begin{bmatrix} 20 & 3 & 2 \\ 3 & -10 & 5 \\ 2 & 5 & -8 \end{bmatrix} \times 10^{-6}.$$

Determine the following values.
(a) the strain invariants
(b) the principal strains
(c) the octahedral shearing strain
(d) the absolute maximum shearing strain
(e) the mean normal strain and the strain deviator.

3.3 With reference to problem 3.2, consider a second coordinate system x_i' in which x_2' is parallel to x_2 and x_1' and x_3' are defined by a 60° counterclockwise rotation about x_2. Find the components of strain with reference to the x_i' system using the strain field from problem 3.2.

3.4 The components of a strain tensor referred to the x_1, x_2, x_3 axes in the figure are

$$\varepsilon = \begin{bmatrix} 0.02 & 0 & 0 \\ 0 & 0.01 & 0 \\ 0 & 0 & 0.03 \end{bmatrix}.$$

In the figure, $OA = OB = OC$ and D is the midpoint of AC. The direction cosines of AC are $(1/\sqrt{2}, 0, -1/\sqrt{2})$ and those of BD are $(-1/\sqrt{6}, \sqrt{2}/\sqrt{3}, -1/\sqrt{6})$. Find:

(a) the elongation of line AC

(b) change of initial right angle BDA.

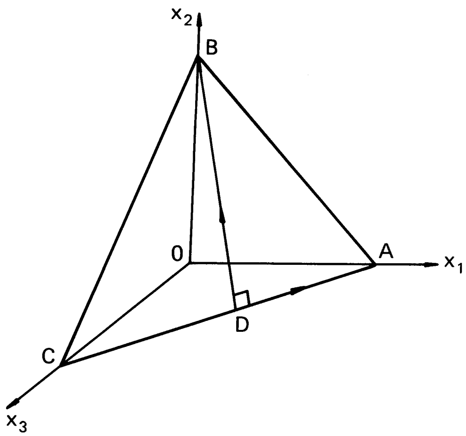

Problem 3.4

3.5 The components of a strain tensor referred to the x_1, x_2, x_3 axes in the figure are given by

$$\varepsilon = \begin{bmatrix} 0.02 & -0.003 & 0 \\ -0.003 & 0.01 & 0.02 \\ 0 & 0.02 & 0.01 \end{bmatrix},$$

and they are constant in the region under consideration. The direction cosines of AC and DB are as given in Exercise 3.4. Find:

(a) the relative elongations of the lines AC and DB

(b) the change of the initially right angle ADB

(c) the first, second and third invariants of strain.

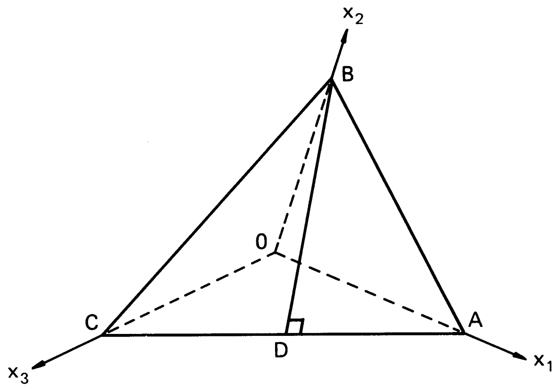

Problem 3.5

3.6 Compute the infinitesimal strains and sketch the deformed configuration of an initially rectangular volume element subject to the following displacement fields (from [3.1]), where A, B, D_{ij} = constants,

(a) Simple extension: $u_1 = A_1 x_1$; $u_2 = u_3 = 0$.

(b) Simple shear: $u_1 = Bx_2$; $u_2 = y_3 = 0$.

(c) Homogeneous deformation: $u_i = D_{ij} x_j$. [See 3.8]

3.7 Consider a (linear) strain field associated with a simply connected region R such that

$$\varepsilon_{11} = Ax_2^2, \quad \varepsilon_{22} = Ax_1^2, \quad \varepsilon_{12} = Bx_1 x_2, \quad \varepsilon_{33} = \varepsilon_{32} = \varepsilon_{31} = 0.$$

Find the relationship between A and B such that it is possible to obtain a single-valued continuous displacement field which corresponds to the given strain field.

3.8 Show that the expression for the tangential component of stress σ_{ns}, given by Eq. 2.19, can be written as [3.9]

$$\sigma_{ns} = [\sigma_{ik}\sigma_{jm} n_k n_m (\delta_{km} - n_k n_m)]^{1/2}$$

3.9 Consider the St. Venant compatibility equations (3.59):

(a)
$$R_1 = \varepsilon_{11,22} + \varepsilon_{22,11} - 2\varepsilon_{12,12} = 0$$
$$R_2 = \varepsilon_{22,33} + \varepsilon_{33,22} - 2\varepsilon_{23,23} = 0$$
$$R_3 = \varepsilon_{33,11} + \varepsilon_{11,33} - 2\varepsilon_{31,31} = 0$$
$$U_1 = -\varepsilon_{11,23} + (-\varepsilon_{23,1} + \varepsilon_{31,2} + \varepsilon_{12,3})_{,1} = 0$$
$$U_2 = -\varepsilon_{22,31} + (\varepsilon_{23,1} - \varepsilon_{31,2} + \varepsilon_{12,3})_{,2} = 0$$
$$U_3 = -\varepsilon_{33,12} + (\varepsilon_{23,1} + \varepsilon_{31,2} - \varepsilon_{12,3})_{,3} = 0$$

(b) Show that these equations satisfy the Bianchi formulas [3.7]:

$$R_{1,1} + U_{3,2} + U_{2,3} = 0$$
$$U_{3,1} + R_{2,2} + U_{1,3} = 0$$
$$U_{2,1} + U_{1,2} + R_{3,3} = 0$$

References

[3.1] Tauchert. T. R., *Energy Principles in Structural Mechanics* (McGraw–Hill Book Company, Inc., New York, 1974).

[3.2] Westergaard, H. M., *Theory of Elasticity and Plasticity* (Dover Publications, Inc., New York, 1964).

[3.3] Filonenko–Borodich, M., *Theory of Elasticity*, translated from Russian by M. Konayeon (Dover Publications, Inc., New York, 1965).

[3.4] Ma, Y., and Desai, C. S., "Alternative Definition of Finite Strains," *Journal of Engineering Mechanics*, ASCE, Vol. 116, No. 4, April, 1990, pp. 901–919.

[3.5] Pearson, C. E., *Theoretical Elasticity* (Harvard Univ. Press, Cambridge, MA, 1959).

[3.6] Ugural, A. C., and Fenster, S. K., *Advanced Strength and Applied Elasticity*, (Elsevier-North Holland, New York, 1975).

[3.7] Malvern, L. E., *Introduction to the Mechanics of a Continuous Medium* (Prentice-Hall, Englewood Cliffs, NJ, 1969).

[3.8] Timoshenko, S. P., and Goodier, J. N., *Theory of Elasticity* (McGraw–Hill Book Company, Inc., New York, 1951).

[3.9] Zubelwicz, A., and Bažant, Z. P., "Constitutive Model with Rotating Active Plane and True Stress," *Journal of Engineering Mechanics*, ASCE, Vol. 113, No. 3, March, 1987, pp. 398–416.

CHAPTER 4
Material Behavior

4.1 Introduction

The need to connect the equilibrium equations derived in Chapter 2 with the kinematic relations developed in Chapter 3 was pointed out earlier. This coupling is accomplished by considering the mechanical properties of the materials for which the theory of elasticity is to be applied and is expressed by *constitutive* or *material* laws.

4.2 Uniaxial Behavior

The most elementary description of material behavior is the well-known *Hooke's law*, stated by Robert Hooke in the late 17th century [4.1], which refers to a one-dimensional extensional test:

$$\sigma_{11} = E\varepsilon_{11}. \tag{4.1}$$

where E is called the *modulus of elasticity*, or *Young's modulus* after Thomas Young who introduced the term in the early 19th century [4.1]. This test also reveals some additional bases of material characterization as shown in Fig. 4.1, which is an automatically recorded plot of two cycles of loading and unloading for mild steel. Branch (1) is the initial elastic response, from which E may be calculated as the slope. In the vicinity of (2), there is a decrease in the slope, commencing at the *proportional limit* and progressing until the *yield point* is reached at (3). Yielding progresses along branch (4) until unloading commences at (5) and continues along (6). The unloading ceases, and reloading begins at (7) to initiate another cycle that extends through (13) when the test is terminated. Region (14) is known as a *hysteresis loop* and is a measure of the energy dissipated through one excursion beyond the yield point.

A material that is loaded only to a level below the yield strain and that unloads along the same path is called *elastic*. If the path is linear as well, the material is said to be *linearly elastic*. It is also possible to have *nonlinear*

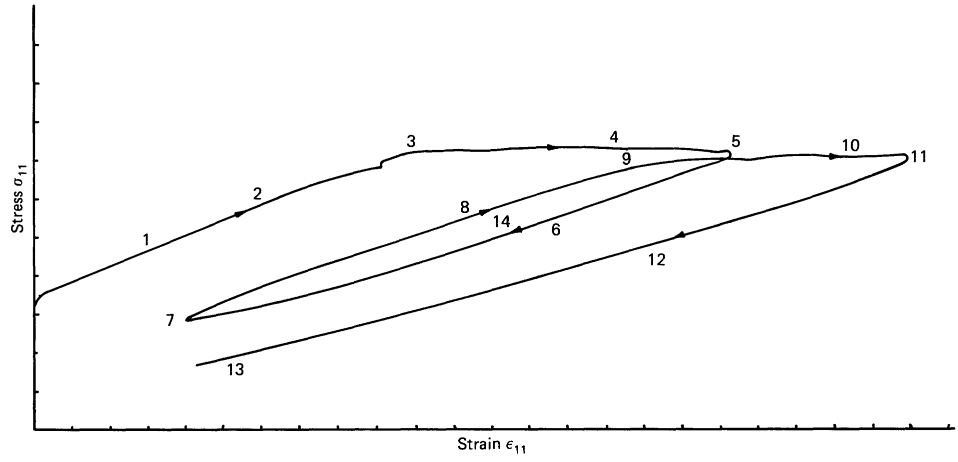

Fig. 4.1. Stress-strain curve.

elastic materials for which the coincident paths are curved. Both of these possibilities are addressed by the theory of elasticity, although only the former case is considered here in any detail. Past the yield point, we have the inelastic regime that requires additional considerations.

Beyond the uniaxial test, the characterization of material behavior is far more involved, from both a theoretical and an experimental standpoint, and is discussed in the following sections.

4.3 Generalized Hooke's Law

As a prerequisite to the postulation of a *linear* relationship between each component of stress and strain, it is necessary to establish the existence of a strain energy density W that is a homogeneous quadratic function of the strain components $W(\varepsilon_{ij})$ [4.2]. This concept is attributed to George Green [4.1]. For a body that is slightly strained by gradual application of the loading while the temperature remains constant, this will produce stress components derivable as

$$\sigma_{ij} = \frac{\partial W}{\partial \varepsilon_{ij}} \tag{4.2a}$$

It is convenient initially to write W in terms of the "engineering" strains $\bar{\varepsilon}_{ij}$ as defined in Section 3.3. Thus,

$$\sigma_{ij} = \frac{\partial W(\bar{\varepsilon}_{ij})}{\partial \bar{\varepsilon}_{ij}} \tag{4.2b}$$

where $\bar{\varepsilon}_{ij} = (2 - \delta_{ij})\varepsilon_{ij}$.

The function should have coefficients such that $W \geq 0$ in order to insure the stability of the body [4.2], with $W(0) = 0$ corresponding to a *natural* or *zero energy state* (unloaded). Energy principles are developed in Chapter 10.

Now, the generalized Hooke's law is written in the form of a fourth-order tensor

$$\sigma_{ij} = E_{ijkl}\varepsilon_{kl} \tag{4.3}$$

in which the 81 coefficients E_{ijkl} are called the elastic constants. Since W is continuous, the order of differentiation in Eq. (4.2) is immaterial and E_{ijkl} is symmetric. Thus the number of independent equations reduces from nine to six, the elastic constants from 81 to 36, and then further to $[(36.6)/2] + 6 = 21$ when only half of the off-diagonal constants are counted. We represent this relationship in matrix form in terms of the engineering strains as

$$\{\boldsymbol{\sigma}\} = [\mathbf{E}]\{\bar{\boldsymbol{\varepsilon}}\}, \tag{4.4}$$

where

$$\begin{Bmatrix} \sigma_{11} \\ \sigma_{22} \\ \sigma_{33} \\ \sigma_{12} \\ \sigma_{23} \\ \sigma_{31} \end{Bmatrix} = \begin{bmatrix} E_{1111} & E_{1122} & E_{1133} & E_{1112} & E_{1123} & E_{1131} \\ & E_{2222} & E_{2233} & E_{2212} & E_{2223} & E_{2231} \\ & & E_{3333} & E_{3312} & E_{3323} & E_{3331} \\ & & & E_{1212} & E_{1223} & E_{1231} \\ & & & & E_{2323} & E_{2331} \\ & & & & & E_{3131} \end{bmatrix} \begin{Bmatrix} \bar{\varepsilon}_{11} \\ \bar{\varepsilon}_{22} \\ \bar{\varepsilon}_{33} \\ \bar{\varepsilon}_{12} \\ \bar{\varepsilon}_{23} \\ \bar{\varepsilon}_{31} \end{Bmatrix}. \tag{4.5}$$

Replacing the awkward quadruple subscripts, we have

$$\begin{Bmatrix} \sigma_{11} \\ \sigma_{22} \\ \sigma_{33} \\ \sigma_{12} \\ \sigma_{23} \\ \sigma_{31} \end{Bmatrix} = \begin{bmatrix} C_{11} & C_{12} & C_{13} & C_{14} & C_{15} & C_{16} \\ & C_{22} & C_{23} & C_{24} & C_{25} & C_{26} \\ & & C_{33} & C_{34} & C_{35} & C_{36} \\ & & & C_{44} & C_{45} & C_{46} \\ & & & & C_{55} & C_{56} \\ & & & & & C_{66} \end{bmatrix} \begin{Bmatrix} \bar{\varepsilon}_{11} \\ \bar{\varepsilon}_{22} \\ \bar{\varepsilon}_{33} \\ \bar{\varepsilon}_{12} \\ \bar{\varepsilon}_{23} \\ \bar{\varepsilon}_{31} \end{Bmatrix}, \tag{4.6}$$

or

$$\{\boldsymbol{\sigma}\} = [\mathbf{C}]\{\bar{\boldsymbol{\varepsilon}}\}. \tag{4.7}$$

The corresponding strain energy function is [4.2]

$$\begin{aligned} 2W = {} & C_{11}\bar{\varepsilon}_{11}^2 + 2C_{12}\bar{\varepsilon}_{11}\bar{\varepsilon}_{22} + 2C_{13}\bar{\varepsilon}_{11}\bar{\varepsilon}_{33} + 2C_{14}\bar{\varepsilon}_{11}\bar{\varepsilon}_{12} + 2C_{15}\bar{\varepsilon}_{11}\bar{\varepsilon}_{23} \\ & + 2C_{16}\bar{\varepsilon}_{11}\bar{\varepsilon}_{31} + C_{22}\bar{\varepsilon}_{22}^2 + 2C_{23}\bar{\varepsilon}_{22}\bar{\varepsilon}_{33} + 2C_{24}\bar{\varepsilon}_{22}\bar{\varepsilon}_{12} + 2C_{25}\bar{\varepsilon}_{22}\bar{\varepsilon}_{23} \\ & + 2C_{26}\bar{\varepsilon}_{22}\bar{\varepsilon}_{31} + C_{33}\bar{\varepsilon}_{33}^2 + 2C_{34}\bar{\varepsilon}_{33}\bar{\varepsilon}_{12} + 2C_{35}\bar{\varepsilon}_{33}\bar{\varepsilon}_{23} + 2C_{36}\bar{\varepsilon}_{33}\bar{\varepsilon}_{31} \\ & + C_{44}\bar{\varepsilon}_{12}^2 + 2C_{45}\bar{\varepsilon}_{12}\bar{\varepsilon}_{23} + 2C_{46}\bar{\varepsilon}_{12}\bar{\varepsilon}_{31} \\ & + C_{55}\bar{\varepsilon}_{23}^2 + 2C_{56}\bar{\varepsilon}_{23}\bar{\varepsilon}_{31} \\ & + C_{66}\bar{\varepsilon}_{31}^2 \end{aligned} \tag{4.8}$$

from which Eqs. (4.2) produces Eq. (4.6).

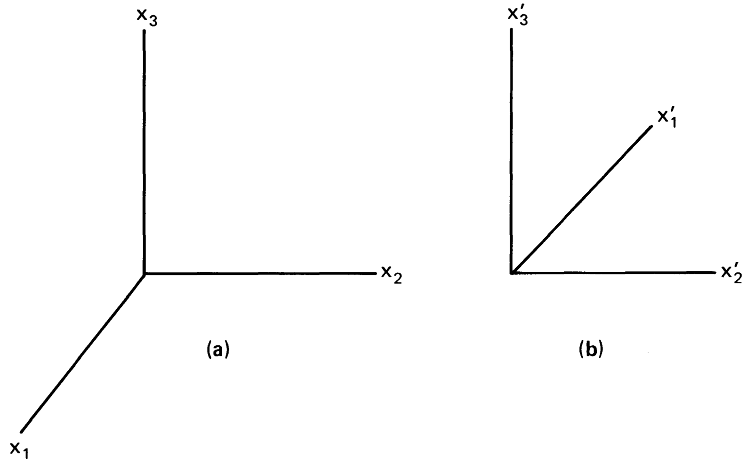

Fig. 4.2. (a) Reference material coordinates; (b) single-plane symmetry.

The preceding characterization is the most general with which we need to be concerned; such a material is termed *anisotropic* [4.3]. Fortunately, most engineering materials possess properties of symmetry about one or more of the planes or axes, which allow the number of independent constants to be reduced. Devising valid experiments to isolate each material constant can be tedious and difficult.

The first reduction is for one plane of symmetry, for example, plane $x_2 x_3$ in Fig. 4.2(a). This implies that the x_1 axis can be reversed as shown in Fig. 4.2(b), which corresponds to a coordinate transformation with direction cosines as shown below [4.4]:

	x_1	x_2	x_3
x'_1	-1		
x'_2		1	
x'_3			1 .

(4.9)

Using Eq. (2.13), $\sigma'_{ij} = \alpha_{ik}\alpha_{jl}\sigma_{kl}$, with the direction cosines given in Eq. (4.9), we find

$$\sigma'_{11} = \sigma_{11}; \quad \sigma'_{22} = \sigma_{22}; \quad \sigma'_{33} = \sigma_{33};$$

$$\sigma'_{12} = -\sigma_{12}; \quad \sigma'_{23} = \sigma_{23}; \quad \sigma'_{31} = -\sigma_{31}.$$

Similarly, using Eq. (3.16), $\varepsilon'_{ij} = \alpha_{ik}\alpha_{jl}\varepsilon_{kl}$, we find

$$\bar{\varepsilon}'_{11} = \bar{\varepsilon}_{11}; \quad \bar{\varepsilon}'_{22} = \bar{\varepsilon}_{22}; \quad \bar{\varepsilon}'_{33} = \bar{\varepsilon}_{33};$$

$$\bar{\varepsilon}'_{12} = -\bar{\varepsilon}_{12}; \quad \bar{\varepsilon}'_{23} = \bar{\varepsilon}_{23}; \quad \bar{\varepsilon}'_{31} = -\bar{\varepsilon}_{31}.$$

The preceding relations are reflected in the material law

$$\begin{Bmatrix} \sigma'_{11} \\ \sigma'_{22} \\ \sigma'_{33} \\ \sigma'_{12} \\ \sigma'_{23} \\ \sigma'_{31} \end{Bmatrix} = \begin{Bmatrix} \sigma_{11} \\ \sigma_{22} \\ \sigma_{33} \\ -\sigma_{12} \\ \sigma_{23} \\ -\sigma_{31} \end{Bmatrix} = \Bigg[\quad \mathbf{C} \quad \Bigg] \begin{Bmatrix} \bar{\varepsilon}'_{11} \\ \bar{\varepsilon}'_{22} \\ \bar{\varepsilon}'_{33} \\ \bar{\varepsilon}'_{12} \\ \bar{\varepsilon}'_{23} \\ \bar{\varepsilon}'_{31} \end{Bmatrix}$$

$$= \Bigg[\quad \mathbf{C} \quad \Bigg] \begin{Bmatrix} \bar{\varepsilon}_{11} \\ \bar{\varepsilon}_{22} \\ \bar{\varepsilon}_{33} \\ -\bar{\varepsilon}_{12} \\ \bar{\varepsilon}_{23} \\ -\bar{\varepsilon}_{31} \end{Bmatrix}. \tag{4.10}$$

Rewriting Eq. (4.10) in the form of Eq. (4.6) gives

$$\begin{Bmatrix} \sigma_{11} \\ \sigma_{22} \\ \sigma_{33} \\ \sigma_{12} \\ \sigma_{23} \\ \sigma_{31} \end{Bmatrix} = \begin{bmatrix} C_{11} & C_{12} & C_{13} & -C_{14} & C_{15} & -C_{16} \\ & C_{22} & C_{23} & -C_{24} & C_{25} & -C_{26} \\ & & C_{33} & -C_{34} & C_{35} & -C_{36} \\ & & & C_{44} & -C_{45} & C_{46} \\ & & & & C_{55} & -C_{56} \\ & & & & & C_{66} \end{bmatrix} \begin{Bmatrix} \bar{\varepsilon}_{11} \\ \bar{\varepsilon}_{22} \\ \bar{\varepsilon}_{33} \\ \bar{\varepsilon}_{12} \\ \bar{\varepsilon}_{23} \\ \bar{\varepsilon}_{31} \end{Bmatrix} \tag{4.11}$$

but, since the constants do not change with the transformation, C_{14}, C_{16}, C_{24}, C_{26}, C_{34}, C_{36}, C_{45}, $C_{56} = 0$ leaving 21 – 8, or 13, constants. Such a material is called *monoclinic* [4.4].

Next, double symmetry is achieved by the transformation

	x_1	x_2	x_3
x'_1	-1		
x'_2		-1	
x'_3			1

(4.12)

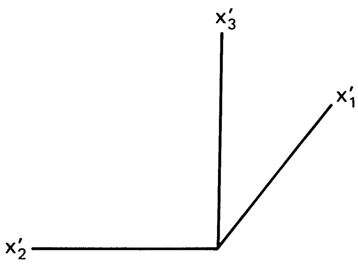

Fig. 4.3. Double-plane symmetry.

as shown in Fig. 4.3. Following a similar argument as before, the number of elastic constants is reduced from 13 to 9 producing an orthorhombic or *orthotropic* material [4.4]. No further reduction is achieved by taking $x_3' = -x_3$, since all of the axes could have been reversed initially in Fig. 4.2(a).

The stress-strain law for an *orthotropic* material is written explicitly as

$$\begin{Bmatrix} \sigma_{11} \\ \sigma_{22} \\ \sigma_{33} \\ \sigma_{12} \\ \sigma_{23} \\ \sigma_{31} \end{Bmatrix} = \begin{bmatrix} C_{11} & C_{12} & C_{13} & 0 & 0 & 0 \\ & C_{22} & C_{23} & 0 & 0 & 0 \\ & & C_{33} & 0 & 0 & 0 \\ & & & C_{44} & 0 & 0 \\ & & & & C_{55} & 0 \\ & & & & & C_{66} \end{bmatrix} \begin{Bmatrix} \bar{\varepsilon}_{11} \\ \bar{\varepsilon}_{22} \\ \bar{\varepsilon}_{33} \\ \bar{\varepsilon}_{12} \\ \bar{\varepsilon}_{23} \\ \bar{\varepsilon}_{31} \end{Bmatrix} \qquad \text{(a)} \quad (4.13)$$

or, in terms of the elastic moduli, as

$$\begin{Bmatrix} \sigma_{11} \\ \sigma_{22} \\ \sigma_{33} \\ \sigma_{12} \\ \sigma_{23} \\ \sigma_{31} \end{Bmatrix} = \begin{bmatrix} E_{1111} & E_{1122} & E_{1133} & 0 & 0 & 0 \\ & E_{2222} & E_{2233} & 0 & 0 & 0 \\ & & E_{3333} & 0 & 0 & 0 \\ & & & E_{1212} & 0 & 0 \\ & & & & E_{2323} & 0 \\ & & & & & E_{3131} \end{bmatrix} \begin{Bmatrix} \bar{\varepsilon}_{11} \\ \bar{\varepsilon}_{22} \\ \bar{\varepsilon}_{33} \\ \bar{\varepsilon}_{12} \\ \bar{\varepsilon}_{23} \\ \bar{\varepsilon}_{31} \end{Bmatrix}. \qquad \text{(b)} \quad (4.13)$$

Additional simplifications are possible if directional independence of the material properties is present. The appropriate relationships are formally derived by interchanging axes. For example, we may interchange x_2 and x_3 by the transformation

	x_1	x_2	x_3
x_1'	1	0	0
x_2'	0	0	1
x_3'	0	1	0

(4.14)

and x_1 and x_2 by

	x_1	x_2	x_3
x_1'	0	1	0
x_2'	1	0	0
x_3'	0	0	1

(4.15)

The result is a *cubic* material with three independent constants.

A final simplification is to enforce rotational independence, in addition to the directional independence, by the transformation

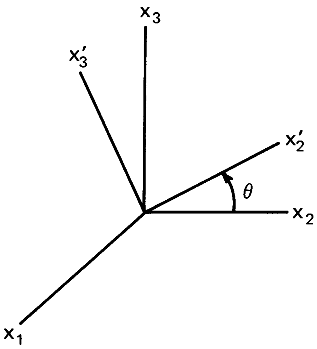

Fig. 4.4. Isotropic condition.

	x_1	x_2	x_3
x_1'	1	0	0
x_2'	0	$\cos\theta$	$\sin\theta$
x_3'	0	$-\sin\theta$	$\cos\theta$

(4.16)

as shown in Fig. 4.4. This reduces the number of constants from three to two, producing the familiar *isotropic* material. These modulii are known as the Lamé constants, since they were correctly established first by Gabriel Lamé in the middle of the 19th century [4.1], and produce the stress-strain relationship written in terms of the tensor components ε_{ij} as

$$\begin{Bmatrix} \sigma_{11} \\ \sigma_{22} \\ \sigma_{33} \\ \sigma_{12} \\ \sigma_{23} \\ \sigma_{31} \end{Bmatrix} = \begin{bmatrix} 2\mu+\lambda & \lambda & \lambda & 0 & 0 & 0 \\ \lambda & 2\mu+\lambda & \lambda & 0 & 0 & 0 \\ \lambda & \lambda & 2\mu+\lambda & 0 & 0 & 0 \\ & & & 2\mu & 0 & 0 \\ & & & & 2\mu & 0 \\ & & & & & 2\mu \end{bmatrix} \begin{Bmatrix} \varepsilon_{11} \\ \varepsilon_{22} \\ \varepsilon_{33} \\ \varepsilon_{12} \\ \varepsilon_{23} \\ \varepsilon_{31} \end{Bmatrix} \tag{4.17}$$

or, in indicial form,

$$\sigma_{ij} = 2\mu\varepsilon_{ij} + \lambda\delta_{ij}\varepsilon_{kk}. \tag{4.18}$$

It is useful to invert Eq. (4.18), expressing the strains in terms of the stresses. This is best accomplished by first setting $i = j$ and expressing ε_{kk} in terms of σ_{kk}, and then solving the resulting Eq. (4.18) for ε_{ij}. This gives

$$\varepsilon_{ij} = \frac{1}{2\mu}\sigma_{ij} - \frac{\lambda}{2\mu(2\mu + 3\lambda)}\delta_{ij}\sigma_{kk}. \tag{4.19}$$

Although the Lamé constants are perfectly suitable from a mathematical standpoint, it is common to use *engineering* material constants that are related to measurements from elementary mechanical tests.

For a uniaxial stress with σ_{11} constant and all other $\sigma_{ij} = 0$,

$$\begin{aligned} \sigma_{11} &= (2\mu + \lambda)\varepsilon_{11} + \lambda\varepsilon_{22} + \lambda\varepsilon_{33}, && \text{(a)} \\ 0 &= \lambda\varepsilon_{11} + (2\mu + \lambda)\varepsilon_{22} + \lambda\varepsilon_{33}, && \text{(b)} \\ 0 &= \lambda\varepsilon_{11} + \lambda\varepsilon_{22} + (2\mu + \lambda)\varepsilon_{33}. && \text{(c)} \end{aligned} \tag{4.20}$$

Solving (4.20b) and (4.20c) for $\varepsilon_{22} + \varepsilon_{33}$ and then substituting into Eq. (4.20a) gives

$$\sigma_{11} = \frac{\mu(2\mu + 3\lambda)}{\mu + \lambda}\varepsilon_{11} = E\varepsilon_{11}. \tag{4.21}$$

Young's modulus, E, was defined in Section 4.2.

From the same uniaxial stress state, the *fractional contraction* may be computed as

$$-\frac{\varepsilon_{22}}{\varepsilon_{11}} = -\frac{\varepsilon_{33}}{\varepsilon_{11}} = \frac{\lambda}{2(\mu + \lambda)} = \nu, \tag{4.22}$$

where ν is Poisson's ratio.

A third engineering constant is obtained from the state of *pure shear* in two dimensions, given by $\sigma_{12} = \sigma_{21} =$ constant, all other $\sigma_{ij} = 0$. From Eq. (4.18),

$$\sigma_{12} = 2\mu\varepsilon_{12} = 2G\varepsilon_{12}, \tag{4.23}$$

where G is the shear modulus.

Although the engineering constants E, ν and G are convenient, we realize that only *two* of these constants are independent since $G = \mu$ and both E and ν are defined in terms of λ and μ. The relationships between the Lamé and engineering constants are collected as

$$\begin{aligned} \mu &= \frac{E}{2(1 + \nu)}, && \text{(a)} \\ \lambda &= \frac{\nu E}{(1 + \nu)(1 - 2\nu)}, && \text{(b)} \\ E &= \frac{\mu(2\mu + 3\lambda)}{\mu + \lambda}, && \text{(c)} \\ \nu &= \frac{\lambda}{2(\mu + \lambda)}, && \text{(d)} \\ G &= \mu. && \text{(e)} \end{aligned} \tag{4.24}$$

Note from Eq. (4.24b) that for λ to remain finite, Poisson's ratio must lie between

$$-1 < \nu < 0.5. \tag{4.25}$$

From Eq. (4.22) it is difficult to visualize a negative value since it implies that an elongational strain in the 1 direction would result in an expansion in the 2 direction as well; but, see Ch. 12. Poisson's ratio is also related to the volume change or dilatation, introduced in Sec. 3.5. We write Eq. (3.41) for an extension of an isotropic material applied along the 1-principal axis as

$$\varepsilon^{(1)} = \bar{\varepsilon}, \tag{4.26}$$

whereupon Eq. (4.22) gives

$$\varepsilon^{(2)} = \varepsilon^{(3)} = -\nu\bar{\varepsilon}. \tag{4.27}$$

Then

$$\Delta = \bar{\varepsilon}(1 - 2\nu). \tag{4.28}$$

If $\nu = 0.5$, the upper positive limit, $\Delta = 0$ and the material is said to be incompressible. Rubber-like materials exhibit this type of behavior.

The explicit form of the generalized Hooke's law in terms of the engineering constants is best written in the inverse form

$$\{\varepsilon\} = [C]^{-1}\{\sigma\}, \tag{4.29a}$$

or

$$\begin{Bmatrix} \varepsilon_{11} \\ \varepsilon_{22} \\ \varepsilon_{33} \\ \varepsilon_{12} \\ \varepsilon_{23} \\ \varepsilon_{31} \end{Bmatrix} = \begin{bmatrix} \frac{1}{E} & -\frac{\nu}{E} & -\frac{\nu}{E} & 0 & 0 & 0 \\ -\frac{\nu}{E} & \frac{1}{E} & -\frac{\nu}{E} & 0 & 0 & 0 \\ -\frac{\nu}{E} & -\frac{\nu}{E} & \frac{1}{E} & 0 & 0 & 0 \\ 0 & 0 & 0 & \frac{1}{2G} & 0 & 0 \\ 0 & 0 & 0 & 0 & \frac{1}{2G} & 0 \\ 0 & 0 & 0 & 0 & 0 & \frac{1}{2G} \end{bmatrix} \begin{Bmatrix} \sigma_{11} \\ \sigma_{22} \\ \sigma_{33} \\ \sigma_{12} \\ \sigma_{23} \\ \sigma_{31} \end{Bmatrix}. \tag{4.29b}$$

The elements of $[C]^{-1}$ have been explicitly defined, with reference to Eqs. (4.21)–(4.23). In general, these coefficients are called compliances. In indicial notation with G, replaced by E using Eqs. (4.24e and a), Eq. (4.29b) becomes

$$\varepsilon_{ij} = \frac{1}{E}[(1 + \nu)\sigma_{ij} - \nu\delta_{ij}\sigma_{kk}]. \tag{4.30}$$

Recalling the discussion at the end of Section 3.6 and comparing the number of equations available (nine) and the number of unknowns introduced (fifteen), we see that the material law provides six additional equations, yet involves no additional unknowns; thus, the set of equations for the linear theory of elasticity is consistent. In the next chapter, we will explore methods of reducing the equations as well as additional constraints on the theory.

4.4 Thermal Strains

Temperature changes may be a source of important stresses in elastic systems. It is reasonable to assume that a linear relationship exists between the temperature difference from the datum value and the corresponding linear strain:

$$\varepsilon_{(ii)}(T) = \alpha[T - T_0], \tag{4.31}$$

in which $\varepsilon_{(ii)}(T)$ is the linear strain due to the temperature difference $T - T_0$, T_0 is the datum temperature, and α the *coefficient of thermal expansion*, assumed here to be a *constant*.

With this concept, it is easy to generalize Eq. (4.30) to become

$$\varepsilon_{ij} = \frac{1}{E}[(1 + \nu)\sigma_{ij} - \nu\delta_{ij}\sigma_{kk}] + \alpha\delta_{ij}[T - T_0]. \tag{4.32}$$

We can also generalize Eq. (4.18) to become

$$\sigma_{ij} = 2\mu\varepsilon_{ij} + \lambda\delta_{ij}\varepsilon_{kk} - \alpha\delta_{ij}(3\lambda + 2\mu)[T - T_0]. \tag{4.33}$$

When these expressions are used in subsequent applications, the thermal terms are carried through as constants and ultimately become grouped with the applied tractions and/or body forces. In this form, they have come to be known as *thermal loads* that can be treated along with mechanical loads as known quantities.

Obvious complications are produced when temperatures outside the normal environmental range are considered since both the material properties such as E and G and the thermal coefficient α may become, possibly nonlinear, functions of the temperature.

4.5 Physical Data

Since the implementation of the various material models is based on physical data, it is necessary either to obtain relevant data or to construct appropriate experiments. The literature is rich with data for a wide variety of materials, but, because they are oriented to specific applications, these data are somewhat scattered. Some procedures are discussed with respect to strength criteria in Ch. 11. For orthotropic materials, a detailed interpretation of the constants in Eq. 4.13 is provided by Vinson and Sierakowski [4.5]. A comprehensive guide to the techniques of constitutive modeling that treats metals, concrete and soils from an elasticity basis may facilitate the collection and interpretation of physical data [4.6].

Exercises

4.1 Derive the generalized Hooke's law for an orthotropic elastic solid, starting with the equations for an anisotropic material [4.3].

4.2 For an isotropic material, obtain the relationship

$$\varepsilon_{ij} = \frac{1}{2\mu}\sigma_{ij} - \frac{\lambda}{2\mu(2\mu + 3\lambda)}\delta_{ij}\sigma_{kk},$$

from the expression

$$\sigma_{ij} = 2\mu\varepsilon_{ij} + \lambda\delta_{ij}\varepsilon_{kk}.$$

4.3 Show that the principal axes of stress correspond with the principal axes of strain for an isotropic, linearly elastic material.

4.4 Extend the stress-strain laws to include thermal effects assuming that the coefficient of thermal expansion is equal to α. How does this complicate the formulation of the elasticity problem?

4.5 For steel, $E = 30 \times 10^6$ and $G = 12 \times 10^6$ (force/length^2). The components of strain at a point within this material are given by

$$\boldsymbol{\varepsilon} = \begin{bmatrix} 0.004 & 0.001 & 0 \\ 0.001 & 0.006 & 0.004 \\ 0 & 0.004 & 0.001 \end{bmatrix}.$$

Compute the corresponding components of the stress tensor.

4.6 Verify the relations (a) and (b) of Eq. (4.24) by using (c) and (d).

4.7 Determine the constitutive relations governing the material behavior of a point having the properties described below. Would the material be classified as anisotropic, orthotropic or isotropic?

(a) A point in the material has a state of stress given by the following:

$$\sigma_{11} = 10.8; \quad \sigma_{22} = 3.4; \quad \sigma_{33} = 3.0$$
$$\sigma_{12} = \sigma_{13} = \sigma_{23} = 0.$$

(b) The material develops the corresponding strain components

$$\varepsilon_{11} = 10 \times 10^{-4}; \quad \varepsilon_{22} = 2 \times 10^{-4}; \quad \varepsilon_{33} = 2 \times 10^{-4};$$
$$\varepsilon_{12} = \varepsilon_{23} = \varepsilon_{31} = 0.$$

(c) When a state of stress of

$$\sigma_{11} = 10; \quad \sigma_{22} = 2; \quad \sigma_{33} = 2;$$
$$\sigma_{12} = \sigma_{23} = \sigma_{31} = 0$$

is applied, the strain components are

$$\varepsilon_{11} = 10 \times 10^{-4}; \quad \varepsilon_{22} = \varepsilon_{33} = \varepsilon_{12} = \varepsilon_{23} = \varepsilon_{31} = 0.$$

(d) When subjected to a shearing stress σ_{12}, σ_{13} or σ_{23} of 10, the material develops no strains except the corresponding shearing strain, with tensor component ε_{12}, ε_{13} or ε_{23}, of 20×10^{-4}.

4.8 Show that the stress-strain relationships for an isotropic material, Eq. (4.18) can be written in the general form of Eq. (4.3) where

(a) $E_{ijkl} = G(\delta_{ik}\delta_{jl} + \delta_{il}\delta_{jk}) + (K - \frac{2}{3}G)\delta_{ij}\delta_{kl}$

where $K = \dfrac{E}{3(1 - 2\nu)}$ is known as the Bulk Modulus [4.7].

(b) $E_{ijkl} = \lambda\delta_{ij}\delta_{lm} + \mu\delta_{il}\delta_{jm} + \mu\delta_{im}\delta_{jl}$ [4.8].

4.9 Consider an isotropic elastic medium subject to a hydrostatic state of stress

$$\sigma^{(1)} = \sigma^{(2)} = \sigma^{(3)} = -p.$$

Show that for this state of stress

$$p = -KR_1$$

where K is the Bulk Modulus and R_1 is the cubical strain (Sec. 3.4). Consider the implications of $\nu > 1/2$ and $\nu < -1$. [4.9]

4.10 For an elastic medium subject to a state of stress σ_{ij}, assume that the deformation is incompressible for $\sigma_{ii} \neq 0$.

(a) Verify that $\nu = 0.5$.

(b) Assume also that $\varepsilon_{33} = 0$ and determine ν. [4.9]

References

[4.1] Westergaard, H. M., *Theory of Elasticity and Plasticity* (Dover Publications, Inc., New York, 1964).

[4.2] Love, A. E. H., *The Mathematical Theory of Elasticity* (Dover Publications, Inc., New York, 1944).

[4.3] Tauchert, T. R., *Energy Principles in Structural Mechanics* (McGraw–Hill Book Company, Inc., New York, 1974).

[4.4] Little, R. W., *Elasticity* (Prentice–Hall, Inc., Englewood Cliffs, NJ, 1973).

[4.5] Vinson, J. R., and Sierakowski, R. L., *The Behavior of Structures Composed of Composite Materials* (Martinus Nijhoff, Dordrecht, 1986).

[4.6] Chen, W. F., and Saleeb, A. F., *Constitutive Equations for Engineering Materials, Vol. 1* (John Wiley-Interscience, New York, 1982).

[4.7] Ohtani, Y. C., and Chen, W. F., "Hypoelasticity-Perfectly Plastic Model for Concrete Materials," *Journal of Engineering Mechanics*, ASCE, Vol. 113, No. 12, December, 1987, pp. 1840–1860.

[[4.8] Meek, J. L., and Lin, W. J., "Geometric and Material Nonlinear Analysis of Thin-Walled Beam Columns," *Journal of Structural Engineering*, Vol. 116, No. 6, June, 1990, pp. 1473–1490.

[4.9] Boresi, A. P., and Chong, K. P., *Elasticity in Engineering Mechanics* (Elsevier, New York, 1987).

CHAPTER 5

Formulation, Uniqueness and Solution Strategies

5.1 Introduction

In the previous chapters, we have derived the essential equations of the linear theory of elasticity. Repeated here in terse form, the equilibrium conditions [Eqs. (2.34)] are

$$\sigma_{ij,i} + f_j = 0; \tag{5.1}$$

the kinematic relations [Eqs. (3.14)] are

$$\varepsilon_{ij} = \tfrac{1}{2}(u_{i,j} + u_{j,i}), \tag{5.2}$$

with the compatibility constraints [Eqs. (3.60)]

$$\varepsilon_{ij,kl} + \varepsilon_{kl,ij} = \varepsilon_{ik,jl} + \varepsilon_{jl,ik}; \tag{5.3}$$

and the constitutive law [Eqs. (4.18) and (4.19)] is given by

$$\sigma_{ij} = \lambda\delta_{ij}\varepsilon_{kk} + 2\mu\varepsilon_{ij} \tag{5.4}$$

or

$$\varepsilon_{ij} = \frac{1}{E}[(1 + \nu)\sigma_{ij} - \nu\delta_{ij}\sigma_{kk}]. \tag{5.5}$$

In this chapter, we combine and reduce these equations, we establish the necessary and sufficient conditions governing the uniqueness of a solution, and we introduce some approaches to the solution of an elasticity problem.

5.2 Displacement Formulation

With a view toward retaining only the displacements u_i, we substitute Eq. (5.2) into Eq. (5.4) to eliminate the strains, yielding

$$\sigma_{ij} = \lambda\delta_{ij}u_{k,k} + \mu(u_{i,j} + u_{j,i}) \tag{5.6}$$

a relationship between stresses and displacements. Next, the stresses in Eq.

(5.1) are replaced by Eq. (5.6) to give

$$\lambda\delta_{ij}u_{k,ki} + \mu(u_{i,ji} + u_{j,ii}) + f_j = 0$$

which reduces to

$$\lambda u_{k,kj} + \mu(u_{i,ji} + u_{j,ii}) + f_j = 0$$

or, using i for the dummy index in all terms,

$$\mu u_{j,ii} + (\lambda + \mu)u_{i,ij} + f_j = 0. \tag{5.7}$$

Equations (5.7) are three equilibrium equations in terms of the displacements and constitute a classical *displacement* formulation. These are known as the *Lamé equations* [5.1] and, in the case where the displacement field u_j is continuous and differentiable, the corresponding strain field ε_{ij} always satisfies Eq. (5.3).

The solution of Eqs. (5.7) produces functions and constants of integration that are evaluated from boundary conditions, expressed in terms of displacements. We may also encounter boundary conditions involving tractions. Fortunately, such conditions can often be incorporated into the loading terms, especially in numerical solutions.

5.3 Force Formulation

An alternate to the classical displacement formulation is to synthesize the equations in terms of the stresses σ_{ij}. If the stresses are known, the strains follow directly from Eq. (5.5), but the displacements remain to be evaluated from Eq. (5.2). In this case, these are six equations to find only three displacements. However, the strains must also satisfy the compatibility constraints Eqs. (5.3) in order to insure that the integration of Eqs. (5.2) provides a single-valued displacement field. With this in mind, it is helpful to rewrite Eqs. (5.3) in terms of the stresses from the outset.

We start by substituting Eq. (5.5) into Eq. (5.3) to produce

$$\sigma_{ij,kl} + \sigma_{kl,ij} - \sigma_{ik,jl} - \sigma_{jl,ik} = \frac{\nu}{1+\nu}(\delta_{ij}\sigma_{tt,kl} + \delta_{kl}\sigma_{tt,ij} - \delta_{ik}\sigma_{tt,jl} - \delta_{jl}\sigma_{tt,ik}) \tag{5.8}$$

which are again 81 equations. We recall from the discussion in Section 3.6 that only six of Eqs. (5.3), corresponding to the conditions $k = l$, are independent, so that Eq. (5.8) reduces to

$$\sigma_{ij,kk} + \sigma_{kk,ij} - \sigma_{ik,jk} - \sigma_{jk,ik} = \frac{\nu}{1+\nu}(\delta_{ij}\sigma_{tt,kk} + \delta_{kk}\sigma_{tt,ij} - \delta_{ik}\sigma_{tt,jk} - \delta_{jk}\sigma_{tt,ik}), \tag{5.9}$$

which are nine equations with free indices i and j.

To simplify the equations somewhat, we recall Eq. (2.59a) where

$$Q_1 = \sigma_{tt} = \text{first stress invariant,} \qquad \text{(a)} \quad (5.10)$$

we use

$$(\ )_{,kk} = \nabla^2(\ ), \text{ from Eq. (1.10b)} \qquad \text{(b)} \quad (5.10)$$

and we note that

$$\begin{aligned} \delta_{kk}\sigma_{tt,ij} &= 3\sigma_{tt,ij} = 3Q_{1,ij} && \text{(c)} \\ \delta_{ik}\sigma_{tt,jk} &= \sigma_{tt,ij} = Q_{1,ij} && \text{(d)} \quad (5.10) \\ \delta_{jk}\sigma_{tt,ik} &= \sigma_{tt,ij} = Q_{1,ij}, && \text{(e)} \end{aligned}$$

so that Eq. (5.9) becomes

$$\nabla^2\sigma_{ij} + Q_{1,ij} - \sigma_{ik,jk} - \sigma_{jk,ik} = \frac{v}{1+v}(\delta_{ij}\nabla^2 Q_1 + 3Q_{1,ij} - 2Q_{1,ij}). \quad (5.11)$$

Furthermore, we recall from Eqs. (5.1) that

$$\sigma_{ik,jk} = -f_{i,j} \qquad \text{(a)}$$

and (5.12)

$$\sigma_{jk,ik} = -f_{j,i}. \qquad \text{(b)}$$

Combining terms and considering the preceding relations, we have

$$\nabla^2\sigma_{ij} + \frac{1}{1+v}Q_{1,ij} - \frac{v}{1+v}\delta_{ij}\nabla^2 Q_1 + f_{i,j} + f_{j,i} = 0. \quad (5.13)$$

Equations (5.13) are nine in number; however, only six are independent since the stress tensor is symmetric. It is possible to reduce the equations further by utilizing the additional Eqs. (5.8), when $k \neq l$. Letting $k = i$ and $l = j$, we have

$$\sigma_{ij,ij} + \sigma_{ij,ij} - \sigma_{ii,jj} - \sigma_{jj,ii} = \frac{v}{1+v}(\delta_{ij}\sigma_{tt,ij} + \delta_{ij}\sigma_{tt,ij} - \delta_{ii}\sigma_{tt,jj} - \delta_{jj}\sigma_{tt,ii}),$$

which is

$$2\sigma_{ij,ij} - 2\nabla^2 Q_1 = \frac{v}{1+v}(2\nabla^2 Q_1 - 6\nabla^2 Q_1),$$

so that

$$\sigma_{ij,ij} = \left(1 - \frac{2v}{1+v}\right)\nabla^2 Q_1$$

or

$$\nabla^2 Q_1 = \frac{1+v}{1-v}\sigma_{ij,ij} = -\frac{1+v}{1-v}f_{j,j} \quad (5.14)$$

from Eq. (5.1). Thus, equilibrium is introduced into Eqs. (5.13) through the substitution of Eq. (5.14) for $\nabla^2 Q_1$

$$\nabla^2 \sigma_{ij} + \frac{1}{1+\nu} Q_{1,ij} = \frac{-\nu}{1-\nu} \delta_{ij} f_{k,k} - (f_{i,j} + f_{j,i}). \tag{5.15}$$

If the body forces are constant, Eq. (5.15) reduces to

$$\nabla^2 \sigma_{ij} + \frac{1}{1+\nu} Q_{1,ij} = 0. \tag{5.16}$$

Furthermore, comparing Eq. (5.16) with Eq. (5.13), also with body forces constant, we deduce that

$$\nabla^2 Q_1 = 0, \tag{5.17}$$

that is, $\nabla^2 \sigma_{ii} = 0$ so that Q_1 is a harmonic function.

Equations (5.15) or (5.16) are a set of compatibility equations in terms of stresses (as opposed to the St. Venant equations that are in terms of strain) for a *body in equilibrium* and are known as the Beltrami–Michell equations [5.1] after the originator Eugenio Beltrami, and John–Henry Michell who treated the case of nonconstant body forces. Together with Eqs. (5.1), they constitute a set of six equations in six unknown components of stress, and they represent a classical *force* formulation. If a stress field is formed that satisfies these equations and the corresponding strains computed from Eq. (5.5) are integrated in Eq. (5.2), the displacement field is insured to be single-valued. However, this process may be quite tedious, as is demonstrated in Section 6.2.

Consideration of boundary conditions involving tractions is straightforward; however, constraints on the displacements are generally deferred until the subsequent integration of the kinematic relations. It is sometimes rather difficult to express such constraints directly as equivalent statements on the stresses.

5.4 Other Formulations

Beyond the classical displacement and force formulations, there remains the possibility of using reduced equations that contain a mixture of stress and displacement and, possibly, strain terms. Such an approach is called a *mixed* formulation [5.1]. Additionally, there is the possibility of employing different formulations in various regions of the domain; for example, a stress formulation on the boundary and a displacement formulation in the interior. This is termed a *hybrid* approach and, obviously, covers many possibilities.

Mixed and hybrid formulations are of considerable interest for numerical solutions in the theory of elasticity and may offer expedient alternatives to the more classical approaches.

5.5 Uniqueness

We seek to prove that a solution to the equations synthesized from Eqs. (5.1) to (5.5) is unique for a given region with reasonable boundary conditions.

A counterargument is followed whereby it is assumed that two distinct solutions, say $u_i^{(1)}$ and $u_i^{(2)}$, exist [5.1]. We designate the *differences* between the solutions by asterisk (*) superscripts, that is,

$$u_i^* = u_i^{(1)} - u_i^{(2)}, \tag{5.18}$$

and endeavor to show that $u_i^* = 0$.

The corresponding differences for the strains and stresses are

$$\begin{aligned} \varepsilon_{ij}^* &= \varepsilon_{ij}^{(1)} - \varepsilon_{ij}^{(2)} \\ &= \tfrac{1}{2}(u_{i,j}^* + u_{j,i}^*) \end{aligned} \tag{5.19}$$

and

$$\sigma_{ij}^* = \sigma_{ij}^{(1)} - \sigma_{ij}^{(2)}. \tag{5.20}$$

Since the body forces are identical, $f_j^* = 0$, and since both systems are in equilibrium

$$\sigma_{ij,j}^* = 0. \tag{5.21}$$

To continue, we consider the energy difference

$$2U^* = \int_V \varepsilon_{ij}^* \sigma_{ij}^* \, dV, \tag{5.22}$$

where U is the strain energy. This expression is non-negative, as discussed in Section 4.3. We replace ε_{ij}^* by Eq. (5.19) to give

$$\begin{aligned} \int_V \varepsilon_{ij}^* \sigma_{ij}^* \, dV &= \int_V \frac{1}{2}(u_{i,j}^* + u_{j,i}^*)\sigma_{ij}^* \, dV \\ &= \int_V u_{i,j}^* \sigma_{ij}^* \, dV, \end{aligned} \tag{5.23}$$

since the i and j become repeated indices. Continuing with the r.h.s. of Eq. (5.23) and using the product differentiation rule $(u_i^* \sigma_{ij}^*)_{,j} = \sigma_{ij}^* u_{i,j}^* + u_i^* \sigma_{ij,j}^*$,

$$\begin{aligned} \int_V \varepsilon_{ij}^* \sigma_{ij}^* \, dV &= \int_V (u_i^* \sigma_{ij}^*)_{,j} \, dV - \int_V u_i^* \sigma_{ij,j}^* \, dV \\ &= \int_A u_i^* \sigma_{ij}^* n_j \, dA - 0, \end{aligned} \tag{5.24}$$

where the first term on the r.h.s. is converted to a surface integral using the divergence theorem in component form, Eq. (2.32), and the second term vanishes by Eq. (5.21).

Noting that in the remaining term $\sigma_{ij}^* n_j = T_i^*$, we may finally write

$$\int_V \varepsilon_{ij}^* \sigma_{ij}^* \, dV = \int_A u_i^* T_i^* \, dA$$
$$= \int_A (u_i^{(1)} - u_i^{(2)})(T_i^{(1)} - T_i^{(2)}) \, dA. \tag{5.25}$$

Now, if the r.h.s. of Eq. (5.25) vanishes, the *energy difference* between the two solutions also vanishes and they are *identical*. Therefore, our proof of uniqueness covers the following conditions for which this occurs:

(1) The displacement field u_i is prescribed on the entire surface, making $u_i^* = 0$.
(2) The tractions T_i are prescribed over the entire surface while overall equilibrium is satisfied, making $T_i^* = 0$.
(3) Displacements u_i are prescribed on part of the surface and tractions T_i on the remainder, so that either u_i^* or $T_i^* = 0$.

It is also of interest to note that the proof of uniqueness, while insuring the same set of stresses and strains in both solutions, does not automatically insure that the displacements are identical. In particular, for condition (2), where the tractions are prescribed over the entire surface, *rigid body displacements* could be added without affecting this condition [5.1].

The preceding constraints are limited to *regular*, *singly-connected* regions where the basic form of the divergence theorem, used in Eq. (5.24), is applicable. Extensions to more complex domains are also possible [5.2].

5.6 Membrane Equation

Several problems in the theory of elasticity lend themselves to solution by analogy. One of the most popular is based on the deflection of a uniformly stretched membrane. In Fig. 5.1 we show such a membrane stretched over a cross section and inflated with a pressure q per unit area with a uniform tension T per unit length of the boundary. We consider a rectangular element abcd and write the equilibrium equation in the z direction, noting that the *slopes* of the membrane change by

$$\frac{\partial u_{z,x}}{\partial x} dx \quad \text{and} \quad \frac{\partial u_{z,y}}{\partial y} dy$$

over the element in the respective directions. Thus, we have

$$q dx dy - T dy u_{z,x} + T dy [u_{z,x} + u_{z,xx} \, dx] - T dx u_{z,y} + T dx [u_{z,y} + u_{z,yy} \, dy] = 0$$

or

$$u_{z,xx} + u_{z,yy} = -\frac{q}{T} \tag{5.26}$$

Also, at the boundary, the deflection $u_z = 0$.

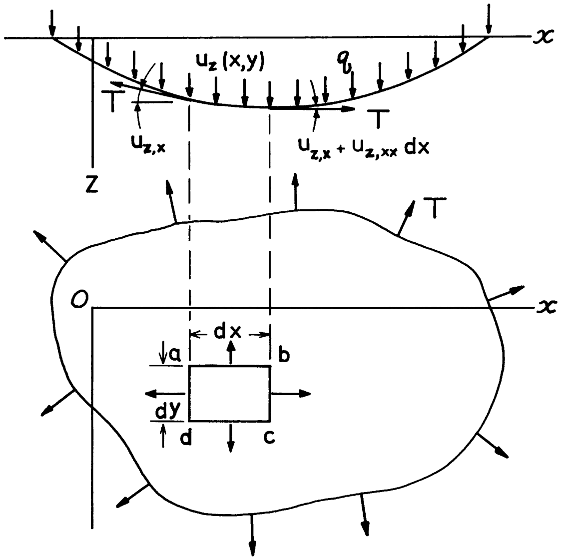

Fig. 5.1. Pressurized membrane. From Timoshenko and Goodier, *Theory of Elasticity*, © 1951. Reproduced with permission of McGraw-Hill.

Equation (5.26) is known as Poisson's equation and occurs repeatedly in the Theory of Elasticity, thereby providing a basis for the so-called membrane analogies, which are used in Ch. 6.

5.7 Solution Strategies

The obvious course is to attempt to carry out a direct integration of the partial differential equations, and then to apply the appropriate boundary conditions. However, the *direct method* is relatively difficult except for some fairly elementary problems.

A second approach is to select stress or strain fields that satisfy the governing differential equations, and then to consider the boundary conditions that are satisfied. Finally, the boundary-value problem that the solution represents is formulated. This is appropriately called the *inverse* method and, at first glance, seems to suggest that one may simply create a problem to fit the available solution, hardly a realistic approach.

The inverse method is meaningful when we look to the origin of stress or strain fields that may satisfy the governing equations. These may be borrowed, in many cases, from a less-rigorous, but hopefully approximately correct, solution to a meaningful problem found from the strength of materials. It is soon realized, however, that such solutions are in some way deficient, so that a third approach is to begin with part of the solution from this source and to develop the remainder by direct integration. This is known as the *semi-inverse* method and is the one of many contributions of Barre'de A. J. C.

St. Venant to the theory of elasticity. The principal historians of the subject, Issac Todhunter and Carl Pearson, devote a major share of their first volume to his memory as the foremost of the modern elasticians [5.3].

In addition to analytical solutions of the governing differential equations, energy-based solutions play an important role in all of solid mechanics. Energy theorems also are the foundation for the powerful finite element method, which has become central to numerical techniques currently in use.

Another notion, attributed to St. Venant, that aids immeasurably in obtaining practical solutions to elasticity problems, is the concept of statically equivalent loads. *St. Venant's principle* [5.2] states that stresses and strains *reasonably distant* from the point of application of an external force are not significantly altered if the applied force is replaced by a *statically equivalent* load. An important consequence of this statement, from an engineering stand-point, is that satisfactory solutions may be obtained for the interior regions of a body without undue concern about the exact local distribution of the applied surface loading or the restraining boundary tractions. While there are some notable exceptions, such as cylindrical shells under concentrated axial edge load, which tend to propagate far into the interior without much diffusion, St. Venant's principle is broadly applicable and is most useful in applied elasticity.

Exercises

5.1 The stress components at point $P(x, y, z)$ are (after [5.4])

$$\begin{aligned} \sigma_{xx} &= y + 3z^2 & \sigma_{xy} &= z^3, \\ \sigma_{yy} &= x + 2z & \sigma_{xz} &= y^2, \\ \sigma_{zz} &= 2x + y & \sigma_{yz} &= x^2. \end{aligned}$$

No body forces are present.

(a) Does this stress field satisfy equilibrium?

(b) Does this stress field satisfy compatibility?

5.2 Write the Beltrami–Michell equations for the case where $\sigma_{zz} = 0$ (plane stress) and show that (after [5.5])

$$\sigma_{ii} = kz + f(x, y),$$

where k is a constant.

5.3 For the following stress field

$$\begin{aligned} \sigma_{xx} &= 80x^3 + y, & \sigma_{xy} &= 1000 + 100y^2, \\ \sigma_{yy} &= 100x^3 + 1600, & \sigma_{xz} &= 0, \\ \sigma_{zz} &= 90y^2 + 100z^3, & \sigma_{yz} &= xz^3 + 100x^2y. \end{aligned}$$

(a) What is the body force distribution required for equilibrium?

(b) What is the stress and body force at (1, 1, 5)?

(c) With $E = 30 \times 10^6$ (force/length^2) and $\nu = 0.3$, what is the strain at (2, 2, 5)?

(d) Does this stress distribution satisfy the equations of compatibility?

References

[5.1] Filonenko–Borodich, M., *Theory of Elasticity*, trans. from Russian by M. Konayeon (Dover Publications, Inc., New York, 1965).

[5.2] Timoshenko, S., and Goodier, J. N., *Theory of Elasticity* (McGraw–Hill Book Company, Inc., New York, 1951).

[5.3] Westergaard, H. M., *Theory of Elasticity and Plasticity* (Dover Publications, Inc., New York, 1964).

[5.4] Volterra, E., and Gaines, J. H., *Advanced Strength of Materials* (Prentice–Hall, Inc., Englewood Cliffs, NJ, 1971).

[5.5] Little, R. W., *Elasticity* (Prentice–Hall, Inc., Englewood Cliffs, NJ, 1973).

CHAPTER 6

Extension, Bending and Torsion

6.1 Introduction

It is instructive to examine some familiar problems, readily solved by elementary theories based on a strength of materials approach, using the theory of elasticity. We anticipate that the elementary solutions are approximately correct, but deficient or incomplete in some way. In each case, the isotropic material law is assumed to be applicable.

6.2 Prismatic Bar Under Axial Loading

We consider the bar shown in Fig. 6.1(a), suspended from a fixed support and loaded by self-weight γ (force/volume) [6.1].

First, we consider the equilibrium condition Eqs. (2.46) with $1 = x$, $2 = y$ and $3 = z$; $f_x = f_y = 0$ and $f_z = -\gamma$; and $\sigma_{ij} = \sigma_{ji}$

$$\begin{aligned} \sigma_{xx,x} + \sigma_{xy,y} + \sigma_{xz,z} &= 0, \\ \sigma_{xy,x} + \sigma_{yy,y} + \sigma_{yz,z} &= 0, \\ \sigma_{xz,x} + \sigma_{yz,y} + \sigma_{zz,z} &= \gamma. \end{aligned} \tag{6.1}$$

We also have an overall equilibrium relationship between the normal component of the traction T_z at $z = l$, $\sigma_{zz}(x, y, L)$, and the self-weight given by

$$\int_{-B/2}^{B/2} \int_{-D/2}^{D/2} \sigma_{zz}(x, y, L)\, dy\, dx = \gamma BDL. \tag{6.2}$$

We invoke St. Venant's principle and seek a solution away from the support region without concern for the exact stress distribution there. The semi-inverse approach discussed in Section 5.7 is followed, whereby the stresses are taken as

$$\begin{aligned} \sigma_{zz} &= \gamma z, \\ \sigma_{xx} = \sigma_{yy} &= \sigma_{xy} = \sigma_{xz} = \sigma_{yz} = 0, \end{aligned} \tag{6.3}$$

which satisfies Eqs. (6.1) and (6.2) for equilibrium. All surfaces except $z = L$

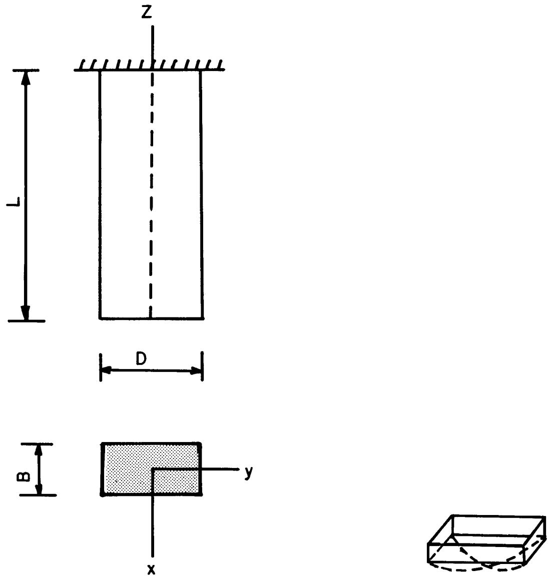

(a) (b)

Fig. 6.1. (a) Prismatic bar in extension; (b) deformed cross section of prismatic bar.

are stress-free, corresponding to condition (2) for uniqueness in Section 5.5; thus, the distribution given by Eq. (6.3) is satisfactory.

Proceeding to the strain-stress relationships Eqs. (4.29b), we have

$$\begin{aligned}
\varepsilon_{xx} &= \frac{1}{E}[\sigma_{xx} - \nu(\sigma_{yy} + \sigma_{zz})] = -\frac{\nu}{E}\gamma z \\
\varepsilon_{yy} &= \frac{1}{E}[\sigma_{yy} - \nu(\sigma_{xx} + \sigma_{zz})] = -\frac{\nu}{E}\gamma z \\
\varepsilon_{zz} &= \frac{1}{E}[\sigma_{zz} - \nu(\sigma_{xx} + \sigma_{yy})] = \frac{1}{E}\gamma z \\
\varepsilon_{xy} &= \frac{1}{2G}\sigma_{xy} = 0 \\
\varepsilon_{yz} &= \frac{1}{2G}\sigma_{yz} = 0 \\
\varepsilon_{xz} &= \frac{1}{2G}\sigma_{xz} = 0.
\end{aligned} \tag{6.4}$$

Since the strains are linear, the compatibility equations Eqs. (3.59), are automatically satisfied.

We should now be able to achieve a single-valued displacement field by the integration of Eqs. (3.15) [6.1], which take the form

$$\varepsilon_{xx} = u_{x,x} = -\frac{\nu}{E}\gamma z \quad \text{(a)}$$

$$\varepsilon_{yy} = u_{y,y} = -\frac{\nu}{E}\gamma z \quad \text{(b)}$$

$$\varepsilon_{zz} = u_{z,z} = \frac{1}{E}\gamma z \quad \text{(c)}$$

$$\varepsilon_{xy} = \tfrac{1}{2}(u_{x,y} + u_{y,x}) = 0 \quad \text{(d)} \qquad (6.5)$$

$$\varepsilon_{yz} = \tfrac{1}{2}(u_{y,z} + u_{z,y}) = 0 \quad \text{(e)}$$

$$\varepsilon_{xz} = \tfrac{1}{2}(u_{x,z} + u_{z,x}) = 0. \quad \text{(f)}$$

Starting with Eq. (6.5c), we integrate to get

$$u_z = \frac{\gamma z^2}{2E} + f(x, y), \qquad (6.6)$$

where $f(x, y)$ is an arbitrary function. Substitution of Eq. (6.6) into Eqs. (6.5e) and (6.5f) yields

$$u_{y,z} = -f_{,y} \quad \text{(a)} \qquad (6.7)$$

$$u_{x,z} = -f_{,x}, \quad \text{(b)}$$

which integrate into

$$u_y = -zf_{,y} + g(x, y) \quad \text{(a)} \qquad (6.8)$$

$$u_x = -zf_{,x} + h(x, y), \quad \text{(b)}$$

where g and h are two more arbitrary functions.

These expressions for u_x, u_y and u_z may now be substituted into Eqs. (6.5a) and (6.5b), which become

$$-zf_{,xx} + h_{,x} = -\frac{\nu}{E}\gamma z \quad \text{(a)} \qquad (6.9)$$

$$-zf_{,yy} + g_{,y} = -\frac{\nu}{E}\gamma z. \quad \text{(b)}$$

It has already been established that f, g, h do not depend on z. Therefore, Eqs. (6.9) may be separated into the following relationships

$$h_{,x} = 0 \quad \text{(a)}$$

$$g_{,y} = 0 \quad \text{(b)} \qquad (6.10)$$

$$f_{,xx} = \frac{\nu}{E}\gamma \quad \text{(c)}$$

$$f_{,yy} = \frac{\nu}{E}\gamma. \quad \text{(d)}$$

Thus far, only Eq. (6.5d) has not been considered. We substitute u_x and u_y from Eq. (6.8) into that equation, producing

$$-2zf_{,xy} + h_{,y} + g_{,x} = 0 \tag{6.11}$$

that separates into

$$h_{,y} + g_{,x} = 0 \quad \text{(a)}$$
$$f_{,xy} = 0 \quad \text{(b)} \qquad (6.12)$$

due to the independence of $h_{,y}$ and $g_{,x}$ from z. Equations (6.10a) and (6.10b) together with Eq. (6.12a) produce expressions for g and h of the form

$$g = C_1 r(x) + C_2 \quad \text{(a)}$$
$$h = C_3 t(y) + C_4 \quad \text{(b)} \qquad (6.13)$$
$$C_3 t_{,y} + C_1 r_{,x} = 0, \quad \text{(c)}$$

where r and t are again arbitrary functions. The foregoing are satisfied by choosing $t(y) = y$, $r(x) = x$ and $C_3 = -C_1$, whereupon

$$g = C_1 x + C_2 \quad \text{(a)}$$
$$h = -C_1 y + C_4. \quad \text{(b)} \qquad (6.14)$$

If we take

$$f = \frac{v}{2E}\gamma(x^2 + y^2) + C_5 x + C_6 y + C_7, \tag{6.15}$$

we see that all of the constraints, Eqs. (6.10c, d) and Eq. (6.12b), are satisfied.

Finally, we are able to write the expressions for the displacements by substituting f, g, h into Eqs. (6.6) and (6.8)

$$u_x = -\frac{v}{E}\gamma xz - C_1 y + C_4 - C_5 z \quad \text{(a)}$$

$$u_y = -\frac{v}{E}\gamma yz - C_1 x + C_2 - C_6 z \quad \text{(b)} \qquad (6.16)$$

$$u_z = \frac{\gamma}{2E}[z^2 + v(x^2 + y^2)] + C_5 x + C_6 y + C_7. \quad \text{(c)}$$

The somewhat tedious calculations for the displacements contain six arbitrary constants, all of which are coefficients of rigid body terms. These constants may be evaluated by imposing constraints on the displacement and on the average rotation at the center of the fixed end, that is, at $(0, 0, L)$, where $u_x = u_y = u_z = 0$ and $\omega_{12} = \omega_{13} = \omega_{23} = 0$. These are written from Eqs. (6.16) and (3.32) to be

$$u_x(0, 0, L) = C_4 - C_5 L = 0 \quad \text{(a)} \qquad (6.17)$$

$$
\begin{aligned}
&u_y(0, 0, L) = C_2 - C_6 L = 0 && \text{(b)} \\
&u_z(0, 0, L) = \frac{\gamma L^2}{2E} + C_7 = 0 && \text{(c)} \\
&\omega_{xy}(0, 0, L) = \tfrac{1}{2}(-C_1 - C_1) = 0 && \text{(d)} \\
&\omega_{xz}(0, 0, L) = \tfrac{1}{2}(-C_5 - C_5) = 0 && \text{(e)} \\
&\omega_{yz}(0, 0, L) = \tfrac{1}{2}(-C_6 - C_6) = 0. && \text{(f)}
\end{aligned}
\tag{6.17}
$$

From the last three equations $C_1 = C_5 = C_6 = 0$, while the first three give

$$
\begin{aligned}
&C_4 = 0 && \text{(a)} \\
&C_2 = 0 && \text{(b)} \\
&C_7 = \frac{-\gamma L^2}{2E}. && \text{(c)}
\end{aligned}
\tag{6.18}
$$

Thus, the final expressions for the displacements become

$$
\begin{aligned}
&u_x = -\frac{\nu}{E}\gamma xz && \text{(a)} \\
&u_y = -\frac{\nu}{E}\gamma yz && \text{(b)} \\
&u_z = \frac{\gamma}{2E}[z^2 + \nu(x^2 + y^2) - L^2]. && \text{(c)}
\end{aligned}
\tag{6.19}
$$

From these results, we make some observations not discernable from the strength-of-materials solution, which is a uniform axial extension along the z axis corresponding to $u_z(0, 0, z)$ in Eq. (6.19c)

(1) All points not on the center line have contractions in the $x - y$ plane given by Eqs. (6.19a, b). This is sometimes called the "Poisson" effect, since it is evidently the motivation for the definition of Poisson's ratio as the fractional contraction (see Section 4.3).
(2) The axial displacement is *not* uniform on the cross section but is a parabolic surface with a peak along the z axis as shown in Fig. 6.1(b).

Finally, in recalling the objectives of examining this problem as outlined in Section 6.1, we find that the theory-of-elasticity solution has confirmed the adequacy of the strength-of-materials solution for defining the equilibrium state and has enhanced the description of the displacements.

6.3 Cantilever Beam Under End Loading

6.3.1 Elementary Beam Theory

Beams have been studied formally since the time of Galileo Galilei, who discussed the cantilever in the middle 17th century. Elastic beam theory

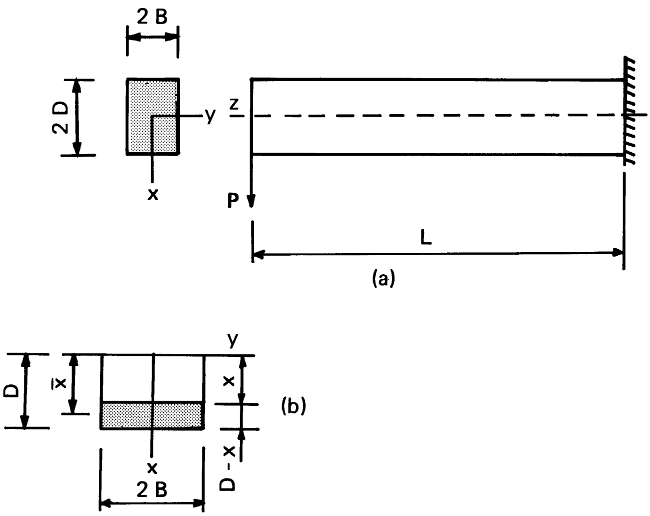

Fig. 6.2. (a) Cantilever beam in bending; (b) location of plane on which horizontal shear acts.

evolved from the contributions of Edme Mariotte, James Bernouilli, Leonhard Euler, Charles A. Coulomb, and, finally L. M. H. Navier in the early 19th century. As an illustration, we consider the cantilever beam shown in Fig. 6.2(a) subjected to a concentrated end load P, neglecting the self-weight.

From elementary beam theory, we may write the solution for the stresses in terms of the shear V and the bending moment M as

$$\sigma_{xx} = \sigma_{yy} = 0 \qquad \text{(a)}$$

$$\sigma_{zz} = \frac{Mx}{I} = \frac{P}{I}(z - L)x \qquad \text{(b)}$$

$$\sigma_{xz} = \sigma_{zx} = \frac{VQ}{2IB} = \frac{P}{2I}(D^2 - x^2) \qquad \text{(c)} \qquad (6.20)$$

$$\sigma_{xy} = \sigma_{yz} = 0, \qquad \text{(d)}$$

where I is the moment of inertia of the cross section equal to $(1/12) \times 2B \times (2D)^3 = (4/3)BD^3$; and Q is the first moment of the area between x and D, as shown on Fig. 6.2(b). For a rectangular cross section

$$Q = (D - x) \times 2B \times \bar{x} = (D - x) \times 2B \times \frac{(D + x)}{2} = (D^2 - x^2)B.$$

Implicit in these expressions is the assumption that the load P and the resulting stresses are uniform over the width of the beam, so that the solution is essentially two-dimensional. Later, we will test this solution against the theory of elasticity.

First, we consider equilibrium Eqs. (2.46), with $1 = x$, $2 = y$ and $3 = z$,

$$\begin{aligned} \sigma_{xx,x} + \sigma_{xy,y} + \sigma_{xz,z} &= 0 + 0 + 0 = 0 && \text{(a)} \\ \sigma_{yx,x} + \sigma_{yy,y} + \sigma_{yz,z} &= 0 + 0 + 0 = 0 && \text{(b)} \quad (6.21) \\ \sigma_{zx,x} + \sigma_{zy,y} + \sigma_{zz,z} &= -\frac{Px}{I} + 0 + \frac{Px}{I} = 0. && \text{(c)} \end{aligned}$$

Thus, equilibrium is satisfied.

Next, we examine the compatibility conditions using the Beltrami–Michell form Eqs. (5.16), since the solution being tested is in terms of stresses. From Eq. (5.10a),

$$Q_1 = \sigma_{tt} = \sigma_{zz} = \frac{P}{I}(z - L)x. \qquad (6.22)$$

Equations (5.16) for $i, j = x, y, z$ become

$$\begin{aligned} \nabla^2\sigma_{xx} + \frac{1}{1+\nu}Q_{1,xx} &= 0 + 0 = 0 && \text{(a)} \\ \nabla^2\sigma_{xy} + \frac{1}{1+\nu}Q_{1,xy} &= 0 + 0 = 0 && \text{(b)} \\ \nabla^2\sigma_{xz} + \frac{1}{1+\nu}Q_{1,xz} &= -\frac{P}{I} + \frac{1}{1+\nu}\frac{P}{I} = \frac{-\nu}{1+\nu}\frac{P}{I} \neq 0 && \text{(c)} \quad (6.23) \\ \nabla^2\sigma_{yy} + \frac{1}{1+\nu}Q_{1,yy} &= 0 + 0 = 0 && \text{(d)} \\ \nabla^2\sigma_{yz} + \frac{1}{1+\nu}Q_{1,yz} &= 0 + 0 = 0 && \text{(e)} \\ \nabla^2\sigma_{zz} + \frac{1}{1+\nu}Q_{1,zz} &= 0 + 0 = 0. && \text{(f)} \end{aligned}$$

One of the compatibility equations, Eq. 6.23(c), will be violated unless $\nu = 0$, but this is implicitly assumed in elementary beam theory.

It is instructive also to consider the compatibility equations in terms of strain Eqs. (3.59) and to identify, specifically, the violation. The relevant equation is Eq. (3.59e), which takes the form

$$\varepsilon_{yz,yx} + \varepsilon_{yx,yz} - \varepsilon_{zx,yy} = \varepsilon_{yy,zx}. \qquad (6.24)$$

We calculate the strains from Eqs. (4.19) and (4.24) as

$$\begin{aligned} \varepsilon_{yz} &= \varepsilon_{yx} = 0 && \text{(a)} \\ \varepsilon_{zx} &= \frac{\sigma_{zx}}{2\mu} = \frac{1}{2G}\frac{P}{2I}(D^2 - x^2) && \text{(b)} \quad (6.25) \\ \varepsilon_{zx,yy} &= 0 && \text{(c)} \end{aligned}$$

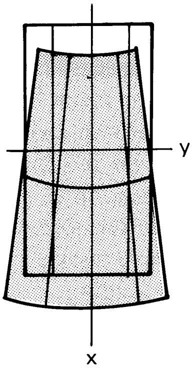

Fig. 6.3. Deformed cross section of cantilever beam (after Ugural and Fenster, *Advanced Strength and Applied Elasticity*, Elsevier, 1975). Reprinted with permission.

$$\varepsilon_{yy} = \frac{-\lambda}{2\mu(2\mu + 3\lambda)}\sigma_{zz} = \frac{-\nu}{E}\frac{P}{I}(z - L)x \qquad \text{(d)}$$

$$\varepsilon_{yy,zx} = \frac{-\nu P}{EI}. \qquad \text{(e)} \qquad (6.25)$$

Thus, Eq. (6.24) becomes

$$0 + 0 + 0 \neq \frac{-\nu P}{EI}. \qquad (6.26)$$

This compatibility equation can be satisfied only through a modification of the assumed stress distribution, considered in the next section. Also, we see that we have a strain ε_{yy}, normal to the plane of bending and proportional to Poisson's ratio, that does not enter into the elementary theory but which may be calculated from Hooke's law in terms of σ_{zz} Eq. (6.25d). This is shown on the deformed cross section in Fig. 6.3. For $x < 0$ and $z < L$, ε_{yy} is negative; while for $x > 0$, it is positive. This distortion from the initially rectangular shape of the cross section is another example of a "Poisson" effect. Of course, so long as σ_{zz} and, hence, ε_{zz} remain independent of y and linear in x for a given value of z, the elementary postulate that "plane sections remain plane" is substantiated.

Finally, we should see if the elementary solution satisfies the boundary conditions. For the lateral boundaries, we have the components of the tractions given in terms of the stresses by Eq. (2.11), $T_i = \sigma_{ji}n_j$.

For the top and bottom of the beam, we consider the normal traction at $x = \pm D$, for which $\mathbf{n} = \pm\mathbf{e}_x$, and

$$n_x = 1, \quad n_y = 0, \quad n_z = 0. \qquad (6.27)$$

Then

$$T_x = \sigma_{jx}(\pm D, y, z)n_j = 0 \times 1 + 0 \times 0 + 0 \times 0 = 0. \tag{6.28}$$

It may be verified that the components T_y and T_z vanish as well. However, it is of interest to note that should the beam be loaded along the top or bottom surface, the solution would *not* automatically satisfy the boundary condition on the normal traction. This is an indication that the theory-of-elasticity solution must account for the variation of a distributed loading through the depth of the beam, in contrast to the elementary solution which is referred to a "neutral" axis, $x = 0$. We have avoided this problem for the present by only considering a concentrated loading.

We may also evaluate the normal traction on the lateral boundaries $y = \pm B$, for which $\mathbf{n} = \pm \mathbf{e}_y$, and

$$n_x = 0, \quad n_y = 1, \quad n_z = 0; \tag{6.29}$$

$$T_y = \sigma_{jy}(x, \pm B, z)n_j = 0 \times 0 + 0 \times 1 + 0 \times 0 = 0. \tag{6.30}$$

The components T_x and T_z also vanish.

At the fixed end $z = 0$, our present solution is insufficient to check the displacement boundary conditions since it violates compatibility, while at $z = L$, we have

$$\begin{aligned} P &= \int_{-D}^{D} \int_{-B}^{B} \sigma_{xz}\, dy\, dx \\ &= \int_{-D}^{D} \int_{-B}^{B} \frac{P(D^2 - x^2)}{2I}\, dy\, dx \\ &= \frac{4}{3}\frac{P}{I}BD^3. \end{aligned} \tag{6.31}$$

With $I = \frac{4}{3}BD^3$, the equation is satisfied. This implies that a concentrated load must be distributed over the depth in accordance with σ_{xz}; that is, parabolically, in order to satisfy the boundary condition exactly. Of course, other distributions are admissible through St. Venant's principle.

We have shown that the elementary beam solution, while satisfying equilibrium in general, fails to account for the lateral contraction or "Poisson" effect and does not recognize the distribution of the applied loading through the depth of the beam.

6.3.2 Elasticity Theory

Again drawing on the work of St. Venant, the semi-inverse approach is followed, whereby it is assumed that the *normal* stresses are identical to those of the elementary theory as given by Eqs. (6.20a, b). Likewise, σ_{xy} is taken as zero as in Eq. (6.20d), but no stipulation is made on the remaining *shearing* stresses σ_{zx} and σ_{zy} that act in the plane of the cross section $x - y$.

The equilibrium equations, Eqs. (2.46), become

$$\sigma_{xz,z} = 0 \quad \text{(a)}$$
$$\sigma_{yz,z} = 0 \quad \text{(b)} \qquad (6.32)$$

$$\sigma_{zx,x} + \sigma_{zy,y} = -\frac{Px}{I}. \quad \text{(c)} \quad (6.32)$$

Equations (6.32a, b) indicate that the shearing stresses do not depend on z, and, therefore, are the same for all cross sections.

We recall the compatibility conditions Eqs. (5.16), which were expanded as Eqs. (6.23). For this case, two are relevant, Eqs. (6.23c) and (6.23e), which are [6.1]

$$\nabla^2\sigma_{xz} = -\frac{1}{1+\nu}\frac{P}{I} \quad \text{(a)}$$
$$\nabla^2\sigma_{yz} = 0. \quad \text{(b)} \qquad (6.33)$$

Also, we must verify that any modified solution continues to satisfy the boundary conditions. Particularly, we consider the components of traction T_z on each face of the beam, found on the top and bottom using Eqs. (6.27) and (6.28) as

$$\sigma_{xz}(\pm D, y, z) = 0, \qquad (6.34)$$

and on the sides using Eqs. (6.29) and (6.30) as

$$\sigma_{yz}(x, \pm B, z) = 0. \qquad (6.35)$$

To continue, we introduce a technique that is very effective in obtaining analytical solutions to a variety of problems in the theory of elasticity [6.1]. We define a *stress function* ϕ such that

$$\sigma_{xz} = \phi_{,z} - \frac{Px^2}{2I} + f(y) \quad \text{(a)}$$
$$\sigma_{yz} = -\phi_{,x}, \quad \text{(b)} \qquad (6.36)$$

which satisfies Eqs. (6.32). Then, Eqs. (6.33) become, respectively,

$$(\phi_{,yxx} + \phi_{,yyy}) - \frac{P}{I} + f_{,yy} = -\frac{1}{1+\nu}\frac{P}{I},$$

or

$$(\phi_{,xx} + \phi_{,yy})_{,y} = \frac{\nu}{1+\nu}\frac{P}{I} - f_{,yy}; \quad \text{(a)} \quad (6.37)$$

and

$$-\phi_{,xxx} - \phi_{,xyy} = 0,$$

or

$$(\phi_{,xx} + \phi_{,yy})_{,x} = 0. \quad \text{(b)} \quad (6.37)$$

Equation (6.37a) integrates to

$$\phi_{,xx} + \phi_{,yy} = \frac{\nu}{1+\nu}\frac{P}{I}y - f_{,y} + C, \tag{6.38}$$

where C is an arbitrary constant. Equation (6.38) also satisfies Eq. (6.37b).

To evaluate C, we consider the average rotation about the z axis, ω_{xy}, as given by Eq. (3.32) with $i = x, j = y$

$$\omega_{xy} = \tfrac{1}{2}(u_{x,y} - u_{y,x}). \tag{6.39}$$

The rate of change of ω_{xy} along z is given by

$$\begin{aligned} \omega_{xy,z} &= \tfrac{1}{2}(u_{x,y} - u_{y,x})_{,z} \\ &= \tfrac{1}{2}[(u_{x,z} + u_{z,x})_{,y} - (u_{y,z} + u_{z,y})_{,x}] \\ &= \varepsilon_{xz,y} - \varepsilon_{yz,x} \end{aligned} \tag{6.40}$$

by Eqs. (3.15e and f). Converting to stresses through Eq. (4.29b), we have

$$\begin{aligned} \omega_{xy,z} &= \frac{1}{2G}(\sigma_{xz,y} - \sigma_{yz,x}) \\ &= \frac{1}{2G}(\phi_{,yy} + f_{,y} + \phi_{,xx}) \end{aligned} \tag{6.41}$$

using Eqs. (6.36). Finally, substituing Eq. (6.41) into the l.h.s. of Eq. (6.38), we find

$$2G\omega_{xy,z} = \frac{1}{1+\nu}\frac{Py}{I} + C. \tag{6.42}$$

We are considering a rectangular cross section, see Fig. 6.2(a), in which the bending is symmetrical about the x axis. At $y = 0$, the average rotation should be zero as well as the rate of change along z, and $C = 0$.

Equation (6.38) now becomes

$$\phi_{,xx} + \phi_{,yy} = \frac{\nu}{1+\nu}\frac{P}{I}y - f_{,y}, \tag{6.43}$$

which is the governing equation for the stress function subject to satisfaction of the boundary conditions Eqs. (6.34) and (6.35). If we introduce $f(y) = PD^2/2I$ into Eqs. (6.36), we may rewrite the boundary conditions directly in terms of the stress function as

$$\begin{aligned} \sigma_{xz}(\pm D, y, z) &= \phi_{,y}(\pm D, y, z) = 0, && \text{(a)} \\ \sigma_{yz}(x, \pm B, z) &= -\phi_{,x}(x, \pm B, z) = 0. && \text{(b)} \end{aligned} \tag{6.44}$$

These are easily satisfied by taking ϕ in a form such that it *vanishes* on the boundary. In many cases, ϕ may be taken to be proportional to the equation of the perimeter of the cross section, which is for this case

$$(x^2 - B^2)(y^2 - D^2) = 0. \tag{6.45}$$

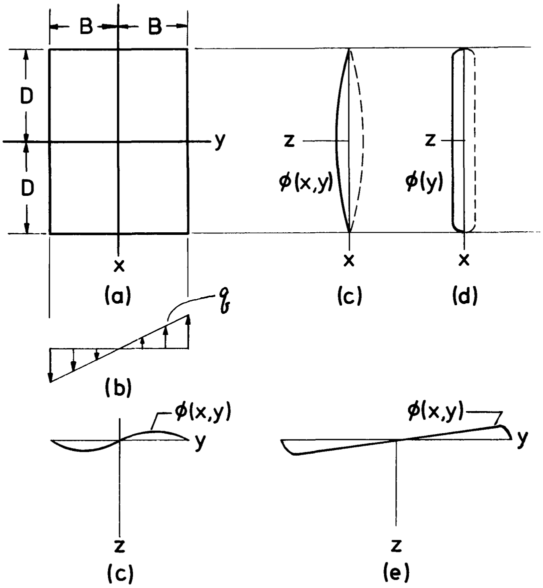

Fig. 6.4. (a) Cross section of membrane analogous to beam; (b) loading and (c) profile of deformed membrane; (d) deep beam; (e) wide beam.

The choice of $f(y)$ to produce Eqs. (6.44) then reduces Eq. (6.43) to

$$\phi_{,xx} + \phi_{,yy} = \frac{\nu}{1+\nu}\frac{Py}{I}. \tag{6.46}$$

Before proceeding with the solution, it is instructive to digress a bit to draw an analogy between Eq. (6.46) and the equation of a uniform *membrane* stretched over the cross section of the beam in Fig. 6.4(a). The equation for a membrane was derived in Sec. 5.6. Except near the boundaries, the height of the membrane $\phi(x, y)$ is proportional to the load intensity q, which is, in turn, analogous to the r.h.s. of Eq. (6.46), $\nu/(1 + \nu)(Py/I)$, as shown in Fig. 6.4(b) [6.1]. In effect, the loading pattern shown in Fig. 6.4(b) would produce a deflected membrane as shown in Fig. 6.4(c). At the edges and along the center line $y = 0$, the height of the membrane must be zero as indicated on the profile in Fig. 6.4(c). Because of the constraint at $y = 0$, the profile is different than in Fig. 5.1. Now we restate the expressions for the stresses from Eq. (6.36), incorporating the chosen $f(y) = PD^2/2I$:

$$\sigma_{xz} = \phi_{,y} - \frac{Px^2}{2I} + \frac{PD^2}{2I} \qquad \text{(a)}$$

$$= \frac{P(D^2 - x^2)}{2I} + \phi_{,y}, \qquad \text{(b)} \tag{6.47}$$

$$\sigma_{yz} = -\phi_{,x}.$$

From Eqs. (6.47), we see that the *changes* in the shearing stresses from the expressions given by the elementary theory, Eqs. (6.20c, d), are proportional to the first derivative or *slope* of the membrane at any point. Examining the profile along y in Fig. 6.4(c), we see that the correction to σ_{xx} has a maximum positive value at the two sides, a maximum negative value in the center, and is zero at the quarter-points. Thus, the *uniformity* of the stress state across the width of the beam inherent in the elementary theory is dispelled. Membrane analogies are often very useful in the theory of elasticity for visualizing and interpreting complex states of stress and strain.

The general solution to Eq. (6.46), as derived by Timoshenko and Goodier [6.1], is rather more complicated than our introductory objectives; however, it is possible to consider some approximate solutions, reasoned from the membrane analogy [6.1].

If the depth of the beam is large compared with the width, $D \gg B$, we may assume that at points sufficiently distant from the short side $x = \pm D$, the surface is cylindrical. As shown in Fig. 6.4(d), this implies that $\phi = \phi(y)$. Then Eq. (6.46) reduces to

$$\phi_{,yy} = \frac{\nu}{1+\nu}\frac{Py}{I}, \tag{6.48}$$

which has a solution of the form

$$\phi(y) = \frac{\nu}{1+\nu}\frac{P}{6I}(y^3 + C_1 y + C_2). \tag{6.49}$$

With the membrane condition $\phi(0) = 0$, see Fig. 6.4(b), $C_2 = 0$, and with $\phi(\pm B) = 0$, $C_1 = -B^2$, so that

$$\phi(y) = \frac{\nu}{1+\nu}\frac{P}{6I}(y^3 - B^2 y); \tag{6.50}$$

from which Eq. (6.47a) gives

$$\sigma_{xz}(x, y) = \frac{P}{2I}\left[(D^2 - x^2) + \frac{\nu}{1+\nu}\left(y^2 - \frac{B^2}{3}\right)\right]. \tag{6.51}$$

Of course, the assumption on ϕ gives $\sigma_{yz} = 0$. At $x = 0$, where the stress computed by the elementary theory is largest,

$$\sigma_{xz}(0, y) = \frac{3}{2}\frac{P}{(2B \times 2D)},$$

the correction given by the second term of Eq. (6.51) is small.

The other extreme is when the width of the beam is large compared to the depth, $B \gg D$. Then, at points sufficiently distant from the short side $y = \pm B$, the function ϕ, representing the deflection of the membrane, is assumed to be linear in y as indicated in Fig. 6.4(e). Thus, Eq. (6.46) reduces to

$$\phi_{,xx} = \frac{v}{1+v}\frac{Py}{I}, \tag{6.52}$$

which is solved as

$$\begin{aligned} \phi_{,x} &= \frac{v}{1+v}\frac{Pyx}{I} + C_1 \\ \phi(x, y) &= \frac{v}{1+v}\frac{Py}{2I}x^2 + C_1 x + C_2. \end{aligned} \tag{6.53}$$

With $\phi(\pm D, y) = 0$, we find

$$C_2 = \frac{-v}{1+v}\frac{Py}{2I}D^2, \tag{6.54}$$

and $C_1 = 0$ so that

$$\phi = \frac{v}{1+v}\frac{Py}{2I}(x^2 - D^2), \tag{6.55}$$

and, from Eqs. (6.47),

$$\begin{aligned} \sigma_{xz} &= \frac{P(D^2 - x^2)}{2I}\left[1 - \frac{v}{1+v}\right] = \frac{1}{1+v}\frac{P(D^2 - x^2)}{2I}, && \text{(a)} \\ \sigma_{yz} &= \frac{-v}{1+v}\frac{P}{I}xy. && \text{(b)} \end{aligned} \tag{6.56}$$

In comparison to elementary theory, σ_{xz} is reduced by the factor $1/(1 + v)$, and σ_{yz} is now available.

For very large values of B/D, both σ_{xz} and σ_{yz} may greatly exceed the $(3/2)[P/(2B \times 2D)]$ peak from elementary theory. At first, this does not seem possible from Eqs. (6.56); however, we recall that the underlying assumption excluded regions near the short sides $y = \pm B$, where actual maximum stress occurs as depicted in Fig. 6.4(e). Moreover, σ_{yz} near the corners, where Eq. (6.56b) would indicate the largest value occurs, may become numerically larger than σ_{xz}.

A final approximate solution is to take ϕ as a multiple of the boundary curve to satisfy the $\phi = 0$ condition. The form

$$\phi = (x^2 - D^2)(y^2 - B^2)(C_1 y + C_2 y^3) \tag{6.57}$$

is satisfactory, but the constants C_1 and C_2 depend on the D/B ratio and must be evaluated from a minimum energy criteria [6.1].

Although we have not derived an elasticity solution to cover all cases, we have shown the limitations of elementary beam theory and have demonstrated how a typical elasticity problem may be approach. Based on the general solution, the error in the maximum stress obtained by the elementary formula for a square beam is about 10% [6.1].

6.4 Torsion

6.4.1 Torsion of Circular Shaft

The circular shaft of radius B shown in Fig. 6.5(a) is subjected to a twisting moment (torque) $M_z(L)$ at the free-end and is restrained against both displacement and rotation at $z = 0$.

This solution for this classical problem was presented by Charles A. Coulomb in the late 18th century and falls within the field of strength of materials. Referring to Figs. 6.5(a) and (b), the Coulomb torsion solution is based on the following assumptions with respect to the shearing stress $\tau(x, y)$.

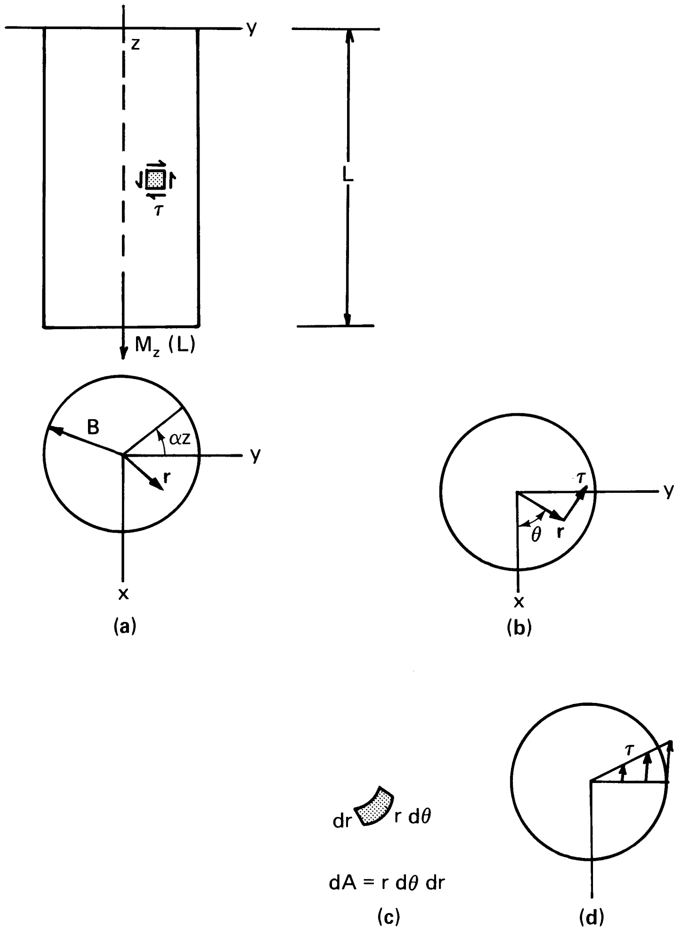

Fig. 6.5. (a) Circular shaft in torsion; (b) Coulomb torsion assumptions; (c) polar area element; (d) shearing stresses.

(1) The shearing stress τ acts in a direction perpendicular to the radius vector **r**.
(2) The shearing stress τ is proportional to $r = |\mathbf{r}|$.
(3) The shearing stress τ is proportional to the angle of rotation per unit length, which is called the rate of twist α.

We see from the differential element on Fig. (6.5a) that the twisting moment produces a state of pure shear stress, so that the proportionality constant in assumption (3) is the shear modulus G; therefore, assumptions (2) and (3) are expressed by

$$\tau = G\alpha r. \tag{6.58}$$

We now consider equilibrium and focus on the polar area element shown in Fig. (6.5c):

$$M_z = \int_A \tau \times r\, dA, \tag{6.59}$$

or, using Eq. (6.58) and taking $dA = r\, dr\, d\theta$,

$$\begin{aligned} M_z &= G\alpha \int_0^B \int_{-\pi}^{\pi} r \times r \times r\, d\theta\, dr \\ &= G\alpha \times 2\pi \int_0^B r^3\, dr \\ &= G\alpha J_c, \end{aligned} \qquad \text{(a)} \quad (6.60)$$

in which

$$J_c = \frac{\pi B^4}{2}, \qquad \text{(b)} \quad (6.60)$$

where J_c is called the *polar moment of inertia*. Then, we may eliminate $G\alpha$ between Eqs. (6.58) and (6.60a) to get

$$\tau = \frac{M_z r}{J_c}. \tag{6.61}$$

Equation (6.61) permits the evaluation of the shearing stress for a known torque and cross section, irrespective of the material and is obviously analogous to Eq. (6.20b) for beam bending. The linear distribution is shown in Fig. 6.5(d). Also, for a given twisting moment, the rate of twist may be computed from Eq. (6.60a) as

$$\alpha = \frac{M_z}{GJ_c}. \tag{6.62}$$

The quantity GJ_c is called the *torsional rigidity* and is a useful parameter for comparing the relative torsional stiffnesses of various cross sections.

With respect to compatibility, since the stresses are linear, the strains will also be linear and the St. Venant equations are thus satisfied. Single-valued displacements may be evaluated from the kinematic relations, but this is not pursued since the angle of twist is of most interest.

Finally, in assessing the admissibility of the strength-of-materials solution as an elasticity solution as well, we examine the boundary conditions. The fixed boundary is bypassed through St. Venant's principle while the loaded boundary is treated by Eq. (6.59). The cylindrical lateral boundary is of primary interest. Assumption (1) guarantees that τ is tangent to the boundary circle and hence has no normal component, so that the boundary must be stress-free.

The satisfaction of the stress-free lateral boundary condition by a shearing stress distribution that is, at the same time, perpendicular to the radius vector is fortuitous, insofar as the solution for the torsional stresses on a *circular* cross section is concerned. The same can be said for an annular or hollow cylindrical section. On the other hand, it is easily shown that for *any* other cross section, it is not possible to have the shearing stress both *tangent* to the boundary and *perpendicular* to the radius vector. Simply visualize the stress distribution shown in Fig. 6.5(d) applied on a rectangular cross section. Except at the major and minor axes intersections with the perimeter, $x = 0$, $y = 0$, simultaneous satisfaction of these conditions cannot be attained. Moreover, the corner presents an additional complication. This condition perplexed early researchers in solid mechanics for some time and was ultimately resolved by a more fundamental approach based on the theory of elasticity, as developed in the following section.

6.4.2 Torsion of Solid Prismatic Shafts

The generalization of the uniform torsion problem from the circular cross-section solution is due to none other than St. Venant and is considered by Westergaard [6.2] to be the most important single contribution of St. Venant to the theory of elasticity. The solution for a noncircular cross section, see Fig. 6.6(a), follows the now familiar semi-inverse approach, whereby all stresses except the in-plane shearing stresses σ_{zx} and σ_{zy} are taken as zero, that is,

$$\sigma_{xx} = \sigma_{yy} = \sigma_{zz} = \sigma_{xy} = 0. \tag{6.63}$$

Considering the equilibrium equations. Eqs. (2.46), in view of Eq. (6.63), with $1 = x$, $2 = y$, $3 = z$ and no body forces,

$$\begin{aligned} \sigma_{xz,z} &= 0, && \text{(a)} \\ \sigma_{yz,z} &= 0, && \text{(b)} \quad (6.64) \\ \sigma_{xz,x} + \sigma_{yz,y} &= 0. && \text{(c)} \end{aligned}$$

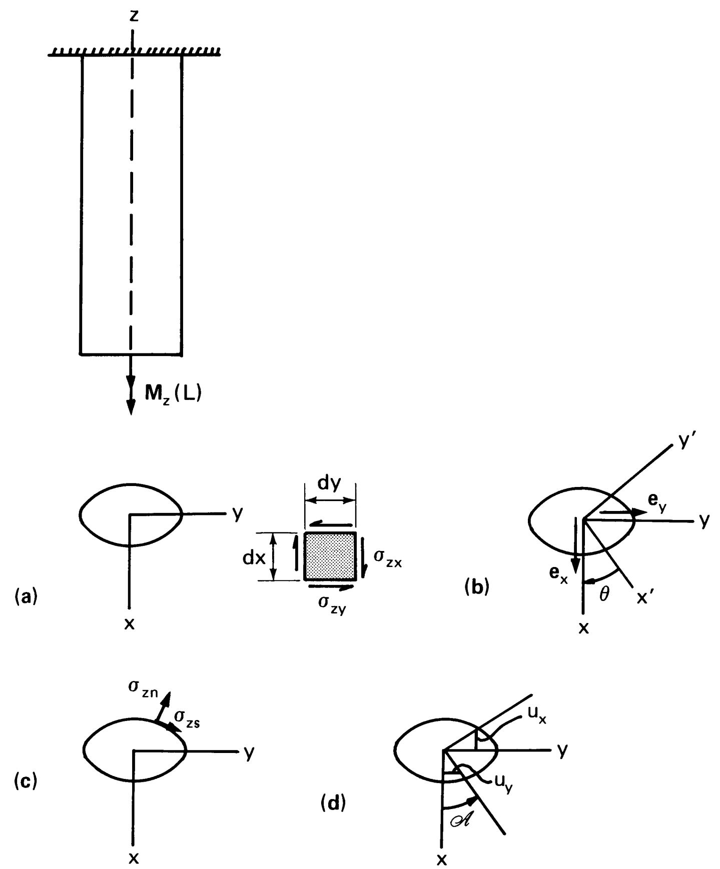

Fig. 6.6. (a) Prismatic shaft in torsion; (b) rotated axes; (c) stresses on lateral surface; (d) angle of rotation.

Equations (6.64a, b) indicate that the shearing stresses are functions of x and y only.

The equations are solved by defining a stress function $\phi(x, y)$ such that

$$\sigma_{xz}(x, y) = \phi_{,y}, \qquad \text{(a)}$$
$$\sigma_{yz}(x, y) = -\phi_{,x}. \qquad \text{(b)} \qquad (6.65)$$

The corresponding strains are computed from Eq. (4.29b) as

$$\varepsilon_{xz}(x, y) = \frac{1}{2G}\sigma_{xz}, \qquad \text{(a)}$$
$$\varepsilon_{yz}(x, y) = \frac{1}{2G}\sigma_{yz}. \qquad \text{(b)} \qquad (6.66)$$

Then, we enter the compatibility Eqs. (3.59), all which are identically satisfied except Eq. (3.59d),

$$\varepsilon_{xy,xz} + \varepsilon_{xz,xy} - \varepsilon_{yz,xx} = \varepsilon_{xx,yz},$$

After eliminating the zero terms $\varepsilon_{xy,xz}$ and $\varepsilon_{xx,yz}$, we have

$$(\varepsilon_{xz,y} - \varepsilon_{yz,x})_{,x} = 0. \tag{6.67}$$

If $\varepsilon_{xz,y} - \varepsilon_{yz,x} =$ constant, then Eq. (6.67) will be satisfied. We may express this requirement in terms of the stress function ϕ by considering Eqs. (6.65) and (6.66),

$$\phi_{,xx} + \phi_{,yy} = H, \tag{6.68}$$

where H is the constant. Equation (6.68) is known as Poisson's equation and expresses the *compatibility* requirements for the torsion problem.

Since the *direction* of the shearing stress was a prime factor in motivating the more general study of torsion, we consider this aspect in detail. We first note that Eqs. (6.65a, b) express the shearing stresses in the x direction σ_{zx} and in the y direction σ_{zy} in terms of the components of the *gradient* of ϕ

$$\begin{aligned} \nabla\phi &= [\nabla\phi]_x \mathbf{e}_x + [\nabla\phi]_y \mathbf{e}_y \\ &= \phi_{,x}\mathbf{e}_x + \phi_{,y}\mathbf{e}_y \end{aligned} \tag{6.69}$$

in the y and x directions, respectively. That is,

$$\begin{aligned} \sigma_{xz} &= [\nabla\phi]_y, && \text{(a)} \\ \sigma_{yz} &= -[\nabla\phi]_x. && \text{(b)} \end{aligned} \tag{6.70}$$

We next evaluate the shearing stresses for a rotated set of axes $x'y'$, see Fig. 6.6(b), using the transformation law, Eq. (2.13),

$$\begin{aligned} \sigma_{x'z} &= \alpha_{x'i}\alpha_{zj}\sigma_{ij}, && \text{(a)} \\ \sigma_{y'z} &= \alpha_{y'i}\alpha_{zj}\sigma_{ij}. && \text{(b)} \end{aligned} \tag{6.71}$$

Expanding these equations gives

$$\begin{aligned} \sigma_{x'z} &= \alpha_{x'x}\alpha_{zz}\sigma_{xz} + \alpha_{x'y}\alpha_{zz}\sigma_{yz} + \alpha_{x'z}\alpha_{zx}\sigma_{zx} + \alpha_{x'z}\alpha_{zy}\sigma_{zy}, && \text{(a)} \\ \sigma_{y'z} &= \alpha_{y'x}\alpha_{zz}\sigma_{xz} + \alpha_{y'y}\alpha_{zz}\sigma_{yz} + \alpha_{y'z}\alpha_{zx}\sigma_{zx} + \alpha_{y'z}\alpha_{zy}\sigma_{zy}, && \text{(b)} \end{aligned} \tag{6.72}$$

where the direction cosines are

	x	y	z
x'	$\cos\theta$	$\sin\theta$	0
y'	$-\sin\theta$	$\cos\theta$	0
z'	0	0	1.

Therefore,

$$\sigma_{x'z} = \sigma_{xz} \cos\theta + \sigma_{yz} \sin\theta, \quad \text{(a)}$$
$$\sigma_{y'z} = -\sigma_{xz} \sin\theta + \sigma_{yz} \cos\theta. \quad \text{(b)} \qquad (6.73)$$

Now, substituting Eqs. (6.70) into Eqs. (6.73), we get

$$\sigma_{x'z} = [\nabla\phi]_y \cos\theta - [\nabla\phi]_x \sin\theta, \quad \text{(a)}$$
$$\sigma_{y'z} = -[\nabla\phi]_y \sin\theta - [\nabla\phi]_x \cos\theta. \quad \text{(b)} \qquad (6.74)$$

Also, we evaluate the unit vectors in the x' and y' vectors from Fig. 6.6(b) as

$$\mathbf{e}_{x'} = \mathbf{e}_x \cos\theta + \mathbf{e}_y \sin\theta, \quad \text{(a)}$$
$$\mathbf{e}_{y'} = \mathbf{e}_y \cos\theta - \mathbf{e}_x \sin\theta. \quad \text{(b)} \qquad (6.75)$$

Now, we see that Eqs. (6.74a, b) can be written as

$$\begin{aligned} \sigma_{x'z} &= [\nabla\phi]_y \cos\theta - [\nabla\phi]_x \sin\theta \\ &= \nabla\phi\cdot\mathbf{e}_y \cos\theta - \nabla\phi\cdot\mathbf{e}_x \sin\theta \qquad \text{(a)} \\ &= \nabla\phi\cdot\mathbf{e}_{y'}, \\ &= [\nabla\phi]_{y'} \qquad (6.76) \\ \sigma_{y'z} &= -[\nabla\phi]_y \sin\theta - [\nabla\phi]_x \cos\theta \\ &= -\nabla\phi\cdot\mathbf{e}_y \sin\theta - \nabla\phi\cdot\mathbf{e}_x \cos\theta \qquad \text{(b)} \\ &= -\nabla\phi\cdot\mathbf{e}_{x'} \\ &= -[\nabla\phi]_{x'}. \end{aligned}$$

From this exercise, we conclude that the shearing stress in *any* direction, say x' or y', at any point (x, y, z) is given by the component of $\nabla\phi$ at *right angles* to that direction, that is, y' or x'. This proves useful in the discussion that follows.

We are now in a position to examine the boundary conditions. At any point on the perimeter, the shearing stress perpendicular to the boundary σ_{zn} must vanish, see Fig. 6.6(c). Only stresses tangent to the boundary are permitted. From Eq. (6.76b) with $x' = s$; $y' = n$; $\mathbf{e}_{x'} = \mathbf{s}$; we find

$$\sigma_{zn} = -\nabla\phi\cdot\mathbf{s} = -[\nabla\phi]_s = -\phi_{,s} = 0. \qquad (6.77)$$

Thus, the stress function ϕ must be *constant* on the boundary. In practice, it is usually sufficient to have ϕ vanish there. This is readily accomplished by selecting ϕ to be proportional to the equation of the perimeter of the cross section. This is similar to the bending stress function discussed in Section 6.3.

We now proceed to the evaluation of the stress function in terms of the applied torque M_z. First, we note that the resultant force on the face is zero. Referring to Fig. 6.6(a) and (b),

$$\int_A (\sigma_{zx}\mathbf{e}_x + \sigma_{zy}\mathbf{e}_y)\, dA = 0. \qquad (6.78)$$

Substituting Eq. (6.65) for the stresses and $dx\,dy$ for dA, we have

$$\int_A (\phi_{,y}\mathbf{e}_x - \phi_{,x}\mathbf{e}_y)\,dx\,dy = 0 \tag{6.79}$$

which separates into two scalar equations

$$\begin{aligned} \int dx \int \phi_{,y}\,dy &= 0, && \text{(a)} \\ -\int dy \int \phi_{,x}\,dx &= 0. && \text{(b)} \end{aligned} \tag{6.80}$$

But $\int \phi_{,y}\,dy = \phi_2(x) - \phi_1(x)$ and $\int \phi_{,x}\,dx = \phi_4(y) - \phi_3(y)$, where $\phi_1 - \phi_4$ are values of $\phi(x, y)$ on the boundary. However, ϕ has been constrained to be *constant* on the boundary, so that the integrals in Eqs. (6.80) are zero, and Eq. (6.78) is satisfied.

Next, we sum moments on the cross section as shown in Fig. 6.6(a).

$$\int_A (-\sigma_{zx}y + \sigma_{zy}x)\,dx\,dy = M_z. \tag{6.81}$$

In terms of the stress function, the l.h.s. is

$$\int_A (-\phi_{,y}y - \phi_{,x}x)\,dx\,dy = -\int dx \int y\phi_{,y}\,dy - \int dy \int x\phi_{,x}\,dx. \tag{6.82}$$

We integrate by parts the inner terms on the r.h.s. of Eq. (6.82) to get

$$\begin{aligned} \int y\phi_{,y}\,dy &= y\phi\Big]_S - \int \phi\,dy && \text{(a)} \\ \int x\phi_{,x}\,dx &= x\phi\Big]_S - \int \phi\,dx, && \text{(b)} \end{aligned} \tag{6.83}$$

where S indicates evaluation of the expression at end points that lie on the boundary. Since ϕ is constant there, the first term of each evaluated integral is zero. Therefore, returning to Eq. (6.81) in view of Eqs. (6.82) and (6.83),

$$\begin{aligned} M_z &= \int dx \int \phi\,dy + \int dy \int \phi\,dx \\ &= 2\int_A \phi\,dA. \end{aligned} \tag{6.84}$$

To complete the solution, we consider the displacements. First, we have the rotation about the z axis, given by Eq. (3.32) with $i = x$ and $j = y$,

$$\omega_{xy} = \tfrac{1}{2}(u_{x,y} - u_{y,x}). \tag{6.85}$$

The rate of change along z is

$$\omega_{xy,z} = \tfrac{1}{2}(u_{x,yz} - u_{y,xz}). \tag{6.86}$$

Considering the terms on the r.h.s. of Eq. (6.86), we have, from Eqs. (3.15) and (4.29b),

$$2\varepsilon_{xz} = u_{x,z} + u_{z,x} = \frac{\sigma_{xz}}{G}, \qquad \text{(a)}$$
$$2\varepsilon_{yz} = u_{y,z} + u_{z,y} = \frac{\sigma_{yz}}{G}. \qquad \text{(b)} \tag{6.87}$$

Next, we take $\partial/\partial y$ [Eq. (6.87a)] and $\partial/\partial x$ [Eq. (6.87b)] to get

$$u_{x,yz} = -u_{z,xy} + \frac{1}{G}\sigma_{xz,y}, \qquad \text{(a)}$$
$$u_{y,xz} = -u_{z,xy} + \frac{1}{G}\sigma_{yz,x}. \qquad \text{(b)} \tag{6.88}$$

Subtracting Eq. (6.88b) from Eq. (6.88a) and substituting into Eq. (6.86) gives

$$\begin{aligned}\omega_{xy,z} &= \frac{1}{2G}(\sigma_{xz,y} - \sigma_{yz,x}) \\ &= \frac{1}{2G}(\phi_{,yy} + \phi_{,xx}) \\ &= \frac{H}{2G}\end{aligned} \tag{6.89}$$

from Eqs. (6.65) and (6.68). Then, the rate of twist α is defined in accordance with the sense of the stresses in Fig. 6.6(a) as

$$\alpha = -\omega_{xy,z} = -\frac{H}{2G}, \tag{6.90}$$

expressed in terms of H which is determined in the course of the solution.

Finding that the angle of rotation per unit length is *constant*, we may compute the total angle of rotation at any cross section $\mathscr{A}$, Fig. (6.6d), as

$$\mathscr{A} = \alpha z = -\frac{Hz}{2G}, \tag{6.91}$$

and the in-plane displacements, shown in Fig. 6.6(d), as

$$-u_x(y, z) = \mathscr{A} y = \alpha yz, \qquad \text{(a)}$$
$$u_y(x, z) = -\mathscr{A} x = \alpha xz. \qquad \text{(b)} \tag{6.92}$$

The normal displacement u_z involves out-of-plane deformations of the cross section, called *warping*, and takes the form [6.1]

$$u_z = \alpha\psi(x, y), \tag{6.93}$$

where ψ is a so-called warping function. Rewriting Eqs. (6.87), in view of Eqs. (6.92) and (6.93), we have

$$\alpha(y + \psi_{,x}) = \frac{\sigma_{xz}}{G}, \quad \text{(a)}$$
$$\alpha(-x + \psi_{,y}) = \frac{\sigma_{yz}}{G}. \quad \text{(b)} \qquad (6.94)$$

For elementary cases, it is sufficient to integrate the equations individually to produce

$$\psi = \frac{1}{2\alpha G}(\sigma_{xz}x + \sigma_{yz}y), \qquad (6.95)$$

anticipating that $u_z(x, y, 0) = 0$ eliminates the extraneous integration functions. Then,

$$u_z = \frac{1}{2G}(\sigma_{xz}x + \sigma_{yz}y). \qquad (6.96)$$

We summarize the main steps to obtain this solution.

(1) The stress function ϕ is selected in a form that is constant along the perimeter of the cross section to satisfy the boundary conditions.
(2) The stress function ϕ is related to the constant H through Eq. (6.68), which expresses compatibility.
(3) The stress function ϕ in terms of H is related to the twisting moment M_z by Eq. (6.84), which is an expression of overall equilibrium.
(4) H is then found in terms of M_z so that ϕ becomes a function of M_z.
(5) The stresses σ_{xz} and σ_{yz} are calculated from Eqs. (6.65).
(6) The rate of twist α is found from Eq. (6.90).
(7) The total angle of rotation $\mathscr{A}$ is given by Eq. (6.91).
(8) The displacements u_x, u_y and u_z are computed from Eqs. (6.92) and (6.96).

6.4.3 Torsion of Elliptical Shaft

As an example of the application of the St. Venant torsion theory, we consider the cross section shown in Fig. 6.7(a). The equation of the boundary is

$$\frac{x^2}{D^2} + \frac{y^2}{B^2} - 1 = 0, \qquad (6.97)$$

so we take

$$\phi = C\left(\frac{x^2}{D^2} + \frac{y^2}{B^2} - 1\right), \qquad (6.98)$$

where C is a constant, to satisfy step (1) of the previous paragraph.

Next, we calculate

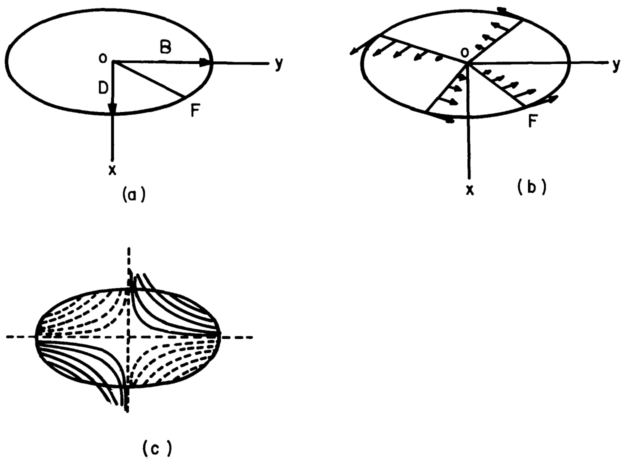

Fig. 6.7. (a) Elliptical cross section; (b) shearing stresses; (c) contours for normal displacement (after Timoshenko and Goodier, *Theory of Elasticity*, McGraw–Hill, 1951). Reprinted with permission.

$$H = 2C\left(\frac{1}{D^2} + \frac{1}{B^2}\right). \tag{6.99}$$

From Eq. (6.68) as suggested in step (2), solve for

$$C = \frac{HD^2B^2}{2(D^2 + B^2)}, \tag{6.100}$$

from which

$$\phi = \frac{HD^2B^2}{2(D^2 + B^2)}\left(\frac{x^2}{D^2} + \frac{y^2}{B^2} - 1\right). \tag{6.101}$$

Proceeding to step (3), we substitute Eq. (6.101) into Eq. (6.84), which becomes

$$\begin{aligned} M_z &= 2\int_A \frac{HD^2B^2}{2(D^2 + B^2)}\left(\frac{x^2}{D^2} + \frac{y^2}{B^2} - 1\right) dx\, dy \\ &= \frac{HD^2B^2}{D^2 + B^2}\left(\frac{1}{D^2} I_{yy} + \frac{1}{B^2} I_{xx} - A\right), \end{aligned} \tag{6.102}$$

in which the moments of inertia and the area for the ellipse are given by

$$I_{yy} = \frac{\pi BD^3}{4}, \qquad \text{(a)}$$

$$I_{xx} = \frac{\pi DB^3}{4}, \qquad \text{(b)} \quad (6.103)$$

$$A = \pi DB. \qquad \text{(c)}$$

Then, following step (4), we substitute Eqs. (6.103) into Eq. (6.102) and simplify to

$$M_z = -\frac{\pi D^3 B^3}{2(D^2 + B^2)} H, \tag{6.104}$$

so that

$$H = -\frac{2(D^2 + B^2)}{\pi D^3 B^3} M_z, \tag{6.105}$$

and, from Eq. (6.101),

$$\phi = \frac{-1}{\pi DB}\left(\frac{x^2}{D^2} + \frac{y^2}{B^2} - 1\right) M_z. \tag{6.106}$$

Now, we evaluate the stresses as suggested in step (5). Equations (6.65) yield

$$\sigma_{xz} = \phi_{,y} = \frac{-2y}{\pi D B^3} M_z, \quad \text{(a)}$$

$$\sigma_{yz} = -\phi_{,x} = \frac{2x}{\pi D^3 B} M_z. \quad \text{(b)} \tag{6.107}$$

Clearly, the maximum values occur at the boundaries and, if $B > D$, the absolute maximum is

$$\sigma_{yz}(D, 0) = \frac{2}{\pi D^2 B} M_z, \tag{6.108}$$

that is, at the extremity of the *minor* diameter. This is perhaps the most startling difference from the Coulomb approach where τ is proportional to r. It is also illustrative to consider a ray, say oF in Fig. 6.7(a), for which x/y is constant. Thus, the ratio of shearing stresses

$$\frac{\sigma_{yz}}{\sigma_{xz}} = -\frac{D^2}{B^2}\frac{x}{y} = \text{constant}. \tag{6.109}$$

This indicates that the *direction* of the resultant shear must likewise be constant. From the boundary requirement, this direction is *tangent* to the perimeter at F. This is illustrated in Fig. 6.7(b) for several rays.

Next, as step (6), the rate of twist is calculated from Eqs. (6.90) and (6.105) as

$$\alpha = -\frac{H}{2G} = \frac{(D^2 + B^2)}{\pi G D^3 B^3} M_z = \frac{M_z}{GJ_e}, \quad \text{(a)}$$

where (6.110)

$$J_e = \frac{\pi D^3 B^3}{D^2 + B^2}. \quad \text{(b)}$$

GJ_e is the torsional rigidity for the ellipse. The total angle of rotation $\mathscr{A}$, step (7), is evaluated at any point along the shaft as z times α, Eq. (6.91).

Finally, the displacements may be found as indicated in step (8). From Eqs. (6.92) and (6.110)

$$u_x = \frac{-M_z}{GJ_e} yz, \quad \text{(a)}$$
$$u_y = \frac{M_z}{GJ_e} xz. \quad \text{(b)} \tag{6.111}$$

Proceeding to the normal displacement and using Eqs. (6.96) and (6.107), we find

$$u_z = \frac{xy}{\pi G} \frac{(B^2 - D^2)}{D^3 B^3} M_z. \tag{6.112}$$

Of interest is the alternating algebraic sign of u_z in each quadrant as shown in Fig. 6.7(c), illustrating the departure from the plane cross section (warping) and the hyperbolic contours of u_z [6.1]. Also, we observe that a classical "fixed" or "built-in" support which is intended to develop an applied M_z may not permit the u_z displacements to occur. If so, a self-equilibrating set of axial stresses would develop near the support, negating Eq. (6.63). This is of comparatively minor importance in solid shafts.

Torsion of rectangular bars is of practical interest but is considerably more complicated [6.3]. An approximate energy-based solution is presented in Section 10.7.3. A distinguishing feature carried over from the elliptical cross-section solution to the rectangular is that the maximum shearing stress occurs at the center of the short side [6.1]. A lesser maximum occurs at the center of the long side, while the corner paradox is resolved by letting the shearing stresses approach zero, as is easily visualized using the membrane analogy discussed in the next section.

The torsional capacity of thin-walled members, comparatively small as previously argued with the membrane analogy, may be considerably enhanced by including the non-uniform torsion associated with the warping [6.4]. However, this discussion is beyond our present scope.

6.4.4 Membrane Analogy

Since the governing equation for the stress function ϕ, Eq. (6.68), is the same as that describing the deflection u_z of a uniformly loaded membrane, Eq. (5.26), we may derive an analogy to assist our understanding and interpretation of the St. Venant torsion problem. This analogy is attributed to Ludwig Prandl [6.1] and was extended into the inelastic range by Arpad Nádái (6.1].

We note from Eq. (6.91) that the r.h.s. of Eq. (6.68) is

$$H = -2G\alpha \tag{6.113}$$

so that replacing the quantity $-q/T$ in Eq. (5.26) by $-2G\alpha$ allows us to establish some important characteristics of the stress distribution on a solid bar under torsion.

(1) From Eq. (6.84), the *total torque* is proportional to the *volume* between the membrane, which follows the stress function, and the cross section of the bar.

(2) From Eq. (6.65), the *shearing stresses* are proportional to the *slope* of the membrane at any point.

To compare the *relative* torsional capacities of two cross sections, we need only visualize a membrane with the same maximum slope (that is, shearing stress) spanning both. It is apparent that a square or circular cross section has considerably more capacity than, say, a long narrow shape of the same area. Also, for a given cross-sectional area, St. Venant showed that the circular cross section is most efficient [6.1].

To illustrate a quantitative application of the membrane analogy, we consider a narrow rectangular bar as shown in Fig. 6.8(a). For the moment we neglect the effects of the short side boundaries and assume that the surface of the membrane is a parabolic cylinder as shown in Fig. 6.8(b).

The deflection of the membrane u_z is written in terms of the maximum deflection at the center, $\delta = u_z(0, 0)$, by the well-known property of the offsets to parabolas,

$$\frac{\delta - u_z}{\delta} = \frac{x^2}{(c/2)^2} \tag{6.114}$$

so that

$$u_z = \frac{4\delta}{c^2}\left[\frac{c^2}{4} - x^2\right]. \tag{6.115}$$

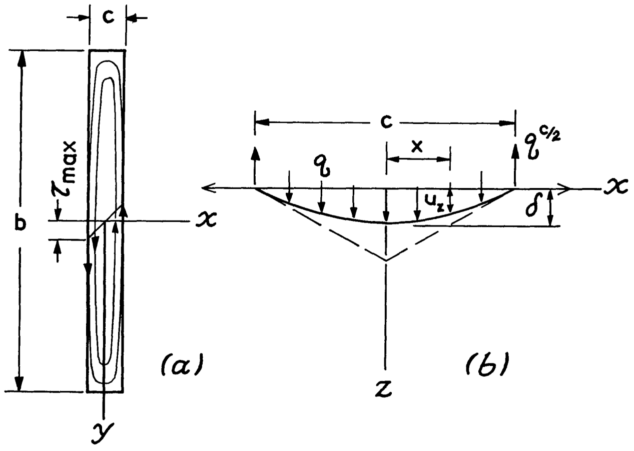

Fig. 6.8. Membrane stretched over narrow rectangular cross section. From Timoshenko and Goodier, *Theory of Elasticity*, © 1951. Reproduced with permission of McGraw-Hill.

The maximum slope is at the intersection of the x axis with the boundary along the long side ($\pm c/2$) and is evaluated from

$$u_{z,x}(x, y) = 8\delta x/c^2 \tag{6.116a}$$

as

$$u_{z,x}(\pm c/2, 0) = 4\delta/c \tag{6.116b}$$

retaining only the positive value because of symmetry.

By considering the statical moment about $x = 0$ in Fig. 6.8(b), we can write the equilibrium equation for a unit width of the parabolic cylinder, essentially the equation of a uniformly loaded string

$$-q\frac{c}{2}\left(\frac{c}{2}\right) + q\frac{c}{2}\left(\frac{c}{4}\right) + T\delta = 0$$

or

$$\delta = qc^2/(8T). \tag{6.117}$$

Therefore, Eq. (6.116b) becomes

$$(u_{z,x})_{\max} = qc/(2T). \tag{6.118}$$

Now we compute the torsion in the bar by evaluating the volume under the membrane

$$\begin{aligned} V &= \tfrac{2}{3}cb\delta \\ &= qbc^3/(12T). \end{aligned} \tag{6.119}$$

Using the analogy and replacing q/T by $2G\alpha$, we have

$$V = \tfrac{1}{6}bc^3G\alpha. \tag{6.120}$$

Inasmuch as M_z is *twice* the volume, as per Eq. (6.84),

$$M_z = \tfrac{1}{3}bc^3G\alpha \tag{6.121}$$

or the rate of twist α is given by

$$\alpha = M_z/(\tfrac{1}{3}bc^3G). \tag{6.122}$$

Turning to the maximum stress in the bar, Fig. 6.8(a), we have from Eqs. (6.65) and (6.118),

$$\begin{aligned} \tau_{\max} &= |(\sigma_{yz})|_{\max} \\ &= |\phi_{,x}|_{\max} \\ &= qc/(2T) \\ &= cG\alpha \\ &= M_t/(\tfrac{1}{3}bc^2). \end{aligned} \tag{6.123}$$

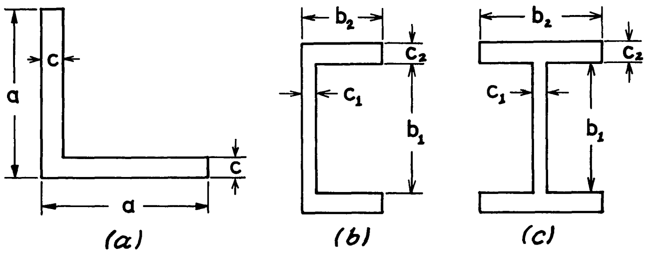

Fig. 6.9. Cross sections of thin-walled members. From Timoshenko and Goodier, *Theory of Elasticity*, © 1951. Reproduced with permission of McGraw-Hill.

The quantities $(\frac{1}{3}bc^3)$ and $(\frac{1}{3}bc^2)$ can be interpreted as section properties of rectangular bars related to torsional stiffnesses, much as moments of inertia relate to bending stiffness.

From Eq. (6.116a), the shearing stresses are distributed linearly across the width of the cross section. It may be shown that the shearing stresses are directed along the contours of the deflected membrane, [6.1] depicted in Fig. 6.8(a). Also, the shearing stresses acting near the short side, σ_{xz}, are not calculated by this simplification. They are smaller in magnitude but further separated than the σ_{yz} stresses and thus contribute equally to the total resistance provided by the cross section to M_z.

Equations (6.122) and (6.123) have great generality. If a thin-walled member, such as those shown in Fig. 6.9, is composed of several long rectangular pieces, each with $c = c_i$ and $b = b_i$, then we can imagine a parabolic cylindrical membrane spanning each segment independently so that

$$\alpha = M_z/(G \sum \tfrac{1}{3} b_i c_i^3) \tag{6.124}$$

and

$$(\tau_i)_{\max} = M_z c_i / \sum \tfrac{1}{3} b_i c_i^3. \tag{6.125}$$

For example, considering the flanges of the H-section shown in Fig. 6.9(c),

$$(\tau_2)_{\max} = M_z c_2 / (\tfrac{1}{3} b_1 c_1^3 + \tfrac{2}{3} b_2 c_2^3). \tag{6.126}$$

Exercises

6.1 Consider the solution for the bending of a cantilever, described in Sec. 6.2 and Sec. 6.3, and sketch a lateral and a top view of the deflected beam using Fig. 6.2 as a reference.

6.2 Investigate the Coulomb (simple) torsion solution, as developed for the circular cross section and for a rectangular cross section. In what respect is it deficient insofar as the theory of elasticity is concerned?

6.3 Two bars made of the same material and having the same length are subjected to the same torque (from [6.5]). One bar has a square cross section of side a and the other bar has a circular cross section of diameter a. Which bar has the greater rate of twist?

6.4 The torsion solution for a cylinder of equilateral triangular cross section is derivable from the stress function [6.6]

$$\phi = C(x - \sqrt{3}y - \tfrac{2}{3}h)(x + \sqrt{3}y - \tfrac{2}{3}h)(x + \tfrac{1}{3}h).$$

Derive expressions for the maximum and minimum shearing stresses and the rate of twist for a torque M_z.

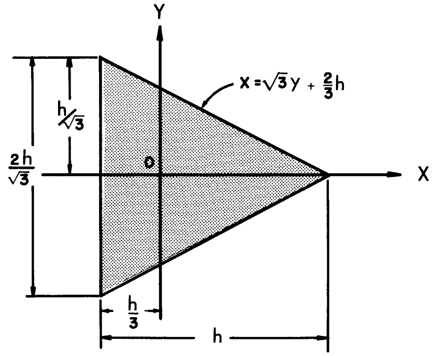

Problem 6.4. (From Ugural and Fenster, *Advanced Strength and Applied Elasticity*, Elsevier, 1975.) Reprinted with permission.

6.5 The torsional rigidity of a circle, an ellipse, and an equilateral triangle are denoted by GJ_c, GJ_e, and GJ_t, respectively. If the cross-sectional areas of these sections are equal, demonstrate that the following relationships exist (from [6.6]):

$$J_e = \frac{2ab}{a^2 + b^2} J_c, \qquad J_t = \frac{2\pi\sqrt{3}}{15} J_c,$$

where a and b are the semi-axes of the ellipse in the x and y directions.

References

[6.1] Timoshenko, S., and Goodier, J. N., *Theory of Elasticity*, 2nd ed. (McGraw–Hill Book Company, Inc., New York, 1951).

[6.2] Westergaard, H. M., *Theory of Elasticity and Plasticity* (Dover Publications, Inc., New York, 1964).

[6.3] Filonenko–Borodich, M., *Theory of Elasticity* (Dover Publications, Inc., New York, 1965).

[6.4] Timoshenko, S., and Gere, J. M., *Theory of Elastic Stability*, (McGraw–Hill Book Company, Inc., New York, 1951).
[6.5] Volterra, E., and Gaines, J. H., *Advanced Strength of Materials* (Prentice–Hall, Inc., Englewood Cliffs, NJ, 1971).
[6.6] Ugural, A. C., and Fenster, S. K., *Advanced Strength and Applied Elasticity* (Elsevier–North Holland, New York, 1975).

CHAPTER 7
Two-Dimensional Elasticity

7.1 Introduction

We briefly mentioned in Section 2.6.2 that an elasticity problem may be reduced from three- to two-dimensions if there is no traction on *one* plane passing through the body. This state is known as *plane stress* since all non-zero stresses are confined to planes parallel to the traction-free plane.

Many physical problems are reducible to two-dimensions, which facilitates the eventual solution. In this regard, we should mention the important engineering theories of plate bending and thin shells. These theories may be regarded as extensions of the elementary theory of beam bending in that the concept of a reference datum (that is, a middle plane or middle surface) is used to reduce the model to two-dimensions. The description of stresses, strains and displacements for points lying *away* from this datum are related to the corresponding quantities *on* the datum through maintenance of plane sections. Also, deformations in the direction normal to the reference datum are neglected. Such problems are not addressed in this book; this is a choice made primarily to reduce the scope of this introductory treatment. However, the epic treastise of August E. H. Love [7.1] on the theory of elasticity includes plate and shell theories, as well as the theory of rods, beam bending, stability and many other topics.[1]

Since we have identified problems *not* strictly within the two-dimensional theory of elasticity, a brief remark on the class of problems that *are* is in order. We have mentioned *plane stress*, which is obviously a possibility for bodies with one dimension much *smaller* than the other two, such as a thin sheet or diaphram loaded in the plane perpendicular to the small dimension. A less obvious case is that of a body in which one dimension is much *greater* than the other two, such as a long pressurized pipe, or perhaps a dam between massive end walls. This is known as *plane strain.*

[1] This prompted a favorite saying among graduate students and professors in an earlier era, that "All you really need is Love."

Our development is confined to the realm of isotropic elasticity but is easily extended to more complex material laws.

7.2 Plane Stress Equations

For plane stress with the z-axis stress-free, we have

$$\sigma_{xz} = \sigma_{yz} = \sigma_{zz} = 0. \tag{7.1}$$

Also, we assume that the remaining stresses do not vary with z, but are only functions of x and y. This reduces the equilibrium equations Eqs. (2.46), with $1 = x$, $2 = y$, $3 = z$, to

$$\begin{aligned} \sigma_{xx,x} + \sigma_{xy,y} + f_x &= 0, && \text{(a)} \\ \sigma_{xy,x} + \sigma_{yy,y} + f_y &= 0, && \text{(b)} \quad (7.2) \\ f_z &= 0. && \text{(c)} \end{aligned}$$

For some linear problems, it is convenient to specify the body force vector in the form

$$\mathbf{f} = -\nabla V = -V_{,i}\mathbf{e}_i, \tag{7.3}$$

where V is a potential function. This corresponds to a body force field that is *conservative* (elaborated in Sec. 10.6.2.). Introducing Eq. (7.3) into Eq. (7.2),

$$\begin{aligned} \sigma_{xx,x} + \sigma_{xy,y} - V_{,x} &= 0, && \text{(a)} \\ \sigma_{xy,x} + \sigma_{yy,y} - V_{,y} &= 0, && \text{(b)} \quad (7.4) \\ V_{,z} &= 0. && \text{(c)} \end{aligned}$$

We now consolidate the equilibrium equations using a technique which we introduced in the study of bending in Section 6.3.2 and of torsion in Section 6.4.2. The stresses are written as

$$\begin{aligned} \sigma_{xx} &= V + \phi_{,yy}, && \text{(a)} \\ \sigma_{yy} &= V + \phi_{,xx}, && \text{(b)} \quad (7.5) \\ \sigma_{xy} &= -\phi_{,xy}, && \text{(c)} \end{aligned}$$

in which ϕ is a stress function named after the astronomer George Airy. Substitution of Eqs. (7.5) into Eqs. (7.4a, b) satisfies these equations identically.

We also develop the constitutive equations in terms of ϕ. First, the generalized Hooke's law Eq. (4.29b) for the plane stress case becomes

$$\begin{aligned} \varepsilon_{xx} &= \frac{1}{E}(\sigma_{xx} - \nu\sigma_{yy}), && \text{(a)} \\ \varepsilon_{yy} &= \frac{1}{E}(\sigma_{yy} - \nu\sigma_{xx}), && \text{(b)} \end{aligned}$$

$$\varepsilon_{zz} = -\frac{\nu}{E}(\sigma_{xx} + \sigma_{yy}), \qquad \text{(c)}$$

$$\varepsilon_{xy} = \frac{1}{2G}\sigma_{xy}, \qquad \text{(d)}$$

$$\varepsilon_{xz} = \varepsilon_{yz} = 0. \qquad \text{(e)} \quad (7.6)$$

From Eqs. (7.6) we see that the strains do not depend on z, only on x and y. However, from Eq. (7.6c), we find a nonzero *strain* in the z direction, indicating that a state of plane stress does *not* imply a corresponding state of plane strain.

It is also convenient to write the stresses in terms of the strains by solving Eqs. (7.6a) and (7.6b) for σ_{xx} and σ_{yy} and Eq. (7.6d) for σ_{xy}:

$$\sigma_{xx} = \frac{E}{(1-\nu^2)}(\varepsilon_{xx} + \nu\varepsilon_{yy}) \qquad \text{(a)} \quad (7.7)$$

$$\sigma_{yy} = \frac{E}{(1-\nu^2)}(\varepsilon_{yy} + \nu\varepsilon_{xx}) \qquad \text{(b)} \quad (7.7)$$

$$\sigma_{xy} = 2G\varepsilon_{xy}. \qquad \text{(c)} \quad (7.7)$$

Introducing Eqs. (7.5) into Eqs. (7.6) produces

$$\varepsilon_{xx} = \frac{1}{E}[(\phi_{,yy} - \nu\phi_{,xx}) + (1-\nu)V], \qquad \text{(a)}$$

$$\varepsilon_{yy} = \frac{1}{E}[(\phi_{,xx} - \nu\phi_{,yy}) + (1-\nu)V], \qquad \text{(b)}$$

$$\varepsilon_{zz} = -\frac{\nu}{E}[(\phi_{,xx} + \phi_{,yy}) + 2V], \qquad \text{(c)} \quad (7.8)$$

$$\varepsilon_{xy} = -\frac{1}{2G}\phi_{,xy} \qquad \text{(d)}$$

$$\varepsilon_{xz} = \varepsilon_{yz} = 0. \qquad \text{(e)}$$

Now, we establish the compatibility equations in terms of the stress function. We consider Eqs. (3.59). First, Eq. (3.59a), with substitution of the strains from Eqs. (7.8), becomes

$$\frac{1}{E}[\phi_{,yyyy} - \nu\phi_{,xxyy} + (1-\nu)V_{,yy} + \phi_{,xxxx} - \nu\phi_{,xxyy} + (1-\nu)V_{,xx}]$$

$$= -\frac{1}{G}\phi_{,xxyy}. \qquad \text{(a)} \quad (7.9)$$

With $E/G = 2(1+\nu)$ from Eqs. (4.24a, e), Eq. (7.9a) reduces to

$$\nabla^4\phi = -(1-\nu)\nabla^2 V. \qquad \text{(b)} \quad (7.9)$$

where the operator $\nabla^4(\ )$ is the two-dimensional contraction of the operator defined in Eq. (1.10c), i.e.,

$$\nabla^4(\ ) = (\ )_{,xxxx} + 2(\ )_{,xxyy} + (\ )_{,yyyy}. \qquad \text{(c)} \quad (7.9)$$

Equations (3.59d, e) are identically satisfied, while the others Eqs. (3.59b, c, f) become

$$\begin{aligned} \varepsilon_{zz,yy} &= \phi_{,xxyy} + \phi_{,yyyy} + 2V_{,yy} = 0, && \text{(a)} \\ \varepsilon_{zz,xx} &= \phi_{xxxx} + \phi_{yyxx} + 2V_{,xx} = 0, && \text{(b)} \quad (7.10) \\ \varepsilon_{zz,xy} &= \phi_{,xxxy} + \phi_{,yyyx} + 2V_{,xy} = 0. && \text{(c)} \end{aligned}$$

Elementary plane stress theory does not consider Eqs. (7.10), but only Eq. (7.9b). In a sense then this is an approximation, but Eqs. (7.10) only contain terms related to ε_{zz} which, although not zero, is but a "Poisson" effect as shown by Eq. (7.8c). Especially for thin members, the error should be negligible. Thus, Eqs. (7.5) and the single compatibility equation Eq. (7.9b) constitute the governing equations for isotropic plane stress theory.

An extension of this theory, in which σ_{zz} is not equal to 0, as stated in Eq. (7.1), but is set to a known or assumed value, is known as generalized plane stress.

7.3 Plane Strain Equations

For plane strain with the z-axis strain-free, we have

$$\varepsilon_{xz} = \varepsilon_{yz} = \varepsilon_{zz} = 0. \qquad (7.11)$$

As in the case of plane stress, all tractions and body forces are functions of x and y only.

To enforce these conditions we use the generalized Hooke's law Eq. (4.29b), with $1 = x$, $2 = y$, $3 = z$,

$$\begin{aligned} \varepsilon_{xx} &= \frac{1}{E}[\sigma_{xx} - \nu(\sigma_{yy} + \sigma_{zz})], && \text{(a)} \\ \varepsilon_{yy} &= \frac{1}{E}[\sigma_{yy} - \nu(\sigma_{xx} + \sigma_{zz})], && \text{(b)} \\ 0 &= \frac{1}{E}[\sigma_{zz} - \nu(\sigma_{xx} + \sigma_{yy})], && \text{(c)} \quad (7.12) \\ \varepsilon_{xy} &= \frac{1}{2G}\sigma_{xy}, && \text{(d)} \\ \varepsilon_{xz} &= \varepsilon_{yz} = 0. && \text{(e)} \end{aligned}$$

Equation (7.12c) indicates that

$$\sigma_{zz} = \nu(\sigma_{xx} + \sigma_{yy}), \tag{7.13}$$

so that the strain-free plane is not stress-free, in general. The equilibrium equations Eqs. (2.46) are almost identical to the plane stress case Eqs. (7.2), except for Eq. (7.2c) where $\sigma_{zz,z}$ remains; while $f_z = 0$, since $\mathbf{f} = \mathbf{f}(x, y)$. With Eq. (7.3) in force, we have

$$\begin{aligned} \sigma_{xx,x} + \sigma_{xy,y} - V_{,x} &= 0, && \text{(a)} \\ \sigma_{xy,x} + \sigma_{yy,y} - V_{,y} &= 0, && \text{(b)} \quad (7.14) \\ \sigma_{zz} &= \text{constant}. && \text{(c)} \end{aligned}$$

Turning to the compatibility equations Eqs. (3.59), all are identically satisfied except for Eq. (3.59a),

$$\varepsilon_{xx,yy} + \varepsilon_{yy,xx} = 2\varepsilon_{xy,xy}. \tag{7.15}$$

This is the same equation from which Eq. (7.9a) was derived. Thus, we again introduce the Airy stress function Eq. (7.5), along with Eq. (7.13), into Eqs. (7.12) which become

$$\begin{aligned} \varepsilon_{xx} &= \frac{1}{E}[(1 - \nu^2)\phi_{,yy} - \nu(1 + \nu)\phi_{,xx} + [1 - \nu(1 + 2\nu)]V], && \text{(a)} \\ \varepsilon_{yy} &= \frac{1}{E}[(1 - \nu^2)\phi_{,xx} - \nu(1 + \nu)\phi_{,yy} + [1 - \nu(1 + 2\nu)]V], && \text{(b)} \quad (7.16) \\ \varepsilon_{xy} &= -\frac{1}{2G}\phi_{,xy}. && \text{(c)} \end{aligned}$$

Then, we write Eq. (7.15), using Eqs. (7.16), as

$$\begin{aligned} &\frac{1}{E}[(1 - \nu^2)\phi_{,yyyy} - \nu(1 + \nu)\phi_{,xxyy} + [1 - \nu(1 + 2\nu)]V_{,yy} \\ &\qquad + (1 - \nu^2)\phi_{,xxxx} - \nu(1 + \nu)\phi_{,xxyy} + [1 - \nu(1 + 2\nu)]V_{,xx}] \\ &= -\frac{1}{G}\phi_{,xxyy}, && \text{(a)} \quad (7.17) \end{aligned}$$

which reduces to

$$\nabla^4\phi = -\frac{(1 - 2\nu)}{1 - \nu}\nabla^2 V, \qquad \text{(b)} \quad (7.17)$$

which is remarkably close to Eq. (7.9b). In fact, for *no body* forces, the two equations are identical. The resulting homogeneous compatibility equation

$$\nabla^4\phi = 0 \tag{7.18}$$

is known as the *biharmonic* equation.

We see that plane strain is exact, insofar as satisfying the St. Venant compatibility equations, while plane stress violates some of the equations. For applications with no body forces, the solution for either case involves the same equations, Eqs. (7.5) and Eq. (7.18); while if body forces are present, a slight alteration of the particular solution for the biharmonic equation is needed between the two theories.

The solution to the biharmonic problem in Cartesian coordinates is most directly written in terms of polynomials having the general form

$$\phi = \sum_m \sum_n C_{mn} x^m y^n. \tag{7.19}$$

Obviously the lower-order terms, that is, $m + n \leq 3$, *each* satisfy the equation identically. However, the linear terms $C_{00} + C_{10}x + C_{01}y$ do not contribute to stresses. The general strategy is to try and construct solutions from the lower-order terms that satisfy the biharmonic equation *individually* and the boundary conditions *collectively*. For more complicated problems, it is necessary to use higher-order terms, that is, $m + n > 3$, and achieve satisfaction of the equation by a combination of the individual terms. Finally, in the nature of general remarks, it is usually required to employ St. Venant's principle to satisfy some of the boundary conditions.

We present some specific applications of this approach in Section 7.9. However, it is instructive to consider the plane stress problem on a circular domain first, both from the standpoints of mathematical simplicity and practical importance.

7.4 Cylindrical Coordinates

7.4.1 Geometric Relations

There are many problems in two-dimensional elasticity that are most conveniently treated in cylindrical coordinates (which degenerate to polar coordinates). Therefore, we develop the appropriate transformations between Cartesian and polar coordinates.

Referring to Fig. 7.1, we have the relations [7.2] between x, y and r, θ as

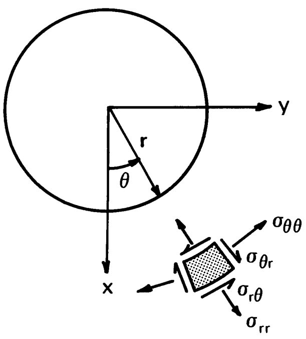

Fig. 7.1. Polar coordinates.

$$x = r\cos\theta, \quad \text{(a)}$$
$$y = r\sin\theta, \quad \text{(b)}$$
$$r = (x^2 + y^2)^{1/2}, \quad \text{(c)} \qquad (7.20)$$
$$\theta = \tan^{-1}\frac{y}{x}. \quad \text{(d)}$$

Also, the derivatives of the polar coordinates with respect to the Cartesian coordinates are of interest

$$r_{,x} = \frac{1}{2}(x^2 + y^2)^{-1/2}(2x) = \frac{x}{r} = \cos\theta, \quad \text{(a)}$$
$$r_{,y} = \frac{y}{r} = \sin\theta, \quad \text{(b)}$$
$$\theta_{,x} = \frac{1}{1 + (y/x)^2}\left(-\frac{y}{x^2}\right) = -\frac{y}{r^2} = -\frac{\sin\theta}{r}, \quad \text{(c)} \qquad (7.21)$$
$$\theta_{,y} = \frac{1}{1 + (y/x)^2}\left(\frac{1}{x}\right) = \frac{x}{r^2} = \frac{\cos\theta}{r}. \quad \text{(d)}$$

Using Eqs. (7.21), we may write the differentiation formulas for functions specified in terms of r and θ as

$$\frac{\partial(\ )}{\partial x} = \frac{\partial(\ )}{\partial r}r_{,x} + \frac{\partial(\ )}{\partial\theta}\theta_{,x}$$
$$= \frac{\partial(\ )}{\partial r}\cos\theta + \frac{\partial(\ )}{\partial\theta}\left(\frac{-\sin\theta}{r}\right), \quad \text{(a)}$$
$$\frac{\partial(\ )}{\partial y} = \frac{\partial(\ )}{\partial r}r_{,y} + \frac{\partial(\ )}{\partial\theta}\theta_{,y} \qquad (7.22)$$
$$= \frac{\partial(\ )}{\partial r}\sin\theta + \frac{\partial(\ )}{\partial\theta}\left(\frac{\cos\theta}{r}\right). \quad \text{(b)}$$

7.4.2 Transformation of Stress Tensor and Compatibility Equation

The stress components are transformed using Eq. (2.13) to become

$$\sigma_{rr} = \alpha_{ri}\alpha_{rj}\sigma_{ij}, \quad \text{(a)}$$
$$\sigma_{\theta\theta} = \alpha_{\theta i}\alpha_{\theta j}\sigma_{ij}, \quad \text{(b)} \qquad (7.23)$$
$$\sigma_{r\theta} = \alpha_{ri}\alpha_{\theta j}\sigma_{ij}. \quad \text{(c)}$$

The direction cosines are

	x	y	z
r	$\cos\theta$	$\sin\theta$	0
θ	$-\sin\theta$	$\cos\theta$	0
z	0	0	1

(7.24)

and Eqs. (7.23) and (7.24) give

$$\begin{aligned}
\sigma_{rr} &= \sigma_{xx}\cos^2\theta + \sigma_{yy}\sin^2\theta + 2\sigma_{xy}\sin\theta\cos\theta, && \text{(a)}\\
\sigma_{\theta\theta} &= \sigma_{xx}\sin^2\theta + \sigma_{yy}\cos^2\theta - 2\sigma_{xy}\sin\theta\cos\theta, && \text{(b)}\\
\sigma_{r\theta} &= -\sigma_{xx}\sin\theta\cos\theta + \sigma_{yy}\sin\theta\cos\theta \\
&\quad + \sigma_{xy}(\cos^2\theta - \sin^2\theta), && \text{(c)}
\end{aligned} \tag{7.25}$$

which should be familiar from the Mohr's circle concept of elementary strength of materials [7.3].

We now introduce the Airy stress function Eq. (7.5) into Eq. (7.25), dropping the body forces terms, to produce

$$\begin{aligned}
\sigma_{rr} &= \phi_{,yy}\cos^2\theta + \phi_{,xx}\sin^2\theta - 2\phi_{,xy}\sin\theta\cos\theta, && \text{(a)}\\
\sigma_{\theta\theta} &= \phi_{,yy}\sin^2\theta + \phi_{,xx}\cos^2\theta + 2\phi_{,xy}\sin\theta\cos\theta && \text{(b)}\\
\sigma_{r\theta} &= -\phi_{,yy}\sin\theta\cos\theta + \phi_{,xx}\sin\theta\cos\theta \\
&\quad - \phi_{,xy}(\cos^2\theta - \sin^2\theta). && \text{(c)}
\end{aligned} \tag{7.26}$$

The next step is to write Eqs. (7.26) entirely in terms of cylindrical coordinates. This involves repeated application of Eq. (7.22), for example,

$$\begin{aligned}
\phi_{,xx} &= \frac{\partial}{\partial x}\left(\frac{\partial\phi}{\partial x}\right) = \frac{\partial}{\partial x}\left[\frac{\partial\phi}{\partial r}\cos\theta - \frac{\partial\phi}{\partial\theta}\frac{\sin\theta}{r}\right]\\
&= \cos\theta\left[\frac{\partial^2\phi}{\partial r^2}\cos\theta - \frac{\partial^2\phi}{\partial r\partial\theta}\frac{\sin\theta}{r}\right] + \frac{\partial\phi}{\partial r}\left[0 + \frac{\sin^2\theta}{r}\right]\\
&\quad - \frac{\sin\theta}{r}\left[\frac{\partial^2\phi}{\partial r\partial\theta}\cos\theta - \frac{\partial^2\phi}{\partial\theta^2}\frac{\sin\theta}{r}\right]\\
&\quad - \frac{\partial\phi}{\partial\theta}\left[-\frac{\sin\theta}{r^2}\cos\theta - \frac{\cos\theta\sin\theta}{r^2}\right]\\
&= \phi_{,rr}\cos^2\theta - 2\phi_{,r\theta}\frac{\sin\theta\cos\theta}{r} + 2\phi_{,\theta}\frac{\sin\theta\cos\theta}{r}\\
&\quad + \phi_{,r}\frac{\sin^2\theta}{r} + \phi_{,\theta\theta}\frac{\sin^2\theta}{r^2}.
\end{aligned} \tag{7.27}$$

Continuing with $\phi_{,yy}$ and $\phi_{,zz}$ and back-substituting into Eqs. (7.25) eventually produces the usable relations [7.4]

$$\sigma_{rr} = \frac{1}{r}\phi_{,r} + \frac{1}{r^2}\phi_{,\theta\theta}, \qquad \text{(a)}$$

$$\sigma_{\theta\theta} = \phi_{,rr}, \qquad \text{(b)} \quad (7.28)$$

$$\sigma_{r\theta} = \frac{1}{r^2}\phi_{,\theta} - \frac{1}{r}\phi_{,r\theta}. \qquad \text{(c)}$$

The (invariant) biharmonic equation in cylindrical coordinates is written by using the appropriate operator. Thus, from Eq. 7.18, the expression

$$\nabla^4\phi = \nabla^2(\nabla^2\phi) = 0 \qquad (7.29)$$

holds, where

$$\nabla^2\phi = \phi_{,rr} + \frac{1}{r}\phi_{,r} + \frac{1}{r^2}\phi_{,\theta\theta} \qquad \text{(a)} \quad (7.30)$$

and

$$\nabla^4\phi = \left[\frac{\partial^2}{\partial r^2} + \frac{1}{r}\frac{\partial}{\partial r} + \frac{1}{r^2}\frac{\partial^2}{\partial\theta^2}\right]\left[\phi_{,rr} + \frac{1}{r}\phi_{,r} + \frac{1}{r^2}\phi_{,\theta\theta}\right], \qquad \text{(b)} \quad (7.30)$$

which constitute the transformation of Eqs. (1–10b,c) into cylindrical coordinates.

7.4.3 Axisymmetric Stresses and Displacements

Many problems in the circular domain are axisymmetric, depending only on r and not on θ. In these cases, we may use a simplified form of the preceding equations

$$\sigma_{rr} = \frac{1}{r}\phi_{,r}, \qquad \text{(a)}$$

$$\sigma_{\theta\theta} = \phi_{,rr}, \qquad \text{(b)}$$

$$\sigma_{r\theta} = 0, \qquad \text{(c)}$$

$$\nabla^2\phi = \phi_{,rr} + \frac{1}{r}\phi_{,r} = \frac{1}{r}[r(\phi)_{,r}]_{,r} \qquad \text{(d)} \quad (7.31)$$

$$\begin{aligned}\nabla^4\phi &= \left[\frac{d^2}{dr^2} + \frac{1}{r}\frac{d}{dr}\right]\left[\phi_{,rr} + \frac{1}{r}\phi_{,r}\right] \\ &= \frac{1}{r}\left[r\left(\frac{1}{r}[r\phi_{,r}]_{,r}\right)_{,r}\right]_{,r} \\ &= 0. \end{aligned} \qquad \text{(e)}$$

The compact forms for $\nabla^2\phi$ and $\nabla^4\phi$ are easily verified by expansion of the terms and are readily integrated as follows.

$$
\begin{aligned}
\frac{1}{r}\left[r\left(\frac{1}{r}[r\phi_{,r}]_{,r}\right)_{,r}\right]_{,r} &= 0 \\
\left[\qquad\qquad\right]_{,r} &= 0 \\
\left[\qquad\qquad\right] &= C_1 \\
\left(\qquad\quad\right)_{,r} &= \frac{C_1}{r} \\
\left(\qquad\quad\right) &= C_1 \ln r + C_2 \\
[\quad]_{,r} &= C_1 r \ln r + C_2 r \\
[\quad] &= C_1\left(\frac{r^2}{2}\ln r - \frac{r^2}{2}\right) + C_2\frac{r^2}{2} + C_3 \\
&= C_1' r^2 \ln r + C_2' r^2 + C_3 \\
\phi_{,r} &= C_1' r \ln r + C_2' r + \frac{C_3}{r} \\
\phi &= C_1\left(\frac{r^2}{2}\ln r - \frac{r^2}{2}\right) + C_2\frac{r^2}{2} + C_3 \ln r + C_4
\end{aligned}
$$

or, redefining the constants,

$$\phi = C_1 r^2 \ln r + C_2 r^2 + C_3 \ln r + C_4. \tag{7.32}$$

The corresponding stresses are found by substituting Eq. (7.32) into Eqs. (7.31a–c)

$$
\begin{aligned}
\sigma_{rr} &= C_1(1 + 2\ln r) + 2C_2 + C_3\frac{1}{r^2}, && \text{(a)} \\
\sigma_{\theta\theta} &= C_1(3 + 2\ln r) + 2C_2 - C_3\frac{1}{r^2}, && \text{(b)} \quad (7.33) \\
\sigma_{r\theta} &= 0. && \text{(c)}
\end{aligned}
$$

The transformation into cylindrical coordinates is sufficient to solve some representative stress analysis problems that are of great practical interest. However, in order to derive the corresponding displacements, we would need to have the kinematic law Eq. (3.14) also transformed into cylindrical coordinates. This is rather involved, but is carried out neatly by Little [7.4] using dyadic notation. Here, we simply record the results without derivation

$$\varepsilon_{rr} = u_{r,r} \qquad \text{(a)}$$

$$\varepsilon_{\theta\theta} = \frac{u_r}{r} + \frac{1}{r} u_{\theta,\theta} \qquad \text{(b)}$$

$$u_r = \frac{1}{E}\left\{C_1 r[(1 - \nu)(2\ln r - 1) - 2\nu] + 2C_2(1 - \nu)r - C_3\frac{(1 + \nu)}{r} + C_4 \sin\theta + C_5 \cos\theta\right\} \qquad \text{(c)}$$

$$u_\theta = \frac{1}{E}[4C_1 r\theta + C_4 \cos\theta - C_5 \sin\theta + C_6 r] \qquad \text{(d)} \quad (7.34)$$

in which $C_4 - C_6$ multiply rigid body terms. Notice that Eqs. (7.34) contain θ-dependent terms, although they are derived from the axisymmetric stress field Eqs. (7.33). This is a so-called "quasi-axisymmetric" case which occasionally proves to be useful, as we will see later.

7.5 Thick-Walled Cylinder or Disk

We examine a thick-walled cylinder constrained along the normal axis, plane strain, or its counterpart—a thin disk with a circular hole in the center, plane stress.

The cylinder is subjected to external and internal pressures shown in Fig. 7.2(a), clearly an axisymmetrical loading case that should exhibit only an axisymmetric response. Thus, Eqs. (7.33) are applicable.

We consider Eqs. (7.33a, b). There are two obvious boundary conditions to evaluate the three constants

$$\sigma_{rr}(R_0) = -p_0, \qquad \text{(a)}$$
$$\sigma_{rr}(R_i) = -p_i, \qquad \text{(b)} \quad (7.35)$$

which give

$$-p_i = C_1(1 + 2\ln R_i) + 2C_2 + \frac{C_3}{R_i^2}, \qquad \text{(c)}$$
$$-p_0 = C_1(1 + 2\ln R_0) + 2C_2 + \frac{C_3}{R_0^2}. \qquad \text{(d)} \quad (7.35)$$

To obtain a third condition, we must resort to the displacement expressions Eqs. (7.34). The expression for u_θ is multi-valued in θ and, since $u_\theta(0) = u_\theta(2\pi) = u_\theta(4\pi)$, etc., we have $C_1 = 0$.

Then, we solve Eqs. (7.35) to get

$$C_2 = \frac{p_i R_i^2 - p_0 R_0^2}{2(R_0^2 - R_i^2)}, \qquad \text{(a)}$$
$$C_3 = \frac{R_i^2 R_0^2 (p_0 - p_i)}{(R_0^2 - R_i^2)}, \qquad \text{(b)} \quad (7.36)$$

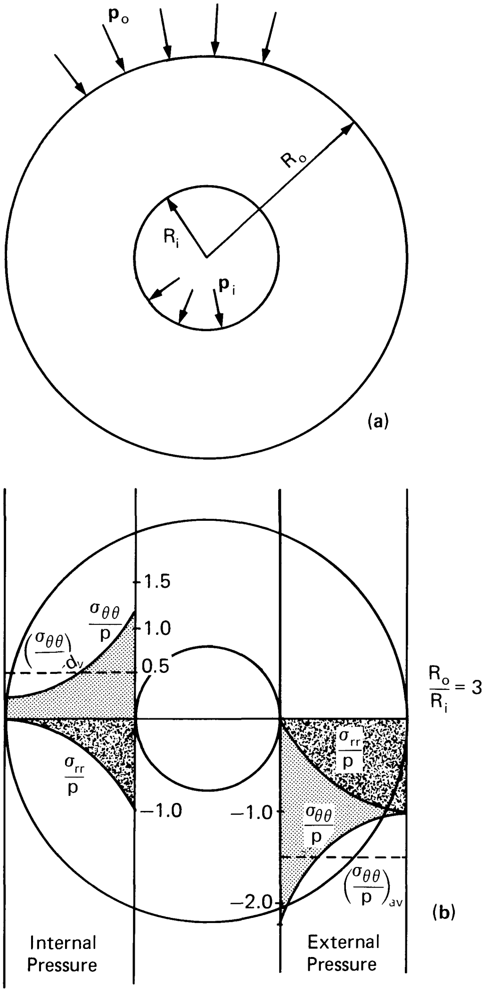

Fig. 7.2. (a) Thick-walled cylinder under external and internal pressure; (b) stress distribution.

which, when substituted into Eqs. (7.33a, b), give the stress distributions

$$\sigma_{rr} = \frac{p_i R_i^2 - p_0 R_0^2}{R_0^2 - R_i^2} + \frac{R_i^2 R_0^2 (p_0 - p_i)}{r^2 (R_0^2 - R_i^2)}, \qquad \text{(a)}$$

$$\sigma_{\theta\theta} = \frac{p_i R_i^2 - p_0 R_0^2}{R_0^2 - R_i^2} - \frac{R_i^2 R_0^2 (p_0 - p_i)}{r^2 (R_0^2 - R_i^2)}, \qquad \text{(b)} \qquad (7.37)$$

and, from Eqs. (7.13) for the constrained (plane strain) case,

$$\sigma_{zz} = \nu(\sigma_{xx} + \sigma_{yy}) = \nu(\sigma_{rr} + \sigma_{\theta\theta})$$
$$= \frac{2\nu(p_i R_i^2 - p_0 R_0^2)}{R_0^2 - R_i^2}. \qquad \text{(c)} \quad (7.37)$$

This solution was presented by G. Lamé [7.2] in the middle 19th century.

The complete solution contains the displacements as well. These may be routinely evaluated from Eqs. (7.34c, d) and are given explicitly by Timoshenko and Goodier [7.2].

We may also obtain the solution for the case of pressure within a small hole in an infinite plane, a two-dimensional static representation of an explosion. We divide the numerator and the denominator of all terms in Eqs. (7.37) by R_0^2, take $p_0 = 0$ and let $R_0 \to \infty$. This leaves only the second terms of Eqs. (7.37a, b), simplified to

$$\sigma_{rr} = -p_i \frac{R_i^2}{r^2}, \qquad \text{(a)}$$
$$\sigma_{\theta\theta} = p_i \frac{R_i^2}{r^2}. \qquad \text{(b)} \quad (7.38)$$

The physical behavior of a thick-walled cylinder is easiest to appreciate by considering the cases of internal pressure and external pressure separately. Results for these two cases and $R_0/R_i = 3$ are shown through the wall thickness on Fig. 7.2(b). For comparison, the nominal circumferential stress from the simple formula of the strength of materials $\sigma_{\theta\theta} = pR/t$; where $R = R_0$ or R_i for p_0 or p_i, respectively, and $t = R_0 - R_i$; is shown as $(\sigma_{\theta\theta})_{av}$. Obviously, the latter formula greatly underestimates the maximum circumferential stress that occurs at the inside wall and also does not recognize the radial stress.

The plane stress counterpart of this solution is a thin disk under radial loading p_0 and p_i. In this case, instead of Eq. (7.37c), we would have from Eq. (7.6c)

$$\varepsilon_{zz} = -\frac{\nu}{E}(\sigma_{rr} + \sigma_{\theta\theta})$$
$$= \frac{2\nu}{E} \frac{(p_0 R_0^2 - p_i R_i^2)}{R_0^2 - R_i^2}. \qquad (7.39)$$

Another variant to the solution is the case of a thick-walled pipe with closed ends. This is neither plane strain nor plane stress, but can be viewed as a superposition of the two-dimensional solution in the cross section, and an axial stress that is uniformly distributed and maintains overall equilibrium in the z direction. The net force is

$$F_z = p_0 \pi R_0^2 - P_i \pi R_i^2 \qquad \text{(a)} \quad (7.40)$$

and

$$\sigma_{zz} = \frac{F_z}{\pi(R_0^2 - R_i^2)} = \frac{p_i R_i^2 - p_0 R_0^2}{R_0^2 - R_i^2}. \qquad \text{(b)} \quad (7.40)$$

The in-plane strains should account for σ_{zz} (Eqs. 7.12a, b).

7.6 Sheet with Small Circular Hole

We consider a sheet of unit thickness under uniaxial uniform tension $\mathbf{T}_x = T_x \mathbf{e}_x$ with a small circular hole of radius A in the interior, as shown in Fig. 7.3(a). Without the hole, the stress would be uniform

$$\sigma_{xx} = T_x, \qquad \text{(a)}$$

$$\sigma_{yy} = \sigma_{xy} = 0. \qquad \text{(b)} \quad (7.41)$$

This distribution should be altered only in the vicinity of the hole, with the stresses maintaining the uniform values in the remainder of the domain by St. Venant's principle. Based on this reasoning, it is convenient to construct a hypothetical circle with a radius equal to the sheet width as shown on the figure, thus facilitating a solution in polar coordinates. We use Eqs. (7.25) to transform the uniform stress state at $r = B$

$$\sigma_{rr}(B, \theta) = T_x \cos^2 \theta = \frac{T_x}{2}(1 + \cos 2\theta), \qquad \text{(a)}$$

$$\sigma_{\theta\theta}(B, \theta) = T_x \sin^2 \theta = \frac{T_x}{2}(1 + \cos 2\theta), \qquad \text{(b)} \quad (7.42)$$

$$\sigma_{r\theta}(B, \theta) = -T_x \sin\theta \cos\theta = -\frac{T_x}{2}\sin 2\theta. \qquad \text{(c)}$$

The stresses along the circular boundary at $r = B$ can be separated into two parts, as shown in Figs. 7.3(b) and (c). On Fig. 7.3(b), we have the axisymmetric stress state

$$\sigma_{rr}^{(1)}(B, \theta) = \frac{T_x}{2}, \qquad \text{(a)}$$

$$\sigma_{r\theta}^{(1)}(B, \theta) = 0. \qquad \text{(b)} \quad (7.43)$$

Of course, $\sigma_{\theta\theta}$ does not act on the boundary. On Fig. 7.3(c), we have a stress state dependent on θ in the form

$$\sigma_{rr}^{(2)}(B, \theta) = \frac{T_x}{2}\cos 2\theta, \qquad \text{(a)}$$

$$\sigma_{r\theta}^{(2)}(B, \theta) = -\frac{T_x}{2}\sin 2\theta. \qquad \text{(b)} \quad (7.44)$$

The advantage to the separation is that we may use the solution for a

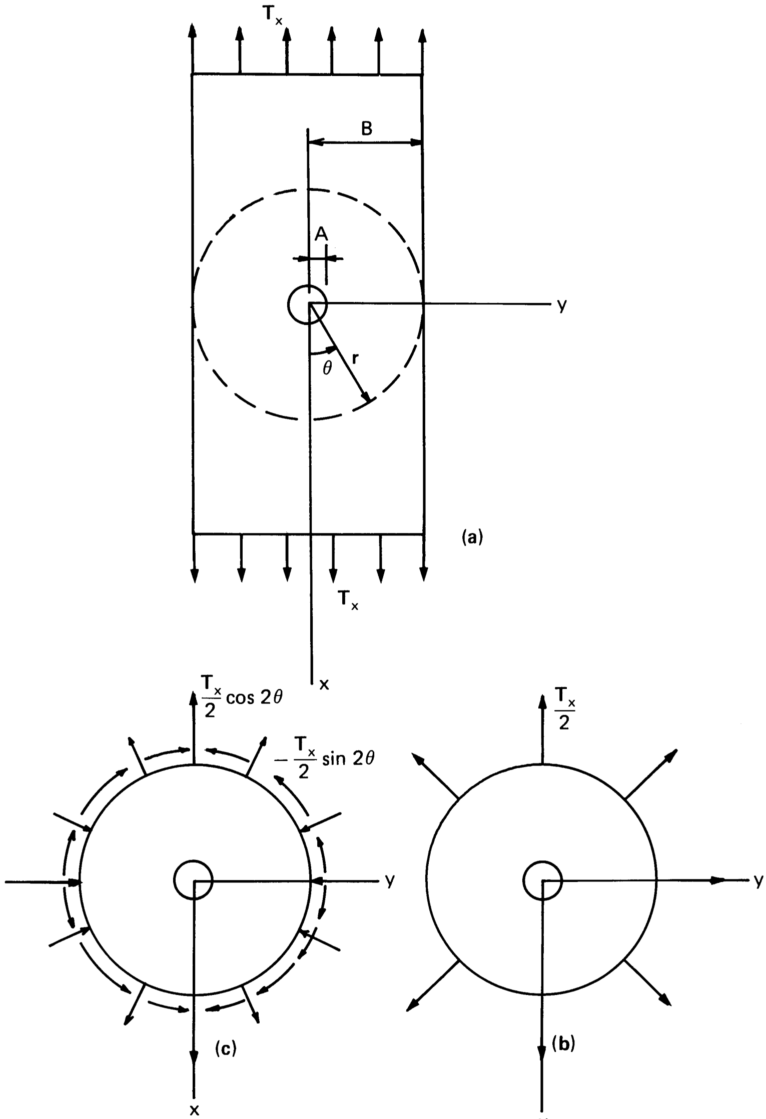

Fig. 7.3. (a) Sheet with small hole under tension; (b) axisymmetric state of stress; (c) θ-dependent state of stress.

thin-disk under axisymmetrical radial load for the first part, Eqs. 7.37(a, b). With $R_i = A$, $R_0 = B$, $p_i = 0$ and $p_0 = -T_x/2$ (since it was originally shown as (+) inward in Fig. 7.2), we have

$$\sigma_{rr}^{(1)} = \frac{T_x}{2}\frac{B^2}{B^2 - A^2} - \frac{T_x}{2}\frac{A^2B^2}{B^2 - A^2}\frac{1}{r^2}, \quad \text{(a)}$$

$$\sigma_{\theta\theta}^{(1)} = \frac{T_x}{2}\frac{B^2}{B^2 - A^2} + \frac{T_x}{2}\frac{A^2B^2}{B^2 - A^2}\frac{1}{r^2}. \quad \text{(b)} \qquad (7.45)$$

Thus, we need only focus on the second part.

We must consider the general form of the biharmonic equation Eq. (7.30b). Recognizing the periodicity of the boundary conditions Eq. (7.44), we assume a solution in the separated form

$$\phi = F(r)\cos 2\theta. \qquad (7.46)$$

If we substitute into Eq. (7.30b), we get an ordinary differential equation

$$\left[\frac{\partial^2}{\partial r^2} + \frac{1}{r}\frac{\partial}{\partial r} + \frac{1}{r^2}\frac{\partial}{\partial \theta^2}\right]\left[\cos 2\theta\left(F_{,rr} + \frac{1}{r}F_{,r} - \frac{4}{r^2}F\right)\right] = 0, \quad \text{(a)} \quad (7.47)$$

which ultimately expands to [7.2]

$$F_{,rrrr} + \frac{2}{r}F_{,rrr} - \frac{9}{r^2}F_{,rr} + \frac{9}{r^3}F_{,r} = 0. \quad \text{(b)} \quad (7.47)$$

The solution to Eq. (7.47b) may be verified by back-substitution to be

$$F(r) = C_1 + C_2r^2 + C_3r^4 + C_4\frac{1}{r^2}. \qquad (7.48)$$

Then,

$$\phi = \left(C_1 + C_2r^2 + C_3r^4 + C_4\frac{1}{r^2}\right)\cos 2\theta. \qquad (7.49)$$

This expression for ϕ is inserted into Eqs. (7.28) to obtain

$$\sigma_{rr}^{(2)} = -\left(4C_1\frac{1}{r^2} + 2C_2 + 6C_4\frac{1}{r^4}\right)\cos 2\theta, \quad \text{(a)}$$

$$\sigma_{\theta\theta}^{(2)} = \left(2C_2 + 12C_3r^2 + 6C_4\frac{1}{r^4}\right)\cos 2\theta, \quad \text{(b)} \quad (7.50)$$

$$\sigma_{r\theta}^{(2)} = \left(-2C_1\frac{1}{r^2} + 2C_2 + 6C_3r^2 - 6C_4\frac{1}{r^4}\right)\sin 2\theta. \quad \text{(c)}$$

The appropriate boundary conditions to evaluate the constants are Eqs. (7.44) and the stress-free conditions at the hole

$$\sigma_{rr}^{(2)}(A,\theta) = 0$$
$$\sigma_{r\theta}^{(2)}(A,\theta) = 0, \qquad (7.51)$$

which leads to

$$\begin{bmatrix} -\frac{4}{A^2} & -2 & 0 & -\frac{6}{A^4} \\ -\frac{2}{A^2} & 2 & 6A^2 & -\frac{6}{A^4} \\ -\frac{4}{B^2} & -2 & 0 & -\frac{6}{B^4} \\ -\frac{2}{B^2} & 2 & 6B^2 & -\frac{6}{B^4} \end{bmatrix} \begin{Bmatrix} C_1 \\ C_2 \\ C_3 \\ C_4 \end{Bmatrix} = \begin{Bmatrix} 0 \\ 0 \\ \frac{T_x}{2} \\ -\frac{T_x}{2} \end{Bmatrix}. \tag{7.52}$$

Equation (7.52) may be simplified for the case where the hole is small compared to the width of the sheet. We first multiply both sides of the fourth equation by $(A/B)^2$ and then let $A/B \to 0$, which gives $C_3 = 0$. Next, we multiply both sides of the third equation by A^2, let $A/B \to 0$, and get $C_2 = -T_x/4$. Then, we have the first and second equations

$$-\frac{4}{A^2}C_1 + \frac{T_x}{2} - \frac{6}{A^4}C_4 = 0 \qquad \text{(a)}$$
$$-\frac{2}{A^2}C_1 - \frac{T_x}{2} - \frac{6}{A^4}C_4 = 0 \qquad \text{(b)} \qquad (7.53)$$

from which $C_1 = (A^2/2)T_x$ and $C_4 = -(A^4/4)T_x$.

Finally, the stresses are found from Eq. (7.50) to be

$$\sigma_{rr}^{(2)} = -\left(2\frac{A^2}{r^2} - \frac{1}{2} - \frac{3}{2}\frac{A^4}{r^4}\right)T_x \cos 2\theta, \qquad \text{(a)}$$
$$\sigma_{\theta\theta}^{(2)} = -\left(\frac{1}{2} + \frac{3}{2}\frac{A^4}{r^4}\right)T_x \cos 2\theta, \qquad \text{(b)} \quad (7.54)$$
$$\sigma_{r\theta}^{(2)} = \left(-\frac{A^2}{r^2} - \frac{1}{2} + \frac{3}{2}\frac{A^4}{r^4}\right)T_x \sin 2\theta. \qquad \text{(c)}$$

We may re-evaluate Eqs. (7.45) by dividing the numerator and denominator of each term by B^2, letting $A/B \to 0$, and then adding the results to Eq. (7.54) to produce, finally, the total solution

$$\sigma_{rr}(r,\theta) = \frac{T_x}{2}\left(1 - \frac{A^2}{r^2}\right) + \frac{T_x}{2}\left(1 - 4\frac{A^2}{r^2} + 3\frac{A^4}{r^4}\right)\cos 2\theta, \quad \text{(a)}$$
$$\sigma_{\theta\theta}(r,\theta) = \frac{T_x}{2}\left(1 + \frac{A^2}{r^2}\right) - \frac{T_x}{2}\left(1 + 3\frac{A^4}{r^4}\right)\cos 2\theta, \qquad \text{(b)} \quad (7.55)$$
$$\sigma_{r\theta}(r,\theta) = -\frac{T_x}{2}\left(1 + 2\frac{A^2}{r^2} - 3\frac{A^4}{r^4}\right)\sin 2\theta. \qquad \text{(c)}$$

Most interesting is to consider the maximum stress that occurs at $r = A$

$$\sigma_{\theta\theta}(A,\theta) = T_x - 2T_x\cos 2\theta, \tag{7.56}$$

which is largest when $\theta = \pi/2$ or $3\pi/2$, that is, at the sides of the hole where the tangent vector is parallel to the direction of the applied $\mathbf{T}_x$,

$$(\sigma_{\theta\theta})_{\max} = \sigma_{\theta\theta}\left(A, \frac{\pi}{2}\right) = \sigma_{xx}(0, A) = 3T_x, \qquad \text{(a)} \quad (7.57)$$

At $\theta = 0$ or π, the sides where the tangent vector is perpendicular to $\mathbf{T}_x$, we find

$$(\sigma_{\theta\theta})_{\min} = \sigma_{\theta\theta}(A, 0) = \sigma_{yy}(A, 0) = -T_x. \qquad \text{(b)} \quad (7.57)$$

The ratio of the maximum to the nominal stress is called the *stress concentration factor* K. In this case, $K = 3$. By superposition, it is easy to see that a uniform biaxial tension would produce $(\sigma_{\theta\theta})_{\max} = 3T_x - T_x = 2T_x$ and $K = 2$, while an equal tension in one direction and compression in the perpendicular direction would give $(\sigma_{\theta\theta})_{\max} = 3T_x + T_x = 4T_x$ and $K = 4$.

It is apparent from the $1/r^2$ and $1/r^4$ factors in Eqs. (7.55), which are indicative of the 'strength' of the singularity, that the high stress concentration is quite localized and decays rapidly away from the hole. It is also obvious that K is *independent* of the actual size of the hole thus making the solution very general. Stress concentrations are of great importance in structural fatigue and crack propagation studies, which are part of a relatively new and important branch of elasticity known as fracture mechanics.

7.7 Curved Beam

We now consider a beam that is curved in the plane of bending, as shown in Fig. 7.4(a). The outside and inside faces are cylindrical, the cross section is rectangular and the loading is a constant bending moment M. With these restrictions, we may consider the stresses to be independent of θ and use the axisymmetric plane stress solution as given by Eqs. (7.33).

We have the stress-free boundary conditions at the upper and lower faces

$$\begin{aligned} \sigma_{rr}(R_0) &= \sigma_{rr}(R_i) = 0 && \text{(a)} \\ \sigma_{r\theta}(R_0) &= \sigma_{r\theta}(R_i) = 0 && \text{(b)} \end{aligned} \tag{7.58}$$

along with the equilibrium conditions

$$\begin{aligned} \int_A \sigma_{\theta\theta}\, dA &= 0 && \text{(a)} \\ \int_A r\sigma_{\theta\theta}\, dA &= M && \text{(b)} \end{aligned} \tag{7.59}$$

where the stresses are shown in Fig. 7.4(b).

Obviously, Eq. (7.58b) is identically satisfied by the axisymmetric solution.

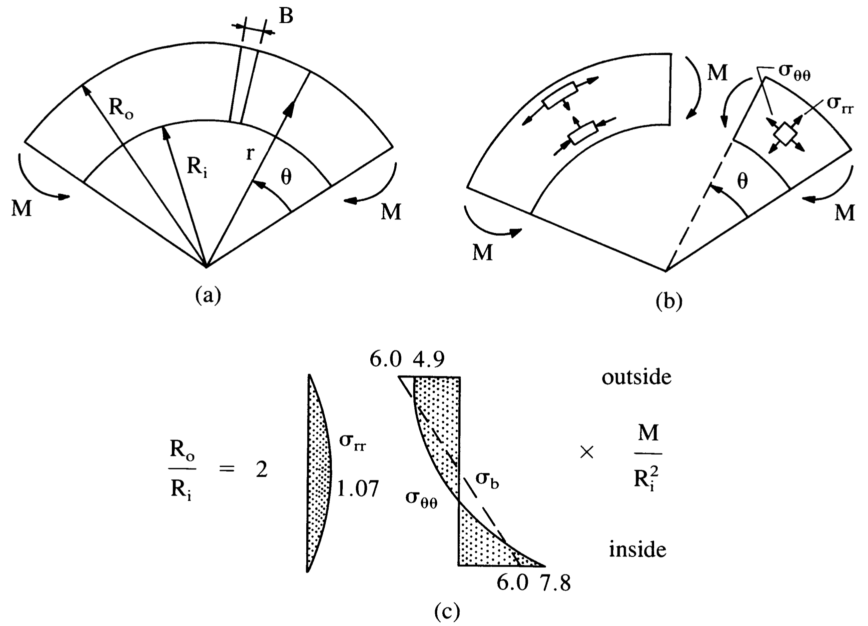

Fig. 7.4. (a) Curved beam in bending; (b) stresses in beam; (c) stress distribution through depth.

However, it appears that the problem may be over-specified, that is, more conditions than unevaluated constants.

We evaluate Eq. (7.33a) for σ_{rr} on the boundaries using Eq. (7.58a) as

$$C_1(1 + 2\ln R_0) + 2C_2 + C_3\frac{1}{R_0^2} = 0, \qquad \text{(a)}$$

$$C_1(1 + 2\ln R_i) + 2C_2 + C_3\frac{1}{R_i^2} = 0. \qquad \text{(b)} \tag{7.60}$$

Next, we have Eq. (7.59a) that may be written in terms of the stress function, using Eq. (7.31b),

$$\int_A \sigma_{\theta\theta}\, dA = B\int_{R_i}^{R_0} \phi_{,rr}\, dr$$

$$= B\left[\phi_{,r}\right]_{R_i}^{R_0}. \tag{7.61}$$

where B is the width of the beam. Noting that $\phi_{,r}$ is proportional to σ_{rr} via Eq. 7.28(a) and comparing the integrated function to Eq. (7.31a) for σ_{rr}, we see that the condition is identical to Eq. (7.58a) that produced Eqs. (7.60). We conclude that $\phi_{,r} = 0$ on the boundaries.

Then, the remaining equilibrium condition is Eq. (7.59b),

$$\int_A r\sigma_{\theta\theta}\, dA = B\int_{R_i}^{R_0} r\phi_{,rr}\, dr = M. \tag{7.62}$$

Considering the integral and using integration by parts,

$$\int_{R_i}^{R_0} r\phi_{,rr}\, dr = r\phi_{,r}\Big]_{R_i}^{R_0} - \int_{R_i}^{R_0} \phi_{,r}\, dr, \tag{7.63}$$

the first term on the r.h.s. is zero since $\phi_{,r}$ has been shown to be zero on the boundaries, while the second term, upon back-substitution into Eq. 7.62, leads to

$$\phi(R_0) - \phi(R_i) = -\frac{M}{B}, \tag{7.64}$$

or, by Eq. (7.32),

$$C_1(R_0^2 \ln R_0 - R_i^2 \ln R_i) + C_2(R_0^2 - R_i^2) + C_3 \ln\frac{R_0}{R_i} = -\frac{M}{B}. \tag{7.65}$$

Thus, we have produced three equations, Eqs. (7.60a, b) and Eq. (7.65), for the constants $C_1 - C_3$. These are solved [7.5] routinely as

$$C_1 = \frac{2M}{NB}(R_0^2 - R_i^2) \qquad \text{(a)}$$

$$C_2 = \frac{-M}{NB}[R_0^2 - R_i^2 + 2(R_0^2 \ln R_0 - R_i^2 \ln R_i)] \qquad \text{(b)} \quad (7.66)$$

$$C_3 = \frac{4M}{NB}R_0^2 R_i^2 \ln\frac{R_0}{R_i}, \qquad \text{(c)}$$

where

$$N = (R_0^2 - R_i^2)^2 - 4R_0^2 R_i^2\left(\ln\frac{R_0}{R_i}\right)^2. \qquad \text{(d)} \quad (7.66)$$

Finally, the stresses are written [7.2] explicitly as

$$\sigma_{rr} = \frac{4M}{NB}\left(R_0^2 R_i^2 \ln\frac{R_0}{R_i}\frac{1}{r^2} + R_0^2 \ln\frac{r}{R_0} + R_i^2 \ln\frac{R_i}{r}\right), \qquad \text{(a)}$$

$$\sigma_{\theta\theta} = \frac{4M}{NB}\left(R_0^2 R_i^2 \ln\frac{R_0}{R_i}\frac{1}{r^2} - R_0^2 \ln\frac{r}{R_0} - R_i^2 \ln\frac{R_i}{r} - R_0^2 + R_i^2\right), \qquad \text{(b)} \quad (7.67)$$

$$\sigma_{r\theta} = 0. \qquad \text{(c)}$$

To be applicable for the entire beam, the end moments M must be distributed in accordance with $\sigma_{\theta\theta}$, see Eq. (7.67b). Otherwise, the results are valid overall, except for the immediate region of moment application, through St. Venant's principle.

In order to study the stress distribution for a typical case, we choose $R_0/R_i = 2$. Then, in Fig. 7.4(c), the stresses σ_{rr} and $\sigma_{\theta\theta}$ are plotted through the depth of the beam along with the straight line distribution obtained from elementary beam theory, $\sigma_b = \sigma_{zz}$ from Eq. (6.20b), [7.2]. Notice that the elementary beam solution underestimates the maximum stress that occurs along the inside boundary and, of course, does not indicate σ_{rr} at all. We may explain heuristically the increase in stress along the inside boundary and the decrease along the outside boundary as compared to elementary theory by recognizing that the inside fibers are shorter and the outside fibers are longer than those along the center-line, which correspond to a straight beam of the same length. Therefore, the same extension or contraction would produce a correspondingly greater, or lesser, strain in these fibers. Also the sense of σ_{rr} may be related to the radial components of the stresses $\sigma_{\theta\theta}$ shown on the left portion of Fig. 7.4(b). Near the outside face, this component is directed inward, while near the outside face it acts outward to produce the radial compression.

It should also be mentioned that there is a strength-of-materials solution for curved beams that produces results for $\sigma_{\theta\theta}$ practically identically to those obtained from the plane stress solution for beams in which the radius of the centroidal axis $1/2(R_0 + R_i)$ is greater than the depth $R_0 - R_i$, but still no values for ϕ_{rr}. This solution is presented in detail in Ref. [7.6] and is adequate for many practical cases.

7.8 Rotational Dislocation

An interesting variant on the thick-walled cylinder problem treated in Section 7.5 is shown in Fig. 7.5 where the ring has been formed as open and separated by an angle α, assumed as the zero stress state, and then forced together and joined. The appropriate boundary conditions are

$$\sigma_{rr}(R_0) = \sigma_{rr}(R_i) = 0, \quad \text{(a)}$$
$$u_\theta(r, 2\pi) = r\alpha. \quad \text{(b)} \qquad (7.68)$$

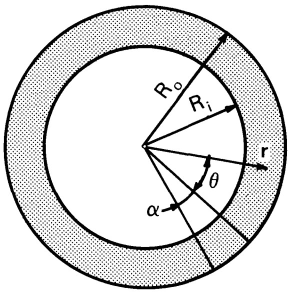

Fig. 7.5. Thick-walled cylinder with rotational dislocation.

The utility of the "quasi-axisymmetric" displacement equations is now apparent, since we may use Eq. (7.34d) to write Eq. (7.68b) as

$$r\alpha = \frac{1}{E} 8\pi C_1 r,$$

or

$$C_1 = \frac{E\alpha}{8\pi}. \tag{7.69}$$

We then introduce the boundary conditions Eq. (7.68a) along with substituting Eq. (7.69) into Eqs. (7.33a and b) producing

$$\begin{aligned} &\frac{E\alpha}{8\pi}(1 + 2\ln R_0) + 2C_2 + \frac{C_3}{R_0^2} = 0, && \text{(a)} \\ &\frac{E\alpha}{8\pi}(1 + 2\ln R_i) + 2C_2 + \frac{C_3}{R_i^2} = 0, && \text{(b)} \end{aligned} \tag{7.70}$$

and yielding

$$\begin{aligned} C_2 &= -\frac{E\alpha}{16\pi} \frac{(1 + 2\ln R_0)R_0^2 - (1 + 2\ln R_i)R_i^2}{R_0^2 - R_i^2}, && \text{(a)} \\ C_3 &= \frac{E\alpha}{4\pi} \frac{R_0^2 R_i^2}{R_0^2 - R_i^2} \ln\frac{R_0}{R_i}, && \text{(b)} \end{aligned} \tag{7.71}$$

which can be back-substituted into Eqs. (7.33) along with C_1 to find σ_{rr} and $\sigma_{\theta\theta}$.

We may easily find the total bending moment across the section from Eq. (7.66a) to be

$$\begin{aligned} M &= \frac{C_1}{2} \frac{NB}{R_0^2 - R_i^2} \\ &= \frac{E\alpha B}{16\pi} \frac{(R_0^2 - R_i^2)^2 - 4R_0^2 R_i^2 \ln(R_0/R_i)^2}{R_0^2 - R_i^2}. \end{aligned} \tag{7.72}$$

7.9 Narrow, Simply Supported Beam

The previous examples of two-dimensional elasticity solutions have focused on problems in cylindrical coordinates. We now turn to a Cartesian domain and again consider the beam bending problem, which was analyzed in Section 6.3 in the context of three-dimensional elasticity.

We examine a simply supported beam of unit width under self-weight as shown in Fig. 7.6, closely following the treatment by Little [7.4]. The supports are precisely located within the depth, since we are seeking an elasticity solution.

We employ the plane strain formulation Eq. (7.9) in terms of the Airy stress

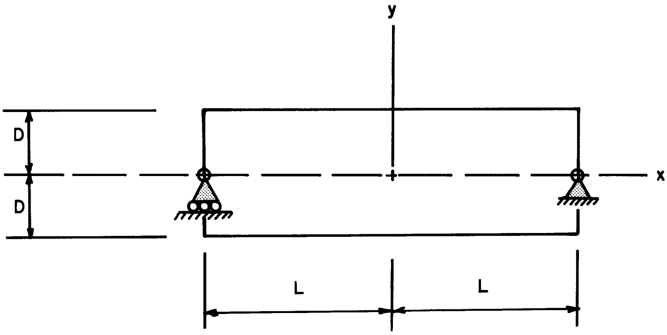

Fig. 7.6. Narrow beam in bending.

function. With the body forces given by

$$\mathbf{f} = -\rho g \mathbf{e}_y, \tag{7.73}$$

where ρ is the mass density and g the acceleration of gravity, the potential V, as defined in Eq. (7.3), becomes

$$V = \rho g y. \tag{7.74}$$

Thus, Eq. (7.9b) takes the form

$$\nabla^4 \phi = -(1 - \nu)\nabla^2(\rho g y). \tag{7.75}$$

The boundary conditions on the top and bottom faces are

$$\sigma_{xy}(x, \pm D) = \sigma_{yy}(x, \pm D) = 0, \tag{7.76}$$

and on the ends,

$$\begin{aligned} &\sigma_{xx}(\pm L, y) = 0, && \text{(a)} \\ &\int_{-D}^{D} \sigma_{xy}(-L, y)\,dy = -2\rho g D L, && \text{(b)} \\ &\int_{-D}^{D} \sigma_{xy}(L, y)\,dy = 2\rho g D L. && \text{(c)} \end{aligned} \tag{7.77}$$

The latter two equations reflect the acceptance of St. Venant's principle for this case.

Once the stress function is found, the stresses can be calculated from Eqs. (7.5)

$$\begin{aligned} \sigma_{xx} &= \rho g y + \phi_{,yy}, && \text{(a)} \\ \sigma_{yy} &= \rho g y + \phi_{,xx}, && \text{(b)} \\ \sigma_{xy} &= -\phi_{,xy}. && \text{(c)} \end{aligned} \tag{7.78}$$

Recalling the idea of expressing the solution ϕ in the form of selected polynomial terms, as suggested in Eq. (7.19), and recognizing that the stress would likely follow an *even* functional distribution in x and an *odd* distribution in y, then we have

$$\phi = C_{21}x^2y + C_{23}x^2y^3 + C_{03}y^3 + C_{05}y^5 \tag{7.79}$$

as proposed in [7.4]. From the discussion in Section 7.3, it is evident that the first and third terms satisfy Eq. (7.75) individually, but the second and fourth terms must satisfy the equation in combination.

Substituting Eq. (7.79) into Eqs. (7.78) yields

$$\begin{aligned} \sigma_{xx} &= \rho g y + 6C_{23}x^2y + 6C_{03}y + 20C_{05}y^3 && \text{(a)} \\ \sigma_{yy} &= \rho g y + 2C_{21}y + 2C_{23}y^3 && \text{(b)} \\ \sigma_{xy} &= -2C_{21}x - 6C_{23}xy^2 && \text{(c)} \end{aligned} \tag{7.80}$$

for the stresses.

Since we have chosen appropriate even or odd functions, we may select either the (+) or (−) conditions in Eqs. (7.76). Using the condition at (+) D,

$$\begin{aligned} \sigma_{xy}(x, D) &= -2C_{21}x - 6C_{23}xD^2 = 0 && \text{(a)} \\ \sigma_{yy}(x, D) &= \rho g D + 2C_{21}D + 2C_{23}D^3 = 0, && \text{(b)} \end{aligned} \tag{7.81}$$

from which

$$\begin{aligned} C_{21} &= -\frac{3}{4}\rho g, && \text{(a)} \\ C_{23} &= \frac{1}{4}\frac{\rho g}{D^2}. && \text{(b)} \end{aligned} \tag{7.82}$$

From Eq. (7.75) applied to Eq. (7.79), we find

$$\begin{aligned} C_{05} &= -\frac{1}{5}C_{23} \\ &= -\frac{1}{20}\frac{\rho g}{D^2}. \end{aligned} \tag{7.83}$$

Finally, we turn to Eq. (7.77a). The form of σ_{xx} in Eq. (7.80a) makes it impossible to satisfy this equation identically in a pointwise fashion. Therefore, we invoke St. Venant's principle whereby

$$\begin{aligned} &\int_{-D}^{D} \sigma_{xx}(L, y)\, dy = 0, && \text{(a)} \\ &\int_{-D}^{D} \sigma_{xx}(L, y) y\, dy = 0. && \text{(b)} \end{aligned} \tag{7.84}$$

Substituting Eq. (7.80a), along with Eqs. (7.82) and (7.83), into Eq. (7.84a), we find that it is satisfied identically since σ_{xx} is an odd function in y. Equation (7.84b) yields

$$\tfrac{2}{3}\rho g D^3 + \rho g L^2 D + 4C_{03}D^3 - \tfrac{2}{5}\rho g D^3 = 0, \tag{7.85}$$

from which

$$C_{03} = -\rho g\left(\frac{1}{15} + \frac{1}{4}\frac{L^2}{D^2}\right). \tag{7.86}$$

Inserting the evaluated constants into Eqs. (7.80) gives

$$\begin{aligned}
\sigma_{xx} &= 3\rho g\left[\frac{1}{5} + \frac{1}{2D^2}(x^2 - L^2)\right]y - \rho g\frac{y^2}{D^2} \\
&= \frac{\rho g D}{I}\left[\frac{2}{5}D^2 y - \frac{2}{3}y^3 + \underline{(x^2 - L^2)y}\right], && \text{(a)} \\
\sigma_{yy} &= -\frac{1}{2}\rho g\left[1 - \frac{y^2}{D^2}\right]y \\
&= \frac{\rho g D}{I}\left[-\frac{D^2 y}{3} + \frac{y^3}{3}\right], && \text{(b)} \qquad (7.87) \\
\sigma_{xy} &= \frac{3}{2}\rho g\left[1 - \frac{y^2}{D^2}\right]x \\
&= \frac{\rho g D}{I}[D^2 x - y^2 x], && \text{(c)}
\end{aligned}$$

where I is the moment of inertia/unit width about the centroidal axis $= \frac{2}{3}D^3$.

Elementary beam theory, which was derived for a cantilever beam in Section 6.3.1, gives only the underlined term in Eq. (7.87a) for σ_{xx}, so that the other terms in Eqs. (7.87a, b) represent the modification due to the two-dimensional stress state produced by the presence of σ_{yy}. The value of σ_{xy} is not changed from the elementary theory result. The analysis may be carried on to produce strains and eventually displacements, but little that is new is revealed [7.4].

Of interest in the family of two-dimensional beam solutions are the various possibilities for applying the transverse loading, in addition to the uniform distribution through the depth studied here. Loading on the top face or the bottom face produces alterations to Eq. (7.87), especially in the σ_{yy} (transverse normal) stresses [7.5].

7.10 Semi-Infinite Plate with a Concentrated Load

A semi-infinite plate of unit thickness under a concentrated vertical loading, shown in Figure 7.7, may be solved in either polar or Cartesian coordinates. The general three-dimensional case is known as the Boussinesq problem and is reknown in the Theory of Elasticity. Here, we present the two-dimensional version in polar coordinates and leave the Cartesian coordinate solution for the exercises.

It is postulated that any element located by (r, θ) is under a state of pure radial compression, i.e.,

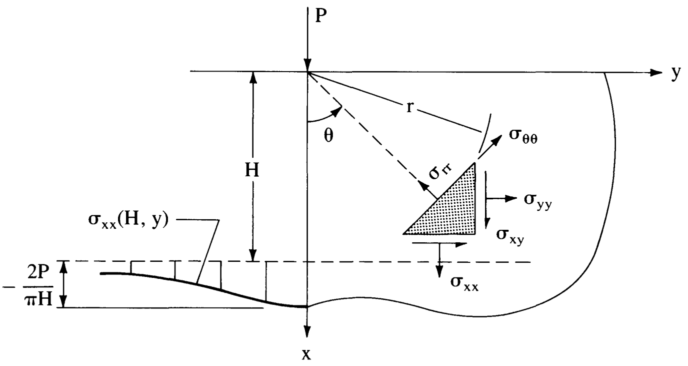

Fig. 7.7. Semi-infinite plate with concentrated load (from Ugural and Fenster, *Advanced Strength and Applied Elasticity*, Elsevi 1975.) Reprinted with permission.

$$\sigma_{rr}(r,\theta) = -2(P/\pi)\frac{\cos\theta}{r} \qquad \text{(a)}$$

$$\sigma_{\theta\theta} = 0 \qquad \text{(b)} \quad (7.88)$$

$$\sigma_{r\theta} = 0 \qquad \text{(c)}$$

which will be verified shortly.

If the vertical component of σ_{rr}, $\sigma_{rr}\cos\theta$, is integrated over a cylindrical surface described by r, we have

$$2\int_0^{\pi/2} (\sigma_{rr}\cos\theta)(rd\theta) = -P \qquad (7.89)$$

so that overall equilibrium is satisfied. Obviously the coefficient $2/\pi$ in Eq. (7.88a) was chosen to scale the integral to the r.h.s. of Eq. (7.89).

The boundary conditions on the free surface are obviously satisfied since the stresses vanish at every point, except under the load where the infinite stress is given by Eq. 7.88 with $\theta = 0$ and $r = 0$.

To complete the solution, it must be shown that local equilibrium and compatibility are also satisfied. It is convenient to use the stress function

$$\phi = -(P/\pi)r\theta\sin\theta \qquad (7.90)$$

which may be substituted into Eqs. 7.28 to confirm that Eqs. 7.88 produce equilibrium and then into Eq. 7.29 to verify compatibility.

We now consider a horizontal plane $x = H$ and compute the Cartesian components of stress using Eq. 2.13. From Fig. 7.7, the direction cosines are found as

	r	θ	z
x	$\cos\theta$	$-\sin\theta$	0
y	$\sin\theta$	$\cos\theta$	0
z	0	0	1

(7.91)

Since

$$\sigma_{rr}(r,\theta) = \sigma_{rr}(H/\cos\theta,\theta) = -2\left(\frac{P}{\pi H}\right)\cos^2\theta \tag{7.92}$$

we find

$$\begin{aligned} \sigma_{xx}(H,\theta) &= \sigma_{rr}\cos^2\theta = -2\left(\frac{P}{\pi H}\right)\cos^4\theta && \text{(a)} \\ \sigma_{yy}(H,\theta) &= \sigma_{rr}\sin^2\theta = -2\left(\frac{P}{\pi H}\right)\sin^2\theta\cos^2\theta && \text{(b)} \quad (7.93) \\ \sigma_{xy}(H,\theta) &= \sigma_{rr}\sin\theta\cos\theta = -2\left(\frac{P}{\pi H}\right)\sin\theta\cos^3\theta. && \text{(c)} \end{aligned}$$

For a point directly beneath the load, $\theta = 0$ and $\sigma_{rr} = \sigma_{xx} = -\dfrac{2P}{\pi H}$. As shown on the figure, the vertical compression attenuates away from the load. A detailed study of the stress distribution is presented in [7.2] along with a solution for a concentrated horizontal force at the origin.

These solutions are of great utility in determining the stresses and the corresponding displacements in soil deposits due to surface loading, such as building columns or vehicular wheels.

Exercises

7.1 Using the element shown in the figure below solve the following problems.

(a) Derive the equilibrium equations in polar coordinates, neglecting body forces.

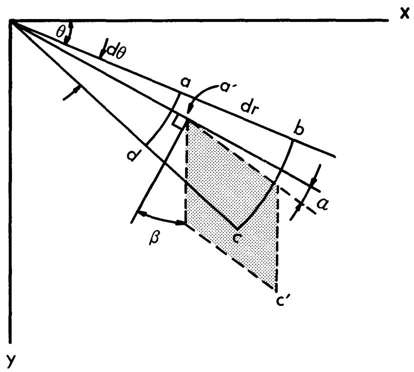

Problem 7.1

Answer: $\sigma_{rr,r} + \dfrac{1}{r}\sigma_{r\theta,\theta} + \dfrac{\sigma_{rr} - \sigma_{\theta\theta}}{r} = 0$

$\dfrac{1}{r}\sigma_{\theta\theta,\theta} + \sigma_{r\theta,r} + \dfrac{2}{r}\sigma_{r\theta} = 0$

(b) Verify that the above equations are satisfied by Eqs. (7.28).

7.2 Consider a thick-walled cylinder with an outside diameter of 5. The internal pressure is 0.5 (force/length^2).

(a) For an inside diameter of 4, compute the maximum normal and circumferential stresses.

(b) How much error would be involved if part (a) were carried out using thin-walled cylinder theory.

(c) Determine the radial displacement of a point on the inside surface.

7.3 A cylinder with inside radius a and outside radius $b = 1.20a$ is subjected to:

(1) internal pressure p_i only,

(2) external pressure p_0 only.

Determine the ratio of maximum to minimum tangential stress for each case (from (7.7]).

7.4 Determine the value of the constant C in the stress function

$$\phi = C[r^2(\alpha - \theta) + r^2 \sin\theta \cos\theta - r^2 \cos^2\theta \tan\alpha]$$

required to satisfy the conditions on the upper and lower edges of the triangular plate shown in the figure. Evaluate the stress components σ_{xx}, σ_{yy}, σ_{xy} at M for the case $\alpha = 30°$. In what way is this solution different from that found by the elementary beam theory?

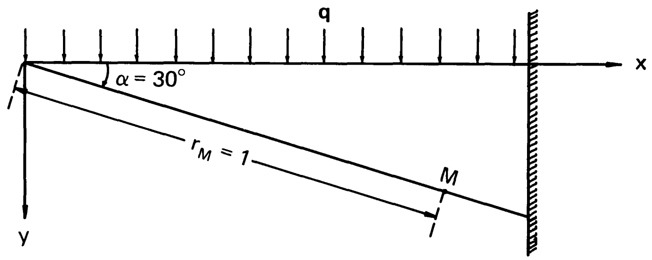

Problem 7.4

7.5 Determine the stress concentration factor for the plate as shown in the figure below.

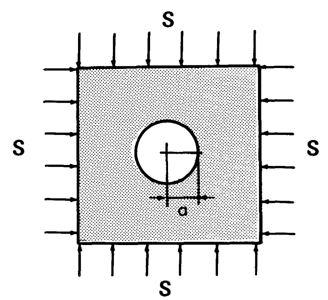

Problem 7.5

7.6 Consider a curved beam as shown in the figure below.

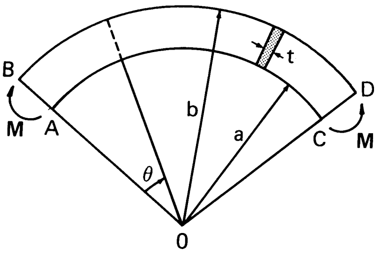

Problem 7.6

The values of the dimensions and moments are

$$a = 10; \quad b = 13; \quad M = 11{,}000 \text{ (length-force)}; \quad t = 0.8.$$

Calculate the maximum stress arising from M and compare this with $\sigma_{\theta\theta} = M(b - a)/2I$, computed from elementary beam theory.

7.7 For problem 5.2, show that the corresponding Airy stress function may be written as

$$\phi = -\frac{1}{2}\frac{v}{1+v}f(x,y)z^2 + A + Bx + Cy + \phi_1(x,y)z + \phi_0(x,y),$$

where ϕ, A, B, C may be functions of z, and ϕ_0 is a specialized Airy stress function for problems symmetrical about the plane $z = 0$ (from [7.4]).

7.8 A stress distribution is given by

$$\sigma_{xx} = C_1 yx^3 - 2C_2 xy + C_3 y$$
$$\sigma_{yy} = C_1 xy^3 - 2C_1 x^3 y$$
$$\sigma_{xy} = -\frac{3}{2}C_1 x^2 y^2 + C_2 y^2 + \frac{1}{2}C_1 x^4 + C_4$$

where $C_1 - C_4$ are constants (from [7.7]).

(a) Show that this field represents a solution for a thin plate as shown below.
(b) Derive the corresponding stress function.
(c) Evaluate the surface forces along the edges $y = 0$ and $y = b$ of the plate.

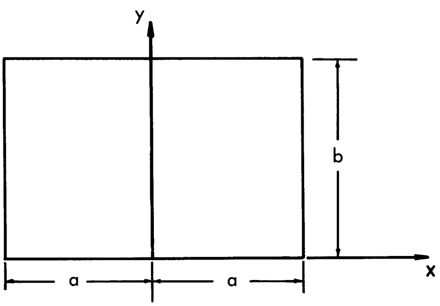

Problem 7.8. (From Ugural and Fenster, *Advanced Strength and Applied Elasticity*, Elsevier, 1975.) Reprinted with permission.

7.9 Consider the semi-infinite plate treated in Section 7.10 using Cartesian coordinates. Show that the stress function $\phi = -(P/\pi)y\tan^{-1}(y/x)$ results in the following stress field within the plate (from [7.7]):

$$\sigma_{xx} = -\frac{2P}{\pi}\frac{x^3}{(x^2+y^2)^2}; \quad \sigma_{yy} = -\frac{2P}{\pi}\frac{xy^2}{(x^2+y^2)^2}; \quad \sigma_{xy} = -\frac{2P}{\pi}\frac{yx^2}{(x^2+y^2)^2}.$$

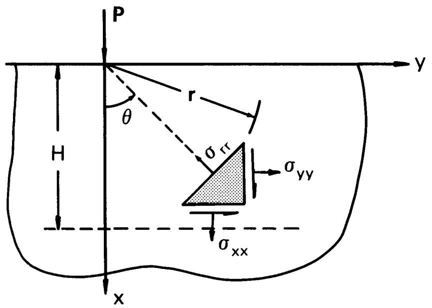

Problem 7.9. (From Ugural and Fenster, *Advanced Strength and Applied Elasticity*, Elsevier, 1975.) Reprinted with permission.

Also, plot the resulting stress distribution for σ_{xx} and σ_{xy} at a constant depth H below the boundary (from [7.7]).

7.10 The thin cantilever beam shown is subjected to a uniform shearing stress τ_0 along the upper surface, $y = +D$; while the surfaces $y = -D$ and $x = L$ are stress-free. Determine if the Airy stress function

$$\phi = \frac{1}{4}\tau_0\left(xy - \frac{xy^2}{D} - \frac{xy^3}{D^2} + \frac{Ly^2}{D} + \frac{Ly^3}{D^2}\right)$$

satisfies the required conditions for this problem (from [7.7]).

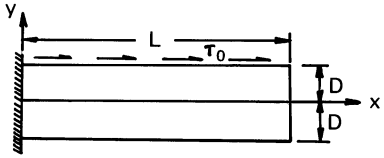

Problem 7.10. (From Ugural and Fenster, *Advanced Strength and Applied Elasticity*, Elsevier, 1975.) Reprinted with permission.

7.11 Show that for the case of plane stress with no body forces present:

(a) The equations of equilibrium may be expressed in terms of displacements u_x and u_y as follows (from [7.7]):

$$\nabla^2 u_x + \left(\frac{1+\nu}{1-\nu}\right)(u_{x,x} + u_{y,y})_{,x} = 0$$

$$\nabla^2 u_y + \left(\frac{1+\nu}{1-\nu}\right)(u_{y,y} + u_{x,x})_{,y} = 0$$

(b) Verify that the indicial form of these equations, following steps analogous to those in Section 5.2, is

$$\nabla^2 u_i + \left(\frac{1+\nu}{1-\nu}\right) u_{j,ji} = 0 \qquad i, j = 1, 2.$$

7.12 For the stress function in Eq. 7.90,

$$\phi = -(P/\pi) r\theta \sin\theta,$$

verify that equilibrium and compatibility are satisfied.

7.13 Refer to the solution in Sec. 7.10.

(a) Compute the Cartesian components of stress as a function of r and θ.

(b) Show that the integral of σ_{rr} along any semicircle about the origin is equal to P (from [7.7]).

7.14 An edge-loaded diaphragm is sometimes called a "deep beam" since it spans between columns and has a depth/span ratio outside the limitations of simple beam theory. For the simply-supported case shown [7.8], based on the assumption that the column reactions are uniformly distributed over the width c, formulate the problem within the theory of elasticity:

(a) State the governing equation.

(b) State the boundary conditions on all edges.

(c) Suppose the load is applied along the lower edge instead. How will the boundary conditions be altered? What limitation of elementary beam theory does this illustrate?

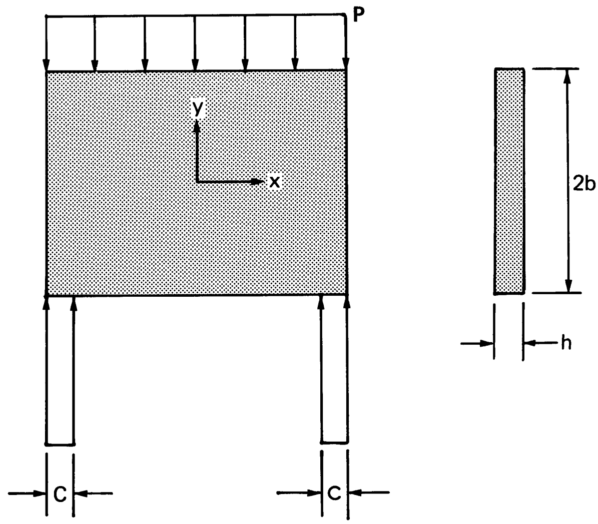

Problem 7.14

7.15 Derive Eqs. 7.28.

7.16 A pipe is composed of two concentric cylinders. The outer radius is $3a$, the radius along the interface is $2a$ and the inner radius is a. For the outer cylinder, $E = E_0$ while for the inner cylinder, $E = E_i = \frac{1}{2}E_0$;

(a) For an internal pressure p, compute the circumferential and radial stress distributions in the pipes.
(b) Evaluate the shear stress along the interface.
(c) Compute the radial displacement at both surfaces.

7.17 Consider the material law stated in Eq. (4.33):
(a) Re-write these equations in terms of the engineering constants E and ν.
(b) Specialize and expand the equations for the cylindrical coordinates r, θ, z introduced in Sec. 7.4.
(c) Consider the concentric cylinders described in Problem 7.16. When the outer cylinder is much stiffer than the inner, $E_o \ll E_i$, the inner cylinder may be considered to be in a state of *generalized plane stress*, with σ_{rr} taken as equal to $-p$, or an assumed $\bar{\sigma}_{rr}(p, z)$, throughout. Show that the remaining stress-strain equations are:

$$\sigma_{\theta\theta} = \frac{E_i}{1 - \nu^2}[\varepsilon_{\theta\theta} + \mu\varepsilon_{zz} - (1 + \nu)\alpha\Delta T] + \frac{\nu}{1 - \nu}\bar{\sigma}_{rr}$$

$$\sigma_{zz} = \frac{E_i}{1 - \nu^2}[\mu\varepsilon_{\theta\theta} + \varepsilon_{zz} - (1 + \nu)\alpha\Delta T] + \frac{\nu}{1 - \nu}\bar{\sigma}_{rr}.$$

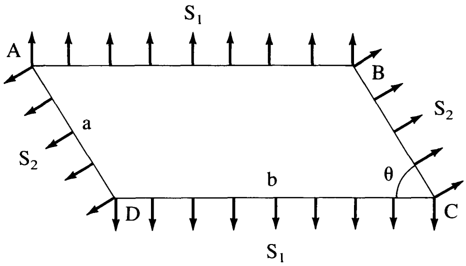

Problems 7.18 and 7.19

7.18 A skewed plate of unit thickness is loaded by uniformly distributed stresses, S_1 and S_2, applied perpendicular to the sides of the plate as shown in the figure. [7.9]
(a) Solve the equilibrium equations for the plate in terms of S_1, S_2, a, b and θ.
(b) Determine the elongation of the diagonal AC under the action of the stresses, S_1 and S_2, assuming that the material is linearly elastic and isotropic and that $\theta = 90°$.

7.19 Now, consider the stresses, S_1 and S_2, to be applied so that they are directed parallel to the edges AB and AD, respectively, of the skewed plate. Derive expressions for the principal stresses and the principal strains in terms of S_1, S_2, a, b, θ, E, and ν where E and ν denote Young's modulus and Poisson's ratio, respectively. [7.9]

7.20 Consider the stress-strain relationships in terms of the engineering constants, Eqs. (7.7), and Eq. (4.13b) simplified for the plane strain case in the x-y plane.
Show that Eqs. (7.7) may be generalized for a homogeneous orthotropic mate-

rial [7.10] defined by

$$E_x \nu_{yx} = E_y \nu_{xy}$$

to the form

$$\sigma_{11} = \frac{E_x}{(1 - \nu_{xy}\nu_{yx})}(\varepsilon_x + \nu_{yx}\varepsilon_y)$$

$$\sigma_{22} = \frac{E_y}{(1 - \nu_{xy}\nu_{yx})}(\nu_{xy}\varepsilon_x + \varepsilon_y)$$

$$\sigma_{xy} = 2G\varepsilon_{xy}$$

7.21 Consider the axisymmetrical thermal elasticity problem in two dimensions. Prove that the compatibility equation in polar coordinates is given by [7.7]

$$\frac{1}{r}(r\phi_{,r})_{,r} + E\alpha\Delta T = 0$$

where

$$\Delta T = T - T_0 \qquad \text{as defined by Eq. (4.31)}$$

and

$$\phi = \text{Airy stress function.}$$

References

[7.1] Love, A. E. H., *A Treatise on the Mathematical Theory of Elasticity*, 4th ed. (Dover Publications, Inc., New York, 1944).

[7.2] Timoshenko, S., and Goodier, J. N., *Theory of Elasticity*, 2nd ed. (McGraw-Hill Book Company, Inc., New York, 1951).

[7.3] Popov, E. P., *Mechanics of Materials*, 2nd ed. (Prentice-Hall, Inc., Englewood Cliffs, NJ, 1978).

[7.4] Little, R. W. *Elasticity* (Prentice-Hall, Inc., Englewood Cliffs, NJ, 1973).

[7.5] Filonenko-Borodich, M., *Theory of Elasticity* (Dover Publications, Inc., New York, 1965).

[7.6] Boresi, A. B., Sidebottom, O. M., Seeley, F. B., and Smith, J., *Advanced Mechanics of Materials*, 3rd ed. (John Wiley & Sons, Inc., New York, 1978).

[7.7] Ugural, A. C., and Fenster, S. K., *Advanced Strength and Applied Elasticity* (Elsevier-North Holland, New York, 1975).

[7.8] Barry, J. E. and Ainso, H., "Single-Span Deep Beams," *Journal of Structural Engineering*, ASCE, V. 109, No. ST3, March, 1983, pp. 646–663.

[7.9] Boresi, A. P., and Chong, K. P., *Elasticity in Engineering Mechanics* (Elsevier, New York, 1987).

[7.10] Little, G. H., "Large Deflections of Orthotropic Plates under Pressure," *Journal of Engineering Mechanics*, ASCE, V. 115, No. 12, December, 1989, pp. 2601–2620.

CHAPTER 8

Bending of Thin Plates

8.1 Introduction

In the preceding chapter, a thin elastic plate loaded *in* the plane of the plate was analyzed. The resulting deformations are confined to the plane of the plate in accordance with the plane strain assumption.

If such a plate is loaded *transverse* to the plane, as shown in Figure 8.1, where a distributed load $q(x, y)$ is applied to the upper surface, the plate bends and the deflection of the surface in the normal direction is predominant. The problem of plate bending is, in part, an extension of the elementary theory of beams. However, plate bending is more complicated than beam bending, or even the compatible bending of a network of orthogonal beams connected at their intersections. In effect, a solid plate is much stiffer than such a gridwork. This will be elaborated on in a later section.

Transversely loaded plates are classifled in terms of their thinness by a characteristic ratio h/l, where h is the thickness and l is a plan dimension such as the length of a side or a radius. If the plate is very thin, $h/l < 0.001$, in-plane or membrane forces are needed to provide equilibrium mobilizing finite deformations. On the other hand, if the plate is thick, $h/l < 0.4$, three-dimensional effects are relevant. Between these bounds lie medium-thin plates which can be analyzed by a linear theory in reference to a middle plane, a two-dimensional analog to the familiar neutral axis of a beam.

8.2 Assumptions

(1) Based on the relative thinness of the plate and the orientation of the loading, the plate is assumed to be approximately in both plane strain and plane stress, i.e.,

$$\varepsilon_{zz} = 0 \quad \text{(a)}$$

and (8.1)

$$\sigma_{zz} = 0 \quad \text{(b)}$$

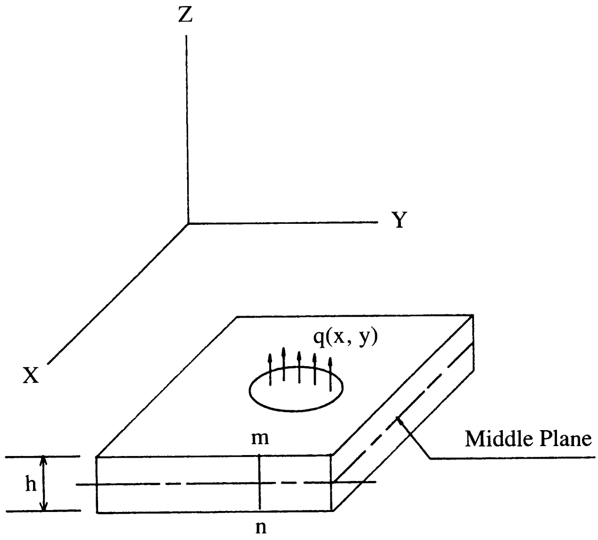

Fig. 8.1. Thin plate under transverse loading.

except directly under a surface load. The corresponding strain-stress equations (7.12 a,b,d) become

$$\varepsilon_{xx} = \frac{1}{E}(\sigma_{xx} - \nu\sigma_{yy}) \quad \text{(a)}$$

$$\varepsilon_{yy} = \frac{1}{E}(\sigma_{yy} - \nu\sigma_{xx}) \quad \text{(b)} \quad (8.2)$$

$$\varepsilon_{xy} = \frac{1}{2G}\sigma_{xy}. \quad \text{(c)}$$

Also, the plate thickness does not change, so that the normal displacement is constant along a normal through the thickness, i.e.,

$$u_z = u_z(x, y). \quad (8.3)$$

(2) The second assumption is stated with respect to the line *mn*, shown in Figure 8.1 and again in the section normal to the x-axis, Figure 8.2. Line *mn* represents all lines initially perpendicular to the undeformed middle plane and is presumed to remain *straight* and *normal* to the deformed middle plane. This is the *hypothesis of linear elements*, attributed to G. Kirchhoff by Filonenko-Borodich [8.1].

Referring to Figure 8.2, the undeflected line *mn* is superimposed on the deflected line *m′n′* in the upper cross section. The rotation of the line is ω_{yz}. By the application of the hypothesis, this rotation is equal to the rotation of

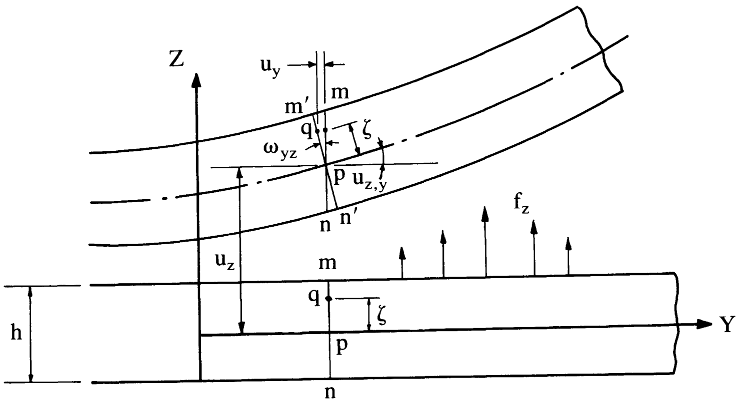

Fig. 8.2. Deformation of thin plate.

a tangent to the middle plane:

$$\omega_{yz} = u_{z,y}. \tag{8.4}$$

(3) The last essential assumption states that the middle plane deflects only in the z direction. Thus, on the middle plane where the normal coordinate $\zeta = 0$,

$$u_x(x, y, 0) = 0 \qquad \text{(a)}$$
$$u_y(x, y, 0) = 0 \qquad \text{(b)} \quad (8.5)$$
$$u_z(x, y, 0) = f(x, y). \qquad \text{(c)}$$

Therefore, there can be no extensional deformations or shears on the middle plane and

$$\begin{aligned} \sigma_{xx}(x, y, 0) &= 0 \\ \sigma_{yy}(x, y, 0) &= 0 \\ \sigma_{xy}(x, y, 0) &= 0. \end{aligned} \tag{8.6}$$

The preceding assumptions enable a classical displacement formulation for transversely loaded medium-thin plates. All stresses, strains and in-plane displacements will be described in terms of the normal displacement $u_z(x, y)$.

8.3 Formulation

8.3.1 Geometric Relationships

We focus on two points which lie on mn, the normal to the middle plane, in Figure 8.2. Point p is also on the middle plane, while point q is initially located a distance ζ away from the plane in the positive z direction.

On the displaced surface, point q remains ζ from point p by Assumption (1) and has the same normal displacement $u_z(x, y)$ by Assumption (3). So the in-plane displacement is given by

$$u_y = -\zeta\omega_{yz} = -\zeta u_{z,y} \tag{8.7}$$

by Assumption (2), Eq. 8.4. The negative sign indicates that a *positive* $\zeta u_{z,y}$ produces a u_y in the *negative* y direction.

A similar section perpendicular to the y-axis would reveal the x-z plane and yield

$$u_x = -\zeta\omega_{xz} = -\zeta u_{z,x}. \tag{8.8}$$

Thus, the in-plane displacements u_x and u_y are functions of the normal displacement u_z.

8.3.2 Strains and Stresses

Using Eqs. (8.7) and (8.8), we may write the in-plane strain-displacement relationships from Eqs. (3.15 a,b,c) with 1, 2, 3 = x, y, z:

$$\begin{aligned}
\varepsilon_{xx} &= u_{x,x} = -\zeta u_{z,xx} && \text{(a)} \\
\varepsilon_{yy} &= u_{y,y} = -\zeta u_{z,yy} && \text{(b)} \quad (8.9) \\
\varepsilon_{xy} &= \tfrac{1}{2}(u_{x,y} + u_{y,x}) = -\zeta u_{z,xy}. && \text{(c)}
\end{aligned}$$

The corresponding stresses are formed by inverting Eqs. (8.2) and substituting Eqs. (8.9).

$$\begin{aligned}
\sigma_{xx} &= \frac{E}{(1-\nu^2)}(\varepsilon_{xx} + \nu\varepsilon_{yy}) \\
&= -\frac{\zeta E}{(1-\nu^2)}(u_{z,xx} + \nu u_{z,yy}) && \text{(a)} \\
\sigma_{yy} &= \frac{E}{(1-\nu^2)}(\varepsilon_{yy} + \nu\varepsilon_{xx}) \\
&= -\frac{\zeta E}{(1-\nu^2)}(u_{z,yy} + \nu u_{z,xx}) && \text{(b)} \quad (8.10) \\
\sigma_{xy} &= 2G\varepsilon_{xy} \\
&= \frac{E}{(1+\nu)}\varepsilon_{xy} \\
&= -\frac{\zeta E}{(1+\nu)}u_{z,xy} \\
&= -\frac{\zeta E}{(1-\nu^2)}(1-\nu)u_{z,xy} && \text{(c)}
\end{aligned}$$

It should be mentioned that efficient application of the theory of plates is facilitated by the introduction of *stress resultants*, which are bending and twisting moments per width of middle surface. However, to retain a strictly pointwise description consistent with the remainder of this text, the resultants are not introduced here.

We now calculate the remaining components of stress from the equilibrium equations, 2.46, again with 1, 2, 3 = x, y, z and Eqs. (8.10). From Eq. (2.46a) and $f_x = 0$,

$$\begin{aligned}\sigma_{xz,z} &= -\sigma_{xx,x} - \sigma_{xy,y} \\ &= -\frac{\zeta E}{(1-\nu^2)}[u_{z,xxx} + \nu u_{z,yyx} + (1-\nu)u_{z,xyy}] \\ &= -\frac{\zeta E}{(1-\nu^2)}(u_{z,xx} + u_{z,yy})_{,x} \\ &= \frac{\zeta E}{(1-\nu^2)}(\nabla^2 u_z)_{,x}.\end{aligned} \tag{8.11}$$

Similarly, from Eq. (2.46b) and $f_y = 0$

$$\sigma_{yz,z} = \frac{\zeta E}{(1-\nu^2)}(\nabla^2 u_z)_{,y}. \tag{8.12}$$

The preceding equations may be integrated with respect to z. Only ζ is a function of z, so that

$$\int \zeta\,dz = \int \zeta\,d\zeta = \frac{\zeta^2}{2} + C. \tag{8.13}$$

Since σ_{xz} and σ_{yz} should vanish at the surfaces $\zeta = \pm\frac{h}{2}$,

$$C = -\frac{h^2}{4}. \tag{8.14}$$

The final expressions for the transverse shearing stresses are found from the integrals of Eqs. (8.11) and (8.12), considering Eq. (8.14), as

$$\sigma_{xz} = \frac{E\left(\zeta^2 - \frac{h^2}{4}\right)}{2(1-\nu^2)}(\nabla^2 u_z)_{,x} \qquad \text{(a)}$$

$$\sigma_{yz} = \frac{E\left(\zeta^2 - \frac{h^2}{4}\right)}{2(1-\nu^2)}(\nabla^2 u_z)_{,y}. \qquad \text{(b)} \tag{8.15}$$

Now, we consider the normal stress σ_{zz} given by Eq. (2.46c), with $f_z = 0$ since there are no body forces:

$$\sigma_{zz,z} = -\sigma_{xz,x} - \sigma_{yz,y}$$
$$= -\frac{E\left(\zeta^2 - \frac{h^2}{4}\right)}{2(1-\nu^2)}(\nabla^4 u_z). \quad (8.16)$$

The stress σ_{zz} is of little practical consequence since, at most, it is equal to the magnitude of the surface loading. However, Eq. (8.16) is useful in establishing the governing equation for the normal displacement.

8.3.3 Plate Equation

We first consider the z-dependent terms $\left(\zeta^2 - \frac{h^2}{4}\right)$ of Eq. (8.16) integrated through the thickness

$$\int_{-h/2}^{h/2}\left(\zeta^2 - \frac{h^2}{4}\right)dz = \int_{-h/2}^{h/2}\left(\zeta^2 - \frac{h^2}{4}\right)d\zeta$$
$$= -\frac{h^3}{6}. \quad (8.17)$$

Substituting Eqs. (8.17) into the integral through the thickness of Eq. (8.16) gives

$$\sigma_{zz}\left(\frac{h}{2}\right) - \sigma_{zz}\left(-\frac{h}{2}\right) = \frac{Eh^3}{12(1-\nu^2)}\nabla^4 u_z. \quad (8.18)$$

Since the load $q(x, y)$ is assumed to be applied to the top surface in the positive z-direction

$$\sigma_{zz}\left(\frac{h}{2}\right) = q(x, y) \quad \text{(a)} \quad (8.19)$$

$$\sigma_{zz}\left(-\frac{h}{2}\right) = 0 \quad \text{(b)} \quad (8.19)$$

while

$$\nabla^4 u_z = q(x, y)/D \quad \text{(a)} \quad (8.20)$$

where

$$D = \frac{Eh^3}{12(1-\nu^2)} \quad \text{(b)} \quad (8.20)$$

is termed the *flexural rigidity* and is roughly equivalent to E times the moment of inertia of a unit width of plate, in consort with the theory of flexure where EI is termed the bending or flexural rigidity.

Equation (8.20a) is widely known as *the* plate equation and is of the same biharmonic form as the compatibility equations encountered in the two-dimensional elasticity formulation in Chapter 7.

Although the parallel between the plate equation and the bending of a beam of unit width is evident, Eq. (8.20a) represents more than one- or even two-directional flexure. Writing the equation in expanded form gives

$$u_{z,xxxx} + 2u_{z,xxyy} + u_{z,yyyy} = q(x,y)/D. \tag{8.21}$$

While the first and third terms on the l.h.s indeed represent flexure in the respective directions, each presumably resisting a portion of the load $q(x, y)$, the second term involves the mixed partial derivative and describes relative twisting of parallel fibers in the plate. It is this torsional resistance which differentiates a plate from a system of intersecting beams and contributes significantly to the overall rigidity of a solid plate.

The goal of the formulation, to express all displacements, strains and stresses in terms of a single displacement component u_z has been achieved. Once Eq. (8.21) is solved, the remaining components of displacement are found from Eqs. (8.7) and (8.8); the in-plane strains are given by Eq. (8.9); and the stresses follow Eqs. (8.10) and (8.15).

8.3.4 Polar Coordinates

For a circular plate, it is expedient to use polar coordinates, Figure 7.1. Inasmuch as the "plate" equation, Eq. (8.20a), and the compatibility equation from two-dimensional elasticity, Eq. (7.18), are essentially the same biharmonic equation, we may directly use the information given in Ch. 7. We simply replace ϕ with u_z in Eqs. (7.30) for the general case $u_z(r, \theta)$ to get

$$\nabla^4 u_z = q(r, \theta)/D \tag{8.22}$$

and in Eq. (7.31e) for the axisymmetric case $u_z(r)$ to get

$$\nabla^4 u_z = q(r)/D \tag{8.23}$$

where the $\nabla^4(\ )$ operator has been transformed to polar coordinates. Of course, appropriate particular solutions will be needed for the plate problem.

8.4 Solutions

8.4.1 Rectangular Plate

Since the theory of thin plates has an extensive specialized literature. residing for the most part outside of elasticity, we shall not pursue the analysis in depth here. However, much insight into the difficulty involved in obtaining analytical solutions may be gained by considering a rectangular plate, such as that shown in Figure 8.1, with plan dimensions a along the x-axis and b

along the y-axis and subjected to an arbitrary distributed loading $q(x, y)$. The origin for x and y is set at one corner of the plate.

If the plate is simply supported, which means that the normal displacement, u_z, and the bending moments, M_x and M_y, are equal to zero on the boundaries, harmonic functions in the form of a double-sine series

$$u_z = \sum_{j=1}^{\infty} \sum_{k=1}^{\infty} u_z^{jk} \sin j\pi \frac{x}{a} \sin k\pi \frac{y}{b} \tag{8.24}$$

identically satisfy the displacement boundary conditions

$$u_z(0, y) = u_z(a, y) = u_z(x, 0) = u_z(x, b) = 0. \tag{8.25}$$

Now, considering the bending moments on the boundary, they are computed from the integrals of the respective extensional stresses $\sigma_{(ii)}$ through the thickness, just as in the case of a beam, see Eq. (7.59b). However, for a plate, each stress is proportional to the curvatures in *both* coordinate directions, Eqs. (8.10 a,b).

This condition is therefore written as

$$M_x \sim u_{z,xx} + \nu u_{z,yy} = 0 \qquad \text{(a)} \quad (8.26)$$

at $(0, y)$ and (a, y) and

$$M_y \sim u_{z,yy} + \nu u_{z,xx} = 0 \qquad \text{(b)} \quad (8.26)$$

at $(x, 0)$ and (x, b). The double-sine function in Eq. (8.24) satisfies these conditions as well.

When the loading is expanded in a similar double series

$$q(x, y) = \sum_{j=1}^{\infty} \sum_{k=1}^{\infty} q^{jk} \sin j\pi \frac{x}{a} \sin k\pi \frac{y}{b}, \tag{8.27}$$

standard Fourier analysis may be used to obtain the solution for a general harmonic jk [8.2],

$$u_z^{jk} = \frac{q^{jk}}{D} \left\{ \frac{1}{\pi^4 \left[\left(\frac{j}{a}\right)^2 + \left(\frac{k}{b}\right)^2 \right]^2} \right\}. \tag{8.28}$$

Then the complete solution for the displacement at any point (x, y) is obtained by superposition from Eq. (8.22) as

$$u_z = \frac{1}{\pi^4 D} \sum_{j=1}^{\infty} \sum_{k=1}^{\infty} q^{jk} \left\{ \frac{1}{\left[\left(\frac{j}{a}\right)^2 + \left(\frac{k}{b}\right)^2 \right]^2} \right\} \sin j\pi \frac{x}{a} \sin k\pi \frac{y}{b}. \tag{8.29}$$

We may verify that Eq. (8.29) is indeed the solution by performing the operations indicated on the l.h.s. of Eq. (8.21). Since the solution is formed by superimposing the individual harmonic contributions, it is sufficient to consider a typical component $\bar{j}\bar{k}$. Common to each term is the function

$$F(x, y; \bar{j}, \bar{k}) = \frac{q^{\bar{j}\bar{k}}}{\pi^4 D} \left\{ \frac{1}{\left[\left(\frac{\bar{j}}{a}\right)^2 + \left(\frac{\bar{k}}{b}\right)^2\right]^2} \right\} \sin \bar{j}\pi\frac{x}{a} \sin \bar{k}\pi\frac{y}{b} \tag{8.30}$$

whereupon

$$u_{z,xxxx} = \left(\frac{\bar{j}\pi}{a}\right)^4 F$$

$$2u_{z,xxyy} = 2\left(\frac{\bar{j}\pi}{a}\right)^2\left(\frac{\bar{k}\pi}{b}\right)^2 F$$

$$u_{z,yyyy} = \left(\frac{\bar{k}\pi}{b}\right)^4 F$$

and the sum is

$$\begin{aligned}\nabla^4 u_z &= \left[\left(\frac{\bar{j}\pi}{a}\right)^4 + 2\left(\frac{\bar{j}\pi}{a}\right)^2\left(\frac{\bar{k}\pi}{b}\right)^2 + \left(\frac{\bar{k}\pi}{b}\right)^4\right] F \\ &= \pi^4\left[\left(\frac{\bar{j}}{a}\right)^2 + \left(\frac{\bar{k}}{b}\right)^2\right]^2 F \\ &= (q^{\bar{j}\bar{k}}/D) \sin \bar{j}\pi\frac{x}{a} \sin \bar{k}\pi\frac{y}{b} \\ &= q(x, y)/D \end{aligned} \tag{8.31}$$

from Eq. (8.27).

It remains to examine the convergence of the series Eq. (8.29) so as to set appropriate truncation limits for j and k. To illustrate, we take the example of a uniformly loaded plate with

$$q(x, y) = q_0 \tag{8.32}$$

and set about to determine the Fourier coefficients q^{jk}.

Starting with Eq. (8.27)

$$q_0 = \sum_{j=1}^{\infty} \sum_{k=1}^{\infty} q^{jk} \sin j\pi\frac{x}{a} \sin k\pi\frac{y}{b}, \tag{8.33}$$

the procedure is to multiply both sides by $\sin m\pi\frac{x}{b} \sin n\pi\frac{y}{b}$, where m and n represent arbitrary harmonics, and integrate over the area:

$$\begin{aligned}&\int_0^a \int_0^b q_0 \sin m\pi\frac{x}{a} \sin n\pi\frac{y}{b}\, dx\, dy \\ &= \sum_{j=1}^{\infty} \sum_{k=1}^{\infty} q^{jk} \int_0^a \sin m\pi\frac{x}{a} \sin j\pi\frac{x}{a}\, dx \int_a^b \sin n\pi\frac{y}{b} \sin k\pi\frac{y}{b}\, dy.\end{aligned} \tag{8.34}$$

For the l.h.s. of Eq. (8.34)

$$\int_0^a \int_0^b q_0 \sin m\pi \frac{x}{a} \sin n\pi \frac{y}{b} \, dx \, dy = q_0 \frac{a}{m\pi}\left[-\cos\frac{m\pi x}{a}\right]_0^a \frac{b}{n\pi}\left[-\cos\frac{n\pi y}{b}\right]_0^b$$

$$= q_0 \frac{a}{m\pi}[\cos m\pi - 1]\frac{b}{n\pi}[\cos n\pi - 1]. \quad (8.35)$$

If m and/or n is an even integer, the expression = 0. But, for m and n both odd,

$$q_0 \frac{a}{m\pi}[\cos m\pi - 1]\frac{b}{n\pi}[\cos n\pi - 1] = \frac{4ab}{\pi^2 mn} q_0. \quad (8.36)$$

Now, considering the r.h.s. of Eq. (8.34),

$$\begin{aligned} \int_0^a \sin m\pi \frac{x}{a} \sin j\pi \frac{y}{a} \, dx &= \frac{a}{2} \qquad m = j \\ &= 0 \qquad m \neq j \\ \int_0^b \sin n\pi \frac{y}{b} \sin k\pi \frac{y}{b} \, dy &= \frac{b}{2} \qquad n = k \\ &= 0 \qquad n \neq k. \end{aligned}$$

Therefore, the entire summation reduces to

$$q^{jk} \frac{ab}{4}. \quad (8.37)$$

Replacing m and n by j and k to denote a general but specific harmonic, we have by equating Eqs. (8.36) and (8.37)

$$q^{jk} = \frac{16}{\pi^2 jk} q_0 \quad (8.38)$$

and the complete displacement function follows from Eq. (8.29) as

$$u_z = \frac{16 q_0}{\pi^6 D} \sum_{j=1}^{\infty} \sum_{k=1}^{\infty} \frac{1}{jk} \left\{ \frac{1}{\left[\left(\frac{j}{a}\right)^2 + \left(\frac{k}{b}\right)^2\right]^2} \right\} \sin j\pi \frac{x}{a} \sin k\pi \frac{y}{b} \quad \begin{matrix} j = 1, 3, 5, \ldots \\ k = 1, 3, 5, \ldots. \end{matrix} \quad (8.39)$$

The series will obviously converge very rapidly since j and k are of the fifth power in the denominator. Also, it should be dominated by the first terms $j = k = 1$; $j = 1, k = 3$; $j = \; = 3, k = 1$; since $j = k = 3$ and higher terms will carry at least $(3)^5$ in the denominator.

Once the displacement function is found, the various stresses are computed routinely. For the in-plane or membrane stresses, σ_{xx}, σ_{yy}, σ_{xy}, we use Eqs. (8.10), which requires differentiating the series. For the transverse shearing stresses, σ_{xz} and σ_{yz}, Eqs. (8.11) and (8.12) respectively are integrated through the thickness.

In considering the truncation of a series such as Eq. (8.39), we must be cautious. We remember that we seek not only the displacements for the plate, but the stresses as well. We see from Eqs. (8.10) that the stresses σ_{ij} are given by various combinations of $u_{z,ij}$. For example,

$$u_{z,xx} = \frac{16}{\pi^4}\frac{q_0}{D}\frac{1}{a^2}\sum_{j=1}^{\infty}\sum_{k=1}^{\infty}\left(\frac{j}{k}\right)\left\{\frac{1}{\left[\left(\frac{j}{a}\right)^2+\left(\frac{k}{b}\right)^2\right]^2}\right\}\sin j\pi\frac{x}{a}\sin k\pi\frac{y}{b}, \quad (8.40)$$

which will converge slower than Eq. (8.39). The expressions for $u_{z,yy}$ and $u_{z,xy}$ are similar.

The double series is known as Navier's solution and is recognized as a great accomplishment in solid mechanics. However, if boundary conditions other than all sides simply supported are encountered or if the planform is other than rectangular or circular, the difficulty of choosing harmonic functions which identically satisfy the boundary conditions increases enormously. Therefore, numerical methods are widely applied to the analysis of plates.

8.4.2 Circular Plate

8.4.2.1 General Solution for Axisymmetric Loading

We consider a circular plate subject to a uniform load q_0, initially without specifying boundary conditions. A plate so loaded will deform uniformly around the circumference so that the axisymmetric form of the governing equation may be considered. The solution to Eq. (8.23) may be written by analogy with Eq. (7.32) as

$$u_z(r) = C_1 r^2 \ln r + C_2 r^2 + C_3 \ln r + C_4 + u_{zp} \quad (8.41)$$

where u_{zp} is a particular solution. For the case of a uniform load, u_{zp} must be proportional to r^4, say Cr^4. Performing the operations indicated by Eq. (7.31e).

$$\nabla^4(Cr^4) = \frac{1}{r}\left[r\left(\frac{1}{r}[r(Cr^4)_{,r}]_{,r}\right)_{,r}\right]_{,r} = 64C. \quad (8.42)$$

With $64C = q_0/D$,

$$C = \frac{q_0}{64D} \quad (8.43)$$

and

$$u_{zp} = \frac{q_0}{64D}r^4. \quad (8.44)$$

A variety of support conditions and geometries may be solved with Eq. (8.41). First, it is convenient to form the first and second derivatives

$$u_{z,r} = C_1 r(2\ln r + 1) + 2C_2 r + C_3\frac{1}{r} + \frac{q_0}{16D}r^3 \qquad \text{(a)}$$

$$u_{z,rr} = C_1(2\ln r + 3) + 2C_2 - C_3\frac{1}{r^2} + \frac{3q_0}{16D}r^2. \qquad \text{(b)} \qquad (8.45)$$

Next, second derivatives of u_z with respect to x and y, which are contained in the simply supported boundary conditions Eqs. (8.26), are transformed into polar coordinates. We refer to Fig. 7.1 and the r-dependent portions of Eqs. (7.22):

$$\frac{\partial(\ )}{\partial x} = \frac{\partial(\ )}{\partial r}r_{,x} = \frac{\partial(\ )}{\partial r}\cos\theta = \frac{\partial(\ )}{\partial r}\frac{x}{r} \qquad \text{(a)}$$

$$\frac{\partial(\ )}{\partial y} = \frac{\partial(\ )}{\partial r}r_{,y} = \frac{\partial(\ )}{\partial r}\sin\theta = \frac{\partial(\ )}{\partial r}\frac{y}{r} \qquad \text{(b)} \qquad (8.46)$$

from which

$$\frac{\partial^2 u_z}{\partial x^2} = \frac{x}{r}\frac{\partial^2 u_z}{\partial r^2} + \frac{\partial u_{z,r}}{\partial r}\left(\frac{r - xr_{,x}}{r^2}\right) \qquad \text{(a)}$$

$$\frac{\partial^2 u_z}{\partial y^2} = \frac{y}{r}\frac{\partial^2 u_z}{\partial r^2} + \frac{\partial u_{z,r}}{\partial r}\left(\frac{r - yr_{,y}}{r^2}\right). \qquad \text{(b)} \qquad (8.47)$$

Taking r along the x-axis in Fig. 7.1, $x = r$, $y = 0$, $r_{,x} = \cos\theta = 1$ and $r_{,y} = \sin\theta = 0$, leaving

$$u_{z,xx} = u_{z,rr} \qquad \text{(a)}$$

$$u_{z,yy} = \frac{1}{r}u_{z,r} \qquad \text{(b)} \qquad (8.48)$$

as the transformed derivatives.

8.4.2.2 Solid Plate

We consider a circular plate with outside radius R_0. Since the terms containing $\ln r$ would be singular at $r = 0$, we may set C_1 and $C_3 = 0$ in Eq. (8.41), which leaves

$$u_z(r) = C_2 r^2 + C_4 + \frac{q_0}{64D}r^4. \qquad (8.49)$$

If the plate is clamped at the boundary, we have $u_z(R_0) = u_{z,r}(R_0) = 0$, or

$$u_z(R_0) = C_2 R_0^2 + C_4 + \frac{q_0}{64D}R_0^4 = 0 \qquad \text{(a)}$$

$$u_{z,r}(R_0) = 2C_2 R_0 + \frac{q_0}{16D}R_0^3 = 0 \qquad \text{(b)} \qquad (8.50)$$

from which

$$C_2 = -\frac{q_0}{32D} R_0^2 \qquad \text{(a)}$$
$$C_4 = \frac{q_0}{64D} R_0^4 \qquad \text{(b)} \tag{8.51}$$

and

$$u_z = \frac{q_0}{64D}(-2R_0^2 r^2 + R_0^4 + r^4)$$
$$= \frac{q_0}{64D}(R_0^2 - r^2). \tag{8.52}$$

If the plate is simply supported at the boundary, we have Eq. (8.50a) along with Eqs. (8. 26), which are written in polar coordinates using Eqs. (8.48) as

$$\left(u_{z,rr} + \frac{v}{r} u_{z,r}\right)_{r=R_0} = 0. \tag{8.53}$$

Substituting Eqs. (8.45),

$$2(1 + v)C_2 + \frac{(3 + v)}{16D} q_0 R_0^2 = 0 \tag{8.54}$$

so that

$$C_2 = -2\left(\frac{3 + v}{1 + v}\right)\frac{q_0 R_0^2}{64D} \tag{8.55a}$$

and from Eq. (8.50a)

$$C_4 = \frac{q_0 R_0^4}{64D}\left[\frac{2(3 + v)}{1 + v} - 1\right]$$
$$= \frac{q_0}{64D}\left[\frac{5 + v}{1 + v}\right] R_0^4 \tag{8.55b}$$

and then from Eq. (8.49)

$$u_z(r) = \frac{q_0}{64D}(R_0^2 - r^2)\left\{\left[\frac{5 + v}{1 + v}\right] R_0^2 - r^2\right\}. \tag{8.56}$$

8.4.2.3 Annular Plate

We may also consider an annular plate with planform as shown in Fig. 7.2(a), but subjected to a *transverse* uniform loading q. We again consider the clamped boundary condition corresponding to

$$u_z(R_0) = u_{z,r}(R_0) = 0 \tag{8.57}$$

at the outer ring and

$$u_z(R_1) = u_{z,r}(R_1) = 0 \tag{8.58}$$

on the inner ring. Since the singularity as $r \to 0$ is not an issue, we retain C_1 and C_3 and evaluate from Eqs. (8.41) and (8.45a):

$$C_1 R_0^2 \ln R_0 + C_2 R_0^2 + C_3 \ln R_0 + C_4 + \frac{q_0}{64D} R_0^4 = 0 \quad \text{(a)}$$

$$C_1 R_0(2 \ln R_0 + 1) + 2C_2 R_0 + \frac{C_3}{R_0} + \frac{q_0}{16D} R_0^3 = 0 \quad \text{(b)}$$

$$C_1 R_1^2 \ln R_1 + C_2 R_1^2 + C_3 \ln R_1 + C_4 + \frac{q_0}{64D} R_1^4 = 0 \quad \text{(c)} \tag{8.59}$$

$$C_1 R_1(2 \ln R_1 + 1) + 2C_2 R_1 + \frac{C_3}{R_1} + \frac{q_0}{16D} R_1^3 = 0. \quad \text{(d)}$$

The equations are best solved using numerical values for R_0 and R_1, whereupon the determined constants are used in Eq. (8.41) and subsequent calculations.

8.4.2.4 Stresses

After the appropriate boundary conditions are applied and the constants determined, the complete displacement function and derivatives are available from Eqs. (8.41), (8.44) and (8.45). Returning to the stresses for the axisymmetric case, σ_{xx} and σ_{yy} in Eqs. (8.10 a,b) become σ_{rr} and $\sigma_{\theta\theta}$. Substituting Eqs. (8.48) for the curvatures gives

$$\sigma_{rr} = -\frac{\zeta E}{1 - \nu^2}\left(u_{z,rr} + \frac{\nu}{r} u_{z,r}\right) \quad \text{(a)}$$

$$\sigma_{\theta\theta} = -\frac{\zeta E}{1 - \nu^2} \frac{1}{r}(u_{z,r} + \nu u_{z,rr}). \quad \text{(b)} \tag{8.60}$$

The evaluation of the stresses, in particular the maximum value through the thickness at $\zeta = \pm\frac{h}{2}$, may proceed routinely.

8.5 Commentary

It should also be mentioned that more refined theories of plates, between the elementary theory presented here and a three-dimensional elasticity solution, are available. Most prominent is a theory which relaxes part of Assumption (2). In effect, the line *mn* remains straight but not necessarily normal to the deformed middle surface. This negates Eq. (8.4) and gives independent rotations ω_{yz} and ω_{xz} in addition to $u_z(x, y)$. The difference between the two deformation fields are due to transverse shearing strains. Although these differences are seldom signficant in magnitude, the inclusion of these deformations often facilitates numerically based solutions [8.2].

Exercises

8.1 Consider a thin plate having the elliptical planform shown in Fig. 6.7(a). Following the strategy used for the torsion problem, the solution is assumed proportional to the equation of the boundary [8.1]

$$u_z = C\left(\frac{x^2}{D^2} + \frac{y^2}{B^2} - 1\right)^2.$$

(a) Show that this solution satisfies the clamped boundary conditions.
(b) For a uniform load, q_0, compute the constant C.
(c) Evaluate the maximum displacement.

8.2 Consider the solution for a simply supported plate, Eq. (8.39), and particularly the displacement at the center of the plate.
(a) Compare the values after 1, 3 and 5 terms.
(b) Repeat the computation for the stress σ_{xx} at the center.

8.3 Consider a clamped solid circular plate of radius R_0 with a "sand heap" loading

$$q(z) = q_0(R - R_0)$$

and determine the deflection function.

8.4 Consider the solutions for the solid plate with both clamped and simply supported boundary conditions.
(a) Why are the values of σ_{rr} and $\sigma_{\theta\theta}$ equal at $r = 0$ in each case?
(b) Evaluate $\sigma_{rr}(0)$ for the two boundary conditions. How does this compare to the difference between a clamped and simply supported beam if $\nu = 0.3$?

References

[8.1] Filonenko–Borodich, M., *Theory of Elasticity* (Dover Publications, Inc., New York, 1965).
[8.2] Gould, P. L., *Analysis of Shells and Plates* (Springer-Verlag, New York, 1988).

CHAPTER 9

Time-Dependent Effects

9.1 Introduction

The strains in an elastic body may be computed from a specified displacement field using the equations of compatibility, regardless of whether the displacements arise from static or dynamic excitation. The corresponding stresses and, indeed, the displacements themselves may be dependent on the rate characteristics of the loading function. Therefore, the time derivatives of the displacements, i.e., velocities and accelerations, enter into these equations.

It is often convenient to separate the response of a linear system into a product of the effects of the *system* and the effects of the *load*. This concept is useful in static cases and is usually based on identifying the Green's function for the system, the response (displacement, strain, stress) due to the application of a *unit* load, and integrating that function over a specified load range to evaluate the corresponding total response. For example, Eqs. 7.93 with $P = 1$ would be Green's functions for a vertical load on a semi-infinite plate.

In the case of dynamic excitation, two important system characteristics are the natural frequencies or their inverse, the periods of vibration, and the corresponding mode shapes. Once these are found by considering the homogeneous part of the governing differential equation, the response to a forcing function may be readily obtained as a particular solution. Also, even if the loading is not specified, these system characteristics are useful for classification. For example, structures are said to be stiff or flexible based on the relative natural frequencies. A related characteristic, which is dependent only on the material properties, is the velocity at which an elastic wave propagates through a medium or a body. Again, this value leads to useful comparative classifications of media and materials.

In dynamic response computations, damping is very important. Damping represents internal energy dissipation and may be dependent on the displacement, the velocity or other rate quantities. In effect, damping is a quantity which is considered at the macro level of linear elasticity but which really represents micro-level molecular processes. Obviously, there are a variety of models which attempt to depict physical reality.

In this chapter, the field equations of linear elasticity will be generalized to include rate-dependent terms. We will first focus on the propagation of waves through the medium and then describe the motion of the particles comprising the medium.

9.2 Vibrations in an Infinite Elastic Medium

9.2.1 Equilibrium Equations

We begin with the Lamé equations (5.7) and consider the body forces to be the inertial forces corresponding to the acceleration, by D'Alembert's principle. Thus, we have

$$\mu u_{j,ii} + (\lambda + \mu) u_{i,ij} - \rho \ddot{u}_j = 0 \tag{9.1}$$

where $(\dot{\ })$ indicates $\dfrac{\partial(\ )}{\partial t}$ and t is the time variable.

Initially, we are not concerned with boundary conditions on u_i since the medium is assumed to be infinite. We follow the treatment of Filonenko–Borodich [9.1] in explicit notation and generalize to the indicial form when convenient.

9.2.2 Longitudinal Vibrations

We refer to a Cartesian coordinate system and consider time-dependent displacements along one axis, say the x-axis in Figure 9.1. For the moment, we do not dwell on the source of the motion but only the response. The displacement field is

$$\begin{aligned} u_x &= u_x(x, t) && \text{(a)} \\ u_y &= 0 && \text{(b)} \\ u_z &= 0. && \text{(c)} \end{aligned} \tag{9.2}$$

Considering the plane L parallel to the y-z plane at a distance x_0 from the origin, it will assume a position $x = x_0 + u_x(x_0, t)$ at any time $t > 0$ during the motion.

If excitations along the x-axis are present, the plane will travel back and forth along the axis. Other planes initially parallel to L will move in a like manner. While the planes will remain parallel, the distance between any two will alternately increase and decrease, creating a state of uniform longitudinal vibration. Two planes initially at $x = x_0$ and $x = x_1$ will be separated by a distance

$$\begin{aligned} d(x_0, x_1, t) &= [x_1 + u_x(x_1, t)] - [x_0 + u_x(x_0, t)] \\ &= x_1 - x_0 + u_x(x_1, t) - u_x(x_0, t) \end{aligned} \tag{9.3}$$

at any time t.

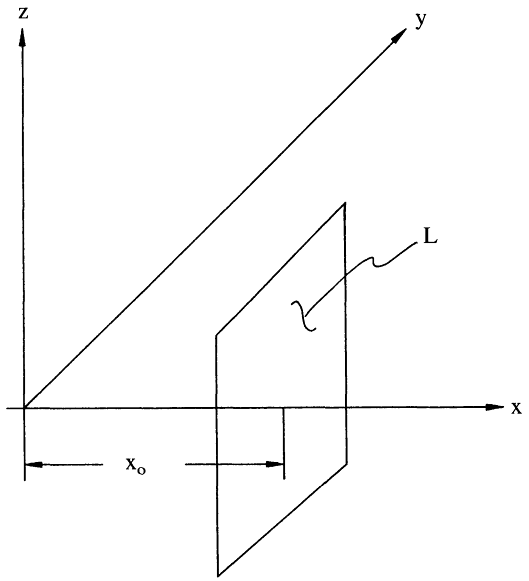

Fig. 9.1. Plane in Cartesian space.

For this case, Eqs. (9.1) with $i = x, y, z$ become

$$\mu u_{x,xx} + (\lambda + \mu)u_{x,xx} - \rho \ddot{u}_x = 0 \tag{9.4}$$

since the motion is uniform and only a function of x. Equation (9.4) may be written as

$$\ddot{u}_x = c_P^2 u_{x,xx} \quad \text{(a)} \quad (9.5)$$

where

$$c_P = \sqrt{\frac{\lambda + 2\mu}{\rho}} = \sqrt{\frac{E(1-\nu)}{\rho(1+\nu)(1-2\nu)}}, \quad \text{(b)} \quad (9.5)$$

which is known as the one-dimensional wave equation.

Thus, longitudinal vibrations described by Eqs. (9.2) are possible if $u_x(x, t)$ satisfies Eq. (9.5a). The parameter c_P will be interpreted later. Since the waves generated oscillate along the axis producing extension and contraction, they are dilation waves, usually called P (for pressure) waves.

The preceding equation may be derived from another approach. The condition of no rotation,

$$\omega_{ij} = \tfrac{1}{2}(u_{i,j} - u_{j,i}) = 0, \tag{9.6}$$

from Eq. (3.32) is satisfied by defining a potential function Φ such that

$$u_i = \Phi_{,i} \quad \text{(a)} \quad (9.7)$$

and

$$u_j = \Phi_{,j} \qquad \text{(b)} \quad (9.7)$$

from which

$$u_{i,i} = \Phi_{,ii}. \qquad (9.8)$$

Then Eq. (9.1) becomes

$$\mu\Phi_{,jii} + (\lambda + \mu)\Phi_{,iij} - \rho\ddot{u}_j = 0. \qquad (9.9)$$

Using Eq. (9.7b) to replace $\Phi_{,j}$, we get

$$(\lambda + 2\mu)u_{j,ii} - \rho\ddot{u}_j = 0 \qquad (9.10a)$$

or

$$(\lambda + 2\mu)\nabla^2 u_j - \rho\ddot{u}_j = 0, \qquad (9.10b)$$

which reduces to Eq. (9.5a) for the one directional motion described by Eq. (9.2). Thus, the specialization which produces *P* waves is known as irrotational wave propagation.

Also, the form of Eq. (9.10) is more general, in that the motion need not be completely uniform throughout the medium so long as it is irrotational.

9.2.3 Transverse Vibrations

Now we choose a displacement field normal to the x-axis, say in the z-direction,

$$u_x = 0 \qquad \text{(a)}$$
$$u_y = 0 \qquad \text{(b)} \quad (9.11)$$
$$u_z = u_z(x, t). \qquad \text{(c)}$$

In this case the plane L and all parallel planes will move perpendicular to the x-axis. All points on L move the same distance u_z, but the planes move relative to one another in the z-direction, setting up a state of uniform transverse vibrations.

Equation (9.1) reduces to

$$\mu u_{z,xx} - \rho\ddot{u}_z = 0 \qquad (9.12)$$

since the motion is still only a function of x, or

$$\ddot{u}_z = c_S^2 u_{z,xx} \qquad \text{(a)} \quad (9.13)$$

where

$$c_S = \sqrt{\frac{\mu}{\rho}} = \sqrt{\frac{E}{2\rho(1 + \nu)}}. \qquad \text{(b)} \quad (9.13)$$

Thus, transverse vibrations described by Eqs. (9.11) may occur if $u_z(x, t)$ satisfies Eq. (9.13a). Again the parameter c_S will be interpreted later. The waves produced are known as shear or S waves since they produce transverse motion but no extensional deformation.

We may also derive the preceding equations by noting that the transverse vibrations cause no volume change. From Eq. (3.41), the dilation

$$\Delta = \varepsilon_{ii} = u_{i,i} = 0, \tag{9.14}$$

Setting $u_{i,i} = 0$ in Eq. (9.1) gives

$$\mu u_{j,ii} - \rho \ddot{u}_j = 0 \qquad \text{(a)} \quad (9.15)$$

or

$$\mu \nabla^2 u_j - \rho \ddot{u}_j = 0, \qquad \text{(b)} \quad (9.15)$$

which reduces to Eq. (9.12) for the motion described by Eq. (9.11). Therefore, the specialization which produces S waves is known as incompressible wave propagation.

It should also be noted that an identical solution could have been constructed for the displacement in the y direction, i.e., $u_y = u_y(x, t)$, so that two orthogonal sets of shear waves, SH and SV waves, may be generated.

Again, the form of Eqs. (9.15) is more general than the reduced Eq. (9.12).

9.2.4 Harmonic Vibrations

9.2.4.1 Longitudinal Motion

We now consider a sinusoidal form for the function u_x in Eq. (9.2a)

$$u_x(x, t) = A \sin 2\pi \left(\frac{x}{l_P} - \frac{t}{T_P} \right). \tag{9.16}$$

The normalizing terms l_P and T_P will be interpreted later. Equation (9.16) is substituted into Eq. (9.5a) to get

$$\frac{1}{T_P^2} = \frac{c_P^2}{l_P^2}. \tag{9.17}$$

Therefore, the conditions on l_P and T_P to produce the motion described by Eq. (9.16) are

$$\frac{l_P}{T_P} = c_P = \sqrt{\frac{\lambda + 2\mu}{\rho}}. \tag{9.18}$$

The amplitude of the vibration, A, is arbitrary.

This motion is represented by the trace of the planes such as L on the x-z plane in Figure 9.2. The term T_P in Eq. (9.16) is called the *period* of the traveling waves. For a point at $x = \bar{x}$, which represents all points on a single plane, the displacement $u_x(\bar{x}, t)$ evaluated at a specific time $\bar{t}$ is

$$u_x(\bar{x}, \bar{t}) = A \left[\sin\left(2\pi \frac{\bar{x}}{l_P}\right) \cos\left(2\pi \frac{\bar{t}}{T_P}\right) - \cos\left(2\pi \frac{\bar{x}}{l_P}\right) \sin\left(2\pi \frac{\bar{t}}{T_P}\right) \right] \tag{9.19}$$

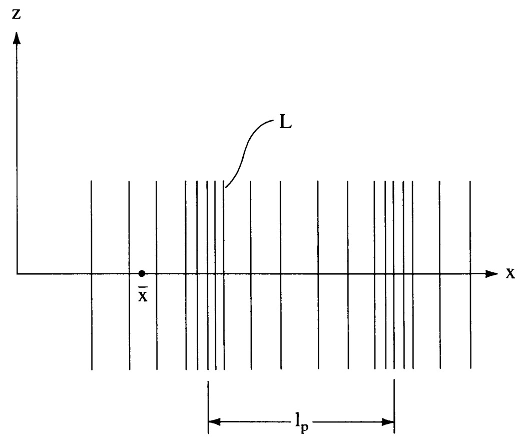

Fig. 9.2. Traces of longitudinally vibrating planes.

while at a time $\bar{t} + T_P$

$$\begin{aligned} u_x(\bar{x}, \bar{t} + T_P) &= A\left[\sin\left(2\pi\frac{\bar{x}}{l_P}\right)\cos\left(2\pi\frac{\bar{t} + T_P}{T_P}\right) - \cos\left(2\pi\frac{\bar{x}}{l_P}\right)\sin\left(2\pi\frac{\bar{t} + T_P}{T_P}\right)\right] \\ &= A\left[\sin\left(2\pi\frac{\bar{x}}{l_P}\right)\cos\left(2\pi + 2\pi\frac{\bar{t}}{T_P}\right) - \cos\left(2\pi\frac{\bar{x}}{l_P}\right)\sin\left(2\pi + 2\pi\frac{\bar{t}}{T_P}\right)\right] \\ &= u_x(\bar{x}, \bar{t}) \end{aligned} \tag{9.20}$$

since $\cos(2\pi + t) = \cos t$ and $\sin(2\pi + t) = \sin t$. The same would be true at $t = \bar{t} + 2T_P$, or $t = \bar{t} + nT_P$, where n is an integer. Thus, the motion is repeated after a duration of T_P.

To interpret parameter l_P, we consider the axial strain Eq. (3.15a)

$$\varepsilon_{xx}(x, t) = u_{x,x} = A\frac{2\pi}{l_P}\cos 2\pi\left(\frac{x}{l_P} - \frac{t}{T_P}\right). \tag{9.21}$$

At an instant in time $t = \bar{t}$, we consider a representative sampling of planes which were equally spaced when the system was at rest. It may be shown that at $t = \bar{t}$, a plane located at $x + l_P$ has the same strain as the plane at x, i.e.,

$$\varepsilon_{xx}(x + l_P, \bar{t}) = \varepsilon_{xx}(x, \bar{t}), \qquad \text{(a)} \quad (9.22)$$

or, in general,

$$\varepsilon_{xx}(x + nl_P, \bar{t}) = \varepsilon_{xx}(x, \bar{t}). \qquad \text{(b)} \quad (9.22)$$

The relationship between equally strained planes is shown in Figure 9.2. The separation l_P is known as the *wave length*. The maximum contraction strain is in the region where the planes are most dense while the maximum extension is in the least dense region. Referring to Eq. (9.21), these maxima occur when

$$\cos 2\pi\left(\frac{x}{l_P} - \frac{t}{T_P}\right) = \pm 1 \qquad \text{(a)} \quad (9.23)$$

or

$$\frac{x}{l_P} - \frac{t}{T_P} = \frac{n}{2} \qquad \text{(b)} \quad (9.23)$$

where n is an integer.

Also, Eq. (9.23b) indicates that the coordinates of these points of extreme strain $x = x_e$ move linearly in time with a velocity

$$\dot{x}_e = \frac{l_P}{T_P}. \tag{9.24}$$

But, from Eq. (9.18),

$$\frac{l_P}{T_P} = c_P = \sqrt{\frac{\lambda + 2\mu}{\rho}} \tag{9.25}$$

so that the parameter c_P encountered originally in Eqs. (9.5) has finally been identified as the velocity of propagation of the pressure waves produced by longitudinal vibrations.

An important application is for sonic vibrations and the associated strains, which occur in the range $\frac{1}{16}$ sec $> T_P > 2 \times 10^{-5}$ sec [9.1]. Such waves propagate through an infinite medium with a velocity dependent on the material properties λ, μ and ρ which enter into Eq. (9.25).

Some closely related applications in the strength of materials are the longitudinal vibration of a bar and longitudinal wave motion in a fluid column.

9.2.4.2 Transverse Motion

If we assume an analogous sinusoidal form for u_z in Eq. (9.11c)

$$u_z = B \sin 2\pi\left(\frac{x}{l_S} - \frac{t}{T_S}\right) \tag{9.26}$$

we describe the transverse vibration of the waves for which the traces are shown in Figure 9.3. The wavelength is l_S and the velocity of propagation is

$$c_S = \sqrt{\frac{\mu}{\rho}}, \tag{9.27}$$

which is smaller than c_P. Here, we have a shear strain computed from Eq. (3.15e) as

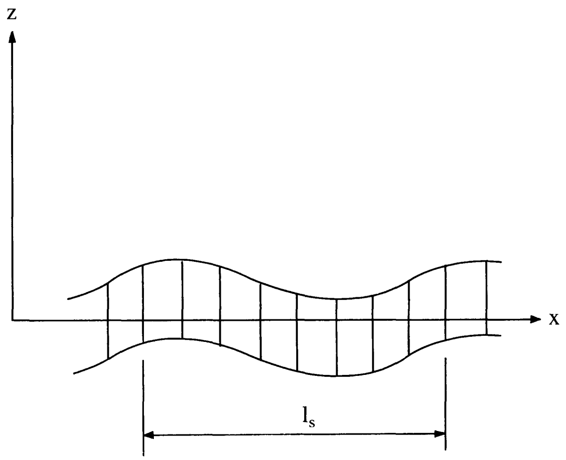

Fig. 9.3. Traces of transversely vibrating planes.

$$\varepsilon_{xz} = \frac{1}{2} u_{z,x}$$

$$= B\frac{\pi}{l_S}\cos 2\pi\left(\frac{x}{l_S} - \frac{t}{T_S}\right). \tag{9.28}$$

The shear strain propagates with the same velocity c_S.

In the strength of materials, the transverse vibration of a shear beam is described by the response to waves propagating with velocity c_S.

To compare the longitudinal and transverse motions, we form the ratio

$$\frac{c_S}{c_P} = \sqrt{\frac{\mu}{\lambda + 2\mu}}. \tag{9.29}$$

Both μ and λ may be expressed in terms of Poisson's ratio ν and Young's modulus E through Eqs. (4.24a and b). Then,

$$\frac{c_S}{c_P} = \sqrt{\frac{1 - 2\nu}{2 - 2\nu}}. \tag{9.30}$$

For $\nu = \frac{1}{3}$,

$$\frac{c_S}{c_P} = \frac{1}{2}.$$

While the velocities c_P and c_S are very large, on the order of 5 km/sec through metal [9.1], the difference in velocities can often be distinguished and the P and S waves thus identified. In Figure 9.4 a seismogram which records the period wave motion is shown [9.2]. The marked record is an earthquake in Alaska recorded in California. The peaks corresponding to the

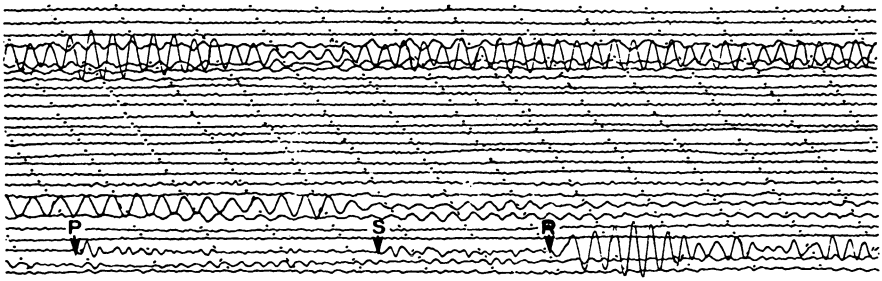

Fig. 9.4. Seismogram from a long-period seismograph showing the vertical component of elastic wave motion recorded at Oroville, California, during part of one day. The third trace from the bottom is from a magnitude-5 earthquake in Alaska. The time between breaks in the trace is 1 min. Bruce A. Bolt, "Elastic Waves in the Vicinity of the Earthquake Source," in *Earthquake Engineering*, Robert Weigel, ed., © 1970, p. 5. Reprinted by permission of Prentice Hall, Englewood Cliffs, New Jersey.

faster-moving P waves followed by the slower S waves are shown, along with peaks due to another even slower moving type of wave, the L or Love waves which are caused by surface effects.

Again we note the possibility of a second orthogonal set of S waves acting in the x-y plane and the multidirectional forms of the wave propagation equations, Eqs. (9.10) and (9.15). However, in any case the velocity of propagation remains a constant dependent only on the properties of the medium. The differences in velocity between the P waves and S waves is used in many geophysical techniques.

9.3 Free Vibration

9.3.1 Equations of Motion

Vibration of elastic bodies is very important in practical engineering and is most often applied to specialized structural forms such as beams and plates. However, the governing equations can be developed to a certain extent within the present context of elasticity.

While the previous sections have focused on the propagation of waves through a medium, we now focus on the motion of particles within the medium. Again, the source of the motion is not germane at this point. We simply assume that the body is vibrating in a normal mode, which means that all particles are moving synchronously and pass through the zero or rest position simultaneously [9.3]. The deformation may be visualized as a series of independently vibrating orthogonal modes, such as sine or cosine curves, which may be superposed to approximate a more complicated motion. This is, of course, the physical interpretation of a Fourier series and is the basis of one of the most powerful analytical tools in mathematical physics, harmonic analysis.

Referring to Eq. (9.1), the displacement is taken as the product of a function, A_j, of the spatial coordinates x_j and a function, f, of the time coordinate t, i.e.,

$$u_j(x_j, t) = A_j(x_j)f(t). \tag{9.31}$$

Substituting into Eq. (9.1) gives

$$\mu\left[A_{j,ii} + \left(\frac{\lambda + \mu}{\mu}\right)A_{i,ij}\right]f = \rho A_j\ddot{f} \tag{9.32}$$

or

$$\frac{\mu}{A_j}\left[A_{j,ii} + \left(\frac{\lambda + \mu}{\mu}\right)A_{i,ij}\right] = \rho\frac{\ddot{f}}{f}. \tag{9.33}$$

With the l.h.s. being a function of x_j and the r.h.s. being a function of t, $\frac{\ddot{f}}{f}$ is at most a constant, i.e.,

$$\frac{\ddot{f}}{f} = -\omega^2. \tag{9.34}$$

Thus,

$$f = C\cos\omega t + D\sin\omega t \tag{9.35}$$

but since the time origin is arbitrary, we may take

$$f = D\sin\omega t. \tag{9.36}$$

Then, the equilibrium equation (9.1) becomes, in view of Eq. (9.34),

$$\mu\left[u_{j,ii} + \left(\frac{\lambda + \mu}{\mu}\right)u_{i,ij} + \frac{\rho}{\mu}\omega^2 u_j\right] = 0 \tag{9.37}$$

or by comparing Equations (5.1) and (5.7) and reintroducing the stress tensor, we can write Eq. (9.37) as

$$\sigma_{ij,i} + \rho\omega^2 u_j = 0. \tag{9.38}$$

Equation (9.38) may also be stated in terms of the engineering constants G and ν using Eqs. (4.24) as

$$u_{j,ii} + \frac{1}{1 - 2\nu}u_{i,ij} + \frac{\rho}{G}\omega^2 u_j = 0. \tag{9.39}$$

For a set of boundary conditions prescribed on the surface of the body, Eqs. (9.38) or (9.39) may be satisfied only for certain values of ω which are called characteristic or eigenvalues. The corresponding u_j are the eigenvectors.

Eigenvalue problems were encountered in the solution for principal stresses in Chapter 2. Within the context of our general treatment, we may proceed with a general proof of the orthogonality condition, which is an important component to this analysis.

9.3.2 Orthogonality Conditions

We seek to derive certain conditions on the solutions of Eqs. (9.39). We select two such solutions, say $u_j^{(1)}$ and $u_j^{(2)}$ and first specialize the equation for $u_j^{(1)}$:

$$u_{j,ii}^{(1)} + \frac{1}{1-2\nu} u_{i,ij}^{(1)} + \frac{\rho}{G}\omega_1^2 u_j^{(1)} = 0 \tag{9.40}$$

or in terms of the stresses, as given by Eq. (9.38),

$$\sigma_{ij,i}^{(1)} + \rho\omega_1^2 u_j^{(1)} = 0. \tag{9.41}$$

We multiply Eq. (9.41) by $u_j^{(2)}$ and integrate over the volume to get

$$\int_V u_j^{(2)}\sigma_{ij,i}^{(1)}\, dV = -\rho\omega_1^2 \int_V u_j^{(2)} u_j^{(1)}\, dV. \tag{9.42}$$

Next, we expand the l.h.s. using integration by parts [9.4] as

$$\int_V u_j^{(2)}\sigma_{ij,i}^{(1)}\, dV = \int_A u_j^{(2)}\sigma_{ij}^{(1)} n_i\, dA - \int_V u_{j,i}^{(2)}\sigma_{ij}^{(1)}\, dV. \tag{9.43}$$

The first term on the r.h.s. of Eq. (9.43) is written in terms of the traction T_j as

$$\int_A u_{ij}^{(2)}\sigma_{ij}^{(1)} n_i\, dA = \int_A u_j^{(2)} T_j^{(1)}\, dA \tag{9.44}$$

using Eq. (2.11). The second term may be manipulated into a form that is symmetric in (1) and (2) by first rearranging the integrand as

$$u_{j,i}^{(2)}\sigma_{ij}^{(1)} = \tfrac{1}{2}\sigma_{ij}^{(1)}(u_{i,j}^{(2)} + u_{j,i}^{(2)}) \tag{9.45}$$

recognizing the summation convention.

Continuing,

$$\tfrac{1}{2}\sigma_{ij}^{(1)}(u_{i,j}^{(2)} + u_{j,i}^{(2)}) = \varepsilon_{ij}^{(2)}\sigma_{ij}^{(1)} \tag{9.46a}$$

We use the constitutive law, Eq. (4.30) to replace $\varepsilon_{ij}^{(2)}$ and produce

$$\begin{aligned}\varepsilon_{ij}^{(2)}\sigma_{ij}^{(1)} &= \frac{1}{E}[(1+\nu)\sigma_{ij}^{(2)}\sigma_{ij}^{(1)} - \nu\delta_{ij}\sigma_{kk}^{(2)}\sigma_{ij}^{(1)}] \\ &= \frac{1}{E}[(1+\nu)\sigma_{ij}^{(2)}\sigma_{ij}^{(1)} - \nu\sigma_{kk}^{(2)}\sigma_{jj}^{(1)}]\end{aligned} \tag{9.46b}$$

Obviously, Eq. (9.46b) is symmetric.

Finally using Eqs. (9.44) and (9.46), Eq. (9.42) becomes

$$\int_A u_j^{(2)} T_j^{(1)}\, dA - \int_V \frac{1}{E}[(1+\nu)\sigma_{ij}^{(1)}\sigma_{ij}^{(2)} - \nu\sigma_{kk}^{(2)}\sigma_{jj}^{(1)}]\, dV = -\rho\omega_1^2 \int_V u_j^{(2)} u_j^{(1)}\, dV \tag{9.47}$$

If the calculations on Eq. (9.39) are repeated for $u_j^{(2)}$, the resulting equation will be identical to Eq. (9.47) with the indices 1 and 2 interchanged. Then subtracting the two equations, we find

$$\int_A (u_j^{(2)}T_j^{(1)} - u_j^{(1)}T_j^{(2)})\,dA = -\rho(\omega_1^2 - \omega_2^2)\int_V u_j^{(2)}u_j^{(1)}\,dV \tag{9.48}$$

recognizing the symmetry. We refer to Betti's Law, in integral form [9.5], which is to be discussed in Sect. 10.5.4, to set the l.h.s. = 0, whereupon

$$-\rho(\omega_1^2 - \omega_2^2)\int_V u_j^{(2)}u_j^{(1)}\,dV = 0 \tag{9.49}$$

Since ω_1 and ω_2 are presumed to be different,

$$\int_V u_j^{(2)}u_j^{(1)}\,dV = 0 \tag{9.50}$$

is the statement of orthogonality.

9.3.3 Rayleigh's Quotient

It is often useful to rewrite Eq. (9.39) in a form in which ω^2 is expressed explicitly. Taking the first two terms in operator form

$$u_{j,ii} + \frac{1}{1-2\nu}u_{i,ij} = L_j(u_j), \tag{9.51}$$

we have

$$L_j(u_j) = -\frac{\rho}{G}\omega^2 u_j. \tag{9.52}$$

We multiply by u_j and integrate to get

$$\omega^2 = -\frac{G}{\rho}\frac{\displaystyle\int_V u_j L_j(u_j)\,dV}{\displaystyle\int_V u_j u_j\,dV}, \tag{9.53}$$

which is called Rayleigh's quotient [9.3].

This form allows the mode shapes to be approximated in the manner of the Rayleigh-Ritz method, Section 10.7.2. So long as the assumed functions satisfy the boundary conditions, good approximations for the eigenvalues, which are the natural frequencies of the system, may be obtained.

9.3.4 Axial Vibration of a Bar

As an elementary example, we consider a slender bar of length H which is oriented along the x-axis in Fig. 9.1 and which vibrates in an axial mode as discussed in Sec. 9.2.2.

In accordance with the elementary theory, we neglect the transverse displacements u_y and u_z. Then Eq. (9.37) becomes

$$(\lambda + 2\mu)u_{x,xx} + \rho\omega^2 u_x = 0 \tag{9.54}$$

in the manner of Eq. (9.4). Equation (9.54) is written compactly as

$$u_{x,xx} - \frac{\omega^2}{c_P^2} u_x = 0 \tag{9.55}$$

following Eq. (9.5). Also, the assumption of one-dimensional motion implies that Poisson's ratio $\nu = 0$ so that

$$c_P = c_{P1} = \sqrt{\frac{E}{\rho}}. \tag{9.56}$$

The spatial solution is taken as

$$u_x(x) = A \sin \frac{\omega}{c_{P1}} x + B \cos \frac{\omega}{c_{P1}} x. \tag{9.57}$$

Now the boundary conditions on the bar must be considered to evaluate ω. For a bar that is free to displace at both ends, the displacement oscillates between $+\bar{u}_x$ and $-\bar{u}_x$ at each end. Since the stress-free condition implies that the axial strain is zero, $u_{x,x} = 0$. Thus, we have

$$u_{x,x}(0, t) = u_{x,x}(H, t) = 0. \tag{9.58}$$

From Eq. (9.57),

$$u_{x,x} = \frac{\omega}{c_{P1}} \left[A \cos \frac{\omega}{c_{P1}} x - B \sin \frac{\omega}{c_{P1}} x \right] \tag{9.59}$$

so that, for a nontrivial solution, we have $A = 0$ and $B \neq 0$ if

$$\sin \frac{\omega}{c_{P1}} H = 0. \tag{9.60}$$

Equation (9.60) is a transcendental equation which is typical of eigenvalue problems. It is satisfied when

$$\frac{\omega}{c_{P1}} H = n\pi \qquad \text{(a)} \quad (9.61)$$

or

$$\omega = \frac{n\pi}{H} c_{P1}$$

$$= \frac{n\pi}{H} \sqrt{\frac{E}{\rho}}. \qquad \text{(b)} \quad (9.61)$$

This result is identical to that obtained from the specialized formulation for a one-dimensional bar [9.5].

The complete solution is found by substituting ω into Eqs. (9.57) and (9.35) and then recombining these equations into Eq. (9.31). Thus,

$$u_x(x) = B\cos\frac{n\pi}{H}x \tag{9.62}$$

$$f(t) = C\cos\omega t + D\sin\omega t \tag{9.63}$$

and

$$u_{xn} = \cos\frac{n\pi}{H}x(C_n\cos\omega_n t + D_n\sin\omega_n t). \tag{9.64}$$

In the last equation, the constants have been combined and the solution specified for a harmonic n.

Free vibration and the propagation of elastic waves discussed in the preceding sections may be initiated by a specified displacement or velocity distribution at $t = 0$. This distribution may be in the form of a single harmonic, i.e., proportional to $\cos\frac{n\pi}{H}x$ or $\sin\frac{n\pi}{H}x$, or may be a more general pattern requiring several terms of the form of Eq. (9.64) to describe. Thus, the complete solution is

$$u_x = \sum_{n=1,2,}^{\infty} \cos\frac{n\pi}{H}x(C_n\cos\omega_n t + D_n\sin\omega_n t). \tag{9.65}$$

Correspondingly, the initial conditions are specified in terms of a similar Fourier series and the constants C_n and D_n are evaluated harmonic by harmonic, using the orthogonality property discussed in Sec. 9.3.2.

Additional details on the vibration of prismatic bars with various boundary conditions are presented in Jacobsen and Ayre [9.5].

9.4 Uniform Rotation of a Beam

9.4.1 Equilibrium Equations

We consider a beam with an arbitrary cross section, as shown Fig. 9.5, which rotates about the x-axis with a constant angular velocity Ω. The cross-sectional x and y are chosen to be principal axes in order to preclude torsion due to asymmetric body forces. The beam is subjected to extension along the z-axis and bending in the y-z plane and is essentially a combination of the problems discussed in Sections 6.2 and 6.3.

This model represents an idealized turbine blade, which is of great practical interest. The self-weight of the member is neglected, as well as the time-

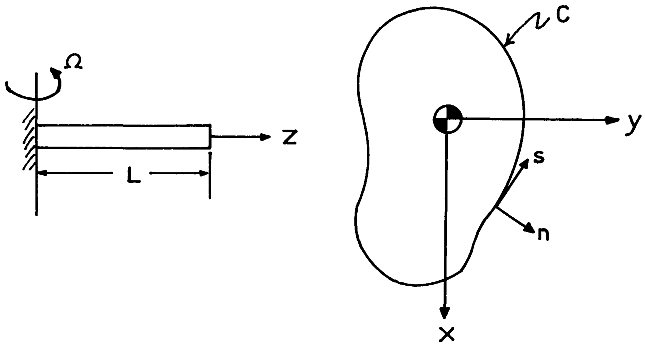

Fig. 9.5. Cross section of rotating beam.

dependent effects in the transient phase while the blade is brought up to speed. Essentially, each point in the member is subjected to a centrifugal acceleration $R\Omega^2\mathbf{e}_z$ where $R(y,z)$ is the projection of the position vector emanating from the origin onto the y-z plane. The components of the inertial force are

$$f_y = \rho R\Omega^2(y/R) = \rho\Omega^2 y \quad \text{(a)}$$

and (9.66)

$$f_z = \rho R\Omega^2(z/R) = \rho\Omega^2 z \quad \text{(b)}$$

respectively and Eqs (2.46) for (x, y, z) become

$$\sigma_{xx,x} + \sigma_{yx,y} + \sigma_{zx,z} = 0 \quad \text{(a)}$$

$$\sigma_{xy,x} + \sigma_{yy,y} + \sigma_{zx,z} + \rho\Omega^2 y = 0 \quad \text{(b)} \quad (9.67)$$

$$\sigma_{xz,x} + \sigma_{yz,y} + \sigma_{zz,z} + \rho\Omega^2 z = 0. \quad \text{(c)}$$

9.4.2 Boundary Conditions

All lateral boundaries and the end $z = L$ are presumed to be traction-free. For the lateral boundaries, we write the components of the traction from Eq. (2.44) as

$$T_x = \sigma_{xx}n_x + \sigma_{yx}n_y = 0 \quad \text{(a)}$$

$$T_y = \sigma_{xy}n_x + \sigma_{yy}n_y = 0 \quad \text{(b)} \quad (9.68)$$

$$T_z = \sigma_{xz}n_x + \sigma_{yz}n_y = 0. \quad \text{(c)}$$

For the end $z = L$,

$$\sigma_{zx} = \sigma_{zy} = \sigma_{zz} = 0. \quad (9.69)$$

9.4.3 Semi-Inverse Solution

Employing the semi-inverse method of St. Venant, which has been discussed in Section 5.7 and used extensively in Chapter 6, Stephen and Wang [9.6] stated the following assumptions:

(a) Shearing stresses and strains in the z direction are zero:

$$\sigma_{xz} = \sigma_{yz} = \varepsilon_{xz} = \varepsilon_{yz} = 0. \tag{9.70}$$

(b) Planar stresses and strains are independent of z:

$$\sigma_{xx}, \sigma_{xy}, \sigma_{yy} \quad \text{and} \quad \varepsilon_{xy} \neq f(z). \tag{9.71}$$

(c) Longitudinal strain taken in the form

$$\varepsilon_{zz} = \varepsilon_0 + \frac{1}{2}\frac{\rho}{E}\Omega^2(L^2 - z^2) - \kappa_0 x - \kappa_0' y + \varepsilon_1(x^2 + y^2) \tag{9.72}$$

where ε_0, ε_1, κ_0 and κ_0' are constants to be determined. In Eq. (9.72) the first two terms are similar to those found in the solution for the extension problem in Section 6.2, Eq. (6.5c), but one degree higher since the loading here is linear in z rather than constant. Similarly, the last term represents the distortion of the cross section into a paraboloid of revolution as described by Eq. (6.19c). The third and fourth terms are associated with bending since they are linear in the cross-sectional coordinates.

With these assumptions, the equilibrium equations (9.67) reduce to

$$\begin{aligned} \sigma_{xx,x} + \sigma_{yx,y} &= 0 && \text{(a)} \\ \sigma_{xy,x} + \sigma_{yy,y} + \rho\Omega^2 y &= 0 && \text{(b)} \\ \sigma_{zz,z} + \rho\Omega^2 z &= 0 && \text{(c)} \end{aligned} \tag{9.73}$$

and the St. Venant compatibility equations, Eqs. (3.59), for (x, y, z) become

$$\begin{aligned} \varepsilon_{xx,yy} + \varepsilon_{yy,xx} &= 2\varepsilon_{xy,xy} && \text{(a)} \\ \varepsilon_{yy,zz} + \varepsilon_{zz,yy} &= 0 && \text{(b)} \\ \varepsilon_{zz,xx} + \varepsilon_{xx,zz} &= 0 && \text{(c)} \\ \varepsilon_{xx,yz} &= 0 && \text{(d)} \\ \varepsilon_{yy,xz} &= 0 && \text{(e)} \\ \varepsilon_{zz,xy} &= 0. && \text{(f)} \end{aligned} \tag{9.74}$$

Note that Eq. (9.72) satisfies Eq. (9.74f).

A stress function $\phi(x, y)$ such that

$$\begin{aligned} \sigma_{xx} &= \phi_{,yy} && \text{(a)} \\ \sigma_{xy} &= -\phi_{,xy} && \text{(b)} \\ \sigma_{yy} &= \phi_{,xx} - \tfrac{1}{2}\rho\Omega^2 y^2 && \text{(c)} \end{aligned} \tag{9.75}$$

satisfies the equilibrium equations Eq. (9.73a,b).

We now consider Hooke's law specialized from the first three of Eqs. (4.29b):

$$\begin{aligned} \varepsilon_{xx} &= (1/E)\sigma_{xx} - (\nu/E)(\sigma_{yy} + \sigma_{zz}) && \text{(a)} \\ \varepsilon_{yy} &= (1/E)\sigma_{yy} - (\nu/E)(\sigma_{xx} + \sigma_{zz}) && \text{(b)} \\ \varepsilon_{zz} &= (1/E)\sigma_{zz} - (\nu/E)(\sigma_{xx} + \sigma_{yy}). && \text{(c)} \end{aligned} \tag{9.76}$$

The first two equations are differentiated with respect to z, recalling Eqs. (9.71), to produce

$$\varepsilon_{xx,zz} = \varepsilon_{yy,zz} = -(\nu/E)\sigma_{zz,zz} = (\nu/E)\rho\Omega^2. \tag{9.77}$$

The last equality is stated after considering Eq. (9.73c). Returning to compatibility equations Eqs. (9.74b,c) gives

$$\varepsilon_{zz,yy} = \varepsilon_{zz,xx} = -(\nu/E)\rho\Omega^2 \tag{9.78a}$$

from which we may assign the value

$$\varepsilon_1 = -\tfrac{1}{2}(\nu/E)\rho\Omega^2 \tag{9.78b}$$

to the constant in Eq. (9.72), since it is the only term which multiplies quadratic functions of x and y.

The remaining extensional stress-strain equation Eq. (9.76c) is now solved for σ_{zz} in terms of the remaining unknown constants in Eq. (9.72):

$$\begin{aligned} \sigma_{zz} = {} & E\varepsilon_0 + \tfrac{1}{2}\rho\Omega^2(L^2 - z^2) - E\kappa_0 x - E\kappa_0' y \\ & -\tfrac{1}{2}\nu\rho\Omega^2(x^2 + y^2) + \nu(\sigma_{xx} + \sigma_{yy}). \end{aligned} \tag{9.79}$$

At this point the evaluation of these constants requires consideration of the resultant force and bending moment on the cross section.

We first form the resultant axial force on the cross section as

$$\begin{aligned} T(z) &= \int_A \sigma_{zz}\,dx\,dy \\ &= EA\varepsilon_0 + \tfrac{1}{2}\rho\Omega^2 A(L^2 - z^2) - \tfrac{1}{2}\nu\rho\Omega^2(I_x + I_y) \\ &\quad + \nu \int_A (\sigma_{xx} + \sigma_{yy})\,dx\,dy \end{aligned} \tag{9.80}$$

where

A = area of cross section,

$$I_x = \int_A y^2\,dx\,dy \qquad \text{(a)}$$

and (9.81)

$$I_y = \int_A x^2\,dx\,dy \qquad \text{(b)}$$

are the principal moments of inertia. Note that the first moment terms in Eq. (9.79) do not contribute to the integral.

Next, we focus on the last term of $T(z)$ and recall the useful relationship between contour and area integrals known as Green's theorem. From Eq. (1.13),

$$\oint_C (P\,dx + Q\,dy) = \int_A (Q_{,x} - P_{,y})\,dx\,dy \tag{9.82}$$

where $P(x, y)$ and $Q(x, y)$ are C^1 continuous functions.

Now we express

$$\int_A (\sigma_{xx} + \sigma_{yy})\,dx\,dy = I_1 + I_2 \tag{9.83}$$

where

$$I_1 = \int_A \{(x\sigma_{xx} + y\sigma_{xy})_{,x} + (x\sigma_{yx} + y\sigma_{yy})_{,y}\}\,dx\,dy \qquad \text{(a)} \quad (9.84)$$

and

$$I_2 = -\int_A \{x(\sigma_{xx,x} + \sigma_{xy,y}) + y(\sigma_{yx,x} + \sigma_{yy,y})\}\,dx\,dy. \qquad \text{(b)} \quad (9.84)$$

The separation of the integral into two parts may be easily verified by expanding the derivatives. Involking Green's theorem Eq. (9.82) with

$$Q = (x\sigma_{xx} + y\sigma_{xy}) \qquad \text{(a)}$$

and (9.85)

$$P = -(x\sigma_{yx} + y\sigma_{yy}) \qquad \text{(b)}$$

$$I_1 = \oint (-x\sigma_{yx}\,dx - y\sigma_{yy}\,dx + x\sigma_{xx}\,dy + y\sigma_{xy}\,dy)$$

$$= \oint \{x(\sigma_{xx}\,dy - \sigma_{yx}\,dx) + y(\sigma_{xy}\,dy - \sigma_{yy}\,dx)\}. \tag{9.86}$$

Further, we may write the contour integral in terms of the differential contour increment ds by noting the $n - s$ coordinates on the contour in Fig. 9.5 and refering to Eq. (2.18) which gives

$$\frac{dy}{ds} = s_y = \mathbf{e}_y \cdot \mathbf{s} = n_x \qquad \text{(a)} \quad (9.87)$$

and

$$\frac{dx}{ds} = s_x = \mathbf{e}_x \cdot \mathbf{s} = -n_y. \qquad \text{(b)} \quad (9.87)$$

Replacing dy and dx in Eq. (9.86) by the relationships in terms of ds produces

$$I_1 = \oint \{x(\sigma_{xx}n_x + \sigma_{yx}n_y) + y(\sigma_{yx}n_x + \sigma_{yy}n_y)\}\, ds \qquad (9.88)$$

which vanishes by virtue of the lateral bounding conditions, Eq. (9.68a,b). Thus, we have remaining in Eq. (9.83)

$$\begin{aligned} I_2 &= \int_A (\sigma_{xx} + \sigma_{yy})\, dx\, dy \\ &= \int_A \rho\Omega^2 y^2\, dx\, dy \end{aligned} \qquad (9.89)$$

by comparison of Eq. (9.84b) to the equilibrium equations, Eqs. (9.73a,b).

Finally, returning to the original term in Eq. (9.80) and noting Eq. (9.81b),

$$\nu \int_A (\sigma_{xx} + \sigma_{yy})\, dx\, dy = \nu\rho\Omega^2 I_x \qquad (9.90)$$

and the resultant axial force becomes

$$T(z) = EA\varepsilon_0 + \tfrac{1}{2}\rho\Omega^2 A(L^2 - z^2) + \tfrac{1}{2}\nu\rho\Omega^2(I_x - I_y). \qquad (9.91)$$

The stress-free end condition

$$T(L) = 0 \qquad (9.92)$$

requires that

$$\varepsilon_0 = -\frac{1}{2}\frac{\nu\rho\Omega^2}{EA}(I_x - I_y) \qquad (9.93)$$

from which

$$T(z) = \frac{1}{2}\rho\Omega^2 A(L^2 - z^2). \qquad (9.94)$$

The constants κ_0 and κ_0' in Eq. (9.79) remain to be evaluated by considering the bending moments on the cross section

$$\begin{aligned} M_x &= -\int_A \sigma_{zz} y\, dx\, dy \qquad &\text{(a)} \\ M_y &= \int_A \sigma_{zz} x\, dx\, dy, \qquad &\text{(b)} \end{aligned} \qquad (9.95)$$

First, consider M_x

$$M_x(z) = -\int_A \sigma_{zz} y\,dx\,dy$$

$$= -\int_A \{E\varepsilon_0 y + \tfrac{1}{2}\rho\Omega^2(L^2 - x^2)y - E\kappa_0 xy - E\kappa'_0 y^2$$

$$- \tfrac{1}{2}\nu\rho\Omega^2(x^2 + y^2)y + \nu(\sigma_{xx} + \sigma_{yy})y\}\,dx\,dy.$$

The first three terms do not contribute since x and y are principal axes, so

$$M_x(z) = E\kappa'_0 I_x + \tfrac{1}{2}\nu\rho\Omega^2 \int_A (x^2 + y^2)y\,dx\,dy - \nu \int_A (\sigma_{xx} + \sigma_{yy})y\,dx\,dy. \tag{9.96}$$

Again, we have an area integral to be transformed,

$$\int_A (\sigma_{xx} + \sigma_{yy})y\,dx\,dy = I_3 + I_4 \tag{9.97}$$

where

$$I_3 = \int_A \{[\tfrac{1}{2}(y^2 - x^2)\sigma_{yy} + xy\sigma_{yx}]_{,y}$$

$$+ [xy\sigma_{xx} + \tfrac{1}{2}(y^2 - x^2)\sigma_{xy}]_{,x}\}\,dx\,dy \qquad \text{(a)}$$

$$I_4 = -\int_A \{xy(\sigma_{xx,x} + \sigma_{xy,y}) + \tfrac{1}{2}(y^2 - x^2)(\sigma_{yx,x} + \sigma_{yy,y})\}\,dx\,dy, \qquad \text{(b)} \tag{9.98}$$

which is easily verified. Then taking

$$P = -[\tfrac{1}{2}(y^2 - x^2)\sigma_{yy} + xy\sigma_{yx}] \qquad \text{(a)}$$

and (9.99)

$$Q = xy\sigma_{xx} + \tfrac{1}{2}(y^2 - x^2)\sigma_{xy} \qquad \text{(b)}$$

in Eq. (9.82),

$$I_3 = \oint \{-\tfrac{1}{2}(y^2 - x^2)\sigma_{yy}\,dx - xy\sigma_{yx}\,dx + xy\sigma_{xx}\,dy + \tfrac{1}{2}(y^2 - x^2)\sigma_{xy}\,dy\}$$

$$= \oint \{xy(\sigma_{xx}\,dy - \sigma_{yx}\,dx) + \tfrac{1}{2}(y^2 - x^2)(\sigma_{xy}\,dy - \sigma_{yy}\,dx)\}. \tag{9.100}$$

The terms in parentheses are identical to those in Eq. (9.86), so that $I_3 = 0$ and

$$I_4 = \int_A (\sigma_{xx} + \sigma_{yy}) y \, dx \, dy$$

$$= \frac{1}{2} \rho \Omega^2 \int_A (y^2 - x^2) y \, dx \, dy \tag{9.101}$$

from Eqs. (9.98b) and (9.73a,b). Continuing from Eq. (9.96) after including Eq. (9.101) multiplied by $-\nu$,

$$M_x(z) = EI_x \kappa_0' + \nu \rho \Omega^2 \int_A x^2 y \, dx \, dy. \tag{9.102}$$

Similarly, we may compute

$$M_y(z) = -EI_y \kappa_0 + \tfrac{1}{2} \nu \rho \Omega^2 \int_A (y^2 - x^2) x \, dx \, dy. \tag{9.103}$$

These expressions are independent of z and are required to vanish at $z = 0$; hence,

$$\kappa_0 = \frac{1}{2} \frac{\nu \rho}{EI_y} \Omega^2 \int_A (y^2 - x^2) x \, dx \, dy \tag{9.104}$$

and

$$\kappa_0' = -\frac{\nu \rho}{EI_x} \Omega^2 \int_A x^2 y \, dx \, dy. \tag{9.105}$$

This completes the general solutions for σ_{zz}, Eq. (9.79), in terms of ε_0, κ_0, κ_0' and ϕ which are functions of the cross-sectional geometry. It is also useful to have expressions for the direct strains as defined in Eq. (9.76), incorporating ε_0 from Eq. (9.93), and κ_0 and κ_0' from Eqs. (9.104) and (9.105) into the equation for σ_{zz}. The results are given by Stephen and Wang [9.6] and are used along with the shear stain ε_{xy}, which may be obtained from Eq. (4.29b), to derive a two-dimensional approximation.

9.4.4 Two-Dimensional Problem

A solution independent of the axial coordinate z is sought by considering the first of the compatibility equations, Eq. (9.74a), in the form

$$\varepsilon_{xx,yy} + \varepsilon_{yy,xx} - 2\varepsilon_{xy,xy} = 0. \tag{9.106}$$

The resulting equation is found from Eqs. (9.76) and (9.75) as

$$\nabla^4 \phi = -\nu \left(\frac{1 + 3\nu}{1 - \nu^2} \right) \rho \Omega^2. \tag{9.107}$$

The remainder of the compatibility equations (9.74) are satisfied identically.

The applicable boundary conditions, Eqs. (9.68a,b), may be written in terms of ϕ and the differential along the contour, ds, by using Eqs. (9.75) for the stress and Eqs. (9.87) for the components of the normal to the contour. The relationships are

$$\begin{aligned} T_x &= \phi_{,yy}\frac{dy}{ds} + \phi_{,xy}\frac{dx}{ds} \\ &= \frac{d}{dy}(\phi_{,y})\frac{dy}{ds} + \frac{d}{dx}(\phi_{,y})\frac{dx}{ds} \\ &= \frac{d}{ds}(\phi_{,y}) \\ &= 0 \end{aligned} \qquad \text{(a)} \quad (9.108)$$

and

$$\begin{aligned} T_y &= -\phi_{,xy}\frac{dy}{ds} - [\phi_{,xx} - \tfrac{1}{2}\rho\Omega^2 y^2]\frac{dx}{ds} \\ &= \frac{d}{ds}(\phi_{,x}) + \tfrac{1}{2}\rho\Omega^2 y^2\frac{dx}{ds} \\ &= 0. \end{aligned} \qquad \text{(b)} \quad (9.108)$$

9.4.5 Circular Cross Section

Stephen and Wang [9.6] give a solution for the stress function for a member with a circular cross section, Fig. 7.1, with the contour equation

$$x^2 + y^2 - r^2 = 0 \qquad (9.109)$$

in the form

$$\begin{aligned} \phi(x, y) = &-\left(\frac{\nu + 3\nu^2}{1 - \nu^2}\right)\frac{\rho\Omega^2}{64}(x^2 + y^2 - r^2)^2 \\ &+ \frac{\rho\Omega^2}{64}(y^4 - \tfrac{5}{3}x^4 + 2x^2y^2 + 14r^2x^2 - 2r^2y^2). \end{aligned} \qquad (9.110)$$

As in previous examples, the equation of the contour is included in the stress function. This function is easily shown to satisfy Eq. (9.107) by differentiation and substitution. Also, it must satisfy Eqs. (9.108). In order to compute the derivatives along the boundary when $\phi = \phi(x, y)$, the chain rule

$$\frac{d(\ )}{ds} = (\ )_{,x}\frac{dx}{ds} + (\ )_{,y}\frac{dy}{ds} \qquad (9.111)$$

is required. For a circular contour,

$$\frac{dx}{ds} = \frac{dx}{d\theta}\frac{d\theta}{ds}; \qquad \frac{dy}{ds} = \frac{dy}{d\theta}\frac{d\theta}{ds}. \tag{9.112}$$

With $x = r\cos\theta$ and $y = r\sin\theta$, Eqs. (7.20a,b), and noting from Fig. 7.1 that $ds = r\,d\theta$

$$\frac{d\theta}{ds} = \frac{1}{r}; \qquad \frac{dx}{ds} = -\sin\theta = \frac{-y}{r}; \qquad \frac{dy}{ds} = \cos\theta = \frac{x}{r} \tag{9.113}$$

so that the differentiation formula, Eq. (9.111), becomes

$$\frac{d(\theta)}{ds} = -(\ )_{,x}\frac{y}{r} + (\ )_{,y}\frac{x}{r}. \tag{9.114}$$

This may be directly applied to Eq. (9.110) to check Eqs. (9.108). To illustrate, consider Eq. (9.108a), and form

$$\begin{aligned}\phi_{,y} = &-\left(\frac{\nu + 3\nu^2}{1-\nu^2}\right)\frac{\rho\Omega^2}{64}4y(x^2 + y^2 - r^2)\\ &+ \frac{\rho\Omega^2}{64}(4y^3 + 4x^2y - 4r^2y)\end{aligned} \tag{9.115}$$

$$\begin{aligned}\frac{d}{ds}(\phi_{,y}) &= -(\phi_{,y})_{,x}\frac{y}{r} + (\phi_{,y})_{,y}\frac{x}{r}\\ &= \left(\frac{\nu + 3\nu^2}{1-\nu^2}\right)\frac{\rho\Omega^2}{16}(2xy)\frac{y}{r} - \frac{\rho\Omega^2}{64}(8xy)\frac{y}{r} \qquad \text{(a)}\\ + (\phi_{,y})_{,y}\frac{x}{r} &= -\left(\frac{\nu + 3\nu^2}{1-\nu^2}\right)\frac{\rho\Omega^2}{16}(x^2 + 3y^2 - r^2)\frac{x}{r}\\ &\quad + \frac{\rho\Omega^2}{64}4(3y^2 + x^2 - r^2)\frac{x}{r}. \qquad \text{(b)}\end{aligned} \tag{9.116}$$

The first set of variable terms becomes

$$x(2y^2 - x^2 - 3y^2 + r^2) \to 0 \quad \text{on } C. \tag{9.117}$$

while the second set is

$$x(-8y^2 + 12y^2 + 4x^2 - 4r^2) \to 0 \quad \text{on } C \tag{9.118}$$

so that Eq. (9.108a) is satisfied. The stresses σ_{xx}, σ_{yy} and σ_{xy} are evaluated from Eqs. (9.75) as

$$\begin{aligned}\sigma_{xx} &= \frac{\rho\Omega^2}{64}\left[12y^2 + 4x^2 - 4r^2 - 4\left(\frac{\nu + 3\nu^2}{1-\nu^2}\right)(x^2 + 3y^2 - r^2)\right] \qquad \text{(a)}\\ \sigma_{yy} &= \frac{\rho\Omega^2}{64}[12x^2 + 4y^2 - 4r^2]\left[1 - \left(\frac{\nu + 3\nu^2}{1-\nu^2}\right)\right]\end{aligned} \tag{9.119}$$

$$+\frac{1}{2}\rho\Omega^2(r^2 - x^2 - y^2) \tag{b}$$

$$\sigma_{xy} = -\frac{(1 - \nu - 4\nu^2)}{8(1 - \nu^2)}\rho\Omega^2 xy. \tag{c}$$

To compute σ_{zz}, we must first consider the geometric constants ε_0, κ_0 and κ'_0. For the circular cross section, $I_x = I_y$ so that $\varepsilon_0 = 0$, Eq. (9.93). Likewise, the functions κ_0 and κ'_0, when evaluated with x and y from Eq. (9.113), vanish for this cross section. Therefore, from Eq. (9.79)

$$\sigma_{zz} = \tfrac{1}{2}\rho\Omega^2[L^2 - z^2 - \nu(x^2 + y^2)] + \nu(\sigma_{xx} + \sigma_{yy}). \tag{9.120}$$

Exercises

9.1 Perform the calculations in Sec. 9.3.2 using $u_j^{(2)}$ in place of $u_j^{(1)}$.

9.2 Assume that the motion of the free-free bar solved in Sec. 9.3.4 is initiated by equal and opposite static forces of magnitude P at each end which are released at $t = 0$. The area and Young's modulus are given by A and E, respectively. Find u_x.

9.3 For the bar solved in Problem 9.2, evaluate the stress.

9.4 Consider the vibration of an elastic bar as solved in Sec. 9.3.4 but with one end fixed and the other free. Determine u_x.

9.5 Repeat Problem 9.2 for the boundary conditions of Problem 9.4.

9.6 Repeat Problem 9.3 for the boundary conditions of Problem 9.4.

9.7 In Ref. [9.6] a solution for the uniform rotation of a shaft with an elliptical cross section with the equation

$$\frac{x^2}{D^2} + \frac{y^2}{B^2} - 1 = 0$$

is given. The cross section is shown in Fig 6.7(a). The stress function is

$$\phi(x, y) = \frac{\Lambda}{8}D^2B^2\left(\frac{x^2}{D^2} + \frac{y^2}{B^2} - 1\right)^2 - \frac{\rho\Omega}{24}\left(\frac{B}{D}\right)^2 x^4 + \frac{\rho\Omega}{4}D^2x^2$$

where

$$\Lambda = \rho\Omega^2\left[\left(\frac{B}{D}\right)^2 - \left(\frac{\nu + 3\nu^2}{1 - \nu^2}\right)\frac{D^2B^2}{3D^4 + 2D^2B^2 + 3B^4}\right].$$

Verify that

(a) ϕ satisfies Eqs. (9.107) and (9.108).

(b) κ_0 and κ'_0 are zero.

(c) And compute the stresses.

References

[9.1] Filonenko–Borodich, M., *Theory of Elasticity* (Dover Publications, Inc., New York, 1965).

[9.2] Bolt, B. A., *Earthquake Engineering*, Ed. R. L. Weigel (Prentice–Hall, Englewood Cliffs, N.J. 1970).

[9.3] Pearson, C. E., *Theoretical Elasticity* (Harvard University Press, Cambridge, Mass., 1959).

[9.4] Pierce, B. C., and Foster, R. M., "A Short Table of Integrals," fourth edition, Ginn and Company, Boston, 1956, p. 117.

[9.5] Jacobsen, L. S., and Ayre, R. S., *Engineering Vibrations* (McGraw–Hill Book Co., New York, 1958).

[9.6] Stephen, N. G., and Wang, P. J., "Stretching and Bending of Rotating Beam," *Journal of Applied Mechanics*, ASME, Vol. 53, December, 1986, pp. 869–872.

CHAPTER 10

Energy Principles

10.1 Introduction

The theory of elasticity may be developed from energy considerations, leading to the field equations in the form of differential equations. This approach does not promise any computational advantage from the standpoint of *analytical* solutions, since the same equations found from the classical formulations are produced. However, for the pursuit of *numerical* solutions, energy methods are extensively developed and are the basis of powerful contemporary programs for solving complex problems in solid mechanics. This development is rather recent and was brought about by the use of the digital computer. This probably explains the relatively few applications of energy methods to *elasticity* problems found in the classical texts. However, even in the 18th century, the mathematician Leonhard Euler contrasted the direct formulation of the governing differential equations, known then as the method of *effective causes*, with the energy approach, known then as the method of *final causes*, in an argument that skillfully blended science and theology (this may have been diplomatic considering the well-known plight of perhaps the first "elastician," Galileo, a century earlier). Euler wrote [10.1]

> "Since the fabric of the universe is most perfect, and is the work of a most wise Creator, nothing whatsoever takes place in the universe in which some relation of maximum and minimum does not appear. Wherefore there is absolutely no doubt that every effect in the universe can be explained as satisfactorily from final causes, by the aid of the method of maxima and minima, as it can from the effective causes themselves..."

In this chapter, we derive the theoretical underpinnings for energy-based numerical methods, but we do not discuss actual solution techniques since that is a vast field in itself.

10.2 Conservation of Energy

Energy methods are developed from the law of conservation of energy. Assuming that a set of loads is applied slowly and that we have an adiabatic deformation process,

$$W_E = W_V, \tag{10.1}$$

where W_E is the work done by the external loading and W_V is the change in internal energy. With an elastic material, the work W_E will be recovered if the loads are removed, so that W_V may be regarded as stored energy, called *strain energy*. We previously introduced this concept in Section 4.3 and will develop it further in the next section.

10.3 Strain Energy

10.3.1 Strain Energy Density

We represent the strain energy in the form

$$W_V = \int_V W\,dV, \tag{10.2}$$

where the general form of the *strain energy density* W has been stated in Eq. (4.8). For the case of isotropic materials, we consider Eqs. (4.2a) to write

$$W = \int_{\varepsilon_{ij}} \sigma_{ij}\, d\varepsilon_{ij}.$$

For the linear elastic case,

$$\begin{aligned} W &= \int_{\varepsilon_{ij}} (2\mu\varepsilon_{ij} + \lambda\delta_{ij}\varepsilon_{kk})\, d\varepsilon_{ij} \\ &= \mu\varepsilon_{ij}\varepsilon_{ij} + \frac{\lambda}{2}(\varepsilon_{kk})^2, \end{aligned} \tag{10.3}$$

using Eq. (4.18).

It is also convenient to define a dual quantity to W, following Eq. (4.2a),

$$\begin{aligned} \varepsilon_{(ii)} &= \frac{\partial W^*}{\partial \sigma_{(ii)}} \\ \varepsilon_{ij} &= \frac{1}{2}\frac{\partial W^*}{\partial \sigma_{ij}} \qquad i \neq j \end{aligned} \tag{10.4}$$

where W^* is called the *complementary* strain energy density. Following Eq. (10.3), we have

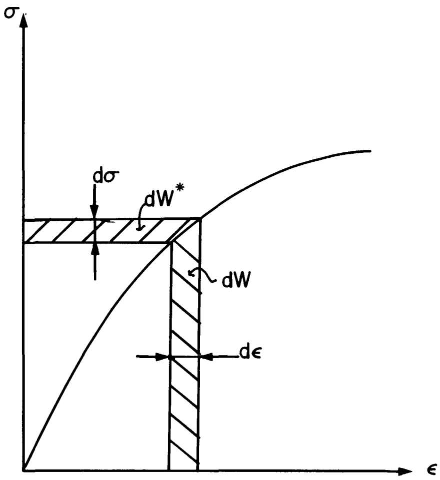

Fig. 10.1. Stress-strain curve for nonlinear elastic material.

$$W^* = \int_{\sigma_{ij}} \varepsilon_{ij}\, d\sigma_{ij}. \tag{10.5}$$

For the linear elastic case, Eq. (4.19) gives

$$W^* = \frac{1}{4\mu}\sigma_{ij}\sigma_{ij} - \frac{\lambda}{4\mu(2\mu + 3\lambda)}(\sigma_{kk})^2 = W \tag{10.6}$$

since the same equation may be obtained from Eq. (10.3) using Eq. (4.19).

It is of interest to graphically interpret the strain energy and complementary strain energy densities for a one-dimensional elastic, but not necessarily linear, material, as shown in Fig. 10.1. For the *linear* case, the densities W and W^* are obviously equal, while for the nonlinear case they are not.

We may illustrate the evaluation of W for a basic problem in elasticity, the prismatic bar under axial load previously solved in Section 6.2. We first rewrite Eq. (10.6) for the principal stress state ($\sigma_{ij} = 0, i \neq j$)

$$W^* = W = \frac{1}{4\mu}\left[1 - \frac{\lambda}{(2\mu + 3\lambda)}\right](\sigma_{kk})^2 \tag{10.7a}$$

In terms of the engineering constants, introducing Eq. (4.24c) gives

$$W = \frac{1}{2E}(\sigma_{kk})^2. \tag{10.7b}$$

When σ_{zz} is the only nonzero stress, Eq. (10.7b) reduces to

$$W = \frac{1}{2E}(\sigma_{zz})^2 \tag{10.7c}$$

and for the bar with $\sigma_{zz} = \gamma z$,

$$W = \frac{\gamma^2}{2E} z^2. \tag{10.7d}$$

Then,

$$W_V = \frac{\gamma^2}{6} \frac{AL^3}{E} \tag{10.8}$$

from Eq. (10.2).

10.3.2 Strain Energy Density of Distortion

We consider the strain energy density in terms of stress, Eq. (10.6), and convert to engineering constants using Eqs. (4.24). The result is

$$W = \frac{1 + \nu}{2E} \sigma_{ij}\sigma_{ij} - \frac{\nu}{2E}(\sigma_{kk})^2. \tag{10.9}$$

Then, we expand the equation for 1, 2, 3 = x, y, z and get

$$\begin{aligned} W = {} & \frac{1 + \nu}{2E}(\sigma_{xx}^2 + \sigma_{yy}^2 + \sigma_{zz}^2 + 2\sigma_{xy}^2 + 2\sigma_{yz}^2 + 2\sigma_{zx}^2) \\ & - \frac{\nu}{2E}(\sigma_{xx}^2 + \sigma_{yy}^2 + \sigma_{zz}^2 + 2\sigma_{xx}\sigma_{yy} + 2\sigma_{yy}\sigma_{zz} + 2\sigma_{xx}\sigma_{zz}) \\ = {} & \frac{1}{2E}[\sigma_{xx}^2 + \sigma_{yy}^2 + \sigma_{zz}^2 - 2\nu(\sigma_{xx}\sigma_{yy} + \sigma_{yy}\sigma_{zz} + \sigma_{xx}\sigma_{zz}) \\ & + 2(1 + \nu)(\sigma_{xy}^2 + \sigma_{yz}^2 + \sigma_{zx}^2)] \end{aligned} \tag{10.10}$$

so that we have separated the normal and shearing contributions.

Equation (10.10) may also be written in terms of the stress invariants, Eqs. (2.59), as

$$W = \frac{1}{2E}[Q_1^2 - 2(1 + \nu)Q_2] \tag{10.11}$$

[10.2], which emphasizes the nondirectionality of energy.

Next, we consider principal stress components

$$\sigma_{xx} = \sigma^{(1)}, \quad \sigma_{yy} = \sigma^{(2)}, \quad \sigma_{zz} = \sigma^{(3)}, \quad \sigma_{xy} = \sigma_{yz} = \sigma_{zx} = 0 \tag{10.12}$$

and rewrite Eq. (10.11) in the form [10.2]

$$\begin{aligned} W = {} & \frac{(1 + \nu)}{6E}\{[\sigma^{(1)} - \sigma^{(2)}]^2 + [\sigma^{(2)} - \sigma^{(3)}]^2 + [\sigma^{(3)} - \sigma^{(1)}]^2\} \\ & + \frac{1 - 2\nu}{6E}[\sigma^{(1)} + \sigma^{(2)} + \sigma^{(3)}]^2, \end{aligned} \tag{10.13}$$

which may be verified by expansion.

The second part of Eq. (10.13) represents the mean stress $\frac{1}{3}[\sigma^{(1)} + \sigma^{(2)} + \sigma^{(3)}]$, which contributes only to volume change, as discussed with respect to the mean strain in Sec. 3.5. Therefore, the first part represents the strain energy density associated with change in shape or *distortion*, and is so defined. Using Eqs. (4.24a, e),

$$W_0 = \frac{1}{12G}\{[\sigma^{(1)} - \sigma^{(2)}]^2 + [\sigma^{(2)} - \sigma^{(3)}]^2 + [\sigma^{(3)} - \sigma^{(1)}]^2\}. \quad (10.14)$$

This quantity is associated with the failure of elastic materials.

The term in brackets is recognized as being proportional to the octahedral shearing stress, Eq. (2.84b), so that the strain energy density of distortion may be written as

$$W_0 = \frac{3}{4G}(\sigma_{ns}^{oct})^2. \quad (10.15)$$

Therefore, the resolution of the strain energy density into the sum of a volume change component and a distortional component corresponds to the state of stress referred to the octahedral planes.

10.4 Work of External Loading

The elastic body is assumed to be loaded by a system of $\bar{Q}$ external forces $\mathbf{F}_Q$, where Q indicates the point of application of the force. It is sufficient for our introductory purposes to assume that the forces are concentrated or *discrete*, as opposed to being distributed. Corresponding to each force is a displacement $\mathbf{u}_Q$. By *correspondence*, we mean that $\mathbf{u}_Q$ is at the same point and in the same direction as $\mathbf{F}_Q$.

The external work produced is then

$$W_E = \sum_{Q=1}^{\bar{Q}} \frac{1}{2}\mathbf{F}_Q \cdot \mathbf{u}_Q \quad (10.16)$$

It turns out that the direct application of the principal of conservation of energy is rather limited so that more useful forms are now sought.

10.5 Principle of Virtual Work

10.5.1 Definitions

Many problems in structural mechanics can be solved by the application of the Principal of Virtual Work, PVW. In this context, the word *virtual* means *not real*, but not necessarily small. As discussed later, the name "work" is somewhat of a misnomer, resulting from the appearance of force-times-distance products having the units of work in the resulting equations.

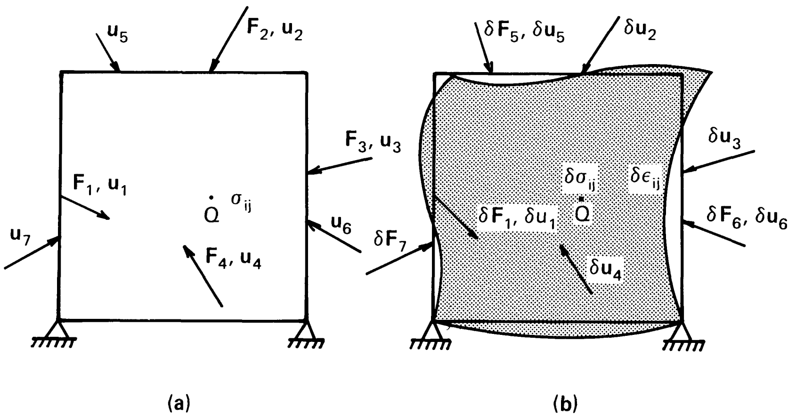

Fig. 10.2. (a) Elastic body in equilibrium under applied forces; (b) elastic body in equilibrium under virtual forces.

We consider a body *in equilibrium* under a set of $\bar{Q}$ applied forces $\mathbf{F}_Q$ as shown in Fig. 10.2(a). At any point Q in the body, the state of stress is given by the components of the stress tensor σ_{ij} that satisfy the equilibrium equations Eq. (2.45). Also indicated are the corresponding displacements $\mathbf{u}_Q$ as well as those at unloaded points that will be of interest later.

Now, the body is subjected to a *second* system of $\bar{Q}$ forces *in equilibrium*, $\delta\mathbf{F}_Q$, as shown in Fig. 10.2(b). This produces a displaced configuration $\delta\mathbf{u}_Q$ that does not violate the prescribed boundary conditions. (This constraint is not strictly necessary, but is sufficient for our purposes.)

Note that the set $\bar{Q}$ includes *all* referenced points in either system. For unloaded points in Fig. 10.2(a), $\mathbf{F}_Q = 0$; and in Fig. 10.2(b), $\delta\mathbf{F}_Q = 0$.

In the *second* system, the stresses, strains and displacement components at Q are $\delta\sigma_{ij}$, $\delta\varepsilon_{ij}$, and δu_i, respectively. The $\delta\mathbf{F}_Q$ are termed *virtual forces*, the $\delta\mathbf{u}_Q$ are called *virtual displacements*, and

$$\delta\varepsilon_{ij} = \frac{1}{2}(\delta u_{i,j} + \delta u_{j,i}) \tag{10.17}$$

are *virtual strains*. Furthermore, the product of *either* $\mathbf{F}_Q \cdot \delta\mathbf{u}_Q$ or $\delta\mathbf{F}_Q \cdot \mathbf{u}_Q$ is known as *external virtual work*. Clearly, the product is *not* conventional work since each component is due to a different source; that is, $\delta\mathbf{u}_Q$ is not due to or caused by $\mathbf{F}_Q$. Since we have stipulated that the virtual forces and virtual distortions, Fig. 10.2(b), are applied *after* the actual or *real* loading system and displacements Fig. 10.2(a), we may envisage virtual work as either the product of a virtual force being "dragged through" a real displacement, or a virtual displacement "acted through" by a real force. The *actual* work performed by the virtual system,

$$\sum_{Q=1}^{\bar{Q}} \frac{1}{2} \delta \mathbf{F}_Q \cdot \delta \mathbf{u}_Q$$

is of no apparent interest here.

10.5.2 Principle of Virtual Displacements

We begin with the virtual work due to virtual displacements $\delta \mathbf{u}_Q$ applied to a system in equilibrium under a set of surface tractions and body forces

$$\delta W_E = \int_A T_i \delta u_i \, dA + \int_V f_i \delta u_i \, dV. \tag{10.18}$$

The surface integral is transformed, using Eq. (2.11) and the divergence theorem in component form, Eq. (2.32), into

$$\begin{aligned} \int_A T_i \delta u_i \, dA &= \int_A \sigma_{ij} n_j \delta u_i \, dA \\ &= \int_V (\sigma_{ij} \delta u_i)_{,j} \, dV. \end{aligned} \tag{10.19}$$

Substituting Eq. (10.19) into Eq. (10.18) gives

$$\begin{aligned} \delta W_E &= \int_V [(\sigma_{ij,j} + f_i) \, \delta u_i + \sigma_{ij} \delta u_{i,j}] \, dV \\ &= \int_V \sigma_{ij} \delta u_{i,j} \, dV, \end{aligned} \tag{10.20}$$

since the first term is the (satisfied) equilibrium equation Eq. (2.45). Next, we introduce Eq. (10.17) into Eq. (10.20), recognizing that both i and j become repeated indices. This produces

$$\delta W_E = \int_V \sigma_{ij} \delta u_{i,j} \, dV = \int_V \sigma_{ij} \delta \varepsilon_{ij} \, dV. \tag{10.21}$$

which may be restated as

$$\delta W_E = \delta W_V \tag{10.22a}$$

where

$$\begin{aligned} \delta W_V &= \int_V \sigma_{ij} \delta \varepsilon_{ij} \, dV \\ &= \textit{internal virtual work}. \end{aligned} \tag{10.22b}$$

This is the *principle of virtual displacements* (PVD) derived for a body in equilibrium that is subjected to virtual displacements produced by a virtual force system also in equilibrium. The important result of this derivation is the converse: If Eq. (10.22a) is satisfied, then the system is in *equilibrium*.

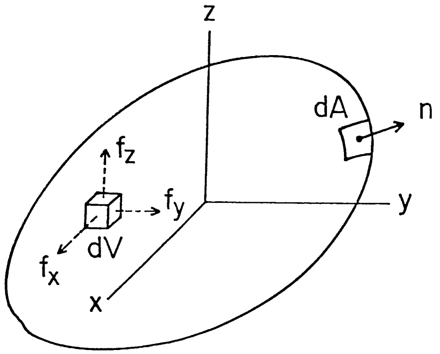

Fig. 10.3. Elastic continuum.

To illustrate an application of the PVD, we attempt to re-derive the equations of equilibrium for an elastic continuum, Fig. 10.3, in terms of displacements. These were previously found in Sec. 5.2 and are given as Eqs. (5.7).

We first treat the internal virtual work. From Eqs. (10.2) and (10.3), the strain energy is

$$W_V = \int_V \left[\mu \varepsilon_{ij} \varepsilon_{ij} + \frac{\lambda}{2} (\varepsilon_{kk})^2 \right] dV. \tag{10.23}$$

Using explicit notation initially, following the presentation of Forray [10.3], and selecting $x_1, x_2, x_3 = x, y, z$, as shown on Fig. 10.3, Eq. (10.23) becomes

$$\begin{aligned} W_V = \int_V \bigg[\left(\frac{\lambda}{2} + \mu \right) & (\varepsilon_{xx}^2 + \varepsilon_{yy}^2 + \varepsilon_{zz}^2) + 2\mu(\varepsilon_{xy}^2 + \varepsilon_{yz}^2 + \varepsilon_{zx}^2) \\ & + \lambda(\varepsilon_{xx}\varepsilon_{yy} + \varepsilon_{yy}\varepsilon_{zz} + \varepsilon_{zz}\varepsilon_{xx}) \bigg] \, dV \end{aligned} \tag{10.24}$$

and the internal virtual work is

$$\begin{aligned} \delta W_V &= \frac{\partial W_V(\varepsilon_{ij})}{\partial \varepsilon_{ij}} \delta \varepsilon_{ij} \\ &= \int_V \bigg[\left(\frac{\lambda}{2} + \mu \right) (2\varepsilon_{xx}\delta\varepsilon_{xx} + 2\varepsilon_{yy}\delta\varepsilon_{yy} + 2\varepsilon_{zz}\delta\varepsilon_{zz}) \\ &\quad + 2\mu(2\varepsilon_{xy}\delta\varepsilon_{xy} + 2\varepsilon_{yz}\delta\varepsilon_{yz} + 2\varepsilon_{zx}\delta\varepsilon_{zx}) \\ &\quad + \lambda(\varepsilon_{xx}\delta\varepsilon_{yy} + \varepsilon_{yy}\delta\varepsilon_{xx} + \varepsilon_{yy}\delta\varepsilon_{zz} \\ &\quad + \varepsilon_{zz}\delta\varepsilon_{yy} + \varepsilon_{zz}\delta\varepsilon_{xx} + \varepsilon_{xx}\delta\varepsilon_{zz}) \bigg] \, dV. \end{aligned} \tag{10.25}$$

The strain-displacement relations are written from Eq. (3.14) as

$$\begin{aligned} \varepsilon_{xx} &= u_{x,x}; \qquad \varepsilon_{yy} = u_{y,y}; \qquad \varepsilon_{zz} = u_{z,z} \\ \varepsilon_{xy} &= \frac{1}{2}(u_{x,y} + u_{y,x}); \qquad \varepsilon_{yz} = \frac{1}{2}(u_{y,z} + u_{z,y}); \qquad \varepsilon_{zx} = \frac{1}{2}(u_{x,z} + u_{z,x}). \end{aligned} \tag{10.26}$$

Now, we apply a virtual displacement consisting of only one component, say δu_x. The corresponding virtual strain-displacement equations are

$$\begin{aligned} \delta\varepsilon_{xx} &= (\delta u_x)_{,x}; \qquad \delta\varepsilon_{yy} = 0; \qquad \delta\varepsilon_{zz} = 0 \\ \delta\varepsilon_{xy} &= \frac{1}{2}(\delta u_x)_{,y}; \qquad \delta\varepsilon_{yz} = 0; \qquad \delta\varepsilon_{zx} = \frac{1}{2}(\delta u_x)_{,z}. \end{aligned} \tag{10.27}$$

Substituting Eqs. (10.26) and (10.27) into Eq. (10.25) yields

$$\begin{aligned} \delta W_V = \int_V \bigg[\left(\frac{\lambda}{2} + \mu\right) 2u_{x,x}(\delta u_x)_{,x} &+ \mu[(u_{x,y} + u_{y,x})(\delta u_x)_{,y} \\ &+ (u_{x,z} + u_{z,x})(\delta u_x)_{,z}] \\ &+ \lambda[(u_{y,y} + u_{z,z})(\delta u_x)_{,x}]\bigg] \, dV. \end{aligned} \tag{10.28}$$

Equation (10.28) may be integrated by parts [10.4] to produce

$$\begin{aligned} \delta W_V = &-\int_V \bigg[\left(\frac{\lambda}{2} + \mu\right) 2u_{x,xx}(\delta u_x) \\ &+ \mu(u_{x,yy} + u_{y,xy} + u_{x,zz} + u_{z,xz})\, \delta u_x + \lambda(u_{y,yx} + u_{z,zx})\, \delta u_x\bigg] \, dV \\ &+ \int_A \bigg[\left(\frac{\lambda}{2} + \mu\right) 2u_{x,n}\, \delta u_x \\ &+ \mu(2u_{x,n} + u_{y,n} + u_{z,n})\, \delta u_x + \lambda(u_{y,n} + u_{z,n})\, \delta u_x\bigg] \, dA \end{aligned} \tag{10.29}$$

where n is directed along the outer normal to the surface, Fig. 10.3. Since the surface terms enter only into the boundary conditions, we concentrate on the first integral and rearrange Eq. (10.29) as

$$\begin{aligned} \delta W_V = &-\int_V [2(\lambda + 2\mu)u_{x,xx} + \mu(u_{x,yy} + u_{y,xy} + u_{x,zz} + u_{z,xz}) \\ &+ \lambda(u_{y,yx} + u_{z,zx})]\, \delta u_x \, dV + [\text{Surface terms}] \\ = &-\int_V [\mu(u_{x,xx} + u_{x,yy} + u_{x,zz}) + (\lambda + \mu)(u_{x,x} + u_{y,y} + u_{z,z})_{,x}]\, \delta u_x \, dV \\ &+ [\text{Surface terms}] \\ = &-\int_V [\mu\nabla^2 u_x + (\lambda + \mu)(\Delta u)_{,x}]\, \delta u_x \, dV + [\text{Surface terms}] \end{aligned} \tag{10.30a}$$

where

$$\nabla^2(\ \ ) = \nabla(\ \ )\cdot\nabla(\ \ ) = (\ \ )_{,ii} \tag{10.30b}$$

$\nabla^2(\ \ )$ is defined in Eq. (1.10b), and

$$\Delta u = \text{div}\, \mathbf{u} = u_{i,i} \tag{10.30c}$$

as defined in Eq. (1.11).

Next, we have the external virtual work, as given by Eq. (10.18) specialized for $u_i = u_x$:

$$\delta W_E = \int_A T_x \delta u_x \, dA + \int_V f_x \delta u_x \, dV$$
$$= \int_V f_x \delta u_x \, dV + [\text{Surface Terms}]. \tag{10.31}$$

We now substitute Eqs. (10.30a) and (10.31) into Eq. (10.21). Since the virtual displacement δu_x is arbitrary, we may equate the coefficients of the volume terms in the integrands to get

$$\mu \nabla^2 u_x + (\lambda + \mu)(\Delta u)_{,x} + f_x = 0 \tag{10.32}$$

which is Eq. (5.7) with $j = x$.

The remaining equations are found by permutation, with a virtual displacement of δu_y and then δu_z.

For completeness, we carry out the same derivation in concise form using indicial notation beginning from Eq. (10.23):

$$\delta W_V = \int_V (2\mu\varepsilon_{ij}\delta\varepsilon_{ij} + \lambda\varepsilon_{kk}\delta\varepsilon_{kk})\, dV \tag{10.33a}$$

where

$$\varepsilon_{ij} = \frac{1}{2}(u_{i,j} + u_{j,i}). \tag{10.33b}$$

With a virtual displacement δu_l,

$$\delta u_l = \delta u_i \delta_{il} = \delta u_j \delta_{jl}$$
$$\delta\varepsilon_{ij} = \frac{1}{2}[(\delta u_i)_{,j}\delta_{il} + (\delta u_j)_{,i}\delta_{jl}]$$
$$= \frac{1}{2}[(\delta u_l)_{,j} + (\delta u_l)_{,i}]. \tag{10.33c}$$

Then, Eq. (10.33a) becomes

$$\delta W_V = \int_V \left[2\mu\left[\frac{1}{2}(u_{i,j} + u_{j,i})\right]\frac{1}{2}[(\delta u_l)_{,j} + (\delta u_l)_{,i}] + \lambda(u_{k,k})(\delta u_l)_{,l}\right] dV$$
$$= \int_V \left[\frac{\mu}{2}[(u_{l,j} + u_{j,l})(\delta u_l)_{,j} + (u_{i,l} + u_{l,i})(\delta u_l)_{,i}] + \lambda(u_{k,k})(\delta u_l)_{,l}\right] dV. \tag{10.33d}$$

Integrating by parts produces typically

$$\int_V u_{i,j}\delta u_{l,j} = u_{i,j}\delta u_l]_{\text{surface}} - \int_V u_{i,jj}\delta u_l \tag{10.33e}$$

so that

$$\delta W_V = -\int_V \left[\frac{\mu}{2}(u_{l,jj} + u_{j,lj} + u_{i,li} + u_{l,ii}) + \lambda(u_{k,k})_{,l}\right] \delta u_l \, dV$$
$$+ \text{[Surface Terms]}$$
$$= -\int_V [\mu(u_l)_{,ii} + (\lambda + \mu)(u_{i,i})_{,l}] \, \delta u_l \, dV$$
$$+ \text{[Surface Terms]} \tag{10.34}$$

with all dummy indices taken as i.

δW_E is given in Eq. (10.31) with $x = l$. Then, setting $\delta W_V = \delta W_E$, equating the volume terms, and changing l to j, we have

$$\mu(u_j)_{,ii} + (\lambda + \mu)(u_{i,i})_{,j} + f_j = 0 \tag{10.35}$$

which is the same as Eq. 5.7. Thus, we see that the PVD is an artifice for establishing *equilibrium* relationships.

We may return to the discrete loading system shown in Fig. 10.1(a) and write

$$\delta W_E = \sum_{Q=1}^{\bar{Q}} \mathbf{F}_Q \cdot \delta \mathbf{u}_Q. \tag{10.36}$$

Of interest in Eq. (10.36), in the context of work, is the absence of the familiar factor of $\frac{1}{2}$ [see Eq. (10.16)]. This is explained by insisting that the real loading *precedes* the virtual distortion, so that the real forces and displacements are at *full* value before the corresponding virtual effects act.

The main use of this form of the PVW is to compute the set of equilibrating forces, one at a time, for a system in which the actual deformations and the corresponding stresses are known. Since the choice of the virtual distortion is open, it is conveniently selected so that the point of application of the single force to be evaluated, say $\mathbf{F}_3$, is given a virtual displacement $\delta \mathbf{u}_3$, while no virtual displacements are permitted at other load points. Equation (10.22a) then reduces to

$$\mathbf{F}_3 \cdot \delta \mathbf{u}_3 = \int_V \sigma_{ij} \delta \varepsilon_{ij} \, dV \tag{10.37}$$

or, for simplicity, choosing $\delta \mathbf{u}_3$ in the direction of $\mathbf{F}_3$,

$$F_3 = \int_V \sigma_{ij} \delta \varepsilon_{ij} \, dV. \tag{10.38}$$

A judicious choice of the virtual deformation allows $\mathbf{F}_3$ to be computed. The procedure may be repeated to calculate the entire set of $\bar{Q}$ loads, provided that the real stresses σ_{ij} and the virtual strains $\delta\varepsilon_{ij}$, corresponding to the particular unit $\delta \mathbf{u}_Q$, can be evaluated. This principle is particularly useful in rigid plastic analysis where the virtual deformation may be discretized at a "plastic hinge."

10.5.3 Principle of Virtual Forces

First we consider the virtual work produced by virtual surface tractions $\delta \mathbf{T}_i$ and virtual body forces $\delta \mathbf{f}_i$.

$$\begin{aligned} \delta W_E^* &= \int_A \delta T_i u_i \, dA + \int_V \delta f_i u_i \, dV \\ &= \int_V \delta \sigma_{ij} \varepsilon_{ij} \, dV \\ &= \delta W_V^* \end{aligned} \tag{10.39}$$

following the same steps as in the previous section, Eqs. (10.19) through (10.22).

This is the so-called *principle of virtual forces* PVF, which describes *compatibility* between internal strains and external displacements.

We now consider the external virtual work produced by virtual forces $\delta \mathbf{F}_Q$

$$\delta W_E^* = \sum_{Q=1}^{\bar{Q}} \delta \mathbf{F}_Q \cdot \mathbf{u}_Q. \tag{10.40}$$

In this form, the principle is useful for computing displacements, one at a time, for a system in which the actual stresses and the corresponding strains are known. If the displacement $\mathbf{u}_3$, is sought, we choose $\delta \mathbf{F}_3 = 1$ with all other $\delta \mathbf{F}_Q = 0$, and Eq. (10.39) becomes

$$u_3 = \int_V \delta \sigma_{ij} \varepsilon_{ij} \, dV. \tag{10.41}$$

Equation (10.41) may be solved, provided that the real strains ε_{ij} corresponding to the particular $\delta \mathbf{F}_Q$ (in this case $\delta \mathbf{F}_3 = 1$) can be evaluated.

A somewhat trivial example is selected to illustrate this technique. The bar shown in Fig. 6.1 is again considered, where it is desired to compute the axial deformation along the centerline $u_z(0, 0, z)$. A unit virtual force produces a stress $\delta \sigma_{ij} = \delta \sigma_{zz} = 1/A$, and the corresponding strain, given by Eq. (6.4), is $\varepsilon_{zz} = (1/E)\gamma z$. Then, Eq. (10.41) becomes

$$\begin{aligned} u_z(0, 0, z) &= \int_L^z \int_A \frac{1}{A} \frac{1}{E} \gamma z \, dA \, dz \\ &= \left[\frac{\gamma z^2}{2E} \right]_L^z = \frac{\gamma}{2E}(z^2 - L^2) \end{aligned} \tag{10.42}$$

which checks with Eq. (6.19c).

10.5.4 Reciprocal Theorems

We again refer to the elastic body in Fig. 10.2(a) subjected, in turn, to two sets of forces $\mathbf{F}_Q$ and $\mathbf{F}_R^*$ which produce displacements $\mathbf{u}_Q$ and $\mathbf{u}_R^*$, respectively. The corresponding displacement components, stresses and strains are

$(u_i, \sigma_{ij}, \varepsilon_{ij})$ and $(u_i^*, \sigma_{ij}^*, \varepsilon_{ij}^*)$. Two sequences are considered:

(1) The $\mathbf{F}_Q$ applied first, then $\mathbf{F}_R^*$;
(2) The $\mathbf{F}_R^*$ applied first, then $\mathbf{F}_Q$.

For the first case, $\mathbf{F}_Q$ may be considered as the real system and $\mathbf{F}_R^*$ as the virtual system; then Eqs. (10.36) and (10.22) give

$$\sum_{Q=1}^{\bar{Q}} \mathbf{F}_Q \cdot \mathbf{u}_Q^* = \int_V \sigma_{ij}\varepsilon_{ij}^* \, dV. \tag{10.43}$$

For the second sequence,

$$\sum_{R=1}^{\bar{R}} \mathbf{F}_R^* \cdot \mathbf{u}_R = \int_V \sigma_{ij}^*\varepsilon_{ij} \, dV. \tag{10.44}$$

In each case the linear elastic stress strain law Eq. (4.3) is applicable. Therefore,

$$\begin{aligned} \sigma_{ij} &= E_{ijkl}\varepsilon_{kl}, & \text{(a)} \\ \sigma_{ij}^* &= E_{ijkl}\varepsilon_{kl}^*. & \text{(b)} \end{aligned} \tag{10.45}$$

After substitution of Eqs. (10.45a and b) into the r.h.s. of Eqs. (10.43) and (10.44), respectively, recognition that the dummy indices may be interchanged, and realization that $E_{ijkl} = E_{klij}$, it is evident that the r.h.s. of the later equations are identical. Then, equating the l.h.s. gives

$$\sum_{Q=1}^{\bar{Q}} \mathbf{F}_Q \cdot \mathbf{u}_Q^* = \sum_{R=1}^{\bar{R}} \mathbf{F}_R^* \cdot \mathbf{u}_R, \tag{10.46}$$

which is known at Betti's law, after Enrico Betti. That is, if a linearly elastic body is subjected to two separate loading systems, the product of the *forces* on the *first* system and the corresponding *displacements* of the *second* system is equal to the product of the *forces* on the *second* system and the corresponding *displacements* of the *first* system.

As a special case, let each loading system be a single unit force, applied at Q and R, respectively. Then Eq. (10.46) reduces to

$$u_Q^* = u_R, \tag{10.47}$$

which is known as Maxwell's law of reciprocal displacements after the 19th century physicist James Clerk Maxwell. That is, the displacement at Q due to a unit force at R is equal to the displacement at R due to a unit force at Q—a remarkable result. Moreover, the unit "forces" do not have to even be of the same type, that is, $\mathbf{F}_Q$ may be an actual force and $\mathbf{F}_R^*$ a unit moment; whereupon $\mathbf{u}_Q^*$ is a displacement, but $\mathbf{u}_R$ is a rotation. Still, they are equal.

10.6 Variational Principles

10.6.1 Definitions

The PVW may be recast in the form of variational theorems to remove the necessity of dealing with the virtual system *per se*. We concisely define the *variation* operation $\delta(\ \ )$ as an arbitrary linear *increment* of a *functional* (a generalized function) that satisfies all constraints on the body, including maintenance of equilibrium. As a simple example, a virtual displacement δu_i may be interpreted as a variation on the displacement field u_i. The variation of a function is computationally the same as the differential, so that

$$\delta(u_i u_i) = \delta(u_i)^2 = 2u_i \delta u_i = 2u_i \delta_{ij} \delta u_j$$

and

$$\delta(\varepsilon_{kk}\varepsilon_{kk}) = \delta(\varepsilon_{kk})^2 = 2\varepsilon_{kk}\delta\varepsilon_{kk} = 2\varepsilon_{kk}\delta_{ij}\delta\varepsilon_{ij}, \text{ etc.}$$

10.6.2 Principle of Minimum Total Potential Energy

Corresponding to δu_i, we have the variation of the strain field $\delta\varepsilon_{ij}$. We now proceed to compute the resulting variation of the internal strain energy Eq. (10.2) with the strain energy density in the form of Eq. (10.3),

$$\begin{aligned} \delta W_V &= \delta \int_V \left[\mu\varepsilon_{ij}\varepsilon_{ij} + \frac{\lambda}{2}(\varepsilon_{kk})^2 \right] dV \\ &= \int_V \left(\left[\mu 2\varepsilon_{ij}\delta\varepsilon_{ij} + \frac{\lambda}{2} 2\varepsilon_{kk}\delta_{ij}\delta\varepsilon_{ij} \right] dV, \right. \end{aligned}$$

or using Eq. (4.18),

$$\delta W_V = \int_V \sigma_{ij}\delta\varepsilon_{ij}\, dV. \tag{10.48}$$

In a similar manner, the external virtual work δW_E may be equated to the work done by the surface tractions T_i and body forces f_i during the variation using Eq. (10.18). It is convenient to represent these contributions in terms of potential functions [10.5]

$$T_i = -\frac{\partial \mathscr{T}}{\partial u_i}, \qquad \text{(a)}$$
$$f_i = -\frac{\partial \mathscr{f}}{\partial u_i}. \qquad \text{(b)} \tag{10.49}$$

When such functions exist, Eq. (10.18) may be written as

$$\begin{aligned} \delta W_E &= \int_A \mathscr{T}_i \delta u_i\, dA + \int_V \mathscr{f}_i \delta u_i\, dV \\ &= -\int_A \frac{\partial \mathscr{T}}{\partial u_i}\delta u_i\, dA - \int_V \frac{\partial \mathscr{f}}{\partial u_i}\delta u_i\, dV \\ &= -\delta \int_A \mathscr{T}\, dA - \delta \int_V \mathscr{f}\, dV \\ &= -\delta V_E, \end{aligned} \tag{10.50}$$

where V_E is defined as the potential of the external forces, given by

$$V_E = \int_A \mathscr{T}\, dA + \int_V \not{f}\, dV. \tag{10.51}$$

Further, it is assumed that the surface and body forces are vector point functions of *position* only; that is, they are *not* dependent on the deformation of the body, either in magnitude or direction. This type of force field is said to be *conservative* and encompasses a large majority of problems in solid mechanics. In this case,

$$\mathscr{T} = -T_i u_i \qquad \text{(a)}$$
$$\not{f} = -f_i u_i, \qquad \text{(b)} \qquad (10.52)$$

and

$$V_E = -\int_A T_i u_i\, dA - \int_V f_i u_i\, dV. \qquad \text{(c)} \quad (10.52)$$

The principle of minimum total potential energy PMPE is properly written as

$$\delta\Pi = \delta(W_V + V_E) = 0, \tag{10.53}$$

in which Π is called the potential energy functional. The form of Eq. (10.53) emphasizes that both terms of Π are subjected to the same variation and that the variation is performed *after* W_V and V_E are evaluated and combined. This is a so-called *extremum* statement since only the first variation is expressed. To show the actual *minimum* character, the second variation would have to be considered, but this is beyond our scope.

This principle implies that the *correct displacement state* of all those states which may satisfy the boundary conditions is that which makes the total potential energy a minimum. The great utility of the PMPE is that it is relatively straightforward *to approximate* displacement fields by *shape functions* that satisfy the kinematic boundary conditions, and to scale these fields by minimizing the resulting total potential energy. We illustrate this point in a later section.

10.6.3 Principle of Minimum Complementary Energy

Recalling that two versions of the virtual work principle were derived, depending on which form of external virtual work was manipulated, it follows that a dual to the PMPE can be created by focusing on the stress field σ_{ij} and the variation $\delta\sigma_{ij}$.

With the strain energy density in the form of Eq. (10.6) and the system subjected to an arbitrary $\delta\sigma_{ij}$, we have

$$\delta W_V^* = \delta \int_V \left[\frac{1}{4\mu} \sigma_{ij}\sigma_{ij} - \frac{\lambda}{4\mu(2\mu + 3\lambda)} (\sigma_{kk})^2 \right] dV$$
$$= \int_V \left[\frac{1}{2\mu} \sigma_{ij}\delta\sigma_{ij} - \frac{\lambda}{2\mu(2\mu + 3\lambda)} \sigma_{kk}\delta_{ij}\delta\sigma_{ij} \right] dV,$$

or, using Eq. (4.19),

$$\delta W_V^* = \int_V \varepsilon_{ij}\delta\sigma_{ij}\, dV \tag{10.54}$$

where δW_V^* is the internal *virtual* work, as derived in Eq. (10.39).

Analogous to Eq. (10.50), we may represent the external virtual work in potential form

$$\delta W_E^* = \int_A \delta T_i u_i\, dA + \int_v \delta f_i u_i\, dV = -\delta V_E^*, \tag{10.55}$$

where $V_E^* = V_E$ as given by Eq. (10.52c), for conservative fields. Finally, the principle of minimum complementary energy PMCE is properly written as

$$\delta\Pi^* = \delta(W_V^* + V_E^*) = 0, \tag{10.56}$$

where Π^* is called the complementary energy functional. Again, it is apparent that the variations are performed on Π^* rather than on the individual terms.

This principle implies that the *correct stress state* of all those that satisfy equilibrium is that which makes the total complementary energy a minimum. In contrast to the attractiveness of selecting displacement functions that satisfy compatibility, it may be more difficult to find stress distributions that satisfy equilibrium.

For an elastic, isotropic structure, $W_V^* = W_V$ and $V_E^* = V_E$. However, the *variations* of these quantities that appear in the foregoing principles are not equal since in the PMPE, the *displacements* are varied; while in the PMCE, the *stresses* are varied.

10.7 Direct Variational Methods

10.7.1 Motivation

As we mentioned in the introductory comments to this chapter, the accelerated prominence of energy methods for the solution of elasticity problems is a fairly recent development. The underlying basis of most of the computer-based techniques, which have come to be known as *finite element* methods, are the previously derived variational principles, together with the appropriate numerical analysis algorithms. Using the PMPE as an example, functions that satisfy the kinematic constraints are selected to represent the dependent variables, which are most frequently generalized displacements. These so-called *shape* or *comparison functions* are scaled in accordance with the PMPE to provide the best approximation to equilibrium. To be specific, recall how a sine wave may closely match the deformation of a simply supported beam, both under static loading and in free vibration.

In the course of introducing shape functions to represent the generalized displacements, the extremum problem of the calculus of variations is transformed to the maximum-minimum problem of the classical calculus. Such techniques are termed *direct* variational methods. The treatment of the vibration of elastic bodies by Lord Rayleigh (John W. Strutt) in *Theory of Sound* [10.6] is probably the origin of this approach, and it is fitting that the *Rayleigh-Ritz method* be recognized as the most prominent direct method.

10.7.2 Rayleigh–Ritz Method

To illustrate the Rayleigh–Ritz idea, we focus on Eq. (10.53) where both W_V and V_E are regarded as functions of the displacement field u_i. We select kinematically admissible polynomials for *each* u_i consisting of n_i terms

$$\begin{aligned} u_i \simeq \bar{u}_i = C_{i0} + C_{i1}x + C_{i2}y + C_{i3}z + C_{i4}x^2 + \cdots \\ + C_{ij}x^m y^p z^q + \cdots + C_{in_i}x^{\bar{m}} y^{\bar{p}} z^{\bar{q}} \quad (i = 1, 2, 3), \end{aligned} \tag{10.57}$$

where the C_{ij} are as yet undetermined coefficients; u_i represents u_x, u_y and u_z, in turn; and m, p and q are the exponents of x, y and z up to $\bar{m}$, $\bar{p}$ and $\bar{q}$, in each polynomial.

After the introduction of the three Eqs. (10.57) into Eq. (10.2), expressed in terms of displacements using Eqs. (10.3) and (3.14), and then into Eqs. (10.52) and (10.53), the subsequent integration and minimization leads to

$$\delta\Pi(\bar{u}_i) = \sum_{j=1}^{n_i} \frac{\partial \Pi}{\partial C_{ij}} \delta C_{ij}, \tag{10.58}$$

where the usual summation convention applies on i.

Since the variations δC_{ij} are arbitrary. Eq. (10.58) may be satisfied only if

$$\frac{\partial \Pi}{\partial C_{ij}} = 0 \qquad i = 1, 2, 3; \qquad j = 1, 2, \ldots, n_i, \tag{10.59}$$

which produce a set of $3(n_i + n_2 + n_3)$ simultaneous *algebraic* equations for the unknown coefficients. With the coefficients C_{ij} evaluated, Eqs. (10.57) represent the displacements over the domain; the strains and stresses may be computed accordingly from the laws of the theory of elasticity.

A similar technique may be applied to minimize the functional Π^* given by Eq. (10.56).

10.7.3 Torsion of Rectangular Cross Section

We return to the St. Venant torsion solution for an illustration of the Rayleigh–Ritz method. Here, we study a rectangular cross section as shown in Fig. 10.4, an elusive problem by analytical means.

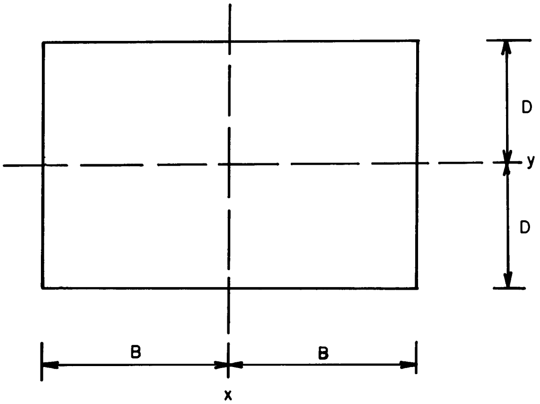

Fig. 10.4. Rectangular cross section.

First, we consider the strain energy W_V defined by Eq. (10.2) with the density W given by Eq. (10.4). Based on the developments in Section 6.4.2, the formulation is in terms of the stress function ϕ:

$$\begin{aligned} W &= \frac{1}{4\mu}\sigma_{ij}\sigma_{ij} \\ &= \frac{2}{4\mu}[(\sigma_{xz})^2 + (\sigma_{yz})^2] \\ &= \frac{1}{2G}[(\phi_{,y})^2 + (\phi_{,x})^2], \end{aligned} \tag{10.60}$$

and the strain energy *per unit length* is given by

$$W_V = \frac{1}{2G}\iint [(\phi_{,y})^2 + (\phi_{,x})^2]\, dx\, dy. \tag{10.61}$$

Next, the corresponding potential of the applied loads is given in the form of Eq. (10.52c), using Eq. (6.84):

$$V_E = -M\alpha = -2\alpha \int_A \phi\, dA. \tag{10.62}$$

Forming the functional as defined in Eq. (10.53), we have

$$\Pi = \iint \left\{ \frac{1}{2G}[(\phi_{,y})^2 + (\phi_{,x})^2] - 2\alpha\phi \right\} dx\, dy. \tag{10.63}$$

At this point, we could address Eq. (10.63) directly, seeking a function ϕ that is a solution to $\delta\Pi = 0$, which is a traditional problem in the calculus of variations. However, we follow the Rayleigh–Ritz approach whereby we assume a solution in the form [10.7].

$$\phi \simeq \bar{\phi} = (x^2 - D^2)(y^2 - B^2) \sum_m \sum_n C_{mn} x^m y^n. \qquad (10.64)$$

This approximation satisfies the condition that ϕ must vanish on the boundaries $x = \pm D$, $y = \pm B$.

The solution proceeds by substituting Eq. (10.64) into Eq. (10.63) and integrating over the area to get the approximate functional $\overline{\Pi}$. Thus, the variational problem is transformed into a calculus problem, for which the equations

$$\frac{\partial \overline{\Pi}}{\partial C_{mn}} = 0 \qquad (10.65)$$

are used to obtain a set of simultaneous equations for the C_{mn} coefficients.

We do not carry out a detailed solution for this problem; however, we may illustrate with a coarse approximation, a single term of Eq. (10.64) and a square cross section $B = D$,

$$\bar{\phi} = C_0(x^2 - B^2)(y^2 - B^2). \qquad (10.66)$$

After evaluating

$$\begin{aligned} \bar{\phi}_{,y} &= 2C_0(x^2 - B^2)y \\ \bar{\phi}_{,x} &= 2C_0(y^2 - B^2)x, \end{aligned} \qquad (10.67)$$

we are ready to substitute Eqs. (10.66) and (10.67) into Eq. (10.63). However, since we may anticipate integrating to find $\overline{\Pi}$ and then taking $\partial\overline{\Pi}/\partial C_0$, it is expedient to commute these operations and write the minimum condition as

$$\frac{\partial \overline{\Pi}}{\partial C_0} = \int_{-B}^{B} \int_{-B}^{B} \left\{ \frac{1}{2G} \left[2\bar{\phi}_{,y} \frac{\partial(\bar{\phi}_{,y})}{\partial C_0} + 2\bar{\phi}_{,x} \frac{\partial(\bar{\phi}_{,x})}{\partial C_0} \right] - 2\alpha \frac{\partial \bar{\phi}}{\partial C_0} \right\} dx\, dy = 0 \qquad (10.68)$$

or

$$\int_{-B}^{B} \int_{-B}^{B} \left\{ \frac{1}{2G} [4C_0(x^2 - B^2)^2 y^2 + 4C_0(y^2 - B^2)^2 x^2] - 2\alpha(x^2 - B^2)(y^2 - B^2) \right\} dx\, dy = 0. \qquad (10.69)$$

After integration and simplification, this gives

$$C_0 = \frac{5}{8} \frac{G\alpha}{B^2}, \qquad (10.70)$$

and, from Eq. (6.84),

$$\begin{aligned} M_z &= 2 \int_A \phi\, dA = 2 \int_{-B}^{B} \int_{-B}^{B} \frac{5}{8} \frac{G\alpha}{B^2} (x^2 - B^2)(y^2 - B^2)\, dx\, dy \\ &= \frac{20}{9} G\alpha B^4, \end{aligned} \qquad (10.71)$$

which differs by just over 1% from the correct solution [10.7]

Timoshenko and Goodier [10.7] have also used a three-term approximation,

$$\bar{\phi} = (x^2 - B^2)(y^2 - B^2)[C_0 + C_1(x^2 + y^2)] \tag{10.72}$$

where C_1 is a combined coefficient due to symmetry. The resulting M_z is but 0.15% from the correct value. However, the corresponding error in the maximum shear stress is about 4%. The distribution of the shearing stresses is quite similar to the elliptical cross section, as previously illustrated in Section 6.4.3, with maxima at the center of the sides decreasing to zero at the corners.

Considering that M_z was approximated almost exactly, the relatively large error in the maximum shear stress may be surprising; however, we recall that the stresses are obtained by *differentiation* of ϕ, Eqs. (6.65), so that they may indeed be less accurate. This demonstrates that extreme care should be exercised in measuring convergence for approximate solutions, specifically the most highly differentiated quantities should be considered. In this case, more terms in the approximation will improve convergence.

10.7.4 Commentary

Although a considerable mathematical simplification is accomplished, in principle, with the Rayleigh–Ritz technique, two rather formidable obstacles are evident once more complex problems are investigated. First, it may be difficult to find kinematically admissible representations for displacement functions over the *entire* domain. Secondly, if appropriate functions are found, the resulting set of simultaneous algebraic equations may be rather large if suitable accuracy is to be achieved.

These obstables have been overcome by two modern developments. The first is the notion that perhaps it is sufficient for the approximate displacement functions to span over only a portion or *element* of the continuum and to be constrained to satisfy interelement continuity. This was apparently recognized early on by Courant and Hilbert [10.8], but was not fully exploited, perhaps since it exacerbates the second obstacle by producing even more simultaneous equations. The ultimate solution is achieved by the use of a high-speed digital computer with its ability for "number-crunching." Properly ordered, tens of thousands of simultaneous equations may be solved routinely.

The prophesy of Euler, quoted in the introductory section of this chapter, has been richly fulfilled by the development of the finite element method. Yet, we should not dismiss the rigorous analytical solutions demanded by the theory of elasticity as archaic, for the finite element solutions are still approximations. They need to be calibrated with selected analytical solutions, both numerically and judgmentally, to establish confidence and to quantify errors. In the opinion of the author, *total* reliance on finite element methods or other numerical techniques that are implemented in "black box" computer programs is surely *unwise*, probably *uneconomical*, and possibly *unsafe*.

Exercises

10.1 Consider the right half of the thin plate shown as Problem 7.8. The boundary conditions, which represent a diaphragm, are given by

$$u_x = 0 \quad \text{along} \quad y = 0 \quad \text{and} \quad y = b$$
$$u_y = 0 \quad \text{along} \quad x = 0 \quad \text{and} \quad x = a$$

For a constant body force $f_y = p$, consider the PVD and the Rayleigh–Ritz method with displacement functions in the form

$$u_x = \sum_{n=1}^{\infty} \left\{ C_{on} + \sum_{m=1}^{\infty} C_{mn} \cos\left(\frac{m\pi x}{a}\right) \right\} \sin\left(\frac{n\pi y}{b}\right)$$
$$u_y = \sum_{m=1}^{\infty} \left\{ D_{om} + \sum_{n=1}^{\infty} D_{mn} \cos\left(\frac{n\pi y}{b}\right) \right\} \sin\left(\frac{m\pi x}{a}\right)$$

Assuming $m = n = 1$, compute the displacements, strains, and stresses for a square plate with $a = b$.

10.2 Use the PVF to verify the solution Eq. (6.62) for the rate of twist in the circular rod subject to a constant torque shown in Fig. 6.5.

10.3 Re-solve the St. Venant torsion of a square cross section discussed in Section 10.7.3 using the improved approximation Eq. (10.72) and evaluate the shear stresses. Compare these results to the values obtained from the one-term approximation.

10.4 Show that Eq. (10.6) can be written in terms of the engineering material constants as [10.9]

$$W = \frac{1}{2E}(\sigma_{11}^2 + \sigma_{22}^2 + \sigma_{33}^2) - \frac{\mu}{E}(\sigma_{11}\sigma_{22} + \sigma_{11}\sigma_{33} + \sigma_{22}\sigma_{33})$$

for a triaxial stress state, $\sigma_{ij} = 0\ (i \neq j)$.

10.5 A state of plane strain relative to the (x, y) plane has a strain energy density function given by

$$W = \tfrac{1}{2}b_{11}\varepsilon_{xx}^2 + b_{22}\varepsilon_{yy}^2 + b_{33}\varepsilon_{xy}^2 + 2b_{12}\varepsilon_{xx}\varepsilon_{yy} + 2b_{13}\varepsilon_{xx}\varepsilon_{xy} + 2b_{23}\varepsilon_{yy}\varepsilon_{xy}$$

where the b_{ij} are elastic coefficients. Derive the equations of equilibrium in terms of the displacements $u_x(x, y)$ and $u_y(x, y)$ including the effects of body forces [10.10].

References

[10.1] Timoshenko, S., *History of Strength of Materials* (McGraw–Hill Book Company, Inc., New York, 1953).

[10.2] Boresi, A. P. et al., *Advanced Methanics of Materials*, third edition (John Wiley & Sons, New York, 1978).

[10.3] Forray, M. J., *Variational Calculus in Science and Engineering* (McGraw–Hill Book Company, Inc., New York, 1968).

[10.4] Pierce, B. O., and Foster, R. M., *A Short Table of Integrals*, Fourth edition (Ginn and Company, Boston, 1950) Formula 969.

[10.5] Tauchert, T.R., *Energy Principles in Structural Mechanics* (McGraw–Hill Book Company, Inc., New York, 1974).
[10.6] Lord Rayleigh, *The Theory of Sound* (Dover Publications, Inc., New York, 1945).
[10.7] Timoshenko, S., and Goodier, J. W., *Theory of Elasticity*, second edition (McGraw–Hill Book Company, Inc., New York, 1951).
[10.8] Courant, R., and Hilbert, D., *Methods of Mathematical Physics*, Vol. 1 (Wiley-Interscience Publications, New York, 1966).
[10.9] Gopu, V. K. A., "Validity of Distortion-Energy-Based Strength Criterion for Timber Members," *Journal of Structural Engineering*, ASCE, Vol. 113, No. 12, December, 1987, pp. 2475–2487.
[10.10] Boresi, A. P., and Chong, F. P., *Elasticity in Engineering Mechanics* (Elsevier, New York, 1987).

CHAPTER 11

Strength and Failure Criteria

11.1 Introduction

The application of the rigorous methods of analysis embodied in the theory of elasticity is naturally of interest to engineers. While a broad discussion of this issue is beyond our scope, it is of interest to introduce the fundamental basis of such application, namely, the comparison of the analytical *results* obtained from an elasticity solution to the expected *capacity* of the resisting material.

Historically, the capacity of a specific material has been stated in terms of a *failure criteria*, whereby the exceedance of a critical value of a controlling parameter marks the limit of the functional range. More recently, it has been recognized that factors other than an explicit extreme failure criterion may govern the limit, such as excessive flexibility or fatigue. Therefore, we choose to add the term *strength criteria*, which implies that there may be additional considerations in assessing the utility of the material. Furthermore, we restrict the discussion to criteria that are correlated to the pointwise focus of the theory, and thereby exclude stability considerations which are strongly controlled by topological parameters.

11.2 Isotropic Materials

11.2.1 Classical Tests

For isotropic materials, it is helpful to discuss the measures of capacity with respect to tests that are easily performed on small specimens. Most common are the uniaxial tensile test and the torsion test, which imparts a state of pure shear. The state of stress in the x-y plane from each of these tests is shown in Figure 11.1. Within each element, the state of stress for a rotation of 45° is shown since this orientation produces the maximum shear stress in the tension test and the maximum extensional stress in the shear test.

For calculation purposes, we assume a circular cross section of radius B

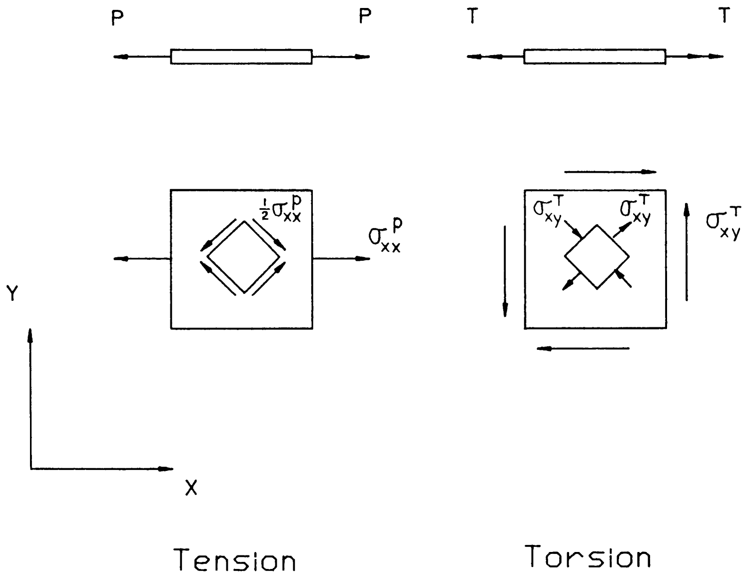

Fig. 11.1. Tension and torsion tests.

for each test with an area $A = \pi B^2$ and polar moment of inertia, Eq. 6.60(b), of $J_c = \dfrac{\pi B^4}{2}$.

It is of interest in what follows to carry out a rather complete analysis and comparison of key parameters in the two classical tests. The parameters of interest are measures of *stress*, *strain* and *energy*.

We first consider stress quantities. In the tensile test, the load produces an axial stress

$$\sigma_{xx}^P = \frac{P}{A} = \frac{P}{\pi B^2} \tag{11.1}$$

while in the torsion test, the torque produces a shearing stress, Eq. (6.61)

$$\sigma_{xy}^T = \frac{TB}{J_c} = \frac{2T}{\pi B^3}. \tag{11.2}$$

On the 45° planes, the respective stresses are

$$\sigma_{x'y'}^P = -\frac{1}{2}\sigma_{xx}^P \tag{11.3}$$

from Eq. (2.13) with $\alpha_{x'x} = \dfrac{\sqrt{2}}{2}$ and $\alpha_{y'x} = -\dfrac{\sqrt{2}}{2}$ for the tensile test, and

$$\sigma_{x'y'}^T = \sigma_{xy}^T \tag{11.4}$$

for the torsion test since the stress state is pure shear.

We may also evaluate the octahedral shearing stresses for each case using Eq. (2.84b). For the tensile test,

$$\sigma_{ns}^{oct\,P} = \frac{1}{3}[(\sigma_{xx}^P)^2 + (-\sigma_{xx}^P)^2]^{1/2}$$

$$= \frac{\sqrt{2}}{3}\sigma_{xx}^P \tag{11.5}$$

$$\sigma_{ns}^{oct\,T} = \frac{1}{3}[(\sigma_{xy}^T + \sigma_{xy}^T)^2 + (-\sigma_{xy}^T)^2 + (-\sigma_{xy}^T)^2]^{1/2}$$

$$= \frac{\sqrt{6}}{3}\sigma_{xy}^T. \tag{11.6}$$

Turning to the strains, for the tensile test the maximum normal strain is

$$\varepsilon_{xx}^P = \frac{\sigma_{xx}^P}{E} \tag{11.7}$$

while the corresponding value in the torsion test may be evaluated from Eq. (4.29b), referred to the 45° axes,

$$\varepsilon_{x'x}^T = \frac{1}{E}[\sigma_{xy}^T - \nu(-\sigma_{xy}^T)]$$

$$= \frac{1+\nu}{E}\sigma_{xy}^T. \tag{11.8}$$

We now consider energy measures. The strain energy density for a uniaxial load is given by Eq. (10.7b), which is for this case

$$W = \frac{1}{2E}(\sigma_{xx}^P)^2. \tag{11.9}$$

In the torsion test

$$W = \frac{1}{2E}[(\sigma_{xy}^T)^2 + (-\sigma_{xy}^T)^2]$$

$$= \frac{1}{E}(\sigma_{xy}^T)^2. \tag{11.10}$$

Finally, we consider the strain energy density of distortion, as derived in Eq. (10.14). For the tensile test,

$$W_0 = \frac{1}{12G}[(\sigma_{xx}^P)^2 + (-\sigma_{xx}^P)^2]$$

$$= \frac{1}{6G}\sigma_{xx}^{P2} \tag{11.11}$$

while for the torsion test,

$$W_0 = \frac{1}{12G}[(2\sigma_{xy}^T)^2 + (-\sigma_{xx}^T)^2 + (-\sigma_{xx}^T)^2]$$

$$= \frac{1}{2G}\sigma_{xy}^{T^2}. \tag{11.12}$$

Recall from Eq. (10.15) that the octahedral shearing stress and W_0 are related.

11.2.2 Failure Theories

We first designate the states of stress, strain and energy for the limit states of the tension and torsion tests by the subscript c, standing for capacity. Thus, the failure loads are P_c and T_c, the stresses $\sigma_{xx}^{P_c}$, etc. Next, strength theories are postulated whereby a *single* parameter, such as a state of stress, strain, and/or energy at a point in an elastic body, is correlated to the like state in either the tensile or torsion test situation. Six such theories, referred to a tension test, are summarized in Table 11.1 [11.1].

It is obvious that a parallel table could be produced with the torsion test limits replacing the tension test values. An interesting format for comparing the dual statements is presented in Table 11.2 after Boresi, et al. [11.1]. Experimental evidence for metals suggests that the shear yield stress $\sigma_{xy}^{T_c}$ is in the range of 0.5 to 0.58 of the tensile yield stress $\sigma_{xx}^{P_c}$, giving credence to the maximum shearing stress and octahedral shearing stress criteria. For more complex materials, it is advantageous to work with nondirectional or invariant quantities such as energy.

11.2.3 Invariants

A direct relationship between the invariants of the stress tensor, which are stated in terms of the principal stresses in Eq. (2.61), and the strain energy of distortion or octahedral shearing stress criteria may be established.

Initially, the hydrostatic stresses are discounted as a contributor to the plastic deformation of metals, in accordance with experimental observations [11.2]. As a result, the mean normal stress as defined in Eq. (3.48) is disregarded. Since this quantity is proportional to the first invariant, we concentrate on the second and third invariants, defined in Eqs. (2.61) and (2.63), respectively, as

$$J_2 = \frac{1}{2}[\sigma^{(1)^2} + \sigma^{(2)^2} + \sigma^{(3)^2}] \tag{11.13}$$

and

$$J_3 = \frac{1}{3}[\sigma^{(1)^3} + \sigma^{(2)^3} + \sigma^{(3)^3}]. \tag{11.14}$$

In Section 3.5, the stress tensor was represented as the sum of a mean normal stress component and a stress deviator component, Eqs. (3.47)–(3.50).

Table 11.1

Theory/Criteria	Statement	Applicability
Maximum principal stress (Rankine's criterion)	Inelastic action begins when the maximum principal stress at any point $\sigma^{(1)}$, reaches the tensile yield stress of the material, $\sigma_{xx}^{P_c}$.	Normal and shear stresses acting on other planes have no influence. Limited to materials that fail by brittle fracture since, for ductile materials, σ^{T_c} is much less than $\sigma_{xx}^{P_c}$.
Maximum shearing stress (Tresca's or Coulomb's criterion)	Inelastic action begins when the maximum shearing stress at any point in a member, $\sigma_{ns}^{\max}$ reaches the value which occurs in a tensile specimen at the onset of yielding, $\frac{1}{2}\sigma_{xx}^{P_c}$.	Justified for ductile materials in which fairly high shears are developed.
Maximum strain (St. Venant's criterion)	Inelastic action begins when the maximum (normal) strain of any point in a member, $\varepsilon^{(1)}$, reaches the value which occurs in a tensile specimen at the onset of yielding, $\frac{1}{E}\sigma_{xx}^{P_c}$.	Improvement over maximum principal stress criterion since it accounts for biaxial and triaxial stress states. Does not reliably predict failures in ductile materials but is widely used for brittle materials such as concrete.
Strain energy density (Beltrami and Haigh criterion)	Inelastic action begins when the strain energy density at any point, W, is equal to the value which occurs in a tensile specimen at the onset of yielding $\frac{1}{2E}(\sigma_{xx}^{P_x})^2$.	Not applicable for biaxial and triaxial stress states.
Strain energy density of distortion (Huber, von Mises, Hencky criterion)	Inelastic action begins when the strain energy density of distortion at any point, W_0, is equal to the value which occurs in a tensile specimen at the onset of yielding $\frac{1}{6G}(\sigma_{xx}^{P_x})^2$.	Accounts for the delay of inelastic action under large hydrostatic stresses. Associates failure with energy absorbed in changing shape, since hydrostatic stresses are associated with volume change only.
Octahedral shearing stress	Inelastic action begins when the octahedral shearing stress at any point, σ_{ns}^{oct}, is equal to the value which occurs in a tensile specimen at the onset of yielding $\frac{\sqrt{2}}{3}\sigma_{xx}^{P_x}$.	Same as strain energy of distortion.

Table 11.2

Failure Criterion	Value from Tensile Test	Value from Torsion Test	Relationship between $\sigma_{xx}^{P_c}$ and $\sigma_{xy}^{T_c}$ if criterion is correct for both states (2) = (3)
(1)	(2)	(3)	(4)
Maximum principal stress	$\sigma^{(1)} = \sigma_{xx}^{P_c}$	$\sigma^{(1)} = \sigma_{xy}^{T_c}$	$\sigma_{xy}^{T_c} = \sigma_{xx}^{P_c}$
Maximum shearing stress	$\sigma_{ns}^{max} = \frac{1}{2}\sigma_{xx}^{P_c}$	$\sigma_{ns}^{max} = \sigma_{xy}^{T_c}$	$\sigma_{xy}^{T_c} = 0.5\sigma_{xx}^{P_c}$
Maximum strain	$\varepsilon^{(1)} = \frac{1}{E}\sigma_{xx}^{P_c}$	$\varepsilon^{(1)} = \frac{1+\nu}{E}\sigma_{xy}^{T_c}$	$\sigma_{xy}^{T_c} = \frac{1}{1+\nu}\sigma_{xx}^{P_c}$
Strain energy density	$W = \frac{1}{2E}(\sigma_{xx}^{P_c})^2$	$W = \frac{1}{E}(\sigma_{xy}^{T_c})^2$	$\sigma_{xy}^{T_c} = 0.707\sigma_{xx}^{P_c}$
Strain energy density of distortion	$W_0 = \frac{1}{6G}(\sigma_{xx}^{P_c})^2$	$W_0 = \frac{1}{2G}(\sigma_{xy}^{T_c})^2$	$\sigma_{xy}^{T_c} = 0.577\sigma_{xx}^{P_c}$
Octahedral shearing stress	$\sigma_{ns}^{oct} = \frac{\sqrt{2}}{3}\sigma_{xx}^{P_c}$	$\sigma_{ns}^{oct} = \frac{\sqrt{6}}{3}\sigma_{xy}^{T_c}$	$\sigma_{xy}^{T_c} = 0.577\sigma_{xx}^{P_c}$

Following a construction suggested by Prager and Hodge [11.3], the normal stress on the octahedral surface is entirely due to $\boldsymbol{\sigma}_M$ while $\boldsymbol{\sigma}_D$ produces only the octahedral shearing stress. Hence, the Cartesian components of the octahedral shearing stress can be computed from Eq. 2.21(a) as

$$\sigma_{ns(k)}^{oct} = T_k \qquad k = 1, 2, 3 \tag{11.15}$$

since $\sigma_{nn(k)}^{oct} = 0$. T_k in each case is found as

$$T_k = \sigma_D^{(k)} n_k \tag{11.16}$$

following Eq. (2.11) written for principal stresses. Since

$$n_k = \frac{1}{\sqrt{3}} \qquad k = 1, 2, 3 \tag{11.17}$$

from Eq. (2.82), the components of T_k are

$$T_1 = \sigma_D^{(1)}\frac{1}{\sqrt{3}}, \qquad T_2 = \sigma_D^{(2)}\frac{1}{\sqrt{3}}, \qquad T_3 = \sigma_D^{(3)}\frac{1}{\sqrt{3}} \tag{11.18}$$

and, from Eq. (2.84b),

$$\sigma_{ns}^{oct} = \left\{\frac{1}{3}[(\sigma_D^{(1)})^2 + (\sigma_D^{(2)})^2 + (\sigma_D^{(3)})^2]\right\}^{1/2} = \left[\frac{2}{3}J_{2D}\right]^{1/2} \tag{11.19}$$

in view of Eq. (11.13).

The octahedral shearing stress is thus shown to be proportional to the second invariant of the stress deviator. Likewise, the strain energy density of distortion is related to that quantity.

11.3 Yield Surfaces

11.3.1 General

Since the state of stress at a point is specified by the value of six independent stress components σ_{ij} referred to an arbitrary set of orthogonal coordinate axes x, y, z, it might seem that a general stress criteria would be a function in six-dimensional space, $f(\sigma_{xx}, \sigma_{yy}, \sigma_{zz}, \sigma_{xy}, \sigma_{yz}, \sigma_{zx}) = 0$. Choosing the principal axes as the basis eliminates the shear stresses σ_{ij} $(i \neq j)$ and does not reduce generality for isotropic systems. This produces yield criteria in terms of a three-dimensional principal stress space $f(\sigma^{(1)}, \sigma^{(2)}, \sigma^{(3)}) = 0$. The states of stress referred to both sets of axes are shown in Fig. 11.2(a).

It is informative to demonstrate these criteria using yield surfaces which are an essential component of the theory of plasticity [11.4]. The yield sur-

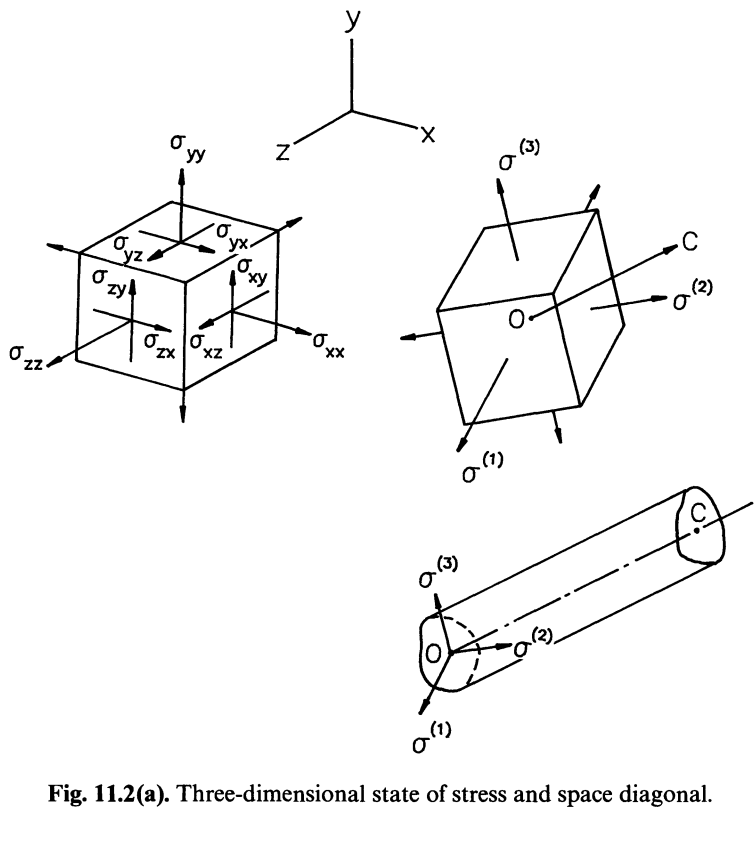

Fig. 11.2(a). Three-dimensional state of stress and space diagonal.

face is produced by all points that satisfy a particular strength criteria. In the three-dimensional principal stress space, the surface may be visualized as a prism, with the axis along the *space diagonal* $\sigma^{(1)} = \sigma^{(2)} = \sigma^{(3)}$, which is the ray OC as shown in Fig. 11.2(a). Since the stress state $\boldsymbol{\sigma}$ may be resolved into a mean normal component $\boldsymbol{\sigma}_M$ and a stress deviator component $\boldsymbol{\sigma}_D$, as discussed in Section 3.5, the cross section of the prism essentially represents $\boldsymbol{\sigma}_D$. Any point on the yield surface may be represented by the sum of the mean and deviatoric components. From Eqs. (3.48)–(3.52), we have

$$(\sigma^{(1)}, \sigma^{(2)}, \sigma^{(3)}) = (\sigma_m, \sigma_m, \sigma_m) = (\sigma_D^{(1)}, \sigma_D^{(2)}, \sigma_D^{(3)}). \tag{11.20}$$

For the principal stresses determined in Section 2.4.3, $\sigma^{(1)} = -1168$, $\sigma^{(2)} = 1380$, $\sigma^{(3)} = 988$.

$$\sigma_m = \frac{1}{3}(-1168 + 1380 + 988) = 400$$

$$\sigma_D^{(1)} = -1168 - 400 = -1568$$

$$\sigma_D^{(2)} = 1380 - 400 = 980$$

$$\sigma_D^{(3)} = 988 - 400 = 588$$

Check: $\sigma_D^{(1)} + \sigma_D^{(2)} + \sigma_D^{(3)} = -1568 + 980 + 588 = 0$ after Eq. (3.54).

The cross section of the prism may be plotted on any plane perpendicular to the space diagonal. Such planes have the equation $\sigma^{(1)} + \sigma^{(2)} + \sigma^{(3)} =$ constant [11.4]. As suggested by Calladine [11.4], the plane passing through the origin is conveniently selected and called the Π-plane, Fig. 11.2(b), and the corresponding cross-sectional boundary is the so-called C-curve, Fig. 11.2(c).

Also, a triangular grid may be inscribed on the π-plane, which represents

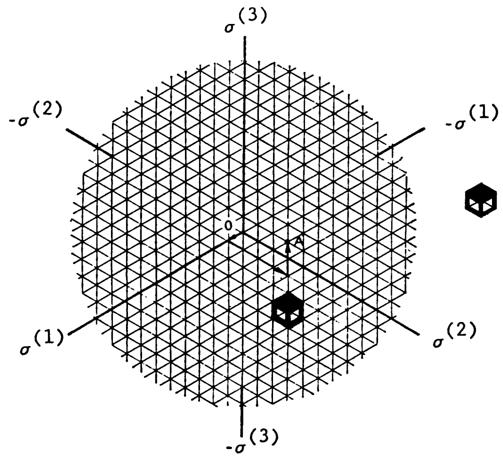

Fig. 11.2(b). Plan view of the π-plane [11.3].

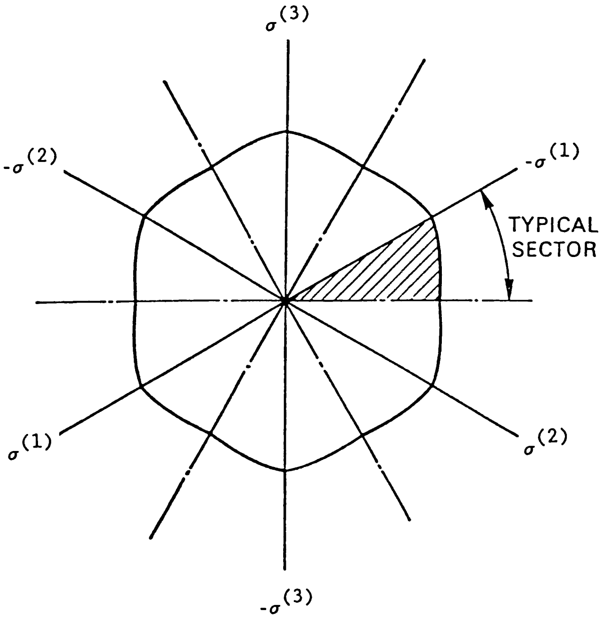

Fig. 11.2(c). *C*-curve in the π-plane and axes of symmetry [11.3].

a view of a cubic lattice in the first octant, as shown by the shaded unit cube and on the inset of Fig. 11.2(b). Point A represents a principal stress state $\sigma^{(i)} = (1, 4, 2)$.

Sliding along the space diagonal gives parallel cross sections corresponding to various values of the hydrostatic stress σ_M. But various yield conditions can be represented on the π-plane.

11.3.2 Tresca Yield Condition

The maximum shearing stress criteria in Table 11.1 may be stated in terms of the principal stresses by Eq. (2.87), which is rewritten for our purposes here as

$$\sigma^{(i)} - \sigma^{(j)} = 2\sigma_{ns}^{\max} = 2k \tag{11.21}$$

where k is the limiting value of the shear stress. Taking for the moment

$$\sigma^{(1)} > \sigma^{(2)} > \sigma^{(3)} \tag{11.22}$$

the projection of the stress point, Eq. (11.21) with $i = 1, j = 3$ lies between the projections of the $(+)\sigma^{(1)}$ axis and the $(-)\sigma^{(3)}$ axis on the π-plane and

$$\sigma^{(1)} - \sigma^{(3)} = 2k \tag{11.23}$$

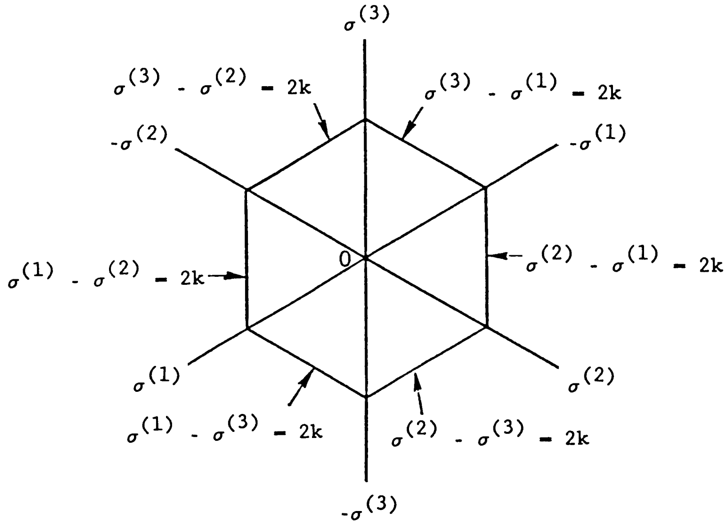

Fig. 11.3. Tresca yield surface: plan view of the π-plane [11.3].

is a straight line perpendicular to the bisector of the boundaries of the region.[1] Each of the other five permutations of Eq. (11.22) will produce similar lines, and the composite C-hexagon is shown in Fig. 11.3.

Within the theory of elasticity we focus on the states of stress within or impinging on the yield surface. From that point, plastic deformation will ensue and a more inclusive theory is required. This is briefly elaborated on in Sec. 11.5.

11.3.3 von Mises Yield Condition

The yield condition attributed to R. von Mises is represented by a circle replacing the hexagon on the π-plane, as shown in Fig. 11.4. The circle is the intersection of a sphere of radius r

$$(\sigma^{(1)})^2 + (\sigma^{(2)})^2 + (\sigma^{(3)})^2 = r^2 \tag{11.24}$$

in the stress space and the plane

$$\sigma^{(1)} + \sigma^{(2)} + \sigma^{(3)} = 0. \tag{11.25}$$

Since Eq. (11.25) is identically satisfied by the components of $\boldsymbol{\sigma}_D$, the required equation is

$$(\sigma_D^{(1)})^2 + (\sigma_D^{(2)})^2 + (\sigma_D^{(3)})^2 = r^2. \tag{11.26}$$

[1] To locate a point along the line defined in Eq. (11.23) on Fig. 11.2(b), find $\sigma^{(1)}$ on the $\sigma^{(1)}$ axis and move along the grid parallel to the $-\sigma^{(3)}$ axis. Then find $\sigma^{(3)}$ on the $-\sigma^{(3)}$ axis and move along the grid parallel to the $\sigma^{(1)}$ axis. The intersection lies on the line.

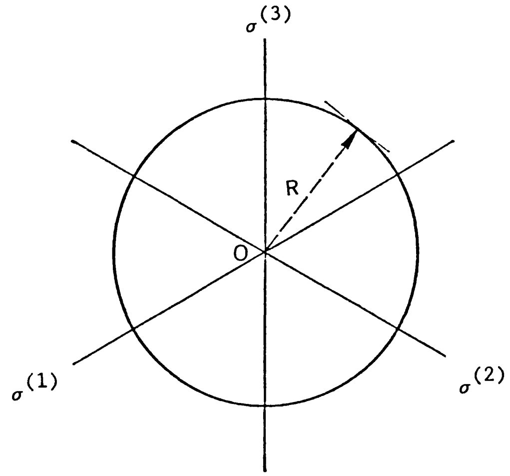

Fig. 11.4. Von Mises yield surface (plan view of π-plane) [11.3].

The radius r is evaluated to make the circle coincide with the Tresca hexagon in the π-plane for states of pure tension and compression. With the yield stress in pure tension $= \sigma_Y$, we compute the radius as the projection of the radius vector $\sigma^{(1)}\mathbf{e}_x = \sigma_Y \mathbf{e}_x$ onto the π-plane. Denoting the angle of inclination between the vector and the Π-plane as θ_x, we have

$$\mathbf{e}_x \cdot \left(\frac{1}{\sqrt{3}}\mathbf{e}_x + \frac{1}{\sqrt{3}}\mathbf{e}_y + \frac{1}{\sqrt{3}}\mathbf{e}_z\right) = \cos\left(\frac{\pi}{2} - \theta_x\right) = \frac{1}{\sqrt{3}} \tag{11.27}$$

since the axis of the prism is along the space diagonal. This simplifies to

$$\sin \theta_x = \frac{1}{\sqrt{3}} \tag{11.28a}$$

or

$$\theta_x = \cos^{-1}\sqrt{\frac{2}{3}} \tag{11.28b}$$

from which

$$r = \sigma_Y \sqrt{\frac{2}{3}} \tag{11.29}$$

and Eq. (11.26) becomes

$$(\sigma_D^{(1)})^2 + (\sigma_D^{(2)})^2 + (\sigma_D^{(3)})^2 = \frac{2}{3}\sigma_Y^2, \tag{11.30a}$$

which may also be written as

$$[\sigma^{(1)} - \sigma^{(2)}]^2 + [\sigma^{(2)} - \sigma^{(3)}]^2 + [\sigma^{(3)} - \sigma^{(1)}]^2 = 2\sigma_Y^2. \tag{11.30b}$$

In terms of the stress deviator invariant given by Eq. (11.13) with $\sigma^{(i)} = \sigma_D^{(i)}$, eq. (11.30a) becomes

$$\sigma_Y = \sqrt{3J_{2D}}. \tag{11.31}$$

The Tresca criterion Eq. (11.21), written in terms of the yield stress $\sigma_Y = 2k$, is

$$\max \text{ of } |\sigma^{(1)} - \sigma^{(2)}|, \quad |\sigma^{(2)} - \sigma^{(3)}|, \quad |\sigma^{(3)} - \sigma^{(1)}| = \sigma_Y. \tag{11.32}$$

Comparing Eq. (11.30b) to Eq. (11.32), Calladine [11.4] observed that the Mises condition is related to the rms of the principal stress differences while the Tresca condition considers only the largest absolute value. He also calculates that the differences between the two criteria are at most 15%.

11.3.4 General Criterion for Isotropic Media

The Tresca and von Mises yield conditions are based on the stress deviator $\boldsymbol{\sigma}_D$ and thus are essentially independent of the mean or hydrostatic stress $\boldsymbol{\sigma}_M$. This is appropriate for ductile materials but is not sufficiently broad to describe all isotropic materials, specifically those where the behavior is dependent on the hydrostatic pressure and the third stress invariant, Eq. (11.14). Examples of such materials cited by Podgorski [11.5] include plain concrete and sand.

The general failure criterion is expressed in terms of the octahedral shearing stress as

$$A_0 + A_1\sigma_{ns}^{oct} + A_2(\sigma_{ns}^{oct})^2 = 0 \tag{11.33}$$

where A_0 is a function of hydrostatic pressure only; and A_1 and A_2 depend on the second and/or third stress invariants. According to Podgorski [11.5], the von Mises yield condition derived in the previous section fits into this form with

$$A_0 = -\sqrt{2/3J_{2D}}$$

$$J_{2D} = \frac{1}{2}\sigma_{D_{ij}}\sigma_{D_{ii}} = \frac{1}{2}[(\sigma_D^{(1)^2}) + (\sigma_D^{(2)^2}) + (\sigma_D^{(3)^2})]$$

and

$$A_1 = 1.$$

Checking, we have

$$A_0 = -\left\{\frac{2}{3}\cdot\frac{1}{2}[(\sigma_D^{(1)})^2 + (\sigma_D^{(2)})^2 + (\sigma_D^{(3)})^2]\right\}^{1/2} = -\sigma_{ns}^{oct}.$$

He also gives the requisite constants for the Tresca conditions. While both the von Mises and Tresca conditions represent yield surfaces with constant cross sections along the main stress axis, OC, in Fig. 11.2(a), yield conditions that reflect dependence on the hydrostatic stress would be nonprismatic.

Conical, pyramidal and paraboloidal surfaces are represented by Eq. (11.33) [11.5].

11.4 Anisotropic Materials

11.4.1 Objectives

For anisotropic materials, it is desirable to have a criterion that is invariant with respect to coordinate transformation; treats interaction terms (such as between normal and shear stresses) as independent components; accounts for the difference in strengths due to positive and negative stresses; and can be specialized to account for different material symmetries, multidimensional space and multiaxial stresses [11.6].

On the other hand, the sixth-order tensor which would emerge from linking all of the stress components is forbidding, and a simpler form is preferred.

11.4.2 Failure Surface

As proposed by Tsai and Wu [11.6], the equation of a failure surface can be written as the sum of a second order tensor and a fourth order tensor.

$$f(\sigma_k) = F_i\sigma_i + F_{ij}\sigma_i\sigma_j = 1 \tag{11.34}$$

in which $i, j, k = 1, 2, \ldots, 6$; F_i and F_{ij} are the components of the strength tensors; and the single subscripted stress σ_i represents the following components of stress:

$$\sigma_1 = \sigma_{11}, \quad \sigma_2 = \sigma_{22}, \quad \sigma_3 = \sigma_{33}$$

$$\sigma_4 = \sigma_{23}, \quad \sigma_5 = \sigma_{13}, \quad \sigma_6 = \sigma_{12}$$

The ordering was apparently chosen to allow planar problems to be considered in the 2-3 plane, so that plane stress can be extracted as the second, third and fourth rows and columns without reordering.

The linear terms σ_i are useful to describe the difference between positive and negative (tension and compression) stress induced failures; and also load reversal phenomena, such as the Bauschinger effect which is a reduction of the yield stress upon loading in the direction opposite from the previous direction [11.5].

The quadratic terms $\sigma_i\sigma_j$ define an ellipsoid in the stress space, which may be considered as a generalization of the sphere described in Sec. 11.3.3.

Following the symmetry argument presented for the generalized Hooke's Law in Sec. 4.3, $[\mathbf{F}_{ij}]$ is taken as symmetric and Eq. (11.34) can be written in matrix form as

$$\{\boldsymbol{\sigma}\}^T\{\mathbf{F}_i\} + \{\boldsymbol{\sigma}\}^T[\mathbf{F}_{ij}]\{\boldsymbol{\sigma}\} = 1 \tag{11.35}$$

in which

$$\{\mathbf{F}_i\} = \{F_1\ F_2\ F_3\ F_4\ F_5\ F_6\} \qquad \text{(a)}$$

$$[\mathbf{F}_{ij}] = \begin{bmatrix} F_{11} & F_{12} & F_{13} & F_{14} & F_{15} & F_{16} \\ F_{12} & F_{22} & F_{23} & F_{24} & F_{25} & F_{26} \\ F_{13} & F_{23} & F_{33} & F_{34} & F_{35} & F_{36} \\ F_{14} & F_{24} & F_{34} & F_{44} & F_{45} & F_{46} \\ F_{15} & F_{25} & F_{35} & F_{45} & F_{55} & F_{56} \\ F_{16} & F_{26} & F_{36} & F_{46} & F_{56} & F_{66} \end{bmatrix} \qquad \text{(b)} \quad (11.36)$$

and

$$\{\boldsymbol{\sigma}\} = \{\sigma_1\ \sigma_2\ \sigma_3\ \sigma_4\ \sigma_5\ \sigma_6\}. \qquad \text{(c)} \quad (11.36)$$

It is necessary to constrain the terms of $[\mathbf{F}_{ij}]$ such that the diagonal terms are positive and dominate the interaction terms. The latter is expressed in terms of a stability condition

$$F_{(ii)}F_{(jj)} - F_{ij}^2 \geq 0. \qquad (11.37)$$

11.4.3 Specializations

Again, guided by the reductions for material symmetry used in Section 4.3, the tensors $\{\mathbf{F}_i\}$ and $[\mathbf{F}_{ij}]$ may be specialized for some special cases. For a specifically orthotropic material, Eqs. (4.13), we assume that the sign of the shear stress does not change the failure stress to eliminate F_4, F_5, F_6 and the shear-normal coupling terms F_{14}, F_{15}, F_{16}, F_{24}, F_{25}, F_{26}, F_{34}, F_{35}, F_{36}. Further, if shear stresses are all uncoupled, we eliminate F_{45}, F_{46}, F_{56}. Remaining are three terms in $\{\mathbf{F}_i\}$ and nine in $[\mathbf{F}_{ij}]$, the same terms as in $[\mathbf{C}_{ij}]$ in Eq. (4.13a). The off-diagonal coefficients F_{12}, F_{13}, F_{23} represent coupling between the normal strengths.

Another common case in composites is transverse or planar isotropy, which refers to a plane such as 2-3 shown in Fig. 11.5. The indices associated with the isotropic plane are identical, i.e.,

$$F_2 = F_3, \quad F_{12} = F_{13}, \quad F_{22} = F_{33}, \quad F_{55} = F_{66}. \qquad (11.38)$$

Thus, Eq. (11.35) becomes

$$\{\boldsymbol{\sigma}\}^T \begin{Bmatrix} F_1 \\ F_2 \\ F_2 \\ 0 \\ 0 \\ 0 \end{Bmatrix} + \{\boldsymbol{\sigma}\}^T \begin{bmatrix} F_{11} & F_{12} & F_{12} & 0 & 0 & 0 \\ F_{12} & F_{22} & F_{23} & 0 & 0 & 0 \\ F_{12} & F_{23} & F_{22} & 0 & 0 & 0 \\ & & & F_{44} & & \\ & & & & F_{55} & \\ & & & & & F_{55} \end{bmatrix} \{\boldsymbol{\sigma}\} = 1. \qquad (11.39)$$

We note that the two stress states shown in Fig. 11.5, pure shear and equal

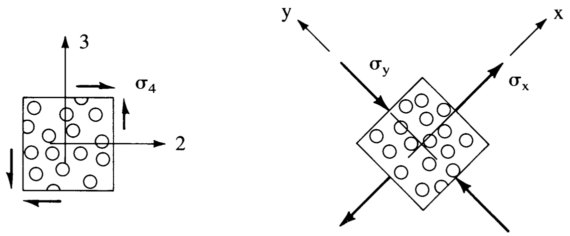

Fig. 11.5. Equivalent states of stress in pure shear and tension-compression.

principal tension and compression, are equivalent. Therefore, we may evaluate Eq. (11.39), first with $\sigma_4(\sigma_{23}) = \bar{\sigma}$, then with $\sigma_2(\sigma_{22}) = \bar{\sigma}$ and $\sigma_3(\sigma_{33}) = -\bar{\sigma}$, and equate the results. This gives an additional relationship between the components

$$F_{44} = 2(F_{22} - F_{23}) \tag{11.40}$$

so that the transverse isotropic case retains two independent F_i components and five F_{ij} components.

By extending Eqs. (11.39) and (11.40) to the other two orthogonal planes, creating a totally isotropic case, we get $F_{11} = F_{22}$, $F_{44} = F_{55}$ and $F_{12} = F_{23}$ with the components related by Eq. (11.39). This leaves one independent component in F_i and two in F_{ij}. Further, if internal stresses are not considered, the F_i component is dropped to produce the expected two-parameter isotropic equation.

Another specialization proposed by Tsai and Wu [11.6] is to eliminate the failures due to the hydrostatic stress state $\sigma^{(i)} = \bar{\sigma}$, as defined in Section 2.6.5. The rationale for this assumption, which is known as zero volume change or *incompressibility*, has been presented in the preceding sections. For the general case, the assumption is implemented by setting $\sigma_1 = \sigma_2 = \sigma_3 = \bar{\sigma}$ in Eq. (11.35), factoring the F_{ij} coefficients of $\bar{\sigma}$, and zeroing the factor. This gives

$$F_{11} + F_{22} + F_{33} + 2(F_{12} + F_{23} + F_{13}) = 0. \tag{11.41}$$

For the isotropic case, the direct stress components corresponding to (1, 2, 3) become identical. Likewise, the shear components (4, 5, 6). Thus, we have

$$\begin{aligned} F_{22} &= F_{33} = F_{11} \\ F_{55} &= F_{66} = F_{44} \\ F_{12} &= F_{23} = F_{13} = -\tfrac{1}{2}F_{11} \end{aligned} \tag{11.42}$$

and, from Eq. (11.40)

$$F_{44} = 2F_{11}[1 - (-\tfrac{1}{2})] = 3F_{11}. \tag{11.43}$$

In summary, for incompressible isotropic materials with zero initial stress

$$\{\mathbf{F}_i\} = 0 \tag{11.44}$$

and

$$[\mathbf{F}_{ij}] = F_{11} \begin{bmatrix} 1 & -\frac{1}{2} & -\frac{1}{2} & 0 & 0 & 0 \\ & 1 & -\frac{1}{2} & 0 & 0 & 0 \\ & & 1 & 0 & 0 & 0 \\ & & & 3 & 0 & 0 \\ & & & & 3 & 0 \\ & & & & & 3 \end{bmatrix}. \tag{11.45}$$

Another case of practical interest is that of plane stress. Considering the 1-2 plane and Eqs. (11.35) and (11.36), we retain

$$\{\mathbf{F}_i\} = \{F_1 \ \ F_2 \ \ F_6\} \qquad \text{(a)} \quad (11.46)$$

and

$$[\mathbf{F}_{ij}] = \begin{bmatrix} F_{11} & F_{12} & F_{16} \\ & F_{22} & F_{26} \\ & & F_{66} \end{bmatrix}, \qquad \text{(b)} \quad (11.46)$$

a total of 9 independent components. If the material is specifically orthotropic,

$$F_6 = F_{16} = F_{26} = 0 \tag{11.47}$$

as discussed earlier in this section. Thus, 2 and 4 components are retained in $\{\mathbf{F}_i\}$ and $[\mathbf{F}_{ij}]$, respectively.

11.4.4 Evaluation of Components

The format presented in Eq. (11.34), or in matrix form in Eq. (11.35), requires the evaluation of the components of the strength tensors, $\mathbf{F}_i$ and $\mathbf{F}_{ij}$. Tsai and Wu [11.6] present a detailed discussion of the evaluation of the key components, which is of interest in providing some physical meaning to strength theories. It is helpful to expand Eq. (11.34) in explicit form as

$$\begin{aligned} &F_1\sigma_1 + F_2\sigma_2 + F_3\sigma_3 + F_4\sigma_4 + F_5\sigma_5 + F_6\sigma_6 \\ &\quad + F_{11}\sigma_1^2 + 2F_{12}\sigma_1\sigma_2 + 2F_{13}\sigma_1\sigma_3 + 2F_{14}\sigma_1\sigma_4 + 2F_{15}\sigma_1\sigma_5 + 2F_{16}\sigma_1\sigma_6 \\ &\qquad + F_{22}\sigma_2^2 + 2F_{23}\sigma_2\sigma_3 + 2F_{24}\sigma_2\sigma_4 + 2F_{25}\sigma_2\sigma_5 + 2F_{26}\sigma_2\sigma_6 \\ &\qquad\quad + F_{33}\sigma_3^2 + 2F_{34}\sigma_3\sigma_4 + 2F_{35}\sigma_3\sigma_5 + 2F_{36}\sigma_3\sigma_6 \\ &\qquad\qquad + F_{44}\sigma_4^2 + 2F_{45}\sigma_4\sigma_5 + 2F_{46}\sigma_4\sigma_6 \\ &\qquad\qquad\quad + F_{55}\sigma_5^2 + 2F_{56}\sigma_5\sigma_6 \\ &\qquad\qquad\qquad + F_{66}\sigma_6^2 = 1 \end{aligned} \tag{11.48}$$

accounting for the symmetry relationship in Eq. (11.36).

To start, assume that a uniaxial stress is imposed on a specimen oriented along the 1-axis, and the measured tensile and compressive failure stresses are σ_1^T and σ_1^C. Substitution into Eq. (11.48) with all other stresses equal to zero gives

$$F_1\sigma_1^T + F_{11}(\sigma_1^T)^2 = 1$$
$$-F_1\sigma_1^C + F_{11}(\sigma_1^C)^2 = 1, \qquad (11.49)$$

which yields

$$F_1 = \frac{1}{\sigma_1^T} - \frac{1}{\sigma_1^C}$$

and

$$F_{11} = \frac{1}{\sigma_1^T\sigma_1^C}. \qquad (11.50)$$

Uniaxial tension and compression tests along the 2 and 3 axes give

$$F_2 = \frac{1}{\sigma_2^T} - \frac{1}{\sigma_2^C}$$
$$F_{22} = \frac{1}{\sigma_2^T\sigma_2^C} \qquad (11.51)$$

and

$$F_3 = \frac{1}{\sigma_3^T} - \frac{1}{\sigma_3^C}$$
$$F_{33} = \frac{1}{\sigma_3^T\sigma_3^C} \qquad (11.52)$$

where σ_2^T, σ_2^C, σ_3^T, σ_3^C are the corresponding failure stresses.

Next, pure shear is imposed in the three horizontal planes producing

$$F_4 = \frac{1}{\sigma_{23}^{S+}} - \frac{1}{\sigma_{23}^{S-}}, \qquad F_{44} = \frac{1}{\sigma_{23}^{S+}\sigma_{23}^{S-}}$$
$$F_5 = \frac{1}{\sigma_{13}^{S+}} - \frac{1}{\sigma_{13}^{S-}}, \qquad F_{55} = \frac{1}{\sigma_{13}^{S+}\sigma_{13}^{S-}} \qquad (11.53)$$
$$F_6 = \frac{1}{\sigma_{12}^{S+}} - \frac{1}{\sigma_{12}^{S-}}, \qquad F_{66} = \frac{1}{\sigma_{12}^{S+}\sigma_{12}^{S-}}$$

where σ_{23}^{S+}, σ_{23}^{S-}; σ_{13}^{S+}, σ_{13}^{S-}; σ_{12}^{S+}, σ_{12}^{S-}; are the positive and negative pure shear strengths in the 2-3, 1-3, and 1-2 planes, respectively.

The preceding procedures established all of the components of $\mathbf{F}_i$ and the diagonal components of $\mathbf{F}_{ij}$ and are relatively straightforward in principle.

The off-diagonal components relate to the interaction of two stress components and require more complicated tests.

A biaxial tension with

$$\sigma_1 = \sigma_2 = \sigma_{12}^T; \qquad \sigma_3 = \sigma_4 = \sigma_5 = \sigma_6 = 0 \tag{11.54}$$

in Eq. (11.48) gives

$$\sigma_{12}^T(F_1 + F_2) + (\sigma_{12}^T)^2(F_{11} + F_{22} + 2F_{12}) = 1 \tag{11.55}$$

from which

$$F_{12} = \frac{1}{2(\sigma_{12}^T)^2}\left[1 - \sigma_{12}^T\left(\frac{1}{\sigma_1^T} - \frac{1}{\sigma_1^C} + \frac{1}{\sigma_2^T} - \frac{1}{\sigma_2^C}\right) - (\sigma_{12}^T)^2\left(\frac{1}{\sigma_1^T\sigma_1^C} + \frac{1}{\sigma_2^T\sigma_2^C}\right)\right]. \tag{11.56}$$

Also, biaxial compression $\sigma_1 = \sigma_2 = \sigma_{12}^2$ could have been applied. Similarly, F_{23} and F_{31} can be determined using biaxial states $\sigma_2 = \sigma_3 = \sigma_{23}^T$ or σ_{23}^C, and $\sigma_1 = \sigma_3 = \sigma_{13}^T$ or σ_{13}^C. There are other tests, specifically 45° specimens, which are preferred by some investigators for determining the interaction terms, as discussed by Tsai and Wu [11.6].

For anisotropic materials, the components F_{16} are determined from an axial-torque combination performed on a tubular specimen with the 1-axis along the tube. This produces the desired tension-shear combination,

$$\sigma_1 = \sigma_6 = \sigma_{16}^{TS}; \qquad \sigma_2 = \sigma_3 = \sigma_4 = \sigma_5 = 0. \tag{11.57}$$

Equation 11.48 becomes

$$\sigma_{16}^{TS}(F_1 + F_6) + (\sigma_{16}^{TS})^2(F_{11} + F_{66} + 2F_{16}) = 1 \tag{11.58}$$

from which

$$F_{16} = \frac{1}{2(\sigma_{16}^{TS})^2}\left[1 - \sigma_{16}^{TS}\left(\frac{1}{\sigma_1^T} - \frac{1}{\sigma_1^C} + \frac{1}{\sigma_{12}^{S+}} - \frac{1}{\sigma_{12}^{S-}}\right) - (\sigma_{16}^{TS})^2\left(\frac{1}{\sigma_1^T\sigma_1^C} + \frac{1}{\sigma_{12}^{S+}\sigma_{12}^{S-}}\right)\right]. \tag{11.59}$$

Also, compression shear $\sigma_1 = \sigma_6 = \sigma_{16}^{CS}$ could have been used. Components F_{26} can be determined by the same test with the 1-axis along the circumference of the tube. If the tube axis coincides with the material symmetry axis, a specifically orthotropic material is produced for which F_{16} and F_{26} are zero.

Finally, it was indicated that such tests as the biaxial and the axial torque can be performed using either tension or compression. This leads to redundant measurements of the interaction terms, which may be used to establish the validity and accuracy of the procedure.

As a numerical illustration, Tsai and Wu [11.6] considered a unidirectional graphite-epoxy composite as a specifically orthotropic material. The 1-axis is oriented along the fibers and the 2-axis transverse to the fibers.

The strengths are

$$\sigma_1^T = 150 \text{ ksi}, \qquad \sigma_1^C = 100 \text{ ksi},$$
$$\sigma_2^T = 6 \text{ ksi}, \qquad \sigma_2^C = 17 \text{ ksi},$$
$$\sigma_{12}^S = 10 \text{ ksi}$$

which gives in Eqs. (11.46)

$$\{\mathbf{F}_i\} = \{F_1 \quad F_2 \quad F_6\} = \{-0.003 \quad +0.108 \quad 0\}$$

and

$$[\mathbf{F}_{ij}] = \begin{bmatrix} 0.00007 & \pm 0.0008 & 0 \\ & 0.0098 & 0 \\ & & 0.01 \end{bmatrix}$$

where F_{12} has been bounded as $F_{12} = \pm\sqrt{F_{11}F_{22}} = \pm 0.0008$ by Eq. (11.37). A more precise determination of F_{12} would require a combined test as discussed previously.

It is evident that the proper determination of material constants requires careful and appropriate testing and evaluation.

11.5 Failure of Structures

The preceding sections are directed toward the establishment of strength limitations based on the *initiation* of inelastic action. Barring premature failure due to loss of stability or fatigue, the loads that produce the yield condition at the critical point can be expected to be lower bounds on the actual capacity of the structure. That is, the entire system may possess the capability to resist loads beyond those corresponding to the criterion. Moreover, the concept of yield is associated with ductile materials, and brittle materials are also of considerable practical interest.

As suggested by Bažant and Mazars, [11.7] the two classical theories for the prediction of complete structural failure are (1) plasticity, which describes material failure distributed over a plastic zone and occurring throughout the entire plastic zone simultaneously; and (2) fracture mechanics, which describes material failure that is concentrated into a very small fracture process zone which propagates throughout the structure. Basically, plasticity would seem to be appropriate for ductile materials while fracture mechanics would apply to brittle materials.

For complex materials such as cement-based aggregate composites (concrete, mortar, fiber-reinforced concrete), rocks and soils, and various fibrous and particulate composites, a more elaborate theory may be appropriate. It has been suggested that the material failure begins simultaneously over a larger zone but then localizes into a relatively small zone that propagates throughout the structure. This concept is complicated by size effects, but promises to somewhat unify some of the basic theories into a more general concept applicable for the prediction of the total failure of arbitrary structures.

Exercises

11.1 A closed ended thin walled cylinder of titanium alloy ($\sigma_Y = 800$ MPa) has an inside diameter of 38 mm and a wall of thickness of 2 mm. The cylinder is subjected to an internal pressure $p = 20.0$ MPa and an axial load $P = 40.0$ kN. Determine the torque T that can be applied to the cylinder if the factor of safety for design is $FS = 2.00$. The design is based on the maximum shearing stress criterion of failure assuming that failure occurs at initiation of yielding [11.1].

11.2 Re-solve Problem 11.1 based on the maximum octahedral shearing stress criterion.

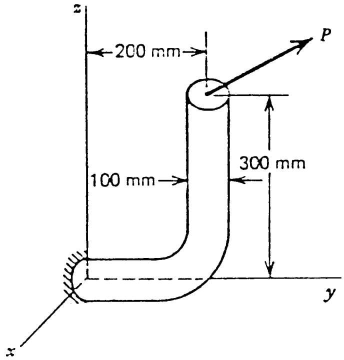

Problem 11.3

11.3 The 100-mm-diameter bar shown is made of a ductile steel that has a yield stress $\sigma_Y = 420$ MPa. The free end of the bar is subjected to a load P making equal angles with the positive directions of the three coordinate axes. Using the maximum octahedral shearing stress criterion of failure, determine the magnitude of P that will initiate yielding.

11.4 Consider a square shaft with a side dimension of 20 mm made of aluminum alloy with $\sigma_Y = 300$ MPa. The shaft is subjected to axial load and $P = 40$ kN.
(a) Determine the torque that can be applied to the shaft to initiate yielding.
(b) Determine the torque that can be applied if the shaft is designed for a factor of safety of 2.0 for both P and T. Base the calculations on the octahedral shear stress criterion.

11.5 Consider the π-plane shown in Fig. 11.2(b). Verify that the lines which bisect the projections of the axes of principal stress correspond to state of pure shear. (Hint: Compute the principal deviatoric stresses corresponding to a state of pure shear and plot them on the Π-plane, or consider any two vectors corresponding to known states of principal stress in the Π-plane, add them to establish the direction of the resultant, and examine the corresponding state of principal stress [11.4].

11.6 Verify the equality of Eqs. (11.30a) and (11.31).

References

[11.1] Boresi, A. P. et al., *Advanced Mechanics of Materials*, 3rd ed. (John Wiley and Sons, New York, 1978).
[11.2] Meek, J. L., and Lin W. J. "Geometric and Material Nonlinear Analysis of Thin-Walled Beam-Columns," *Journal of Structural Engineering*, ASCE, Vol. 116, No. 6, June 1990, pp. 1473–1489.
[11.3] Prager, W., and Hodge, P. G., *Theory of Perfectly Plastic Solids*, (John Wiley and Sons, New York, 1951).
[11.4] Calladine, C. R., *Plasticity of Engineers* (Ellis Howard, Ltd., Chichester, 1985).
[11.5] Podgórski, J., "General Failure Criterion for Isotropic Media," *Journal of Engineering Mechanics*, ASCE, Vol. 111, No. 2, February 1985, pp. 188–201.
[11.6] Tsai, S. W., and Wu, E. M., "A General Theory of Strength for Anisotropic Materials," *Journal of Composite Materials*, Vol. 5, January 1971, pp. 58–80.
[11.7] Bažant, Z. P., and Mazars, J., "France—U.S. Workshop on Strain Localization and Size Effect Due to Cracking and Damage," *Journal of Engineering Mechanics*, ASCE, Vol. 116, No. 6, June 1990, pp. 1412–1424.

CHAPTER 12

Something New

It was stated in the first introductory Section 1.1 that the theory of elasticity originated in the first half of the 19th century. Most of the original work supporting the presentation in this introductory text is many decades old.

Occasionally new developments emerge, even in such a mature theory. A recent contribution, notable because it is attributed to an elementary course in elasticity theory, was developed by Prof. R. Lakes of the University of Iowa. Spurred by the common notion that a real material cannot have a negative Poisson's ratio, as noted in Section 4.3, he developed a substance called antirubber that bulges in the middle when the ends are pulled, an indication of a negative Poisson's ratio. This was accomplished by collapsing or folding cells of polyurethane into a configuration, which is solidified after heating. Then, as the foam is pulled apart, the cells unfold and expand in the direction being pulled and in lateral directions.

The process is shown in Fig. 12.1, which may be the only fundamental development in the theory of elasticity reported in a newspaper article in quite a while [12.1].

There may indeed be something new under the sun.

Reference

[12.1] *Chicago Sunday Tribune*, Aug. 6, 1989.

Antirubber. Roderic Lakes of the University of Iowa has developed a material that, when pulled apart on two sides, expands on all sides. When pushed together, it contracts on all sides. It also absorbs energy more effectively than other materials.

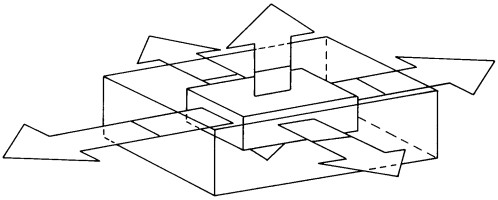

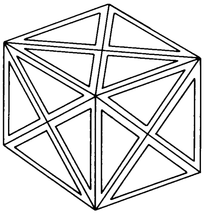

Uncompressed cell. Antirubber is created by transforming the open-cell structure in normal polyurethane or metal foam.

Collapsed cell. The foam is compressed by putting pressure on it from all directions. The cells collapse or fold in upon themselves, and after heating, are solidified into the collapsed configuration.

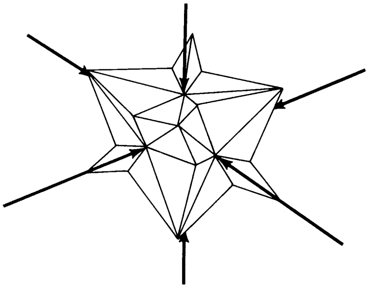

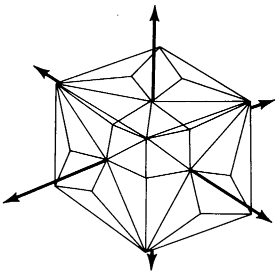

Expanded cell. It's the new, collapsed internal structure that produces the antirubber characteristics. As the foam is pulled apart, the cells unfold and open up in the direction being pulled as well as in all other directions.

Fig. 12.1. Antirubber.

Index